ELIMINACIÓN DE HERBICIDAS Y METALES PESADOS EN AGUAS MEDIANTE EL USO DE HIDRÓXIDOS DOBLES LAMINARES

UNIVERSIDAD DE CÓRDOBA

DEPARTAMENTO DE QUÍMICA INORGÁNICA E INGENIERÍA QUÍMICA

FACULTAD DE CIENCIAS

Memoria de tesis presentada por **Mª Ángeles González Millán**

para aspirar al grado de Doctor con mención internacional por la

Universidad de Córdoba

Córdoba, marzo de 2016

TITULO: *ELIMINACIÓN DE HERBICIDAS Y METALES PESADOS EN AGUAS MEDIANTE EL USO DE HIDRÓXIDOS DOBLES LAMINARES*

AUTOR: *María de los Ángeles González Millán*

Campus de Rabanales
Ctra. Nacional IV, Km. 396 A
14071 Córdoba

www.uco.es/publicaciones
publicaciones@uco.es

TÍTULO DE LA TESIS: ELIMINACIÓN DE HERBICIDAS Y METALES PESADOS EN AGUAS MEDIANTE EL USO DE HIDRÓXIDOS DOBLES LAMINARES

DOCTORANDO/A: Mª Ángeles González Millán

INFORME RAZONADO DEL/DE LOS DIRECTOR/ES DE LA TESIS

(se hará mención a la evolución y desarrollo de la tesis, así como a trabajos y publicaciones derivados de la misma).

La Lcda. Mª Angeles González Millán ha llevado a cabo con éxito el desarrollo de la Tesis Doctoral *"Eliminación de herbicidas y metales pesados en aguas mediante el uso de hidróxidos dobles laminares"*, bajo la dirección de las doctoras abajo firmantes en los laboratorios del Departamento de Química Inorgánica e Ingeniería Química y en el marco del desarrollo del Proyecto Nacional CTM2011-25325.

Este trabajo ha permitido avanzar en la línea de investigación del grupo FQM-214, dedicado al estudio de los procesos de eliminación de contaminantes de aguas y su potencial aplicación y ha contribuido a la formación de la doctoranda tanto en el uso de la instrumentación científica como en la discusión e interpretación de los resultados obtenidos. La intensa labor investigadora realizada por la Lda. González ha permitido alcanzar los objetivos marcados en el Proyecto inicial de la Tesis Doctoral de manera sobresaliente, obteniendo resultados relevantes que han dado lugar a la publicación de cuatro artículos científicos en revistas internacionales de prestigio (Q1) y cuatro comunicaciones en congresos científicos.

En nuestra opinión, la memoria que se presenta reúne los requisitos necesarios para optar al grado de Doctor por la Universidad de Córdoba

Por todo ello, se autoriza la presentación de la tesis doctoral.

Córdoba, 15 de marzo de 2016

Firma del/de los director/es

Fdo.: Cristobalina Barriga Carrasco

Fdo.: Ivana Pavlovic Millicevic

Dª Ivana Pavlovic Milicevic, Profesora Contratada Doctora y Dña. Cristobalina Barriga Carrasco, Catedrática de Universidad de Química Inorgánica del Departamento de Química Inorgánica e Ingeniería Química de la Universidad de Córdoba

CERTIFICAN:

Que el presente Trabajo de Investigación, **Eliminación de herbicidas y metales pesados en aguas mediante el uso de hidróxidos dobles laminares** y que constituye la Memoria que presenta la Lda. Dña. Mª Angeles González Millán para aspirar al Grado de Doctor por la Universidad de Córdoba en Ciencias Químicas, ha sido realizado en los laboratorios del Departamento de Química Inorgánica e Ingeniería Química, bajo nuestra dirección, y reúne las condiciones exigidas para ser presentado como Tesis Doctoral.

Y para que conste, expedimos y firmamos el presente certificado en Córdoba, a 15 de marzo de 2016.

.

Fdo.: Cristobalina Barriga Carrasco

Fdo.: Ivana Pavlovic Milicevic

A mi familia

A Rafa

"Me enseñaron que el camino del progreso no es ni rápido ni fácil"

Marie Curie

El camino hacia la meta ha sido duro pero muy satisfactorio. Como no podría ser de otra manera, quiero expresar mi más sincero agradecimiento a todas aquellas personas e instituciones que han hecho posible el desarrollo de esta tesis doctoral.

En primer lugar, me gustaría agradecer a la Prof. Mª Ángeles Ulibarri, por la confianza depositada en mí para la realización de este trabajo. Sus enseñanzas, compromiso y dedicación por la Química Inorgánica dejaron una huella significativa durante mis años de carrera.

De igual modo, a mis directoras de tesis, la Prof. Cristobalina Barriga y la Prof. Ivana Pavlovic, por haberme iniciado en el mundo de la investigación, por su compresión tanto a nivel profesional como personal, y como no por la valiosa formación que me han dado. Gracias a vuestros consejos he aprendido mucho en esta etapa de mi vida.

Por otro lado, agradecer al Prof. Fabio La Mantia el haberme acogido en la Universidad de Bochum (Alemania) y hacerme sentir que era una más del grupo nada más comenzar. Su interés por mi trabajo y porque volviera de nuevo me ayudaron a creer en mí. Nunca olvidaré aquellos group meetings y discusiones en el laboratorio, los cuales resultaron muy enriquecedores.

Al Prof. José María Fernández, por sus enseñanzas y porque su sentido del humor siempre traía un momento de alegría. A los profesores Álvaro Caballero, Manolo Cruz, Luis Sánchez, Carlos Pérez y Jesús Santos, por sus sabias explicaciones, porque siempre han estado dispuestos a echarme una mano cuando lo he necesitado y por el gran aprecio que les tengo.

A las diferentes instituciones que han financiado este proyecto, al Ministerio de Ciencia e Innovación (CTM 2011-25325) y la Junta de Andalucía, mediante el grupo de investigación FQM-214. Así como al SCAI por la asistencia técnica recibida y al personal técnico del departamento de Química Inorgánica (Mari Carmen) por toda la ayuda prestada.

A mis compañeras/os de laboratorio, a todos y a cada uno de los que han pasado por el departamento durante este periodo y hemos compartido

experiencias e inquietudes juntos, pero en especial a: Rafa S. por sacarme miles de sonrisas, a Jose, siempre dispuesto a solucionar los problemas informáticos, a Óscar por su amabilidad y compañerismo, a Almudena, siempre encantada de ayudar en todo, a Noe porque su ironía me hacía reír muchisimo, a Pepi por tantos mimos cuando más lo necesitaba y por sentirte cerca aunque estés lejos, a Maika, Mari Jose y Naci, con los que he compartido muchas charlas, y como no, a la gente de mi grupo, a mi Fredy, que vino cargado de alegría y buen rollo desde Honduras, y a Chari, Rosalía y Rocío, de las que he aprendido mucho sobre todo en mis inicios. Chicos/as siempre recordaré aquellas intensas y agitadas charlas durante el almuerzo, no tenían desperdicio alguno. Agradecer también a miembros del Departamento de Química Orgánica, como son Alfonso y Susana. A ti Alfonso, gracias por tu ayuda durante todo este tiempo y por ser un amigo de los que ya no quedan, y a ti Susana, porque sé que aunque nos veamos poco te tengo para toda la vida. Finalmente, acabo con mis compis de Bochum, quienes siempre estuvieron dispuestos a tenderme la mano e hicieron que mi estancia fuese más agradable cada día. Anastasia, gracias por ser la mejor compañera y amiga que se puede tener, a Andjela por todo lo que hemos compartido y vivido juntas, a Ghoncheh, Mu y Dulce, mis compañeros de mesa, con los que he charlado mucho y me he sentido muy cómoda, a Guoquing por ser tan apañado conmigo y por tu peculiar sentido del humor, a Giorgia, siempre haciéndome reír nada más hablar, a Alberto, cuyos conocimientos de alemán me ayudaron bastante y cuyas historias no olvidaré, y como no a Francesca, mi organizadora de eventos favorita. No solo me llevo grandes momentos sino a grandes personas.

A mis amigas, en especial a Ana Rosa, Ana Belén, Salud, Mari Ángeles, Isa, Elena, Fátima y Dolores, porque de un modo u otro habéis estado siempre ahí y los momentos que hemos pasado han sido inolvidables. Chicas espero que nuestra amistad perdure muchos años.

Como no podía ser de otra manera, a mi familia. A mis primillos además de amigos, Rafa, Rafael Mª, Angy y Mari Carmen, por vuestro ánimo y por los momentos tan divertidos que hemos compartido juntos. A mis tías, tita Rosario nunca olvidaré tus sabios consejos, y a mis abuelos porque son muy importantes para mí y cada día que puedo disfrutar de ellos, es un motivo más para sonreír.

De manera muy especial a Rafa Trócoli, este trabajo me dio la oportunidad de conocerte y descubrir una gran persona. Siempre me has hecho ver el lado positivo de las cosas y sin tu apoyo y cariño esto no hubiese sido posible. Como olvidar que aquello que me pareció una locura al principio puesto que se salía un poco de las directrices de esta tesis, se convirtió en algo muy interesante y motivador. Hablo de la realización de mi estancia en Bochum, mi vida allí fue más fácil gracias a ti. Me iniciaste en otro ámbito de la química que no conocía y supiste transmitirme tus conocimientos a la perfección. Allí no solo descubrí a un gran investigador sino a un excelente compañero, siempre dispuesto a ayudar a todo el mundo. Mi tiempo allí acabó convirtiéndose en la parte más positiva de este trabajo. Por tu ayuda incondicional en este viaje, por tu paciencia y por formar parte de mi vida, MIL GRACIAS.

Dedicatorias

A mis padres

A ti papá, agradecerte el esfuerzo que haces diariamente por querer darme lo mejor y motivarme a escalar a lo más alto. Tu interés por las cosas y tu curiosidad por aprender cada día algo nuevo me hace sentir muy feliz. A ti mamá porque siempre te enorgullece todo lo que decido hacer, porque no hay día ni momento que no estés dispuesta a ayudarme sin importar el cuándo y el por qué. Porque tienes un corazón enorme y has hecho un mundo mejor para mí. Sin duda, vuestro cariño, ánimos incansables, comprensión y apoyo ha sido vital durante estos años.

"El único amor perfecto de este mundo es aquel de los padres por sus hijos"

A mi hermana

Inmaculada (Macu para mi), agradecerte el apoyo que me has brindado siempre, tu interés por saber lo que hago me llena de alegría. Como no, siempre dispuesta a ayudarme y empatizar conmigo como nadie puede hacerlo. Gracias por ser una hermana diez y saber transmitirme el significado de la "psicología positiva". Antonio (cuñi), nos conocemos de no hace mucho pero te doy las gracias por entrar en nuestras vidas y estar siempre ahí para todos nosotros.

CAPÍTULO I
Introducción

PREÁMBULO

El uso de sustancias tóxicas inorgánicas y orgánicas en los suelos agrícolas, como por ejemplo pesticidas, residuos urbanos que contienen metales pesados, subproductos de transformación de la industria alimentaria, etc. así como el vertido accidental de residuos o su enterramiento en lugares inadecuados ha agravado de forma notable los problemas de contaminación ambiental en suelos y aguas [1-4]. También, como consecuencia de la fabricación y manufacturación de una gran cantidad de productos, numerosos contaminantes llegan a los cauces públicos donde pueden quedar disueltos en el agua o retenidos por las partículas en suspensión y sedimentos.

El desarrollo de técnicas de remediación ha experimentado un auge en los últimos años para lograr la protección y recuperación de suelos y aguas contaminadas. En esta tesis doctoral se estudia dos metodologías encaminadas a la eliminación de contaminantes químicos potencialmente tóxicos presentes en aguas: adsorción de pesticidas y metales pesados y electrodeposición de metales pesados.

La adsorción es una técnica prometedora para la eliminación de contaminantes, tanto orgánicos como inorgánicos especialmente para bajas concentraciones, de una manera rápida, eficaz y sin introducir especies nocivas al medio. Existen numerosos compuestos que pueden utilizarse como adsorbentes, algunos ejemplos son la alúmina activada [5], zeolitas [6], residuos de agricultura [7], arcillas y minerales de arcilla [8,9], etc. Otra técnica novedosa ha sido la electrodeposición de metales, la cual permite su eliminación del agua contaminada.

Los compuestos tipo Hidrotalcita (HT), también denominadas arcillas aniónicas o Hidróxidos Dobles Laminares (HDLs) han sido propuestos y estudiados como adsorbentes de pesticidas y metales pesados, asi cómo sustratos electroquímicos para la deposición de plomo y cadmio. Las características estructurales que poseen los HDLs y sus propiedades tales como baja toxicidad, posibilidad de modificar su carácter hidrófilico a hidrofóbico a través de su adecuada funcionalización, composición química variable, selectividad,

reciclabilidad, elevada estabilidad, bajo coste, etc. permiten ampliar su rango de actuación [10- 13].

I.1. CONTAMINACIÓN DE LAS AGUAS NATURALES

El agua es esencial para la vida y como tal debe ser controlada para la protección de la vida acuática además de la salud pública. Los ríos, lagos y océanos de la Tierra se encuentran en un proceso muy grave de deterioro ya que están siendo amenazados por la contaminación ambiental. Por tanto, la calidad del agua potable es una cuestión social que preocupa en países de todo el mundo, tanto en desarrollo como industrializados, por su repercusión en la salud de la población y en el bienestar humano.

En general, se considera **"contaminante"** a una sustancia presente en concentración mayor que la natural como resultado de la actividad humana, que tiene un efecto perjudicial neto en el medio ambiente o sobre algo de valor en ese ambiente [14].

¿Cómo se contaminan las aguas?

La contaminación de las aguas subterráneas puede venir de la superficie de la tierra, de los suelos sobre el nivel freático, o de sedimentos debajo del nivel freático. Los sitios donde los contaminantes entran al ambiente subterráneo puede afectar la calidad de las aguas subterráneas. En el caso del vertido de un contaminante sobre la tierra, este puede atravesar varias capas de materiales antes de alcanzar las aguas subterráneas, y esto disminuye el nivel de contaminación. El movimiento del contaminante a través de capas de sedimento funciona como un proceso de filtración, dilución y descomposición que puede disminuir el impacto final en las aguas subterráneas. Si el contaminante es introducido directamente en el área debajo del nivel freático, el proceso principal que puede disminuir el impacto del contaminante es la dilución [15].

I.1.1. Clases de componentes químicos y origen

Las sustancias que pueden contaminar las aguas subterráneas pueden dividirse en dos categorías: aquellas que ocurren naturalmente y las sustancias introducidas por actividades humanas, Tabla I.1.

Tabla I.1. Clasificación de los componentes químicos en función de su origen [16]

Origen de componentes químicos	Ejemplos de orígenes
Origen natural	Rocas, suelos y los efectos del marco geológico y el clima
Fuentes industriales y núcleos habitados	Minería (industrias extractivas) e industrias de fabricación y procesamiento, aguas residuales, residuos sólidos, escorrentía urbana, fugas de combustibles
Actividades agropecuarias	Estiércoles, fertilizantes, prácticas de ganadería intensiva y plaguicidas
Tratamiento del agua o materiales en contacto con el agua de consumo	Coagulantes, SPD, materiales de tuberías
Plaguicidas añadidos al agua por motivos de salud pública	Larvicidas utilizados en el control de insectos vectores de enfermedades
Cianobacterias	Lagos eutróficos

Las sustancias de origen natural incluyen minerales como hierro, calcio y selenio. Las sustancias que resultan de las actividades humanas incluyen sal, bacterias y virus, productos químicos e hidrocarburos (por ejemplo los disolventes, pesticidas, y productos petrolíferos), y lixiviación de depósitos de basura (líquidos que se han filtrado del depósito y que llevan sustancias disueltas de la basura) que contienen sustancias como metales pesados [17].

Generalmente, los metales pesados son más persistentes en el medio ambiente que los contaminantes orgánicos como por ejemplo los pesticidas, pudiendo llegar a ser móviles según el pH del suelo y su especiación.

I.2. PLAGUICIDAS O PESTICIDAS

I.2.1. Definición y origen

Estos compuestos agroquímicos resultan imprescindibles para cubrir las necesidades de la sociedad ya que, según la Organización de las Naciones Unidas para la Alimentación y la Agricultura (FAO), el cese del empleo de estos productos fitosanitarios en un país desarrollado como EEUU reduciría el rendimiento de las cosechas y del ganado en un 30-40 % y aumentaría el precio de los productos agrícolas en un 50-70 % [18].

La FAO establece que un **plaguicida o pesticida** es cualquier sustancia o mezcla de sustancias destinadas a prevenir, destruir o controlar cualquier plaga, incluyendo los vectores de enfermedades humanas o animales, especies no deseadas de plantas o animales que causan perjuicio o de otra manera que interfieren con la producción, transformación, almacenamiento, transporte o comercialización de alimentos, productos agrícolas, madera y productos de madera o alimentos para animales, o sustancias que puedan administrarse a los animales para el control de insectos, arácnidos u otras plagas sobre sus cuerpos [19].

Algunos pesticidas se utilizan por motivos de salud pública, como los que se añaden al agua para controlar la presencia de larvas acuáticas de insectos perjudiciales. Al considerar los plaguicidas que pueden añadirse al agua destinada al consumo humano, los valores de referencia establecidos no son tan estrictos. Este planteamiento permite alcanzar un equilibrio adecuado entre la protección de la calidad del agua de consumo y el control de insectos perjudiciales para la salud pública. Los pesticidas también pueden generarse por las actividades agropecuarias, estos se añaden en exceso y tan solo el 1% alcanzan su objetivo, aunque su presencia dependerá de numerosos factores, y no todos ellos se utilizan en todas las circunstancias o climas. Diferentes sustancias pueden ser usadas como pesticidas: agentes químicos, biológicos, antimicrobianos o desinfectantes. La

clasificación de los pesticidas resulta de sus características pudiendo llegar a ser bastante amplia.

I.2.2. Clasificación

Los pesticidas pueden ser clasificados de distintas formas, dependiendo del tipo de plaga que combaten, modo de acción, persistencia o toxicidad, naturaleza química, formulación, etc. La clasificación principal es atendiendo a la actividad del pesticida en cuanto al tipo de plaga como se muestra en la Tabla I.2.

Tabla I.2. Clasificación de los pesticidas según el organismo al que interesa controlar [20]

TIPO DE PESTICIDA	ORGANISMO QUE CONTROLA
Insecticida	Larvas de insectos, hormigas, pulgas, piojos, pulgones y mosquitos
Acaricida	Ácaros
Nematicida	Nematodos
Molusquicida	Moluscos
Rodenticida	Roedores
Bactericida	Bacterias
Fungicida	Hongos
Herbicida	Malas hierbas

La Organización Mundial de la Salud (OMS) ha recomendado (sujeta a actualizaciones periódicas) una clasificación de pesticida según el grado de peligrosidad, entendiendo ésta como su capacidad de producir daño agudo a la salud cuando se dan una o múltiples exposiciones en un tiempo relativamente corto.

I.2.2.a. Tipo de pesticida: Herbicidas

Actualmente, el principal grupo de pesticidas usado en todo el mundo son los “herbicidas”. Estos son productos químicos que inhiben o interrumpen el crecimiento y desarrollo de una planta. La aplicación de la mecanización en la agricultura ha incrementado la habilidad del ser humano de controlar las hojas y

cultivar la cosecha. Los herbicidas a su vez siguen diversos criterios de clasificación, como comentamos a continuación.

Algunos ejemplos de herbicidas de acuerdo a su composición química se detallan a continuación [21]:

- Amidas: Propanil, Alaclor, Metolaclor
- Ácidos benzoícos: Dicamba, Cloroben
- Carbamatos: Cloropropham, Propham, EPTC
- Nitrilos: Bromoxynil, Ioxynil
- Nitroanilinas: Pendimetalina, Butralina
- Organofosforados: Glifosato, Glufosinato de amonio
- Fenoxiácidos: 2.4D, 2.4DB, Mecoprop-P, MCPA
- Piridinas y compuestos de amonio cuaternarios: Paraquat, Diquat
- Piridazinas y piridazonas: Cloridazona, Norflurazona, Piridato
- Triazinas: Atrazina, Simazina, Metribuzina, Terbutrina, Metramitrón
- Fenilureas: Diurón, Linurón, Fenurón
- Sulfonilureas: Clorosulfurón, Triasulfurón, Prosulfurón

Según la acción que ejercen sobre la planta, estos compuestos pueden ser totales o selectivos. Estos últimos pueden controlar la hierba sin afectar al cultivo, mientras que los totales pueden matar toda la vegetación. Finalmente, según la época en que deben aplicarse, los herbicidas pueden ser: preemergentes (PRE) son aquellos que se aplican antes de la emergencia o germinación del cultivo. Presentan una gran interacción con algunas características del suelo como textura, pH y materia orgánica que pueden afectar la cantidad de herbicida disponible en el suelo para controlar la maleza. La otra clase son los postemergentes (POST) que se aplican después de la emergencia o germinación del cultivo y la maleza. Su actividad depende de su grupo químico, especies de maleza presentes y condiciones climáticas. Existen herbicidas que pueden ser aplicados en preemergencia o postemergencia según sea el cultivo, el terreno, la climatología y otros factores.

I.2.3. Relevancia ambiental

En España, el consumo de productos fitosanitarios para la protección de los cultivos se ha incrementado paulatinamente desde la mitad de los años noventa (Figura I.1), siendo los herbicidas los productos más demandados en Andalucía caracterizada por las numerosas hectáreas de olivar. La utilización de productos fitosanitarios puede tener efectos no deseables y es imprescindible que estos efectos no sean en ningún momento peligrosos para la salud humana, ni tampoco que lleguen a presentar niveles de riesgo elevados para el medio ambiente. A este respecto, el Real Decreto 1311/2012, tiene por objeto establecer el marco de acción para conseguir un uso sostenible de los productos fitosanitarios mediante la reducción de los riesgos y los efectos de su empleo en la salud humana y el medio ambiente. Además, el Real Decreto también tiene como objetivo el fomento de la gestión integrada de plagas y de planteamientos o técnicas alternativas tales como los métodos no químicos [22].

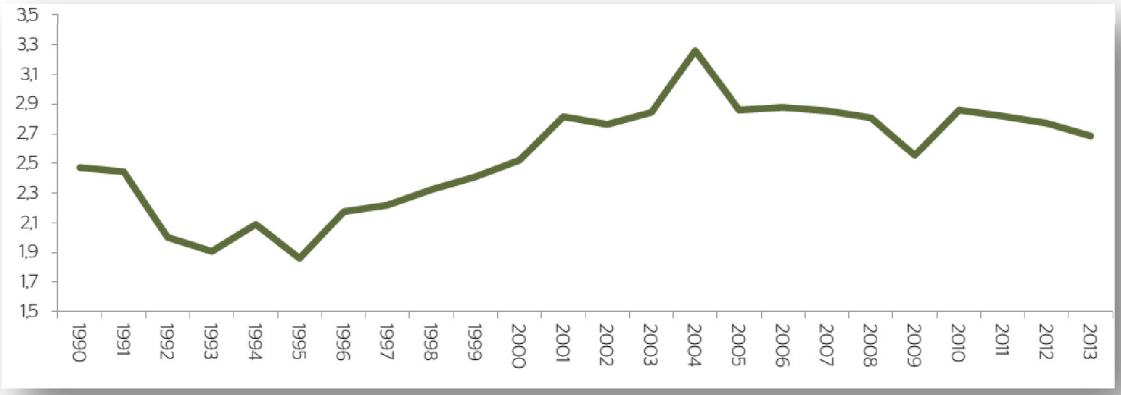

Figura I.1. Consumo de productos fitosanitarios (Kg ingrediente activo/ha) en España

Según la "Encuesta de Comercialización de Productos Fitosanitarios" realizada por el Ministerio de Agricultura, Alimentación y Medio Ambiente en el año 2013, la cual se basa en el conocimiento de las sustancias activas comercializadas dentro del marco nacional de las empresas titulares de productos fitosanitarios, se obtuvieron los siguientes datos (Tabla I.3).

Tabla I.3. Productos fitosanitarios comercializados en España en el año 2013 (expresados en Toneladas)

PRINCIPALES GRUPOS DE SUSTANCIAS QUÍMICAS	TONELADAS
Fungicidas y Bactericidas	32400
Herbicidas	14.719
Insecticidas y Acaricidas	6.909
Molusquicidas, Reguladores de Crecimiento y Otros	17519

I.2.4. Factores y procesos que afectan al transporte de pesticidas

El movimiento de los pesticidas hacia las aguas subterráneas viene condicionado por las características intrínsecas de los productos y está estrechamente ligado con las propiedades del medio en que se encuentren [23].

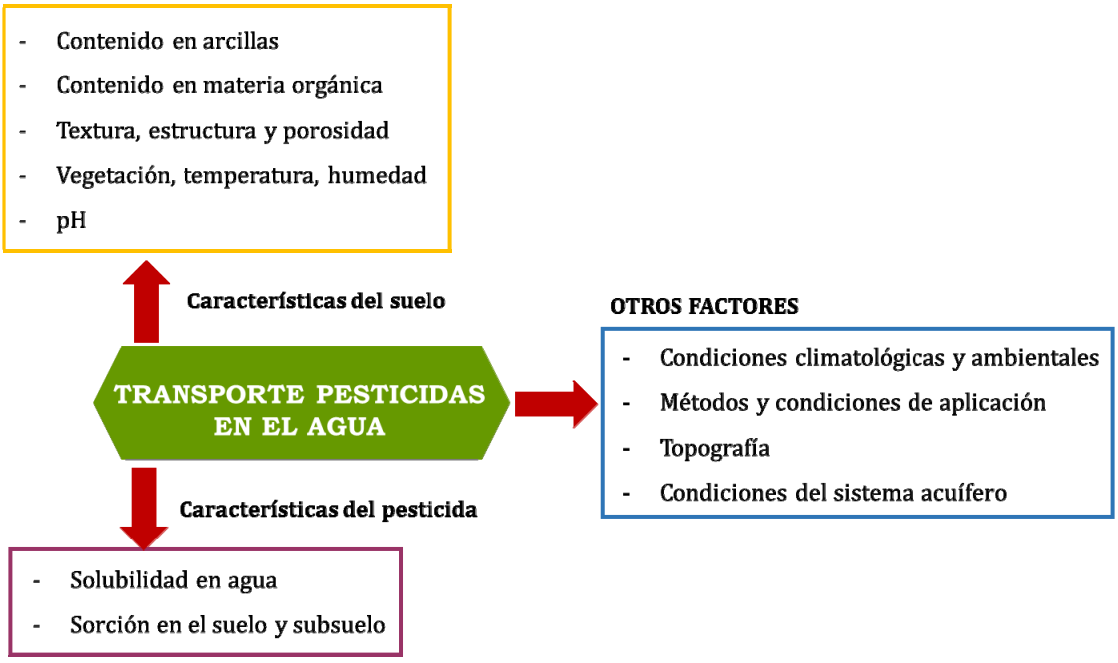

Figura I.2. Factores que afectan al transporte de los pesticidas hacía las aguas subterráneas

Además de los factores relativos a las características del suelo y de los pesticidas que afectan a su movimiento y transporte hacia los acuíferos hay otros factores que pueden alterar los mecanismos físicos, químicos y biológicos de estos contaminantes, Figura I.2. Por consiguiente, es necesaria la información acerca de la topografía, tipos de suelo y ubicación, tipo de cubierta del suelo, precipitación

anual, condiciones de temperatura, entre otros, para poder estimar hacia donde pudiera desplazarse el pesticida aplicado.

El transporte ambiental involucra los movimientos de gases, líquidos y partículas sólidas dentro de un medio determinado y a través de las interfaces entre el aire, agua, sedimento, suelo, plantas y animales (Figura I.3).

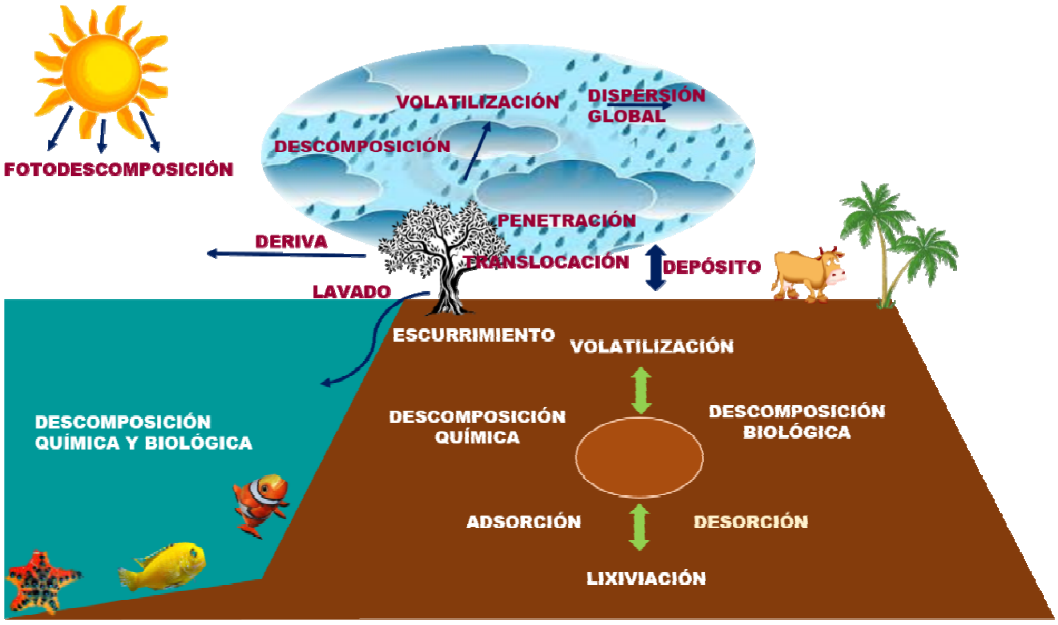

Figura I.3. Posibles mecanismos de transporte y transformación de pestidas en el ambiente

Probablemente la propiedad que más afecta el movimiento del pesticida hacia la atmósfera después de su aplicación es la **volatilización**. El ritmo de volatilización va a depender de su presión de vapor, de la temperatura, de su volatilidad intrínseca y de la velocidad de difusión hacia la superficie de evaporación. El parámetro más importante de evaluación del movimiento de una sustancia en el suelo es la **lixiviación**. Es un proceso que depende de las características químicas del plaguicida, de las propiedades químicas y físicas del suelo y de la dinámica del agua. Los compuestos aplicados al suelo tienden a desplazarse con el agua y lixiviar a través del perfil, alcanzando las capas más profundas y el acuífero. Mediante **difusión**, los contaminantes se pueden mover desde las zonas más concentradas a las menos concentradas. Para ello es necesario considerar la interacción conjunta de una serie de parámetros como son procesos de adsorción, naturaleza del

compuesto, porosidad, etc. Según el tipo de suelo, la **adsorción** o transferencia del pesticida a las partículas del suelo, cambia de acuerdo al % de materia orgánica, arcilla y arena. Factores como la humedad, pH y temperatura del suelo afectan también a dicho proceso. Se trata de un proceso físico-químico mediante el cual un pesticida presente en la disolución del suelo interacciona enlazándose a sus partículas. El proceso inverso, la desorción, conlleva a que los pesticidas estén disponibles para su transporte y procesos de degradación. Otro de los procesos de transporte que se dan en el suelo es la **absorción**, los pesticidas son capaces de penetrar en plantas y microrganismos. Muchas sustancias son absorbidas por plantas, insectos, nematodos, etc., pudiendo degradarse o quedarse asociados a residuos de plantas y organismos. Finalmente, en muchas situaciones se producen **escorrentias** que contaminan las aguas superficiales con los pesticidas, factores como el riego, lluvias y efectos de deriva son las causas principales de esta situación. De acuerdo a las propiedades y las características químicas del plaguicida como del entorno en el que se encuentra depositado, la vida media de ellos puede variar de días a meses. Mediante procesos de transformación, muchos plaguicidas se degradan rápidamente en el suelo, proceso denominado **mineralización** en donde, el pesticida es transformado en compuestos más simples como CO_2, NH_3 y H_2O. El resultado de este proceso es causado por reacciones de hidrólisis, fotólisis y también por procesos de **degradación** metabólica mediada por microorganismos, los cuales utilizan los pesticidas como fuente de carbono [24].

I.3. METALES PESADOS

I.3.1. Definición y origen

El término “metales pesados” se refiere a aquellos elementos metálicos y metaloides que poseen una densidad relativamente alta, entre 3.5 y 7g cm^{-3} y son tóxicos o venenosos a bajas concentraciones. Ejemplos de ellos son: mercurio (Hg), plomo (Pb), cadmio (Cd), cromo (Cr), níquel (Ni), arsénico (As), zinc (Zn), cobre (Cu) y talio (Tl) [25].

Los metales pesados pueden alcanzar los sistemas acuáticos procedentes de la actividad humana, tales como desechos municipales (aguas residuales domésticas),

la minería, procesos industriales (fertilizantes, papel, curtido de pieles, tintes, aleaciones, galvanoplastia, textil, baterías, munición, fotografía, electrónica, etc.), la actividad agrícola (pesticidas y fertilizantes), etc. Estos contaminantes también derivan de fuentes naturales como pueden ser las rocas y minerales. Los metales pesados muestran persistencia ya que no son biodegradables y además pueden ser acumulados por los organismos vivos. Si se ingieren cantidades superiores al límite permisible, podrían ocasionar trastornos en la salud y enfermedades graves.

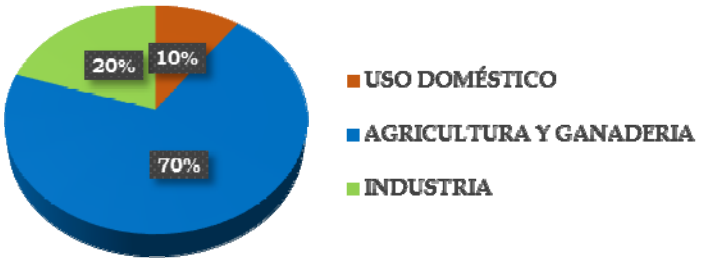

Figura I.4. Fuentes humanas de contaminación de agua

I.3.2. Propiedades químicas y especiación

El destino y transporte de un metal en el suelo y en el agua depende significativamente de su especiación química. En ambientes acuáticos, los metales pesados suelen existir en formas catiónicas, oxoaniones o formas orgánicas. Su movilidad va a estar limitada por las numerosas reacciones que pueden tener lugar: ácido-base, precipitación/disolución, oxidación/ reducción, absorción, adsorción o procesos de intercambio iónico, captación biológica, entre otros [26]. La velocidad y extensión de estas reacciones dependerá de las condiciones físico-químicas del medio (temperatura, humedad, pH, etc.) y de factores como potencial redox, complejación química con otros constituyentes disueltos, sorción y capacidad de sorción de materiales geológicos y contenido de materia orgánica [27, 28]. Algunas de estas reacciones transfieren metales pesados desde la hidrosfera a otros compartimentos ambientales, estos procesos son a menudo reversibles.

La toxicidad, movilidad y reactividad de metales pesados depende de las diferentes formas químicas en las que pueden existir dichos elementos en el medio acuático, y por consiguiente de las numerosas interacciones que pueden tener lugar [29]. Un estudio termodinámico y cinético de estos metales potencialmente tóxicos sería

interesante para determinar su destino final y a lo sumo sus impactos ambientales [30-32].

I.3.3. Efectos en la salud y en los ecosistemas

Aunque algunos de los elementos metálicos son micronutrientes necesarios para la vida de los seres vivos y deben ser absorbidos por las raíces de las plantas o formar parte de la dieta de los animales, muchos de ellos son peligrosos porque tienden a acumularse en los suelos, aguas o los seres vivos. Por tanto, debido a su toxicidad pueden causar problemas severos de salud en los humanos y animales además de problemas en las plantas.

Los efectos típicos que pueden ocasionar los metales estudiados (Cu, Pb y Cd) son los siguientes [25, 33]:

El **cadmio** no es un elemento esencial para los animales o plantas. Afecta de manera adversa a varias enzimas importantes; también puede causar la osteomalacia (dolorosa enfermedad de los huesos) y daños a los riñones. La inhalación de polvos y humos de óxido de cadmio produce la neumonitis del cadmio caracterizada por edema y necrosis del epitelio pulmonar (muerte del tejido que recubre los pulmones).

El **plomo** no es un elemento esencial para las plantas o animales y puede ser tóxico para ambos. El plomo se acumula principalmente en los huesos, el cerebro, los riñones y los músculos. Provoca la inhibición de la síntesis de la hemoglobina, enfermedades renales, y afecta adversamente al sistema nervioso central y periférico.

El **cobre** es un elemento esencial para la vida humana y un micronutriente para la planta. Además se requiere para la activación de algunas enzimas durante la fotosíntesis. En altas dosis puede causar anemia, daño del hígado y del riñón, y la irritación del estómago e intestino.

I.3.4. Tecnologías de remediación para aguas contaminadas por metales pesados

Cuando se produce contaminación de las aguas por metales pesados, es necesario considerar el uso de tratamientos para su eliminación. Varias tecnologías han sido desarrolladas recientemente destinadas a la eliminación de un amplio rango de metales pesados encontrados en efluentes de agua potable y residual. Entre ellas cabe destacar la precipitación química, coagulación-floculación, adsorción, métodos electroquímicos e intercambio iónico [34-37]. Este último es el método más frecuentemente usado para la eliminación de contaminantes iónicos de efluentes acuáticos. En la última década, muchos investigadores se han centrado en el desarrollo de nuevos intercambiadores híbridos multifuncionales. La precipitación química es el método más ampliamente usado cuando los metales se encuentran disueltos en el agua. Los factores que controlan dicho proceso son la concentración de iones metálicos presentes en disolución, el precipitante usado y la presencia si la hubiera de otros constituyentes que pudieran inhibir la reacción. Otros procesos que muestran un gran potencial son aquellos basados en sistemas de filtración de membranas, como son ultrafiltración, osmosis inversa, nanofiltración y electrodiálisis. Aunque hay una diversidad de métodos empleados para la eliminación de metales pesados en aguas, las ventajas no son las mismas y aún quedan muchas limitaciones que solventar [38]. En muchos casos, dos o más técnicas pueden trabajar sinérgicamente obteniéndose mejores resultados. Como tecnología económica, eficiente, efectiva y a su vez popularmente usada destaca la adsorción. Mediante el uso de adsorbentes adecuados y una funcionalización correcta es posible lograr la eliminación de una gran cantidad de contaminantes de distinta naturaleza y sin dar lugar a la formación de sustancias perjudiciales [39]. Finalmente, las técnicas de tratamiento electroquímico han sido menos extendidas debido al consumo energético que suponen [40] pero la eficiencia que puede llegar a conseguirse puede ser óptima para ciertos metales, además de otras múltiples ventajas, siendo la recuperación de metales una de ellas. Aunque hay varias alternativas a la eliminación de estos contaminantes potencialmente tóxicos, cada método presenta algunas ventajas y desventajas, como se resume a continuación en la Tabla I.4 [38].

Tabla I.4. Tecnologías actuales para la eliminación de metales pesados vía procesos físicos y/o químicos

MÉTODO	VENTAJAS	DESVENTAJAS
OXIDACIÓN	Proceso rápido	Coste alto de energía, formación de subproductos
INTERCAMBIO IÓNICO	Alta capacidad de eliminación y eficiencia de un amplio rango de metales pesados	Regeneración del adsorbente o eliminación
TECNOLOGÍAS FILTRACIÓN MEMBRANA	Alta eficiencia de eliminación, fácil operación	Producción de lodo, caro, proceso complejo
OZONACIÓN	Aplicadas en estado gas: alteración del volumen	Tiempo de vida medio corto
COAGULACIÓN/ FLOCULACIÓN	Factible económicamente, mejor deshidratación lodos	Alta producción de lodo y formación de grandes partículas, uso de varios productos químicos
FOTOQUÍMICA	No hay producción de lodo	Formación de subproductos
IRRADIACIÓN	Efectividad a escala de laboratorio	Requiere mucho O_2 disuelto
COAGULACIÓN ELECTROCINÉTICA	Factible económicamente	Alta producción de lodo
TRATAMIENTO BIÓLOGICO	Factible en la eliminación de algunos metales	Aún no está establecida y comercializada
PRECIPITACIÓN QUÍMICA	Simplicidad del proceso, equipos de bajo costo, condiciones seguras	Se requieren grandes cantidades de productos químicos, excesiva producción de lodo
TRATAMIENTO ELECTROQUÍMICO	Proceso rápido y efectivo para ciertos iones metálicos, menor generación de lodo	Elevado coste energético, formación de subproductos
ADSORCIÓN	Flexibilidad diseño, eficiencia alta, sencillez del proceso y bajo coste	Trabaja mejor a bajas concentraciones de metal

I.4. REGULACIÓN DEL AGUA DE CONSUMO

Para la protección de la vida acuática y el agua de consumo, la Directiva CE sobre agua potable 80/778/EC y la nueva directiva 98/83/CE de la Unión Europea establece un límite de 0.1 μg L^{-1} para un solo ingrediente activo de pesticidas, y 0,5 μg L^{-1} para la suma de todos los ingredientes activos individuales detectados y cuantificados [41]. Por el contrario, los límites de residuos y los niveles de referencia establecidos por la Organización Mundial de la Salud (OMS) o la Agencia de Protección Ambiental de Estados Unidos (USEPA) dependen de la toxicidad de las sustancias activas y se determinan mediante una evaluación basada en el riesgo. Los valores de referencia están comprendidos en el rango: 0.03-200 μg L^{-1} para 32 pesticidas individuales y 0.2-700 μg L^{-1} para 21 pesticidas según la OMS y la USEPA respectivamente [42, 43]. En el caso de los metales pesados, la mayoría de ellos deben encontrarse por debajo de 10 μg L^{-1} (Pb, As, Se…) aunque otros no deben sobrepasar los 5 μg L^{-1} e incluso 1 μg L^{-1} (Cd, Sb) y Hg, respectivamente. De acuerdo a la OMS y la USEPA, los límites máximos permisibles para los contaminantes metálicos, objeto de estudio en esta tesis doctoral, se especifican en la Tabla I.5 [44, 45].

Tabla I.5. Límites máximos aceptables de varios iones metálicos tóxicos en el agua según las regulaciones de la OMS y la USEPA

CONTAMINANTE	RANGO DE TOXICIDAD[a]	OMS (mg L^{-1})	U.S. EPA (mg L^{-1})
Cu	118	2	1.3
Pb	2	0.010	0.015
Cd	7	0.003	0.005

a=rank of 2015 substance priority list

La presencia de pesticidas y metales pesados en agua tiene una repercusión económica desfavorable en los procesos de potabilización [46]. Estas sustancias tóxicas pueden provocar efectos indeseables, cuyos impactos negativos pueden ser tan importantes que probablemente podrían afectar a todo el esquema evolutivo de la humanidad.

I.5. ADSORCIÓN

El término "adsorción" generalmente se refiere al proceso mediante el cual las partículas de un gas o un soluto en disolución se acumulan en la superficie de un sólido. La sustancia que se adsorbe se denomina **adsorbato** y el material sobre el cual se adsorbe se denomina **adsorbente** (Figura I.5). Este se va a unir a las moléculas/iones mediante fuerzas de atracción física, intercambio iónico y/o enlaces químicos.

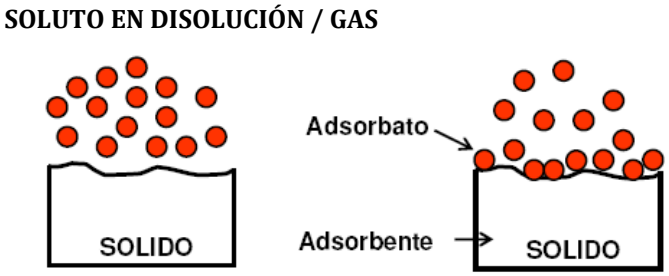

Figura I.5. Esquema del fenómeno de adsorción

Hay dos tipos básicos de adsorción: adsorción física, o fisisorción y adsorción química, o quimisorción. Si la atracción entre la superficie del sólido y las moléculas adsorbidas es de naturaleza física, hablamos de "fisisorción". Generalmente la interacción es de tipo Van der Waals, fuerzas débiles y como resultado el proceso de adsorción es reversible. Si las fuerzas de atracción son debidas a enlaces químicos, el proceso de adsorción es conocido como "quimisorción". Como consecuencia el proceso es irreversible dada la mayor fuerza de interacción de las especies quimisorbidas. Este tipo de adsorción depende principalmente de las características de reactividad química del adsorbato y adsorbente, mientras que en fisisorción la fuerza de la interacción va a depender de la geometría del adsorbato. Ambos tipos de interacciones quedan ilustradas en la Figura I.6.

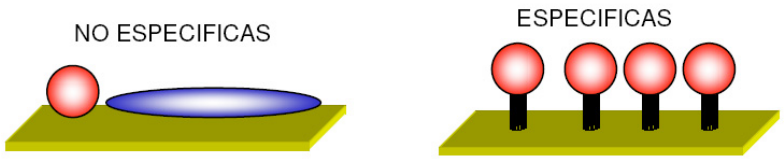

Figura I.6. Tipos de interacciones: no específicas (fisisorción) y específicas (quimisorción)

Por tanto, el fenómeno de adsorción incluye adsorción física [47], complejación [48], precipitación [49], intercambio iónico [50], reducción [51], y coordinación [52], como las principales etapas de reacción.

I.5.1. Factores que afectan al proceso de adsorción

El estudio de los parámetros que afectan a la adsorción es esencial, para lograr una mayor efectividad del proceso. Los factores más importantes son discutidos a continuación:

- **pH:** el pH influencia las características superficiales de adsorbente (carga) y por ello es un factor determinante en la efectividad del mismo [53]. A bajos valores de pH, hay más protones disponibles para reaccionar con grupos activos en la superficie del adsorbente, por tanto, pueden competir con los metales pesados cuando tiene lugar la adsorción [54].
- **Cantidad del adsorbente:** la aplicación de una relación óptima de dosis de adsorbente es crucial para la efectividad y coste del proceso [55].
- **Tiempo de contacto:** la adsorción va a ir aumentando a la vez que lo hace el tiempo de contacto. Es importante conocer el tiempo óptimo de contacto necesario para que se alcance el equilibrio de adsorción. Los datos cinéticos obtenidos se analizan en términos de modelos matemáticos de ecuaciones (pseudo primer orden, pseudo segundo orden, difusión intrapartícula, etc.).
- **Velocidad de agitación:** el efecto del incremento de la velocidad de agitación se traduce con la disminución de la resistencia de la capa límite (boundary layer) a la transferencia de masa [56] y por tanto se favorece el proceso de adsorción.
- **Temperatura:** usualmente, la adsorción aumenta con el incremento de la temperatura debido a la naturaleza endotérmica de la reacción de

adsorción. A altas temperaturas, mas reacciones endotérmicas tienen lugar y el número y tamaño de poros activos en la superficie del adsorbente aumenta [53].

- **Concentración de contaminante:** es importante optimizar el rango de concentración inicial teniendo en cuenta una serie de parámetros (producto de solubilidad, pH, etc.), para garantizar un equilibrio real. Se aplican dos ecuaciones de isotermas de adsorción (Freundlich, Langmuir, entre otras) para la descripción cuantitativa de los datos experimentales de adsorción.
- **Competencia de moléculas e iones:** la adsorción competitiva tiene lugar cuando la adsorción de una mezcla de adsorbatos se lleva a cabo en una superficie. Algunos de los componentes presentes en el agua podrían inducir a la adsorción de otros o bien podrían co-adsorberse con otros componentes. En 2003 Chiou y col. [57, 58] mostraron que la presencia de otras moléculas podrían afectar a la adsorción de una molécula particular. Los adsorbatos presentes en disolución podrían competir entre ellos por ocupar los sitios disponibles en el adsorbente.
- **Fuerza iónica:** generalmente no tiene un efecto significativo en el proceso de adsorción. La fuerza iónica puede influenciar la adsorción a través del potencial de la superficie, del coeficiente de actividad de los iones metálicos en disolución y del grado de complejidad entre el contaminante y los aniones del electrolito [55].

I.5.2. Desorción

La desorción es el proceso contrario a la adsorción, por el que las moléculas de adsorbato previamente adsorbidas son transferidas a la disolución. Cuando la desorción es total, se habla de que el proceso de adsorción es reversible. Sin embargo, es habitual encontrar desorción parcial del adsorbato o incluso nula, cuando parte o todo el adsorbato está irreversiblemente adsorbido [59]. Sin embargo, este proceso es esencial para conocer la distribución y predecir la dinámica del contaminante en el medio y de esta manera poder desarrollar tecnologías de remediación adecuadas a este fin.

El estudio de la isoterma de desorción suele llevarse a cabo mediante diluciones sucesivas, por las que, tras la medida de la adsorción (plateau de la isoterma), se

sustituye parte de la disolución de equilibrio por una disolución libre de contaminante permitiendo que se restablezca el equilibrio. Cuando la isoterma de desorción del contaminante no coincide con la de su adsorción se dice que existe el fenómeno de histéresis.

I.5.3. Equilibrio de adsorción

Los procesos de adsorción y desorción de moléculas sobre la superficie de un adsorbente son dinámicos y relacionados entre sí, dándose de forma continuada a lo largo del tiempo. En este equilibrio la concentración de moléculas de adsorbato en la superficie del adsorbente (C_s) alcanza un equilibrio con su concentración en la disolución (C_e) en contacto con dicho sólido. El equilibrio de adsorción se expresa como:

$$Ce \leftrightharpoons Cs$$

I.5.3.a. Estudio cinético

Uno de los factores más importantes que controla el destino y transporte de muchos contaminantes en el medio ambiente es la "cinética de adsorción". El estudio cinético puede ser utilizado para calcular la velocidad en la que tiene lugar la adsorción en un sistema dado, de manera que nos conduce a expresiones de velocidad características de posibles mecanismos de adsorción, los cuales nos proporcionan información útil para el diseño y operación de un reactor o sistema adecuado para el tratamiento de aguas residuales. Por tanto, estos resultados son necesarios para entender las variables que influyen en la adsorción de dichos contaminantes en el agua.

En la literatura, han sido ampliamente usados tres modelos cinéticos (Tabla I. 6) para investigar los mecanismos de adsorción: (i) modelo cinético de pseudo primer orden (modelo de Lagergren) [60]; (ii) modelo cinético de pseudo segundo orden (modelo de Ho y Mckay) [61]; y modelo de difusión intraparticula (modelo de Webber y Morris) [62].

Tabla I.6. Modelos cinéticos más populares y sus formas lineales

MODELO	ECUACIÓN	FORMA LINEAL
Pseudo primer orden	$log\ \frac{q_e}{q_e - q_t} = \frac{K_1}{2.303} t$	$log\ (q_e - q_t) = log\ q_e\ - \frac{k_1}{2.303}\ t$
Pseudo segundo orden	$\frac{1}{q_e - q_t} = \frac{1}{q_e} + k_2 t$	$\frac{t}{q_t} = \frac{t}{q_e} + \frac{1}{k_2\, q_e^2}$
Difusión Intraparticula		$q_t = k_p\, t^{1/2} + C$

Los parámetros q_t y q_e hacen referencia a las cantidades de adsorbato adsorbidas (mg g^{-1}) al tiempo t (min) y en el equilibrio, respectivamente. k_1 y k_2 son las constantes de velocidad de los modelos de pseudo primer y pseudo segundo orden, expresadas en (min^{-1}) y (g mg^{-1} min^{-1}), respectivamente. Estos valores de las constantes se obtienen de la representación lineal de $log\ (q_e - q_t)$ y t/q_t frente a t para primer y segundo orden, respectivamente. En el modelo propuesto por Weber y Morris, la cantidad de adsorbato adsorbida varía proporcionalmente con $t^{1/2}$, siendo k_p la constante de velocidad de la difusión intrapartícula (mg g^{-1} $min^{0.5}$) y C (ordenada) nos da una idea del espesor la capa límite (boundary layer).

En el caso de la ecuación de Weber y Morris, si la representación de la cantidad adsorbida frente a $t^{1/2}$ da una línea recta que pasa por el origen la difusión intraparticula podría ser el paso limitante de la velocidad, en caso contrario es indicativo de un cierto grado de control de la capa límite y de que la difusión intrapartícula no es el único paso determinante de la velocidad. En este caso, otros procesos podrían controlar la velocidad de adsorción. En general, la representación de Weber y Morris presenta multilinealidad, que indica que el proceso tiene lugar en dos o más etapas. Cuando en la representación hay tres porciones diferentes, la primera parte de la curva es debida adsorción en la superficie y una difusión externa rápida (boundary layer diffusion). El segundo tramo lineal corresponde a una etapa de adsorción gradual donde la difusión intraparticula es la etapa determinante de la velocidad. El último tramo es la etapa de equilibrio final, donde la difusión intraparticula es más lenta debido a la baja concentración de soluto en disolución [63, 64].

I.5.3.b. Isotermas de Adsorción

Una de las características más importantes de un adsorbente es la cantidad de adsorbato que puede acumular, lo cual se lleva a cabo mediante "isotermas de adsorción". Por tanto, definen la relación de equilibrio entre la cantidad de adsorbato por unidad de adsorbente (C_s) y la concentración de la disolución en equilibrio (C_e).

La forma de la isoterma podría ser considerada como una manera de predecir si el proceso de adsorción es favorable o desfavorable. Además, puede proporcionar información cualitativa de la naturaleza de la interacción del soluto en la superficie [63]. La clasificación más conocida de las isotermas de adsorción ha sido propuesta por Giles y col [65] y son cuatro las clases que han sido identificadas, basadas en la configuración de la parte inicial de la isoterma, Figura I.7.

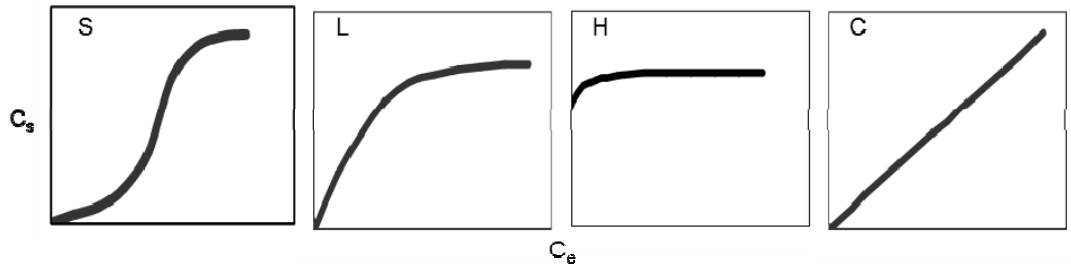

Figura I. 7. Tipos de isotermas de adsorción según la clasificación de Giles y col., 1960

Tipo S: la curvatura inicial de la isoterma muestra que la adsorción llega a ser más fácil a medida que aumenta la concentración de soluto. Esto implica que al principio la adsorción es más baja, pero posteriormente la asociación de moléculas adsorbidas ayudará que el resto de moléculas de soluto disueltas se adsorban.

Tipo L: La curvatura inicial nos indica que la mayoría de sitios en el sustrato comienzan a llenarse, lo cual dificulta que una molécula de soluto pueda encontrar un sitio vacante. Ello implica que la molécula de soluto adsorbida no está verticalmente orientada o que no hay una fuerte competición delsoluto/disolvente.

Tipo H: Es un caso especial de la isoterma tipo L, en la cual el soluto tiene tan alta afinidad por el adsorbato que en disoluciones diluidas, se adsorbe completamente, o al menos la cantidad que queda en disolución no es apreciable. Las especies adsorbidas son a menudo grandes unidades, como por ejemplo micelas iónicas o moléculas poliméricas, pero a veces son iones aparentemente simples que se intercambian con otros de afinidad mucho menor por la superficie. Este tipo de isoterma sugiere que la captación de los contaminantes por los distintos materiales tiene lugar a través de interacciones químicas más que atracción física.

Tipo C: este tipo muestra una linealidad entre la cantidad de soluto adsorbido y la concentración en la disolución de equilibrio. Es un tipo de curva obtenida por la partición de un soluto entre dos disolventes inmiscibles. Con la mayoría de compuestos químicos en un estrecho rango de bajas concentraciones se obtiene este tipo de isotermas en cualquier adsorbente.

Hay varios modelos de isotermas válidos para el análisis de los datos experimentales y para la descripción del equilibrio de adsorción. Las dos ecuaciones más frecuentemente usadas aplicadas a sistemas sólido-liquido son los modelos de Langmuir [66] y Freundlich [67]. En la Tabla I.7 aparecen las correspondientes ecuaciones que pueden ser usadas para el ajuste de los datos experimentales, siendo la regresión lineal la más frecuentemente usada para determinar el modelo.

Tabla I.7. Ecuaciones de equilibrio (isotermas) más populares

ISOTERMA	LANGMUIR	FREUNDLICH
SUPUESTOS	-Adsorción (monocapa) -La adsorción tiene lugar en sitios específicos del adsorbente -El adsorbente tiene una capacidad limitada para el adsorbato (en el equilibrio, se alcanza un punto de saturación) -Todos los sitios son idénticos y energéticamente equivalentes -El adsorbente es estructuralmente homogéneo	-Adsorción (multicapa) -El modelo se aplica a la adsorción en superficies heterogéneas con interacción entre moléculas adsorbidas -La energía de adsorción disminuye exponencialmente al irse agotando los centros adsorción de un adsorbente -Es una ecuación empírica empleada para describir sistemas heterogéneos
ECUACIÓN	$C_s = C_m \frac{K_L C_e}{1+K_L C_e}$	$C_s = K_F \cdot C_e^{n_F}$
FORMA LINEAL LOGARITMICA	$\frac{C_e}{C_s} = \frac{C_e}{C_m} + \frac{1}{C_m K_L}$	$\log C_s = \log K_F + n_F \log C_e$

Los parámetros de las ecuaciones de Langmuir y Freundlich se definen de la siguiente manera:

C_m es la cantidad de adsorbato correspondiente a una monocapa de soluto adsorbida (mmol g^{-1}) y K_L (L $mmol^{-1}$) una constante relacionada con la energía de adsorción. Los valores de dichas constante pueden obtenerse del ajuste lineal de los datos de $\frac{C_e}{C_s}$ frente a C_e.

C_e y C_s hacen referencia a las concentraciones del contaminante en el equilibrio (mmol L^{-1}) y la cantidad de soluto adsorbida en condiciones de equilibrio (mg g^{-1}) respectivamente. K_F y n_F son las constantes de equilibrio relacionadas con la capacidad de adsorción (mmol^{1-nF} L^{nF} g^{-1}) y la intensidad de la adsorción o grado de favorabilidad de la adsorción respectivamente. Un valor grande de n_F implica una interacción fuerte entre el adsorbente y el adsorbato. Los valores de dichas constantes pueden obtenerse del ajuste lineal de los datos de $\log C_s$ frente a $\log C_e$ [63].

I.5.4. Análisis termodinámico

Generalmente, la adsorción de los contaminantes aumenta con la temperatura ya que a temperaturas altas la velocidad de difusión de las moléculas de adsorbato de la disolución al adsorbente es más rápida. Sin embargo, la adsorción de compuestos orgánicos es un proceso exotérmico y las uniones físicas entre estos compuestos y los sitios activos se debilitan con el aumento de la temperatura. También dicho aumento provocara un aumento de la solubilidad de los mismos. Por tanto, las fuerzas de interacción entre el soluto y el disolvente serán más fuertes que aquellas entre el soluto y el adsorbente, y por consiguiente es más complicado que el soluto se adsorba [64].

El efecto de la temperatura en el proceso de adsorción puede ser confirmado por el cálculo de los parámetros termodinámicos, tales como la energía libre de Gibbs (ΔG^0), entalpía (ΔH^0) y entropía (ΔS^0). Estos se correlacionan con la isoterma de Langmuir para su estimación. $\Delta G°$ es criterio de espontaneidad y un valor negativo indica que la reacción es espontánea. $\Delta G°$ se asocia con la constante de equilibrio de la isoterma de Langmuir obtenida para cada temperatura mediante la siguiente ecuación (Gibbs):

$$\Delta G° = -RT ln\, K_L \qquad \text{(I.1)}$$

Los cambios de entalpía y entropía están relacionados también con la constante de equilibrio de Langmuir por la siguiente expresión (Van´t Hoff):

$$ln\, K_L = \frac{\Delta S°}{R} - \frac{\Delta H°}{RT} \qquad \text{(I. 2)}$$

Los valores de $\Delta H°$ (KJ mol^{-1}) y $\Delta S°$ (KJ mol^{-1}) se obtienen de la pendiente y la ordenada de la representación de $ln\, K_L$ y 1/T. La naturaleza endotérmica o exotérmica de la reacción viene determinada por $\Delta H°$. Valores positivos de $\Delta H°$ indican que el proceso de adsorción es endotérmico, mientras que valores negativos indican que es exotérmico. Valores positivos de $\Delta S°$ representa el aumento de la entropía en la interfaz sólido-disolución [68].

I.5.5. Uso de adsorbentes

El adsorbente más utilizado por su efectividad y fácil manejo es el carbón activo, pero debido a su elevado coste se han buscado otras alternativas. El interés por los "**adsorbentes de bajo coste**", capaces de eliminar contaminantes químicos de aguas, se ha intensificado en los últimos años. Materiales naturales como las zeolitas [69], las arcillas catiónicas (montmorillonita, bentonita, caolinita, etc.) [70], el quitosano [71], o incluso productos de desecho procedentes de operaciones industriales, como cenizas volantes, carbón y óxidos de algunos metales, residuos industriales como lignina, hidróxido de hierro (III), lodos generados en las plantas de fertilizantes, lodo rojo, entre otros, han sido explorados para **aguas contaminadas por la presencia de metales pesados** [72-75]. Los residuos agrícolas también han sido estudiados, aunque en menor extensión pero todos ellos son alternativas prometedoras a la captación de metales pesados, obteniéndose altas eficiencias y capacidades de adsorción comparables a las del carbón activo. El uso combinado de adsorbentes complementarios de distinta naturaleza podría proporcionar otra solución factible al tratamiento de aguas que contienen mezclas de contaminantes orgánicos e inorgánicos [76, 77]. Las capacidades de adsorción para ciertos metales pesados de algunos de los adsorbentes mencionados previamente se reflejan gráficamente en la Figura I.8.

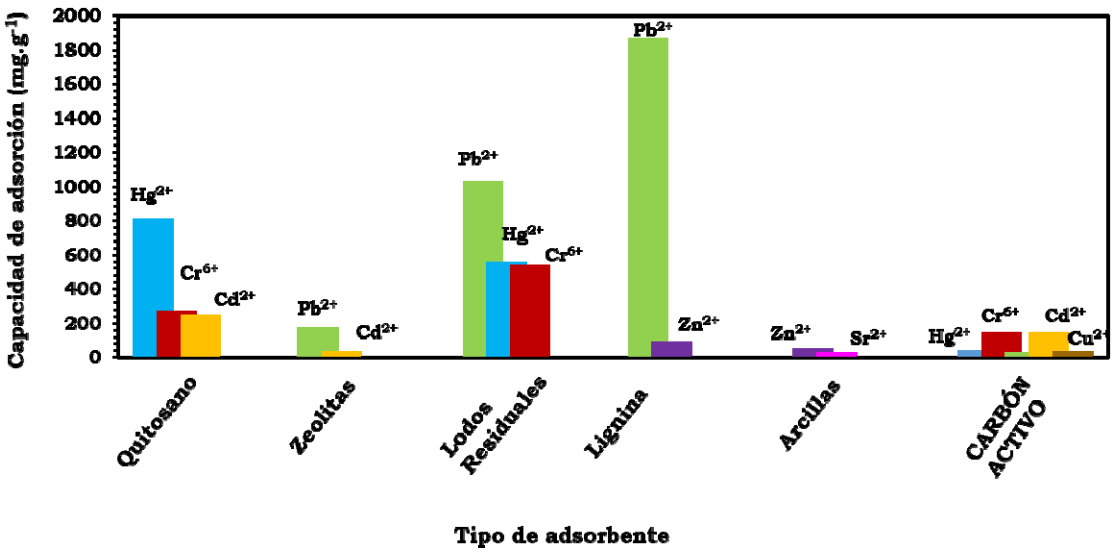

Figura I.8. Capacidades de adsorción de algunos adsorbentes de bajo coste

En los últimos años, se han utilizado para la **eliminación de pesticidas**, entre otros adsorbentes, cáscaras de semillas de arroz y aceite de girasol, lodos de

depuradora compostados [78], membranas de biopolímeros naturales [79], paja, estiércol de vaca, virutas de coco, compost de residuos de jardinería, etc. [80]. Los HDLs son compuestos prometedores en este campo debido a su gran versatilidad química y sus propiedades adsorbentes. Además, la posible modificación de su estructura los convierte en materiales multifuncionales, siendo una de ellas adsorbentes de contaminantes de distinta naturaleza en aguas.

I.6. ELECTRODEPOSICIÓN

La electrodeposición de metales es uno de los procesos electroquímicos de mayor interés tecnológico con aplicaciones muy diversas, como la obtención de recubrimientos metálicos industriales: cobre, cinc, cadmio, níquel, cromo, estaño, latón, plata, oro, rodio y paladio tanto en el campo de la decoración como en el campo tecnológico (electrónica, construcción, alimentación, automoción, aeronáutica, entre otras) [81]. Además de los clásicos recubrimientos de cobre, zinc, níquel, cromo, estaño, etc. se están electrodepositando actualmente aleaciones binarias e incluso ternarias [82]. Estas aplicaciones, en las que se manipula un alto tonelaje de material, constituyen las ramas más importantes de la actual industria electroquímica. La práctica de los procesos de electrodeposición ha sido ampliamente estudiada desde hace muchos años, habiendo alcanzado un desarrollo empírico considerable. El conocimiento teórico es menos extenso, aunque se han dilucidado las etapas electroquímicas del proceso la interpretación de los fenómenos de cristalización que conducen al crecimiento y compactación del depósito presenta ciertas dificultades. Otro problema consiste en determinar el mecanismo de actuación de los aditivos en el proceso, de los que se tiene una elevada información empírica, y cuya intervención influye de manera fundamental en las características y propiedades del depósito. Los procesos de electrodeposición dependen de numerosos factores, tales como la naturaleza del metal a depositar y del sustrato, las características fisicoquímicas de la superficie de éste, las características cristalográficas y morfológicas del metal y las condiciones electroquímicas bajo las que se realiza la experiencia (composición de las disoluciones, potencial aplicado, pH, temperatura, etc.) [83].

I.6.1. Fundamento de la electrodeposición de metales

La electrodeposición es un proceso electroquímico donde los cationes metálicos contenidos en una disolución acuosa se depositan en un electrodo, llamado cátodo o **electrodo de trabajo**. El proceso utiliza una corriente eléctrica para reducir sobre la superficie del electrodo los cationes.

La reacción por la que se deposita material se puede representar mediante la ecuación siguiente:

$$Me^{n+}(aq) + ne^- \Leftrightarrow Me(s) \qquad (I.3)$$

donde n indica el número de electrones involucrados en la reacción. Para que la reacción electroquíimica ocurra es necesario una reacción de oxidación que aporte los electrones necesarios. Esta reacción ocurre en el ánodo o **contraelectrodo**. En general, los ánodos suelen ser de un material inerte, para que no interfiera en la reacción, o de algún material cuyos iones estén ya presentes en el electrolito evitando así la posible contaminación del mismo. El electrodo de trabajo y contraelectrodo están sumergidos en una disolución que contiene los iones de los metales que se quieren depositar. Esta disolución se denomina **electrolito**. Por lo general, se introduce un tercer electrodo, **electrodo de referencia**, para que de esta forma sea posible separar la contribución del potencial del cátodo y el ánodo. Mediante un potenciostato se mide la variación del potencial entre el cátodo y el electrodo de referencia causado por el flujo de corriente eléctrica impuesto. La Figura I.9 muestra una celda electroquímica basada en los componentes anteriormente descritos.

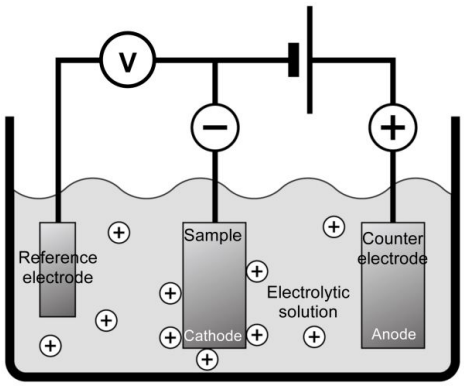

Figura I.9. Esquema de una celda electroquímica con tres electrodos

Un ejemplo de este tipo de celda es la que se puede utilizar en la eliminación de cadmio de un agua contaminada, cuyo proceso viene definido por las siguientes reacciones:

Electrodo de trabajo: $CdCl_{2\,(aq)} + 2e^- \leftrightarrow Cd_{(e)} + 2Cl^-$ (I.4)

Contraelectrodo: $2Ag_{\,(e)} \leftrightarrow 2Ag^+_{(e)} + 2e^-$ (I.5)

Reacción global: $\boldsymbol{CdCl_{2\,(aq)} + 2Ag_{(e)} \leftrightarrow Cd_{(e)} + 2AgCl_{(e)}}$ (I.6)

Donde $e =$ electrodo y aq = acuoso (electrolito)

A partir de la ley de Faraday es posible calcular la cantidad teórica de metal depositado.

I.6.2. Etapas de electrodeposición

En el proceso de formación de una nueva fase metálica o de electrodeposición se pueden distinguir las siguientes etapas (Figura I.10), las cuales están gobernadas por los procesos arriba descritos:

1) Transporte de los iones metálicos solvatados Me^{n+} desde el seno de la disolución hasta las proximidades de la superficie del electrodo (hasta el plano externo de Helmholtz).

2) Transferencia electrónica o reacción de transferencia de carga dentro de las dimensiones de la doble capa.

3) Pérdida parcial o total de la esfera de hidratación que acompaña al ion original, formándose así un átomo depositado sobre la superficie del electrodo. (Los pasos 2 y 3 pueden ocurrir en orden inverso o simultáneamente.)

4) Difusión superficial de los átomos (adsorbidos sobre la superficie del electrodo) hasta sitios energéticamente más favorables.

5) Agrupación de átomos en ciertos sitios, originando la formación de núcleos lo suficientemente grandes como para ser estables (nucleación).

6) Crecimiento generalizado de los núcleos formados por incorporación de nuevos átomos adsorbidos/depositados sobre la superficie del electrodo, pudiendo originar la formación de una fase bidimensional (2D) y/o tridimensional (3D).

7) Solapamiento generalizado de unos núcleos con otros.

8) Crecimiento 3D masivo de la fase metálica.

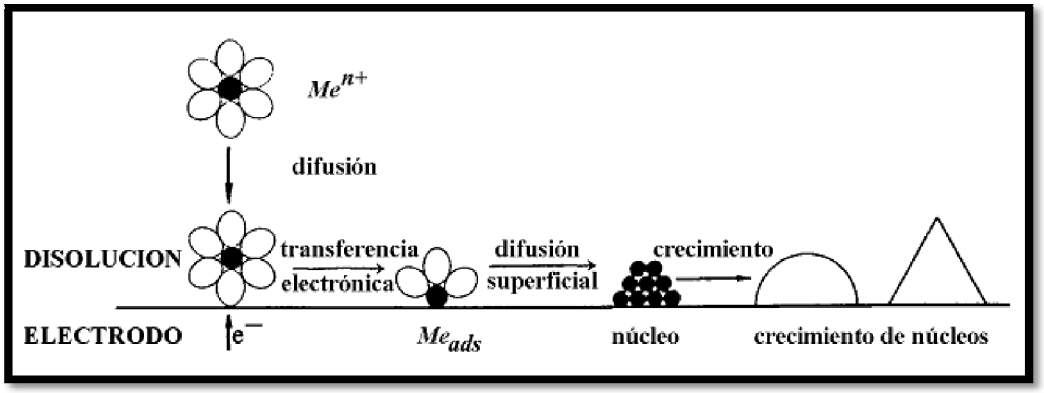

Figura I.10. Etapas de la formación de una nueva fase metálica sobre un sustrato [83]

I.6.3. Procesos involucrados en la electrodeposición

Cuando se aplica un potencial/corriente de reducción (dependiendo de la técnica electroquímica usada) en el cátodo, la concentración de iones en las proximidades de la superficie disminuye. Se crea entonces un gradiente de concentración de iones en la zona del electrolito cercana al cátodo que se denomina capa de difusión (Figura I.11).

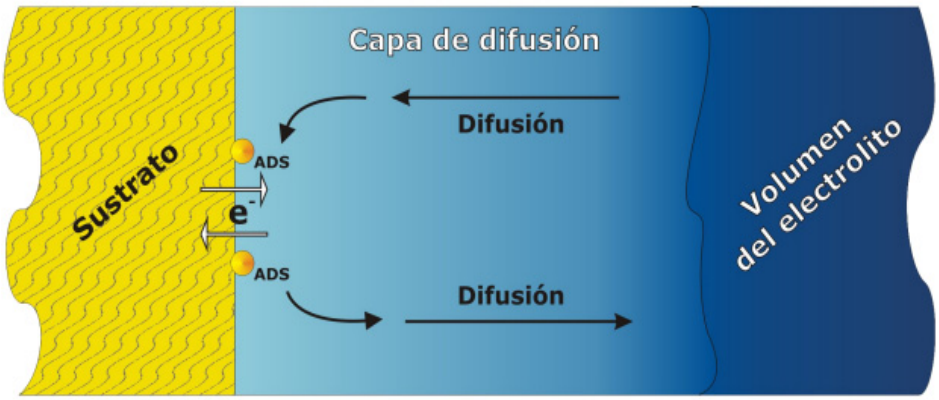

Figura I.11. Esquema de los procesos involucrados en una reacción electroquímica: difusión, adsorción y transferencia de electrones [84]

Para que se pueda dar la electrodeposición, los iones en disolución tienen que llegar a las proximidades del cátodo, adsorberse y, una vez allí, reaccionar con el cátodo mediante una reacción de transferencia de electrones. Los productos, una vez reducidos, pueden ser incorporados a la superficie del

cátodo, o bien pueden desorberse y volver a difundir hacia el volumen del electrolito.

Hay por tanto dos procesos involucrados en la electrodeposición, procesos que están sucediendo de manera continua y simultánea: transporte de masa y transferencia de electrones. El proceso que sea más lento será el proceso limitante de la reacción (generalmente transporte de masa).

Transferencia de masa

La transferencia de masa es el movimiento de material desde un lugar en la disolución a otro, y surge de cualquiera de las diferencias de potencial eléctrico o químico en las dos ubicaciones o del movimiento de un elemento de volumen de la disolución. Los modos de transferencia de masa son [84, 85]:

1. Migración → movimiento de un cuerpo cargado bajo la influencia de un campo eléctrico (un gradiente de potencial eléctrico). Generalmente, este campo eléctrico es aplicado externamente mediante una fuente de potencial. El fenómeno de migración provoca un movimiento cuya dirección queda prácticamente determinada por la geometría del electrodo. En el caso más común de un electrodo plano (tipo estudiado en el presente trabajo), las líneas de campo son perpendiculares a la superficie del mismo. Los iones se dirigirán al electrodo de polaridad opuesta siguiendo la misma dirección de las líneas de campo (no se consideran efectos de borde).

2. Convección → agitación o transporte hidrodinámico. Generalmente el flujo de fluido se produce a causa de la convección natural (gradientes de densidad) y convección forzada, y puede ser caracterizado por regiones inactivas, flujo laminar y flujo turbulento.

3. Difusión → movimiento de una especie bajo la influencia de un gradiente de potencial químico (es decir, un gradiente de concentración). Cuando en el cátodo se produce la reacción, la concentración de iones en la superficie disminuye, siendo menor que la concentración de especies en el volumen del electrolito. Aparece una zona del electrolito en la cual la concentración de iones varia (capa de difusión). En la mayoría de los experimentos, el espesor de esta capa va aumentando con el tiempo hasta que se alcanza un valor estacionario. La difusión es el mecanismo

más importante de movimiento de iones en los procesos de electrodeposición y tiene un papel determinante en las propiedades del material depositado.

Transferencia de electrones

En general, cuando un metal se sumerge en una disolución que contiene sus mismos iones, los átomos de la superficie del metal se hidratan y se disuelven. Así mismo, los iones de la disolución se depositan sobre el metal. El potencial para el que la tasa de estas dos reacciones es la misma se denomina potencial de equilibrio.

Si consideramos una celda general para la cual la semireacción (reducción) es la siguiente:

$$pP + ze^- \leftrightarrow qQ \qquad (I.7)$$

La expresión matemática que relaciona la concentración de especies con el potencial de equilibrio de la reacción de reducción/oxidación se denomina ecuación de Nernst:

$$E = E^o + \frac{RT}{zF} \ln \frac{a_P^p}{a_Q^q} \qquad (I.8)$$

donde R es la constante de los gases (8.3145 J mol^{-1} K^{-1}), T es la temperatura, F es la constante de Faraday (96485.3 C mol^{-1}), z es el número de electrones que se transfieren, E^0 es el potencial estándar (valor del potencial de equilibrio, V, cuando todos los reactivos y productos tienen actividad igual a 1). Para concentraciones diluidas, actividad ≃ concentración, lo que simplifica los cálculos. Experimentalmente no es posible medir valores absolutos de potencial sino que medimos diferencias de potencial. Esto hace que sea necesario disponer de un electrodo de referencia. Los potenciales estándar de electrodo están tabulados para muchas reacciones. En la Tabla I.8. se recogen algunos de los potenciales estándar para las especies utilizadas en esta Tesis Doctoral.

Tabla I.8. Potenciales estándar del electrodo

REACCIÓN	E° / V
$AgCl(s)+e- \leftrightarrow Ag(s) + Cl^-$	0.2223
$2H^+ + 2e^- \leftrightarrow H_2(g)$	0.0000
$2H_2O + 2e^- \leftrightarrow H_2 + 2OH^-$	-0.8277
$Cd^{2+} + 2e^- \leftrightarrow Cd$	-0.4030
$Pb^{2+} + 2e^- \leftrightarrow Pb$	-0.1262

En electrolitos acuosos, la **evolución de hidrógeno** es una de las reacciones parásitas más importantes. El hecho de que haya otra reacción desarrollándose al mismo tiempo que se deposita el metal deseado, implica que la eficiencia de la reacción será más baja, y que al involucrar protones puede haber cambios de pH en las proximidades de la superficie del cátodo, e incluso puede haber un bloqueo parcial de la superficie debido a burbujas de H_2 gas adheridas a las superficie. [86].

Generalmente, el potencial real de un proceso electroquímico difiere del termodinámico (calculado mediante la ecuación de Nerst). Pero para que tenga lugar la reacción deseada a una velocidad apreciable es necesario aplicar un potencial adicional, denominado **sobrepotencial** (η).

$$\eta = E - E_{eq} \qquad (I.9)$$

E=potencial real del electrodo

Este sobrepotencial (η) o polarización de activación es el cambio de potencial en el electrodo debido a la superación de la barrera de energía de la etapa más lenta de la reacción electroquímica o lo que es lo mismo a una inhibición cinética de una etapa de reacción del proceso electroquímico. Por tanto, puede haber diferentes contribuciones de sobrepotencial asociadas con diferentes etapas de reacción: sobrepotencial asociado a la transferencia de carga, a la transferencia de masa, a una reacción precedente, etc. Un caso a considerar especialmente en un proceso electroquímico es cuando aplicamos una corriente próxima al valor teórico de la corriente límite, en ese caso se requiere un gran sobrepotencial para poder reducir las especies, ya que estas no tienen tiempo suficiente de difundir desde el seno de la disolución hasta la superficie del electrodo. Por consiguiente, llamamos

corriente límite a la corriente máxima que puede ser empleada en un proceso, la cual determina la difusión de las especies desde el electrolito hasta el electrodo.

La corriente límite se define como:

$$I_l = nFAD\frac{C_b}{\delta} \qquad \text{(I.110)}$$

donde A es el área del electrodo , D el coeficiente de difusión, C_b es la concentración de la especie en el volumen de la disolución, δ es el espesor de la capa de difusión y *n* el número de electrones intercabiados en la reaccción .

Para finalizar, es necesario considerar que una vez que las especies electroactivas han alcanzado las proximidades del electrodo mediante los procesos de transferencia de masa descritos anteriormente, estas se reducen mediante transferencia electrónica e inmediatamente después los metales formados son adsorbidos en la superficie del electrodo mediante el proceso denominado **ADSORCIÓN.** Esto va a generar una redistribución de cargas electrónicas, modificando la superficie del electrodo. Tanto el proceso de adsorción como la transferencia electrónica pueden ocurrir en orden inverso o simultáneamente como se ha indicado en el apartado I.6.2.

I.7. SUSTANCIAS HÚMICAS (SH)

Las sustancias húmicas son macromoléculas polieletrolíticas de elevado peso molecular. Contienen un esqueleto de carbono con un elevado grado de aromaticidad y con un alto porcentaje de peso molecular incorporado en grupos funcionales, la mayoría de los cuales contienen oxígeno. La composición elemental de la mayoría de las sustancias húmicas está dentro de los siguientes intervalos: C, 45-55%; O, 30-45%; H, 3-6%; N, 1-5%; y S, 0-1%. Las sustancias húmicas son resistentes a la degradación y se forman a partir de la vegetación depositada en el suelo, en sedimentos de los pantanos, turba, carbón, lignito o en casi cualquier lugar donde se hayan deteriorado grandes cantidades de vegetación.

Las sustancias húmicas (SH) se clasifican según su **solubilidad**:

- Ácido fúlvico (AF) es la fracción de la materia orgánica que es soluble en soluciones acuosas que abarcan todos los valores de pH.
- **Ácido húmico (AH)** es insoluble bajo condiciones ácidas pero soluble en álcali.
- Humina (Hu) es insoluble en agua a todos los valores de pH.

Debido a sus propiedades ácido-base, de sorción y para formar complejos, las SH tanto solubles como insolubles tienen un fuerte efecto en la calidad del agua. Por ejemplo, el AH permanece insoluble y afecta la calidad del agua a través del intercambio de especies, como cationes o materiales orgánicos con el agua [14]. El carácter ácido del material húmico está asociado en gran parte con los grupos carboxilato y fenólicos. El primero tiene valor de pKa en el rango entre 2.5 y 5 dependiendo de la proximidad de los átomos electronegativos. En el caso de los grupos fenólicos, estos tienen valores de pKa tales que son ácidos suficientemente fuertes que permanecen sustancialmente desprotonados cuando se disuelven en agua.

Reactividad de las SH en el agua

La presencia de SH en las aguas naturales genera un color amarillento. El ácido húmico es un coloide complejo orgánico relativamente estable, difícil de degradarse en condiciones naturales. La materia orgánica disuelta puede formar complejos con metales pesados, dar lugar a compuestos organoclorados potencialmente tóxicos, como los trihalometanos, los ácidos cloroacéticos, las cloroacetonas y los haloacetonitrilos, también puede acumular microcontaminantes orgánicos, tales como pesticidas, entre otros.

Por ello, en este trabajo, se va a estudiar la interacción del anión humato (sal sódica de ácido húmico) con la HT debido a su carácter intercambiador y su posterior utilización como adsorbente de cationes metálicos. Las SH pueden formar fuertemente complejos con iones metálicos y por consiguiente, modificar su retención, adsorción, migración y biodisponibilidad en el medio ambiente [87-92].

I.8. HIDRÓXIDOS DOBLES LAMINARES (HDLs)

I.8.1. Antecedentes históricos

Los hidróxidos dobles laminares (HDLs) también son denominados compuestos tipo hidrotalcita (HT), debido a su estructura análoga con la hidrotalcita, la cual es el mineral más representativo del grupo de las arcillas aniónicas. La HT es un hidroxicarbonato de magnesio y aluminio y se encuentra en la naturaleza en forma de láminas o como masas fibrosas. La primera fórmula exacta de la hidrotalcita, $Mg_6Al_2(OH)_{16}\cdot(CO_3)\cdot 4H_2O$ fue presentada por E. Manasse en 1915 [93]. En 1942, Feitknecht sintetizó una gran cantidad de compuestos con estructura de hidrotalcita y concluyó que estos compuestos estaban constituidos por una lámina de hidróxidos de un catión intercalada con otra lámina del otro catión [94, 95]. Posteriormente, mediante análisis de DRX llevados a cabo por Allmann y Taylor se demostró que los cationes metálicos estaban situados en la misma lámina de hidróxidos, mientras que los iones carbonato y las moléculas de agua estaban localizados en la interlámina [96, 97].

I.8.2. Estructura

La estructura de los HDLs está basada en la brucita, $Mg(OH)_2$, Figura I.12. Estos compuestos cristalizan con una estructura tipo CdI_2, presentando un empaquetamiento hexagonal compacto de iones hidroxilo con iones Mg^{2+} ocupando la totalidad de los huecos octaédricos en láminas alternadas.

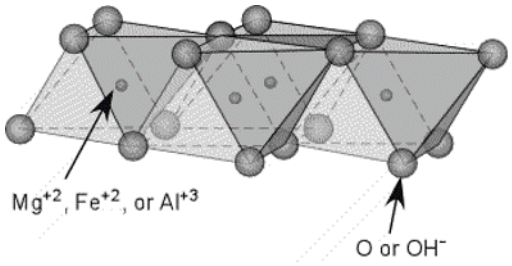

Figura I.12. Estructura tipo brucita [98].

En la hidrotalcita algunos de los cationes de Mg^{2+}, coordinados octaédricamente por grupos hidroxilos en la estructura laminar, son sustituidos isomorficamente por Al^{+3} lo que da lugar a un exceso de carga positiva laminar. Los aniones carbonatos son intercalados entre las láminas para así mantener la

electroneutralidad. Las moléculas de agua unidas mediante enlaces de hidrógeno a las láminas pueden ocupar el espacio restante en la región interlaminar, Figura I.13. Las moléculas de agua se encuentran en los sitios no ocupados por los aniones. No obstante, también hay moléculas de agua adsorbidas en la superficie de la HT. El contenido en agua va a depender de la naturaleza y del tamaño del anión y de las condiciones de lavado y secado.

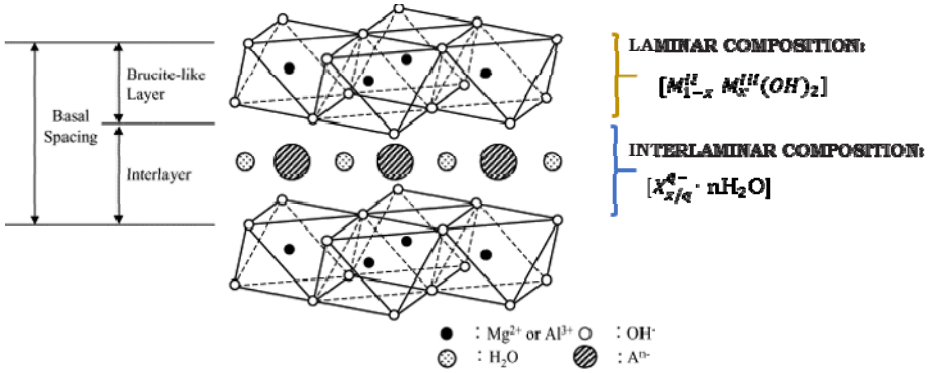

Figura I.13. Representación esquemática de la estructura HT

La fórmula general de otros compuestos de la familia, basados en la combinación de cationes metálicos divalentes y trivalentes, pueden ser escritos como $[M^{II}_{1-x}\ M^{III}_{x}(OH)_2]^{x+}\ [X^{q-}_{x/q}\cdot\ nH_2O]$, donde $[M^{II}_{1-x}\ M^{III}_{x}(OH)_2]^{x+}$ representa la composición laminar y $[X^{q-}_{x/q}\cdot\ nH_2O]$ la composición interlaminar. Las láminas de brucita en el HDL pueden apilarse de diferente manera, dando lugar a diferentes politipos, siendo ABC los sitios de los hidróxidos en el empaquetamiento. Esto podría dar lugar a la secuencia BC-CA-AB-BC, es decir tres láminas hidroxiladas en la celda unidad (grupo espacial 3R) o BC-CB-BC, con dos láminas en la celda unidad con simetría hexagonal (grupo espacial 2H). La HT cristaliza en una simetría 3R romboédrica, siendo los parámetros de la celda unidad a y c= 3c´donde c´ es el espesor de una lámina y una interlámina. Esta simetría ha sido encontrada principalmente en la naturaleza, mientras que el politipo hexagonal podría ser una forma de alta temperatura de la simetría romboédrica [99]. Mediante XAFS, se observó que muchos metales de la primera serie de transición pueden ser incorporados en el interior de la lámina de hidroxilo de la HT [100]. Por ello, la formación de precipitados secundarios mixtos de metal-

Al puede ser un mecanismo de reacción posible para la adsorción de metales de transición en arcillas aniónicas.

La gran versatilidad de estos materiales se debe a diversos parámetros tales como, composición química de las láminas, relación M^{2+}/M^{3+} y naturaleza de anión interlaminar.

I.8.2.a. Composición química de las láminas

Los iones M(II) y M(III) pueden ser fácilmente alojados en los huecos octaédricos de las láminas de brucita, siempre y cuando el radio iónico de ambos no sea muy diferente, es decir las sustituciones isomórficas quedan regidas por consideraciones de tamaño de radio iónico. La estructura HDL no es estable con cationes divalentes de radio iónico menor de 0.06nm, puesto que son demasiados pequeños para la coordinación octaédrica. Todos los elementos trivalentes a excepción del V y el Ti con radios atómicos en un rango de 0.5-0.8Å forman compuestos tipo HT. Algunos de los minerales más representativos con estructura tipo HT se muestran en la Tabla I.9. En el caso del Cu solo forma HDL en presencia de otro catión divalente (Be, Mg, Ni, Co, Zn, Fe, Mn, Cd y Ca), siempre y cuando la relación $Cu^{2+}/M(II)$ sea menor o igual a l. Esto es debido al efecto Jahn Teller que presenta el Cu^{2+} [99]. También, otra clase de HDL compuestos de cationes monovalentes y trivalentes ha sido sintetizada como por ejemplo $[LiAl_2(OH)_6]^+A^-$ [101-104].

Tabla I.9. Algunos minerales con estructura tipo HT

M^{2+}	M^{3+}	FÓRMULA	NOMBRE
Mg	Al	$Mg_6Al_2(OH)_{16}\cdot(CO3)\cdot4H2O$	Hidrotalcita
Mg	Fe	$Mg_6Fe_2(OH)_{16}\cdot(CO_3)\cdot4H_2O$	Pyroaurita
Mg	Cr	$Mg_6Cr_2(OH)_{16}\cdot(CO_3)\cdot4H_2O$	Stichtita
Ni	Fe	$Ni_6Fe_2(OH)_{16}\cdot(CO_3)\cdot4H_2O$	Reevesita
Ni, Zn	Al	$(Ni,Zn)_6Al_2(OH)_{16}\cdot(CO_3)\cdot4H_2O$	Eardlegita
Mg	Ni, Fe	$Mg_6(Ni,Fe)_2(OH)_{16}\cdot(CO_3)\cdot4H_2O$	----------
Ni	Al	$Ni_6Al_2(OH)_2\cdot(CO_3)_{16}\cdot4H_2O$	Takovita
Mg	Mn	$Mg_6Mn_2(OH)_2\cdot(CO_3)_{16}\cdot4H_2O$	Desautelsita

I.8.2.b. Relación M^{2+}/M^{3+}

En muchos casos la relación M(II)/M(III) podría variar de acuerdo a las condiciones de coprecipitación y concentraciones iniciales de las sales [105]. La fracción x del catión trivalente determina la carga electrostática de las láminas. Muchos estudios han demostrado que es posible obtener HT puras para $0.1< x <$ 0.33. Para valores mayores de x se incrementa el número de octaedros de Al vecinos, lo cual lleva a la formación de $Al(OH)_3$, mientras que para valores bajos de x la alta densidad de octaedros de Mg actúa como núcleo para la formación de $Mg(OH)_2$.

I.8.2.c. Naturaleza de anión interlaminar

Para la preparación de los HDLs una amplia variedad de aniones tanto orgánicos como inorgánicos pueden ser usados:

Haluros: F^-, Cl^-, Br^-, I^- [106].

Oxoaniones no metálicos: BO_3^{3-},CO_3^{2-}, NO_3^-, HPO_4^{2-}, SO_4^{2-}, ClO_4^-, AsO_4^{3-} SeO_4^{2-}, BrO_4^-, etc. [107].

Oxoaniones metálicos: VO_4^{3-}, CrO_4^{2-}, MnO_4^-, $V_{10}O_{28}^{6-}$, $Cr_2O_7^{2-}$, $Mo_7O_{24}^{6-}$, $PW_{12}O_{40}^{3-}$, etc. [105].

Ácidos Orgánicos: ácido adípico, succínico, oxálico, malónico, sebático [108], tetradecanodioíco, dodecilsulfónico [109], dietilentriaminopentaacético [110], etc.

Polímeros aniónicos: PSS, PVS, etc. [111].

Biomoléculas: ADN, aminoácidos [112], polisacáridos, etc.

I.8.3. Métodos de síntesis

Existen diversos métodos que permiten la preparación de estos compuestos laminares adecuados según sus aplicaciones. Los tres más utilizados son:

I.8.3.a. Coprecipitación

Es el método más simple y más usado de los conocidos [113]. Se usan dos tipos de condiciones de coprecipitación:

Coprecipitación a <u>baja sobresaturación</u>: se basa en la adición de las sales metálicas (M^{2+} y M^{3+}) lentamente en el reactor que contiene la disolución acuosa del anión

interlaminar deseado. Al mismo tiempo una disolución de un álcali se añade para mantener el pH idóneo para la coprecipitación de las dos sales metálicas.

Coprecipitación a alta sobresaturación: requiere la adición de la disolución de las sales mixtas a una disolución alcalina que contiene el anión interlaminar. Generalmente, este método da lugar a compuestos menos cristalinos comparado con el método a baja sobresaturación, debido a la formación de un gran número de núcleos de cristalización.

Tras la síntesis se suele usar un tratamiento hidrotermal para aumentar la cristalinidad de estos materiales. Cuando se pretende introducir aniones diferentes al CO_3^{2-} hay que trabajar en atmosfera inerte (nitrógeno) para evitar la presencia de CO_2 en la disolución. El carbonato tiene mucha afinidad hacia la interlamina del HDL y compite con los demás aniones o moléculas en la región interlaminar, por ello es común también usar agua descarbonatada. Este procedimiento permite la síntesis de un gran número de HDLs con distintos aniones interlaminares como precursores de reacciones posteriores como por ejemplo intercambio aniónico. Crepaldi y col. [114] demostraron que los materiales preparados por este método mostraron propiedades interesantes para aplicaciones tecnológicas, como alta cristalinidad, tamaño de partícula pequeño, alta superficie específica y un valor promedio alto de diámetro de poro.

I.8.3.b. Método de intercambio iónico

Este procedimiento está basado en el intercambio de un anión presente en disolución en una HT con un anión fácilmente intercambiable (Cl^-, NO_3^-). Este intercambio va a depender principalmente de las interacciones electrostáticas entre las cargas positivas de las láminas hidroxiladas y los aniones intercambiadores y de las constantes de equilibrio de la reacción. El orden de preferencia por aniones inorgánicos sencillos (o capacidad para ser retenidos entre las láminas) en orden creciente es el siguiente [115, 105].

$$NO_3^- < Br^- < Cl^- < F^- < OH^- < MoO_4^{2-} < SO_4^{2-} < CrO_4^{2-} < HAsO_4^{2-} , HPO_4^{2-} < , CO_3^{2-}$$

Este método de síntesis es especialmente útil cuando el catión divalente o los aniones involucrados son inestables en disoluciones alcalinas, o cuando la reacción entre los cationes metálicos y el anión entrante es más favorable a un pH más bajo.

Por este método es posible modificar la HT mediante el intercambio de un gran número de aniones orgánicos e inorgánicos [116].

I.8.3.c. Método de reconstrucción

Consiste en la deshidratación reversible y la eliminación de los aniones interlaminares y grupos hidroxílicos que experimentan las HTs cuando se calcinan a una temperatura de 400-600ºC dando lugar a óxidos metálicos. Es decir, a bajas temperaturas la HT pierde el agua fisisorbida y posteriormente el agua interlaminar (hasta 250ºC), entre 250ºC-500ºC la estructura laminar colapsa y el HDL se convierte en un óxido mixto. Este óxido mixto formado, se puede rehidratar en una disolución acuosa con aniones afines a la interlámina, recuperándose la estructura tipo HT. Esta propiedad es conocida como "efecto memoria" [117]. La facilidad de reconstrucción de la HT va a depender de la naturaleza de los cationes metálicos que constituyen las láminas. Por el contrario, si seguimos calcinando el óxido mixto formado a temperaturas alrededor de los 900ºC tiene lugar la formación de la espinela que ya es un proceso irreversible, Figura I.14.

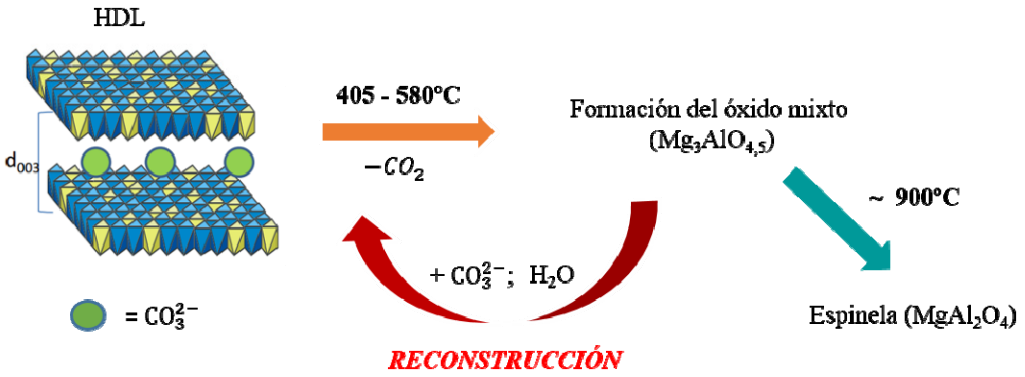

Figura I.14. Proceso de calcinación y reconstrucción de un LDH

Éste método es adecuado para la preparación de HDLs híbridos con aniones orgánicos de gran tamaño [118, 119].

I.8.4. Propiedades de los HDLs

La capacidad de los HDLs para actuar como adsorbente se basa en sus propiedades, entre las que destacan:

- Capacidad de cambio iónico debido a la carga laminar y al hinchamiento de su espaciado interlaminar. Por ello, estos compuestos tienen un gran interés en aplicaciones de descontaminación. Esta propiedad se representa mediante la siguiente reacción:

  $[M^{II}_{1-x}\ M^{III}_{x}(OH)_2\ X^{q-}_{x/q}]\cdot\ nH_2O$ + (x/q)Y^{q-} →$[M^{II}_{1-x}\ M^{III}_{x}(OH)_2\ Y^{q-}_{x/q}]\cdot\ nH_2O$ + (x/q)X^{q-}

- "Efecto memoria", basado en la recuperación de la estructura laminar por reconstrucción de la HT calcinada (oxido mixto) en presencia de agua y aniones.

  $[M^{II}_{1-x}\ M^{III}_{x}(OH)_2\ X^{q-}_{x/q}]\cdot\ nH_2O \xrightarrow{500ºC} [M^{II}_{1-x}\ M^{III}_{x}\ O_{1+x/2}] + (1+\frac{x}{2}+\text{n})\ H_2O$

  $[M^{II}_{1-x}\ M^{III}_{x}\ O_{1+x/2}] + \frac{x}{q}X^{q-} + (1+\frac{x}{2}+\text{n})\ H_2O \rightarrow [M^{II}_{1-x}\ M^{III}_{x}(OH)_2\ X^{q-}_{x/q}]\cdot\ nH_2O + xOH^-$

  De esta manera se pueden incorporar en su estructura los aniones contaminantes de agua. Además, la calcinación permite el reciclado y reutilización del adsorbente [120, 121].

- Capacidad de funcionalización, lo que permite modificar las propiedades de adsorción. Un gran número de aniones orgánicos han sido intercalados, permitiendo el cambio del espaciado interlaminar de hidrofílico a hidrofóbico. De esta forma, se pueden adsorber no solo los contaminantes hidrofílicos sino también los hidrofóbicos [122, 123].
- Propiedades tampón, es decir estos compuestos tienden a mantener el pH de la disolución.
- "Wheathering reactions" en medio ácido que pueden ser escritas de la siguiente manera:

  $[M^{II}_{1-x}\ M^{III}_{x}(OH)_2\ X^{q-}_{x/q}]\cdot\ nH_2O + 2H^+ \rightarrow$ (1-x) M^{II} + xM^{III} + (2+n)H_2O+ $\frac{x}{q}X^{q-}$

  Estas reacciones presentan gran importancia para su aplicación como adsorbentes de metales pesados. El incremento de pH que se produce lleva

a la eliminación de metales pesados mediante la precipitación de sus hidróxidos, ya sea como parte de la estructura de HDL o en una fase separada [124, 125].

Otras propiedades interesantes son:

- La estabilidad térmica de los HDLs fue ampliamente investigada ya que los productos de descomposición térmica de estos compuestos tienen propiedades interesantes como catalizadores. El comportamiento durante la descomposición térmica es prácticamente similar en todos los casos, hasta 250ºC se libera agua interlaminar, seguido por la deshidroxilación de las láminas, y la descomposición o eliminación de los aniones interlaminares ocurre a temperaturas más altas [107]. Sin embargo, la descomposición térmica en los correspondientes óxidos se afecta por la naturaleza del anión interlaminar, lo cual va a determinar la mayor o menor estabilidad térmica [126, 127].
- Estabilidad química, la cual es importante para muchas aplicaciones prácticas, como por ejemplo, sumidero de iones metálicos radioactivos [128]. En evaluaciones geoquímicas es importante la estabilidad del HDL en términos de solubilidad [129, 130].

I.8.5. Aplicaciones

Entre las múltiples aplicaciones de los hidróxidos dobles laminares cabe mencionar algunas de las más importantes:

- **Catálisis**: Se utilizan en reacciones catalíticas de síntesis orgánica, como por ejemplo polimerización de etileno [131], evolución de oxígeno [132], hidrogenación [133], epoxidación de estireno [134], condensación [135], hidroxilación de fenoles [136], etc.
- **Farmacia:** Principalmente como antiácido [137], para combatir la "hiperfosfatemia" [138], como adsorbente de fosfato que se libera en el tracto intestinal, como intercambiadores de aniones tales como medicamentos, biomoléculas [139, 140], soportes de fármacos para la liberación posterior gradual dentro del organismo, como por ejemplo antibióticos [141, 142], antiinflamatorios como el ibuprofeno [143, 144], el diclorofenac [145, 146], entre otros.

- **Descontaminación:** Inmovilizador de isótopos radioactivos [147], reducción de gases de efecto invernadero [148, 149] y en reducción catalítica de nitratos en agua [150]. En adsorción, es usado como adsorbente para la eliminación tanto de contaminantes inorgánicos (aniones como fosfatos, arseniatos, seleniatos, antimoniatos, haluros, etc. y metales pesados) [151-154, 110] como orgánicos, entre ellos pesticidas polares [120] y apolares [155, 156], surfactantes [157], ácidos húmicos [158, 159], colorantes [160, 119]. Finalmente, su uso como soportes en formulaciones para la liberación lenta de herbicidas ha sido ampliamente estudiado como objetivo de minimizar el impacto ambiental [161, 156].
- **Industria:** Retardante de llama [162] estabilizadores de polímeros, etc. [163, 164].
- **Fotoquímica:** Diferentes HTs y reacciones se han utilizado en esta área como por ejemplo, la fotodimerización de especies carboxilato insaturadas intercaladas [165], fotoisomerización de moléculas fotocrómicas [166, 167], fotoestabilidad y termoestabilidad de diversos pigmentos aniónicos tras su intercalación [168], etc.
- **Electroquímica:** Utilización como electrodos modificados, desarrollo de sensores de Hidrógeno [169], material anódico en baterías secundarias Zn-Ni [170, 13], material para electrolitos sólidos [171].
- **Otras:** Cosmética [143], aplicación como materiales magnéticos [172, 173], en construcción como materiales para la intercalación de mezclas orgánicas para la liberación controlada de hormigón [174], intercalación de otras moléculas biológicamente interesantes como nucleótidos [175, 176], vitaminas [177] o péptidos [178, 112], etc.

Referencias

[1] R. Carabias-Marínez, E. Rodríguez-Gonzalo, M.E. Fernández-Laespada, L. Calvo-Seronero, F.J. Sánchez-San Román, *Water Res*. 37 (2003) 928-938.

[2] M.J. Sánchez-Martin, M. Sánchez-Camazano, L.F. Lorenzo, *Agrochimica* 48 (2003) 192-203.

[3] A. Hildebrandt, S. Lacorte, D. Barceló, *Anal. Bioanal. Chem.* 387 (2007)1459-1468.

[4] K. Goh, T. Lim, Z. Dong, *Water Res*. 42 (2008) 1343-1368.

[5] B. J. Kasprzyk-Hordern, *Adv. Colloid Interfac*. 110 (2004) 19-48.

[6] P. Misaelides, *Micropor. Mesopor. Mat.* 144 (2011) 15-18.

[7] M. Cruz-Guzmán, R. Celis, R, M.C. Hermosín, W. Koskinen, J. Cornejo, *J. Agr. Food Chem*. 53 (2005) 7502-7511.

[8] J. Cornejo, R. Celis, I. Pavlovic, M.A. Ulibarri, *Clay Miner.* 43 (2008) 155–176.

[9] B. Gámiz, R. Celis, L. Cox, M.C. Hermosín, J. Cornejo, *Sci. Total Environ.* 429 (2012) 292–299.

[10] V. Rives, 2001. "Layered Double Hydroxides: Present and Future", Ed. Nova Science Publishers, Inc., New York.

[11] E. Cardoso, J.B. Valim, *J. Phys. Chem. Solids* 67 (2006) 987-993.

[12] F. Li, X. Duan, *Struct. Bond*. 119 (2006) 193-223.

[13] T. Wang, Z. Yang, B. Yang, R. Wang, J. Huang, *J. Power Sources* 257 (2014) 174-180.

[14] E.S. Manahan, 2007. "Introducción a la química ambiental", Ed. Reverté, Unam.

[15]http://water.epa.gov/infrastructure/drinkingwater/sourcewater/protection/

[16] http://www.who.int/water_sanitation_health/

[17]http://water.epa.gov/infrastructure/drinkingwater/sourcewater/protection/

[18] M.B. Green, 1984. "PLAGUICIDAS, BENEFICIOSOS O PERJUDICIALES, LOS", Ed. Academia SL.

[19] http://www.fao.org/docrep/

[20] R. Cervantes, 2008. "Manual de Diagnóstico y Tratamiento de Prevención de Intoxicaciones Agudas por Plaguicidas", Fundación Plagbol.

[21] J. L. Tadeo, C. Sánchez-Brunete, L. González, 2008. Pesticides: Classification and Properties, In: J.L. Tadeo, (Ed.), Analyses of Pesticides in Food and Environmental Samples, CRC Press.

[22] http://www.juntadeandalucia.es/agriculturaypesca/

[23] http://www.igme.es/

[24] http://www2.inecc.gob.mx/sistemas/plaguicidas/

[25]R. K. Gautam, S.K. Sharma, S. Mahiya, M.C. Chattopadhyaya, 2015. Contamination of Heavy Metals in Aquatic Media: Transport, Toxicity and Technologies for Remediation, In: S.K. Sharma, (Ed.), Heavy Metals in Water: Presence, Removal and Safety, Royal Society of Chemistry.

[26] K. Ikehata, Y. Jin, N. Maleky, A. Lin, 2015. Heavy Metal Pollution in Water Resources in China—Occurrences and Public Health Implications, In: S.K. Sharma, (Ed.), Heavy Metals in Water: Presence, Removal and Safety, Royal Society of Chemistry.

[27] J.P. Allen, I.G. Torres, 1991. Physical separation techniques for contaminated sediment, In: N.N. Li, (Ed.), Recent Developments in Separation Science, CRC Press.

[28] M.A. Hashim, S. Mukhopadhyay, J. N. Sahu, B. Sengupta, *J. Environ. Manage*. 92 (2011) 2355-2388.

[29] A. Jeske, B. Gworek, *J. Hazard. Mat.* 30 (2012) 315-322.

[30] Y. Li, Q. Yue, B. Gao, *J. Hazard. Mat.* 178 (2010) 465-461.

[31] M. McKay, M. S. Otterburn, A.G. Sweeney, *Water Res*. 14 (1980) 15-20.

[32] X. Huang, N-y. Gao, Q-l. Zhang, *J. Environ. Sci*. 19 (2007) 1287-1292.

[33] G. Lofrano, M. Carotenuto, R. K. Gautam, G. Mahesh, M.C. Chattopadhyaya, 2015. Heavy Metals in Tannery Wastewater and Sludge: Environmental Concerns and Future Challenges, In: S.K. Sharma, (Ed.), Heavy Metals in Water: Presence, Removal and Safety, Royal Society of Chemistry.

[34] K.G. Karthikeyan, H.A Elliott, F.S. Cannon, *Environ. Sci. Technol*. 31 (1997) 2721–2725.

[35] J.B. Brower, R.L. Ryan, M. Pazirandeh, *Environ. Sci. Technol*. 31 (1997) 2910-2914.

[36] C. A. Basha, M. Somasundaram, T. Kannadasan, C.W. Lee, *Chem. Eng. J.* 171 (2011) 563-571**.**

[37] G. Kim, E. T. Igunnu, G.Z. Chen, *Chem. Eng. J.* 244 (2014) 411-421.

[38] M.A. Barakat, R. Kumar, 2015. Modified and New Adsorbents for Removal of Heavy Metals from Wastewater, In: S.K. Sharma, (Ed.), Heavy Metals in Water: Presence, Removal and Safety, Royal Society of Chemistry.

[39] D. L. Sparks, *Elements* 1 (2005) 193-197.

[40] T. A. Kurniawan, G.Y.S. Chan, W-H. Loa, S. Babel, *Chem. Eng. J.* 118 (2006) 83-98.

[41] The Council of the European Union, Council Directive 98/83/EC of 3 November 1998 on the Quality of Water intended for Human Consumption. Official Journal of the European Communities (1998).

[42] United States Environmental Protection Agency, National Primary Drinking Water Regulations. Safe Drinking Water Act (2009).

[43] World Health Organization, 2011. "Guidelines for Drinking-Water Quality", 4th ed.

[44]http://www.atsdr.cdc.gov/SPL/

[45] http://www.epa.gov/superfund/policy/cercla.htm

[46] J. Mallevialle, I. H. Suffet, U.S. Chan, 1992. "Influence and Removal of Organics in Drinking Water", Lewis Publishers, Boca Raton.

[47] K. Chojnacka, *Pol. J. Environ. Stud*. 15 (2006) 845-852.

[48] Y. Wu, T. Li, L. Yang, *Bioresour. Technol*. 107 (2012) 10-18.

[49] M. Gräfe , M. Nachtegaal, D. L. Sparks, *Environ. Sci. Technol*. 38 (2004) 6561–6570.

[50] B. Bolto, D. Dixon, R. Eldridge, S. King, K. Linge, *Water Res.* 36 (2002) 5057–5065.

[51] C. Quintelas, B. Fonseca, B. Silva, H. Figueiredo, T. Tavares, *Bioresour. Technol.* 100 (2009) 220-226.

[52] M. Tsezos, E. Remoudaki, V. Angelatou, *Int. Biodeter. Biodegr*. 35 (1995) 129-153.

[53] J. Fang, B. Gao, Y. Sun, M. Zhang, S.K. Sharma, 2015. Use of Industrial and Agricultural Waste in Removal of Heavy Metals Present in Water, In: S.K. Sharma, (Ed.), Heavy Metals in Water: Presence, Removal and Safety, Royal Society of Chemistry.

[54] C. P. Huang, C.P. Huang, A. L. Morehart. *Water. Res*. 25 (1991) 1365-1375.

[55] X. Liang, Y. Zang, Y. Xu, X. Tan, W. Hou, L. Wang, Y. Sun, *Colloids Surf. A.* 433 (2013) 122–131.

[56] G. McKay, S.J. Allen, I.F. McConvey, *J. Colloid Interface Sci.* 80 (1981) 323-339.

[57] M.S. Chiou, H.Y. Li, *Chemosphere* 50 (2003) 1095-1105.

[58] M.S. Chiou, W.S. Kuo, H.Y. Li, *J. Environ. Sci. Health A. Toxic/ Hazard. Substances Environ. Eng*. 38 (2003) 2621-2631.

[59] R. Celis, W.C. Koskinen, *J. Agric .Food Chem*. 47 (1999) 782-790.

[60] S.Z. Lagergren, *Handlingar* 24 (1898) 1-39.

[61] Y-S. Ho, G. Mckay, *Trans. Chem. Eng*. 76 (1998) 183-191.

[62] W.J. Weber, J.C. Morris, *J. Sanitary Eng. Div. Am. Soc. Civ. Eng.* 89 (1963) 31-59.

[63] G. Crini, P-M. Badot, *Prog. Polym. Sci.* 33 (2008) 399-447.

[64]F. Reanult, N. Morin-Crini, F. Gimbert, P-M. Badot, G. Crini, *Bioresource Tecnol.* 99 (2010) 7573-7586.

[65] C. H. Giles, T. H. MacEwan, S.N. Nakhwa, D. Smith, *J. Chem. Soc.* (1960) 3973-3993.

[66] I. Langmuir, *J. Am. Chem. Soc*. 38 (1916) 2221–2295.

[67] H.M.F. Freundlich, *Z. Phys. Chem*. 57 (1906) 385-470.

[68] R.K. Gautam, S. K. Sharma, M.C. Chattopadhyaya, 2015. Functionalized Magnetic Nanoparticles for Heavy Metals Removal from Aqueous Solutions, In: S.K. Sharma, (Ed.), Heavy Metals in Water: Presence, Removal and Safety, Royal Society of Chemistry.

[69] P. Misaelides, *Micropor. Mesopor. Mat.* 144 (2011) 15-18.

[70] E. Padilla-Ortega, R. Leyva-Ramos, J.V. Flores-Cano, *Chem. Eng. J.* 225 (2013) 535–546.

[71] W.S. Wan Ngah, I.M. Isa, *J. Appl. Polym. Sci*. 67 (1998) 1067-1070.

[72] S.M. Lee, A.P. Davis*, Water Res*. 35 (2001) 534-540.

[73] S.K. Srivastava, A.K. Singh, A. Sharma, *Environ. Technol.* 15 (1994) 353-361.

[74] M.S. Al-Harahsheha, K. Al-Zboonb, L. Al-Makhadmehc, M. Hararahc, M. Mahasneh, *J. Environ. Chem. Eng.* 3 (2015) 1669–1677.

[75] M. Hua, S. Zhang, B. Pan, W. Zhang, L. Lv, Q. Zhang, *J. Hazard. Mat.* 211-212 (2012) 317-331.

[76] S. Babel, T. A. Kurniawan, *J. Hazard. Mat.* B97 (2003) 219-243.

[77] G. San Miguel, S. D. Lambert, N. J.D. Graham*, J. Chem. Technol. Biotechnol.* 81(2006) 1685–1696.

[78] R. Rojas, E. Vanderlinden, J. Morillo, J. Usero, H. El Bakouri, *Sci. Total Environ*. 488-489 (2014) 124-135.

[79] R.T. Carneiro, T.B. Taketa, R.J. Gomes Neto, J.L. Oliveira, E.V. Campos, M.A. de Moraes, C.M. da Silva, M.M. Beppu, L.F. Fraceto, *J. Environ. Manage.* 151 (2015) 353-360.

[80] T. De Wilde, P. Spanoghe, J. Ryckeboer, P. Jaeken, D. Springael, *Chemosphere* 75 (2009) 100–108.

[81] J. M. Costa, 1982. "Fundamentos de Electródica. Cinética Electroquímica y sus Aplicaciones", Ed. Alhambra S.A., Madrid.

[82] E. Julve, 2013. "Recubrimientos. La electrodeposición de metales industriales en el actual mundo tencnológico", Facultad de Ciencias, Universidad Autónoma de Barcelona.

[83] H. Martín Hernández, 2001. Tesis Doctoral, Universidad de la Laguna.

[84] A. Llavona Serrano, 2013. Tesis Doctoral, Universidad Complutense de Madrid.

[85] A.J. Bard, L.R. Faulkner, 2001. "Electrochemical Methods: Fundamentals and Applications", 2nd ed., Wiley, New York.

[86] J. O´M. Bockris, S. U. M. Khan, 1993. "Surface electrochemistry: a molecular level approach", Plenum Press, New York.

[87]D. Xu, X.K. Wang, C.L. Chen, X. Zhou, X.L. Tan, *Radiochim. Acta* 94 (2006) 429-434.

[88] D. Xu, X. Zhou, X.K. Wang, *Appl. Clay Sci*. 39 (2008) 133-141.

[89] X. Wang, D. Xu, C. Chen, X. Tan, X. Zhou, A. Ren, C. Chen, *Appl. Radiat. Isot*. 64 (2006) 414–421.

[90]C.L. Chen, X.K. Wang, *Appl. Geochem.* 22 (2007) 436–445.

[91] X.L. Tan, P.P. Chang, Q.H. Fan, X. Zhou, S.M. Yu, W.S. Wu, X.K. Wang, *Colloids and Surfaces A: Physicochem. Eng. Aspects* 328 (2008) 8–14.

[92] S. Wang, J. Hu, J. Li, Y. Dong, *J. Hazard. Mat*. 167 (2009) 44–51.

[93] E. Manasse, *Atti Soc. Toscana Sc. Nat., Proc. Verb.* 24 (1915) 92.

[94] W. Feitknecht, *Helv*. *Chim. Acta* 25 (1942) 131-137.

[95] W. Feitknecht, *Helv*. *Chim. Acta* 25 (1942) 555-569.

[96] R. Allmann, *Acta Cryst.* B24 (1968) 972-977.

[97] HF.W. Taylor, *Miner. Mag.* 37 (1696) 338-342.

[98]C. Klein, C. Hurbut, 1999. "Manual of Mineralogy (after James D. Dana) Twenty-First Edition", J. Wiley & Sons, New York.

[99]F. Cavani, F. Trifiró, A. Vaccari, *Catal. Today* 11 (1991)173-301.

[100]A.M. Scheidegger, D.G. Strawn, M. Geraldine, G. M. Lamble, D.L. Sparks, *Geochim. Cosmochim. Acta* 62 (1998) 2233.

[101] A.V. Besserguenev, A.M. Fogg, R.J. Francais, S. J. Price, D. O'Hare, V.P. Isupov, B.P. Tolochko, *Chem. Mater*. 9 (1997) 241–247.

[102] M. Nayak, T.R.N. Kutty, V. Jayaraman, G. Periaswamy, *J. Mater. Chem*. 7 (1997) 2131–2137.

[103] G.R. Williams, A.J. Norquist, D. O´ Hare, *Chem. Mater.* 16 (2004) 975–981.

[104] N.S. Kottegoda, W. Jones, *Macromolec. Symp.* 222 (2005) 65–71.

[105] C. Forano, T. Hibino, F. Leroux, C. Taviot-Gheho, 2006. LAYERED DOUBLE HYDROXIDES, In: F. Bergaya, B.K.G. Theng, G. Lagaly, (Eds.), Handbook of Clay Science, Development in Clay Science.

[106] S. Mandal, S. Tripathy, T. Padhi, M. K. Sahu, R. K. Patel, *J. Environ Sci.* 25 (2013) 993-1000.

[107] K-H. Goh, T-T. Lim, Z. Dong, *Water Res.* 42 (2008) 1343-1368.

[108] S. Miyata, T. Kumura*, Chem.Letters* 8 (1973) 843-848.

[109] R. Otero, J.M. Fernandez, M.A. Ulibarri, R. Celis, F. Bruna, *Appl. Clay Sci*. 65–66 (2012) 72–79.

[110] I. Pavlovic, M.R. Pérez, C. Barriga, M.A. Ulibarri, *Appl. Clay Sci*. 43 (2009) 125–129.

[111] O.C. Wilson, T. Olorunyolemi, A. Jaworski, L. Borum, D. Young, A. Siriwat, E. Dickens, C. Oriakhi, M. Lerner, *Appl. Clay Sci.* 15 (1999) 265–279.

[112] H. Nakayama, N. Wada, M. Tsuhako, *Int. J. Pharm.* 269 (2004) 469–478.

[113] W.T. Reichle, *Solid State Ionics* 22 (1986) 135-141.

[114] E.L. Crepaldi, P.C. Pavan, J.B. Valim, *J. Brazil. Chem. Soc.* 11 (2000) 64-70.

[115] S. Miyata, *Clay. Clay. Miner.* 31 (1983) 305-311.

[116] V. Rives, M.A. Ulibarri, *Coordin. Chem. Rev*. 181 (1999) 61-120.

[117] S. Miyata, *Clay. Clay. Miner.* 28 (1980) 50-56.

[118] L. Latterini, F. Elisei, G. G. Aloisi, U. Constantino, M. Nocchetti, *Phys. Chem. Chem. Phys.* 4 (2002) 2792-2798.

[119] R. Extremera, I. Pavlovic, M.R. Pérez, C. Barriga, *Chem. Eng. J.* 213 (2012) 392-400.

[120] I. Pavlovic, C. Barriga, M.C. Hermosín, J. Cornejo, M.A. Ulibarri, *Appl. Clay Sci.* 30 (2005) 125–133.

[121] C. Barriga, M. Gaitán, I. Pavlovic, M.A. Ulibarri, M.C. Hermosin, J. Cornejo, *J. Mat. Chem.* 12 (2002) 1027-1034.

[122] P. Wu, T. Wu, W. He, L. Sun, Y. Li, D. Sun, *Colloid. Surface. A*. 436 (2013) 726-731.

[123] G. Zhang, T. Wu, Y. Li, X. Huang, Y. Wang, G. Wang, *Chem. Eng. J*. 191 (2012) 306–313.

[124] R. Rojas, M.C. Palena, A.F. Jimenez-Kairuz, R.H. Manzo, C.E. Giacomelli, *Appl. Clay Sci*. 62-63 (2012) 15-20.

[125] M. Park, C. L. Choi, Y.J. Seo, S.K. Yeo, J. Choi, S. Komarneni, J.H. Lee, *Appl. Clay Sci.* 37 (2007) 143-148.

[126] Z.P. Xu, H.C. Zeng, *Chem. Mater.* 13 (2001)4564-4572.

[127] Z.P. Xu, H.C. Zeng, *J. Phys. Chem-Us.* 105 (2001)1743-1749.

[128] R.K. Allda, A. Navrotsky, H.T Berbeco, W.H. Casey, *Science* 296 (2002) 721-723.

[129] R.G. Ford, A.C. Sheinost, K.G. Schekel, D.L. Sparks, *Environ. Sci. Technol.* 33 (1999) 3140-3144.

[130] K.G. Schekel, A.C. Scheinost, R.G. Ford, D.L. Sparks, *Geochim. Cosmochim. Ac.* 64 (2000) 2727-2735.

[131] F-A. He, L-M. Zhang, *Compos. Sci. and Technol.* 67 (2007) 3226–3232.

[132] Y. Zhao, B. Li, Q. Wang, W. Gao, C. J. Wang, M. Wei, D.G. Evans, X. Duan, D. O´Hare, *Chem. Sci.* 5 (2014) 951-958.

[133] Y. Huang, X. Chen, Y. Deng, D. Zhou, L. Wang, *Chem. Eng. J*. 269 (2015) 434-443.

[134] B. Tyagi, U. Sharma, R.V. Jasra, *Appl. Catal. A-Gen.* 408 (2011) 171-177.

[135] U. Constantino, M. Curini, F. Montanari, M. Nochetti, O. Rosati, *J. Mol. Catal. A: Chem.* 195 (2003) 245-252.

[136] A. Dubey, V. Rives, S. Kannan, *J. Mol. Catal. A: Chem.* 181 (2002) 151-160.

[137] A.I. Khan, L. Lei, A.J. Norquist, D. O´Hare, *Chem Commun*. (2001) 2342-2343.

[138] A. Ookubo, K. Ooi, H. Hayashi, *J. Pharm. Sci.* 81 (1992) 1139-1140.

[139] J-H. Choy, S-Y. Kwak, J-S. Park, Y-J. Jeong, *J. Mat. Chem*. 11 (2001) 1671-1674.

[140] J-H. Choy, S-J. Choi, J-M. Oh, T. Park, *Appl. Clay Sci*. 36 (2007) 122-132.

[141] L. Mohanambe, S. Vasudevan, *Langmuir* 21 (2005) 10735-10742.

[142] W-Z. Li, J. Lu, J-S. Chen, G-D. Li, Y-S. Jiang, L-S. Li, B-Q. Huang, *J. Chem. Technol. Biot.* 81 (2006) 89-93.

[143] V. Ambrogi, G. Fardella, G. Grandolini, L. Perioli, *Int. J. Pharm.* 220 (2001) 23-32.

[144] H. Zhang, D. Pan, X. Duan, *J. Phys. Chem. C.* 113 (2209) 12140-12148.

[145] V. Ambrogi, G. Fardella, G. Grandolini, L. Perioli, M.C. Tiralti, *AAPS Pharm. Sci. Tech.* 3 (2002) E26.

[146] F.P. Bonina, M.L. Giannossi, L. Medici, C. Puglia, V. Summa, F. Tateo, *Appl. Clay Sci.* 41 (2008) 165-171.

[147] J. Serrano, V. Bertín, S. Bulbulian, *Langmuir* 16 (2000) 3355-3360.

[148] Z. Yong, V. Mata, A.E. Rodrigues, *Sep. Purif. Technol.* 26 (2002) 185-195.

[149] H. Th. J. Reijers, S.E.A. Valster-Shiermeier, P.D. Cobden, R.W. Van den Brink, *Ind. Eng. Chem. Res.* 45 (2006) 2522-2530.

[150] A.E. Palomares, J.G. Prato, F. Rey, A. Corma, *J. Cat*. 221 (2004) 62-66.

[151] H. Lu, Z. Zhu, H. Zhang, J. Zhu, Y. Qiu, *Chem Eng. J.* 276 (2015) 365-375.

[152] S. Paikaray, M. J. Hendry, J. Essilfie-Dughan, *Chem. Geol.* 345 (2013) 130-138.

[153] P. Cai, H. Zheng, C. Wang, H. Ma, J. Hu, Y. Pu, P. Liang, *J. Hazard. Mat.* 213-214 (2012)100-108.

[154] M.R. Pérez, I. Pavlovic, C. Barriga, M.A. Ulibarri, J. Cornejo, M.C. Hermosín, *Appl. Clay Sci.* 32 (2006) 245-251.

[155] F. Bruna, I. Pavlovic, C. Barriga, J. Cornejo, M.A. Ulibarri, *Appl. Clay Sci*. 33 (2006) 116-124.

[156] F. Bruna, I. Pavlovic, R. Celis, C. Barriga, J. Cornejo, M.A. Ulibarri, *Appl. Clay Sci.* 42 (2008) 194-200.

[157] M.A. Ulibarri, I. Pavlovic, C. Barriga, M.C. Hermosín, J. Cornejo, *Appl. Clay Sci.* 18 (2001) 17-27.

[158] G. Onkal-Engin, R. Wibulswas, D.A. White, *Environ. Technol*. 21 (2000) 167-175.

[159] G. Zhang, T. Wub, Y. Li, X. Huang, Y. Wang, G. Wang, *Chem. Eng. J*. 191 (2012) 306-313.

[160] N.K. Lazaridis, T.D. Karapantsios, *Water Res.* 37 (2003) 3023-3033.

[161] M.Z. bin Hussein, A. H. Yahaya, Z. Zainal, L. H. Kian, *Sci. Technol. Adv. Mat*. 6 (2005) 956-962.

[162] C. Nyambo, E. Kandare, D. Wang, C. A. Wilkie, *Polym. Degrad. Stabil.* 93 (2008) 1656-1663.

[163] D.G. Evans, X. Duan, *Chem. Commun.* 5 (2006) 485□496.

[164] Y-J. Lin, D-Q. Li, D.G. Evans, X. Duan, *Polym. Degrad. Stabil.* 88 (2005) 286-293.

[165] K. Takagi, T. Shichi, H. Usami, Y. Sawaki, *J. Am. Chem. Soc.* 115 (1993) 4339-4344.

[166] H. Tagaya, T. Kuwahara, S. Sato, J. Kadokawa, M. Karasu, K. Chiba, *J. Mat. Chem.* 3 (1993) 317-318.

[167] H. Tagaya, S. Sato, T. Kuwahara, J. Kadokawa, K. Masa, K. Chiba, *J. Mat. Chem.* 4 (1994) 1907-1912.

[168] S. Guo, D. Li, W. Zhang, M. Pu, D.G. Evans, X. Duan, *J. Solid State Chem.* 177 (2004) 4597-4604.

[169]A. de Roy, J.P. Besse, P. Bondot, *Mater. Res. Bull*. 20 (1985) 1091-1098.

[170] X. Fan, Z. Yang, R. Wen, B. Yang, W. Long, *J. Power Sources* 224 (2013) 80-85.

[171] C.S. Liao, W.B. Ye, *Electrochim. Acta* 49 (2004) 4993-4998.

[172] J. Liu, F. Li, D. G. Evans, X. Duan, *Chem Commnun*. 4 (2003) 542-543.

[173] B. Lotsch, F. Millange, R.I. Walton, D. O´Hare, *Solid State Sci.* 3 (2001) 883-886.

[174] L. Raki, J.J. Beaudoin, L. Mitchell, *Cement. Concrete. Res*. 34 (2004) 1717-1724.

[175] H. Tamura, J. Chiba, M. Ito, T. Takeda, S. Kikkawa, *Solid State Ionics* 172 (2004) 607-609.

[176] S. Aisawa, H. Kudo, T. Hoshi, S. Takahashi, H. Hirahara, Y. Umetsu, E. Narita, *J. Solid State Chem.* 177 (2004) 3987-3994.

[177] S. Aisawa, N. Higashiyama, S. Takahashi, H. Hirahara, D. Ikematsu, H. Kondo, H. Nakayama, E. Narita*, Appl. Clay Sci*. 35 (2007) 146-154.

[178] S. Aisawa, A. Yasutake, S. Takahashi, H. Hirahara, E. Narita, *J. Nanosci. Nanotechnol.* 8 (2008) 428-431.

CAPÍTULO II
Hipótesis y Objetivos

La presente memoria de Tesis Doctoral se encuadra en la línea de investigación que desarrolla actualmente el grupo FQM-214 de la Universidad de Córdoba. Los trabajos realizados han contribuido en el desarrollo de los siguientes proyectos de I+D: **"Formulaciones de herbicidas soportados en hidróxidos dobles laminares: Biodisponibilidad y Comportamiento bajo ciertas prácticas agronómicas en suelos agrícolas de la Cuenca del Guadalquivir"** (AGL 2008-04031-CO2-02) e "**Hidrotalcitas modificadas con ácido húmico como filtros de descontaminación de pesticidas y metales pesados en aguas potables"** (CTM 2011-25325). Finalmente, dos estancias de investigación se llevaron a cabo en Ruhr-Universität Bochum (Alemania) en el grupo de investigación Semiconductor & Energy Conversion, para complementar esta formación doctoral.

Hipótesis de partida

La presencia de niveles elevados de sustancias tóxicas ya sean inorgánicas u orgánicas en las aguas naturales puede provocar graves problemas de salud en los humanos y en los seres vivos en general. Por tanto, es necesario una búsqueda continua de nuevas tecnologías y materiales que logren disminuir su impacto ambiental.

Con este fin, el **objetivo global** del presente trabajo se centra en la eliminación de contaminantes químicos de distinta naturaleza en ambientes acuáticos mediante tecnologías limpias, simples, económicas y altamente efectivas.

Hipótesis 1

Debido al amplio uso en la agricultura de los pesticidas además de otros campos de actividad, su presencia ha afectado al abastecimiento de agua potable de numerosos municipios y obligado a la implantación de procesos especiales de potabilización con un alto coste económico. Cuando se requiere una inmovilización o recuperación rápida de suelos y aguas afectadas por las altas concentraciones de contaminantes, se suele recurrir a los métodos de adsorción. Los hidróxidos dobles laminares (HDLs), también conocidos como hidrotalcitas (HTs), son materiales que han mostrado buenas propiedades adsorbentes gracias

a sus características estructurales y superficiales, además de su fácil síntesis, baja toxicidad, precio y posibilidad de reciclabilidad. La modificación del espacio interlaminar de los HDLs con aniones orgánicos permite ampliar su uso como adsorbente de especies contaminantes no iónicas o de baja polaridad. Por ello los HDLs pueden ser de gran utilidad como adsorbentes de contaminantes en aguas.

Objetivo 1

Preparación y caracterización estructural de una hidrotalcita modificada con el anión caprilato. La modificación del espacio interlaminar mediante la intercalación de un anión orgánico proporciona un medio adecuado para la adsorción de los pesticidas linurón, 2,4-DB y metamitrón permitiendo la adsorción de estos pesticidas a través de interacciones hidrofóbicas

Objetivo 2

Evaluación de la capacidad adsorbente de la hidrotalcita con caprilato por los pesticidas seleccionados. Para ello, es necesario el estudio de la influencia de una serie de factores en el proceso de adsorción, tales como pH, tiempo de contacto (cinéticas de adsorción), concentración inicial del metal (isotermas de adsorción).

Objetivo 3

Estudio de la cinética de adsorción de los pesticidas mediante el uso de los modelos cinéticos más ampliamente usados en la literatura.

Objetivo 4

Caracterización estructural de los productos de adsorción (complejos adsorbente-adsorbato). El análisis mediante DRX junto con la espectroscopia IR permitirá obtener información sobre cómo se incorpora el adsorbato en el sólido.

Objetivo 5

Realización de experimentos de desorción de los pesticidas con diferentes disolventes (agua, etanol y acetona). La regeneración del adsorbente es de gran interés para abaratar los costes del proceso, ya que abre la posibilidad de

recuperación tanto del adsorbente como del contaminante extraído de la disolución.

Estos objetivos 1, 2, 3, 4 y 5 se abordan en el trabajo *"Caprylate intercalated layered double hydroxide as adsorbent of the linuron, 2,4-DB and metamitron pesticides from aqueous solution"*

Hipótesis 2

Los "metales pesados" son contaminantes altamente peligrosos dada su toxicidad, persistencia y acumulación en organismos vivos. Por ello, hay un gran interés en el desarrollo de procesos para la eliminación de metales pesados en aguas. Entre estos destaca la adsorción como una de las alternativas más eficaces cuando se trata de eliminar estas sustancias tóxicas. Los HDLs pueden ser modificados mediante la intercalación de agentes quelatantes que contengan grupos funcionales (ligandos) que permitan la adsorción de cationes metálicos vía formación de complejos y/o quelatos.

Objetivo 6

Síntesis y caracterización estructural de una hidrotalcita modificada con el anión humato. Esta HT funcionalizada permitirá la adsorción de cationes metálicos, tales como cobre, plomo y cadmio a través de los grupos funcionales del humato, existentes en forma aniónica en un amplio rango de pH, mediante interacciones electrostáticas y enlaces de coordinación entre el metal y los grupos funcionales del anión humato.

Objetivo 7

Estudio de la influencia de varios factores físico-químicos que pueden afectar la adsorción de metales *tales como* pH, tiempo de contacto, concentración inicial y adsorción simultánea de los tres iones metálicos en la disolución (experimentos de competencia).

Objetivo 8

Comparación de la capacidad adsorbente del híbrido LDH-humato (LDH-H) con la hidrotalcita LDH-Cl es decir HT con cloruro como anión interlaminar, y el humato sódico en disolución, ya que todos presentan capacidades adsortivas por los metales pesados.

Los objetivos 6, 7 y 8 se abordan en el trabajo *"Removal of Cu^{2+}, Pb^{2+} and Cd^{2+} by layered double hydroxide–humate hybrid. Sorbate and sorbent comparative studies"*

Objetivo 9

Determinación de las condiciones óptimas de adsorción (Cu^{2+}, Pb^{2+} y Cd^{2+}), a través del estudio de la influencia del tiempo de contacto, concentración inicial y temperatura por los siguientes adsorbentes: LDH-Cl y dos HT híbridas conteniendo distinta cantidad del anión humato (LDH-H50 y LDH-H100).

Objetivo 10

Cálculo de los parámetros cinéticos y termodinámicos de la adsorción de metales en los tres adsorbentes mencionados previamente.

Objetivo 11

Estudio de experimentos de competición hacia el adsorbente en disoluciones binarias y ternarias de metales para así lograr una mejor comprensión del proceso de eliminación de metales en estos materiales. Además, se estudió la influencia de la presencia del anión humato en la disolución multicomponente en la adsorción.

Los objetivos 9, 10 y 11 se abordan en el trabajo *"Cu(II), Pb(II)and Cd(II) sorption on different layered double hydroxides. A kinetic and thermodynamic study and competing factors"*

Hipótesis 3

Recientemente, los compuestos tipo HT han despertado un gran interés en electroquímica por su estructura laminar, capacidad de intercalación, estabilidad, bajo coste e inocuidad para el medio ambiente. Su uso como materiales activos y colectores en baterías alcalinas y en supercondesadores, exhibió propiedades electroquímicas superiores a los materiales tradicionales. La incorporación de compuestos tipo HT a electrodos usados como sustratos electroquímicos, destinados a la remediación de aguas contaminadas por la presencia de metales pesados, podría suponer una nueva estrategia para la purificación de aguas. Los HDLs pueden actuar como matrices altamente estables homogeneizando la deposición de algunos metales y reduciendo la presencia de reacciones secundarias, lo que origina un incremento de la eficiencia del proceso de descontaminación.

Objetivo 12

Optimización de diversos parámetros de la celda electroquímica *t*ales como, proporción de aditivos, contenido del sustrato, concentración de electrolito, colector usado, área del electrodo y corriente usada para reducir las reacciones secundarias.

Objetivo 13

Eliminación de cadmio y plomo mediante electrodeposición usando HDLs como substratos y utilizando los parámetros experimentales óptimos alcanzados tras la consecución del objetivo 12. De manera independiente para los metales Cd y Pb se evaluará el efecto de la densidad de corriente (Cd) y concentración de metal (Pb) en el % de metal eliminado y en el potencial de reducción. Finalmente, se evaluará el efecto de los HDLs en la capacidad de eliminación mediante su comparación con otras tecnologías de remediación usadas en tratamientos de aguas.

Objetivo 14

Recuperación y concentración de los metales depositados electroquímicamente procedentes de las disoluciones contaminadas mediante la consecución del objetivo 13. Optimización de diversas variables que controlan el proceso de recuperación (volumen, densidad de corriente, diseño de la celda…).

Objetivo 15

Estudio de los mecanismos de reacción que se dan en el proceso de eliminación y la presencia de posibles reacciones secundarias mediante caracterización estructural mediante DRX de los electrodos antes y tras el proceso electroquímico.

Los objetivos 12, 13, 14 y 15 fueron abordados en el trabajo *"Capturing Cd(II) and Pb(II) from contaminated water sources by electro-deposition on Hydrotalcites-like Compounds"*

CAPÍTULO III
Materiales y Métodos

III.1. MATERIALES

III.1.1. Herbicidas

Los herbicidas estudiados fueron Linurón, 2,4-DB y Metamitrón. Todos ellos suministrados por Sigma-Aldrich de la marca Fluka y aprobados para su uso en gran parte de la Unión Europea. La estructura molecular de los herbicidas estudiados se muestra en la Tabla III.1.

Tabla III.1. Representación esquemática de la estructura molecular de los herbicidas estudiados

HERBICIDA	ESTRUCTURA QUÍMICA	DIMENSIONES
LINURÓN	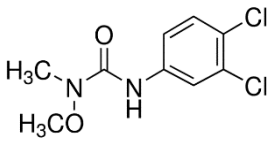	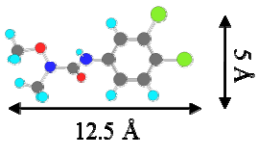
2,4-DB	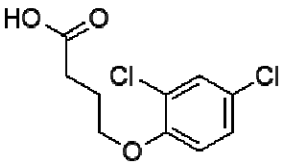	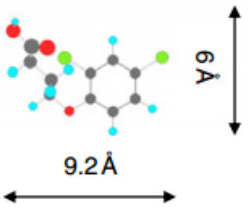
METAMITRÓN	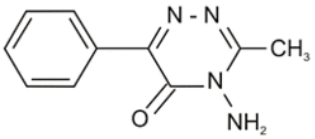	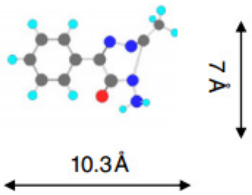

C ● Cl ● O ● N ● H ●

III.1.1.a. Linurón

Linurón es el nombre comercial del 3-(3,4-diclorofenil)-1-metoxi-1-metilurea. Pertenece al grupo químico de las fenilureas. Es un herbicida usado para el control pre y post-emergencia de las malas hierbas anuales. Ha sido ampliamente utilizado en agricultura, en el control del crecimiento de cultivos como el girasol, patata, zanahoria, maíz, guisantes y habas verdes, etc. A

continuación se detalla información sobre la composición química de este producto y algunas propiedades físico-químicas de importancia, Tabla III.2.

Tabla III.2. Información general del Linurón [1]

FÓRMULA	$C_9H_{10}Cl_2N_2O_2$
NÚMERO CAS	330-55-2
MODO DE ACCIÓN	Selectivo, sistémico con el contacto y la acción residual. Inhibe la fotosíntesis (fotosistema II)
ASPECTO	Polvo cristalino
COLOR	Blanco
PESO MOLECULAR	249.09g mol^{-1}
PUNTO DE FUSIÓN (°C)	94
SOLUBILIDAD EN AGUA a 20°C (mg L^{-1})	63.8
SOLUBILIDAD EN SOLVENTES ORGÁNICOS a 20°C (mg L^{-1})	395000 (Acetona); 292000 (Acetato de Etilo); 170000 (Metanol); 75000 (Tolueno)
pka	12.1
MÁXIMO ABSORCIÓN UV-vis	211nm
DEGRADACIÓN DE SUELO (DT50) EN DIAS	48 (Persistente moderado)

III.1.1.b. 2,4-DB

2,4-DB es el nombre comercial del ácido 3-(2.4-Diclorofenoxi) butírico. Pertenece al grupo químico del ácido ariloxialcanoico. Es utilizado para el control de post-emergencia de muchas malezas de hojas anchas anuales y perennes. En la agricultura se emplea principalmente en cultivos de alfalfa, cacahuate y soya. Este herbicida no es volátil pero puede ser lixiviado a las aguas subterráneas en ciertas condiciones. Es moderadamente tóxico para las aves, las lombrices de tierra, las abejas y la mayoría de organismos acuáticos. También lo es para los mamíferos por lo que hay cierta preocupación en cuanto a su potencial de bioacumulación. Algunas de sus propiedades físico-químicas se describen a continuación (Tabla III.3).

Tabla III.3. Información general del 2,4D-B [1]

FÓRMULA	$C_{10}H_{10}Cl_2O_3$
NÚMERO CAS	94-82-6
MODO DE ACCIÓN	Selectivo, sistémico. Auxina sintética que causa malformaciones de tallo y hojas que llevan a la muerte
ASPECTO	Polvo cristalino
COLOR	Blanco
PESO MOLECULAR	249.09g mol^{-1}
PUNTO DE FUSIÓN (°C)	115
SOLUBILIDAD EN AGUA a 20°C (mg L^{-1})	4385
SOLUBILIDAD EN SOLVENTES ORGÁNICOS a 20°C (mg L^{-1})	185200 (Acetona); 90700 (Acetato de Etilo); 113800 (Metanol); 10500 (Xileno)
pka	4.1 (carácter ácido débil)
MÁXIMO ABSORCIÓN UV-vis	230nm; 284nm; 291nm
DEGRADACIÓN DE SUELO (DT50) EN DIAS	16 (No persistente)
CLASIFICACIÓN US EPA (formulación)	III (ligeramente tóxico)

III.1.1.c. Metamitrón

Metamitrón es el nombre comercial del 4-amino-3-metil-6-fenil-1,2,4-triazin-5 (4H)–ona. Pertenece al grupo químico de la triazinona. Es utilizado de forma eficaz contra las malezas de hojas anchas. Es catalogado de pre y post emergencia. Algunas de sus propiedades físico-químicas quedan reflejadas en la Tabla III.4.

Tabla III.4. Información general del metamitrón [1]

FÓRMULA	$C_{10}H_{10}N_4O$
NÚMERO CAS	41394-05-2
MODO DE ACCIÓN	Selectivo, sistémico, absorbido principalmente por las raíces y translocado. Inhibe la fotosíntesis (fotosistema II)
ASPECTO	Sólido cristalino
COLOR	Amarillo
PESO MOLECULAR	202.21g mol^{-1}
PUNTO DE FUSIÓN (°C)	166.6
SOLUBILIDAD EN AGUA a 20°C (mg L^{-1})	1770
SOLUBILIDAD EN SOLVENTES ORGÁNICOS a 20°C (mg L^{-1})	37000 (Acetona); 20000 (Acetato de Etilo); 2000 (Xileno); 33000 (cloruro de metileno)
pka	2.9 (Carácter de base débil)
MÁXIMO ABSORCIÓN UV-vis	311.1nm
DEGRADACIÓN DE SUELO (DT50) EN DIAS	30 (persistente moderado)
CLASIFICACIÓN US EPA (formulación)	III (ligeramente tóxico)

III.1.2. Metales

Los metales pesados estudiados fueron: cobre, plomo y cadmio. Se utilizaron sales de nitrato y cloruro, las cuales fueron suministradas por Sigma-Aldrich. Algunas de sus propiedades físico-químicas se detallan a continuación (Tabla III.5).

Tabla III.5. Información de algunas propiedades físicas y químicas de los metales pesados estudiados [2]

DISOLUCIONES CONTAMINANTES	$Cu(NO_3)\cdot 3H_2O$	$Pb(NO_3)$ / $PbCl_2$	$Cd(NO_3)_2\cdot 4H_2O$ / $CdCl_2$
ESTADO FÍSICO			
PUREZA (%)	99-104	≥99.0	98
PESO MOLECULAR (g mol^{-1})	241.60	331.21 / 278.11	308.48 / 183.32
SOLUBILIDAD g/100g H_20 (25°C)	125	59.7 / 1.08	156 / 120
Ps $M(OH)_2$	1.10^{-20}	$2.5\cdot10^{-16}$	$3.2\cdot10^{-14}$

Siendo M= metal y Ps=Produto de solubilidad

III.1.2.a. Cobre

El cobre es introducido en la atmósfera por la industria de fertilizantes, siderurgia, la quema de madera, descarga de residuos mineros y la eliminación de cenizas volantes y desechos municipales e industriales [3]. El cobre existe en los estados de oxidación 0, +1 y +2. El ión cúprico, Cu(II) es la forma más tóxica del cobre además se ha demostrado que los iones $Cu(OH)^+$ y $Cu_2(OH)_2^{2+}$ son también bastante tóxicos. Sin embargo, en grandes cantidades todas las formas del Cu son extremadamente tóxicas para los organismos vivos. En sistemas alcalinos y aeróbios, el $CuCO_3$ es la especie más soluble y en ambientes anaeróbios el CuS(s) se formará en presencia de sulfuro. También el cobre forma complejos con diferentes ácidos orgánicos en disolución y entre ellos el ácido húmico [4].

III.1.2.b. Plomo

El plomo se considera uno de los contaminantes más peligrosos, puede ser liberado al medioambiente por diversas actividades antropogénicas mediante procesos industriales como fabricación de baterías y enchapado y acabado de metales. En los últimos años la contaminación por plomo ha disminuido debido a que algunas fuentes antropogénicas de plomo han sido eliminadas o estrictamente reguladas debido a su persistencia y toxicidad, como la gasolina con plomo, la pintura con base de plomo, soldadura de plomo en las latas de alimentos,

pesticidas con plomo-arseniato y el uso de municiones en la caza. Este metal existe en los estados de oxidación 0 y +2. El Pb(II) es la forma más común y reactiva de plomo. Este junto con los complejos de hidróxido de plomo son las formas más estables. También forman compuestos de baja solubilidad con aniones inorgánicos (Cl^-, CO_3^{2-}, SO_4^{2-}, PO_4^{3-}) y ligandos orgánicos (ácidos húmicos y fúlvicos, EDTA, aminoácidos). Los procesos primarios que determinan el destino del plomo en los diferentes compartimentos ambientales son adsorción, intercambio iónico, precipitación y complejación con la materia orgánica [4].

III.1.2.c. Cadmio

El cadmio junto con el Pb y el Hg, es uno de los metales pesados más tóxicos. Es introducido en el medioambiente por fuentes naturales como la erosión de las rocas parentales, actividad volcánica e incendios forestales. Debido a sus propiedades químicas, físicas y mecánicas únicas, el cadmio es utilizado en un número importante de aplicaciones industriales y de consumo. Por lo tanto, la principal fuente de contaminación es de naturaleza antropogénica. Podemos citar como ejemplos las baterías de niquel-cadmio, aleaciones fusibles y soldaduras, placas fotográficas y celdas fotoeléctricas. El cadmio existe en los estados de oxidación 0 y +2. Las formas más comunes son Cd(II), $Cd(OH)_2$ y los complejos con cianuro. Su hidróxido y carbonato predominan a pH altos, mientras que el Cd(II) y especies sulfatadas a pH más bajos. El cadmio precipita en presencia de fosfato, arseniato, cromato, sulfato, etc. y muestra movilidad en el rango de pH 4,5-5,5 [3, 4].

III.1.3. Preparación de adsorbentes: Hidróxidos dobles laminares

III.1.3.a. HDL conteniendo cloruro como anión interlaminar (LDH-Cl)

Para la obtención de la hidrotalcita $[Mg_3Al(OH)_8]Cl{\cdot}nH_2O$ que se denominará LDH-Cl, se utilizó el método de coprecipitación [5]. Para ello, desde un embudo de decantación, se añaden 200ml de una disolución que contiene 0.75M $MgCl_2.6H_2O$ y 0.25M de $AlCl_3.6H_2O$ a una disolución de NaCl 0.25M dentro de la cual está circulando una corriente de nitrógeno, de esta manera se evita la disolución del CO_2 atmosférico y consecuentemente la incorporación del carbonato

al sólido. La adición de los iones metálicos se ha llevado a cabo lentamente, con agitación constante y controlando el pH a 8 mediante la adición de NaOH 1M. Una vez finalizada la síntesis, la suspensión obtenida se sometió a tratamiento hidrotermal a 80°C durante 24 horas. Transcurrido dicho tiempo, se procedió al lavado de la hidrotalcita usando agua descarbonatada y repitiendo el proceso unas cuatro veces para así eliminar cualquier impureza. Finalmente, esta fue secada en estufa a 60ºC durante 24h aproximadamente.

III.1.3.b. HDL modificado con el anión caprilato (LDH-Cap)

La sal aniónica seleccionada para la síntesis de esta organohidrotalcita es el "caprilato sódico (Cap)" y fue suministrada por Sigma-Aldrich. También es conocida como la sal sódica del ácido caprílico/octanoico y su estructura química queda reflejada en la Figura III.1.

Figura III.1. Estructura química 2D del caprilato sódico

Algunas de sus propiedades físico-químicas se definen a continuación [2, 6, 7]:

Número CAS: 1984-06-1

Fórmula molecular: $C_8H_{15}NaO_2$

Estado físico: Sólido blanquecino

Peso molecular: 166.19 g mol^{-1}

Punto de fusión: 300°C

pKa = 4.895 a 25°C

Solubilidad en agua: 50 mg ml^{-1}

La preparación del adsorbente $[Mg_3Al(OH)_8][CH_3(CH_2)_6COO]\cdot nH_2O$ que se denominará como LDH-Cap, se llevó a cabo mediante el método de intercambio iónico. La síntesis consiste en adicionar lentamente la disolución que contiene el anión caprilato que queremos intercalar a la suspensión del precursor obtenido previamente por coprecipitación (LDH-Cl). Un diagrama del procedimiento de síntesis se describe en la Figura III.2.

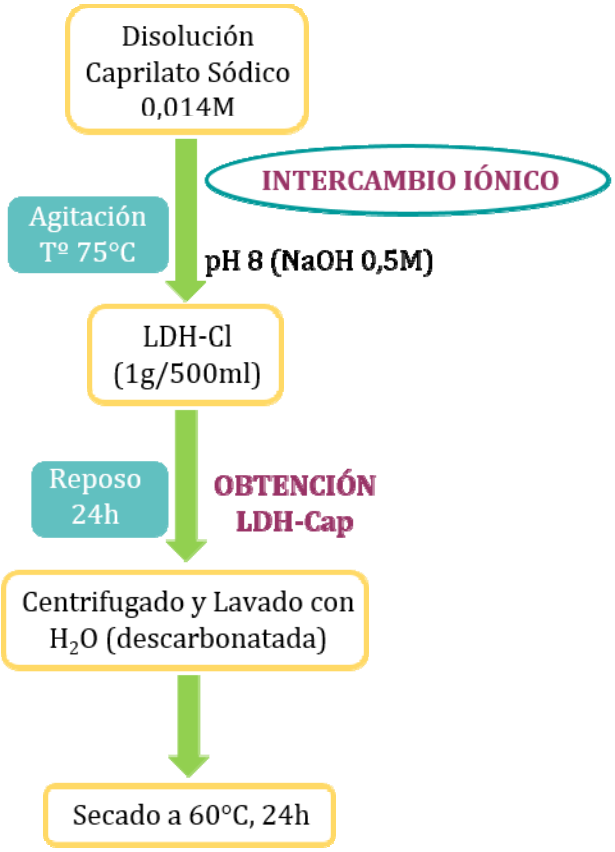

Figura III.2. Diagrama del procedimiento de síntesis del LDH-Cap

III.1.3.c. HDL modificado con el anión humato (LDH-H)

La sal sódica de ácido húmico utilizada fue suministrada por Aldrich. El nombre sistemático de este compuesto es biciclo disódico [2.2.1] hept-5-eno-2,3-dicarboxilato y su estructura química se muestra en la Figura III.3.

El ácido húmico posee una capacidad complejante excelente con los metales pesados y está presente en gran parte de la materia orgánica del suelo y en las aguas.

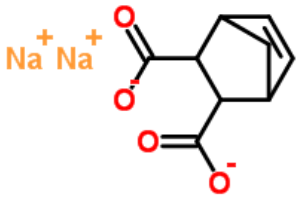

Figura III.3. Estructura química 2D de la sal sódica del ácido húmico

Algunas de sus propiedades se definen a continuación [2, 6, 7]:

Número CAS: 68131-04-4
Fórmula molecular: $C_9H_8Na_2O_4$
Estado físico: Sólido pardo oscuro
Peso molecular: 226.14 g mol^{-1}
Punto de fusión: >300°C
pKa (grupos carboxilato): 4
Solubilidad en agua: 369 g l^{-1} a 20 °C

El anión humato fue empleado para la modificación de LDH-Cl y se obtuvieron dos adsorbentes híbridos a los cuales se les incorporó distinta concentración de humato, para compensar la carga laminar. Estos adsorbentes híbridos se componen de:

- HDL con cloruro interlaminar modificado con el anión humato, conteniendo el 100% de la concentración estequiométrica **(LDH-H100)**.
- HDL con cloruro interlaminar modificado con el anión humato, conteniendo el 50% de la concentración estequiométrica **(LDH-H50)**.

Ambos adsorbentes, de fórmula teórica $[Mg_3Al(OH)_8]\cdot(H)_{0.5}\cdot nH_2O$, fueron preparados mediante el método de síntesis de intercambio iónico a partir del precursor LDH-Cl (procedimiento similar al de obtención del LDH-Cap). Por tanto, se adicionó lentamente una disolución de sal sódica de ácido húmico (100% y 50% de la concentración estequiometria en cada caso) sobre una suspensión del precursor, en agitación constante y manteniendo el pH a 8 con una disolución de NaOH 1M. La suspensión obtenida se dejó reposar durante 24h. A continuación, se

centrifugó y se lavó para así quitar el exceso de humato. Finalmente, se dejó secar en estufa a 80ºC para su posterior caracterización.

III.1.4. Sustratos electroquímicos: HDLs

Una innovadora aplicación de estos materiales tan versátiles llevada a cabo en esta tesis doctoral ha sido su utilización como sustratos electroquímicos para la deposición de metales pesados, por su características estructurales [8], estabilidad en un amplio rango valores de pH, bajo coste, así como sus propiedades redox, magnéticas y catalíticas.

III.1.4.a. HDL conteniendo carbonato como anión interlaminar (ZnAl-CO_3)

Este compuesto de fórmula teórica $[Zn_4Al(OH)_{10}](CO_3)_{0.5}\cdot nH_2O$ fue preparado por el método de coprecipitación. Disoluciones de sales de nitrato que contenían los cationes metálicos, Na_2CO_3 y NaOH, se añadieron lentamente desde los correspondientes embudos de decantación, a un vaso de precipitado que contenía 50ml de agua (Figura III.4). La síntesis se llevó a cabo a temperatura ambiente y manteniendo el pH a 9.

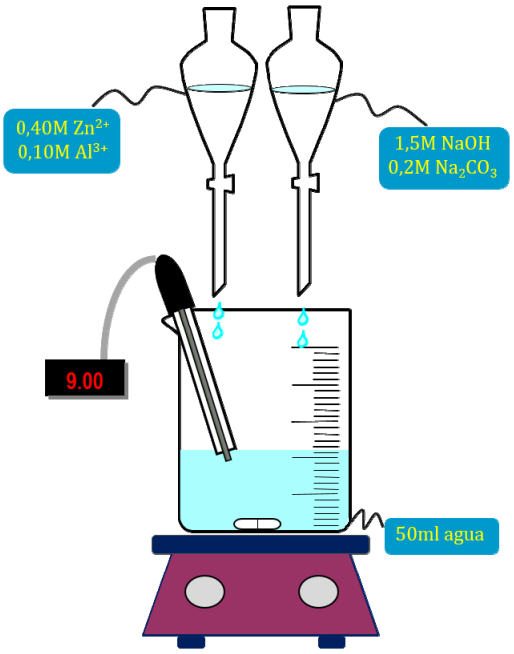

Figura III.4. Esquema del procedimiento de síntesis del ZnAl-CO_3

La suspensión obtenida se mantuvo durante 2h con agitación constante. A continuación fue sometido a tratamiento hidrotermal 24h a 85ºC. Finalmente, se

procedió al centrifugado, lavado y secado del compuesto siguiendo procedimientos anteriores.

El HDL que contiene humato (LDH-H100), cuya síntesis ha sido descrita anteriormente (apartado III.1.3.c.), también ha sido usado como sustrato electroquímico para la deposición de plomo y cadmio.

III.1.5. Preparación de electrodos

Con objeto de potenciar las propiedades mecánicas y eléctricas del material activo se usa normalmente ciertos aditivos junto al material activo, y de esta forma se obtiene un material electródico de uso adecuado en electroquímica. Como material activo se usaron los HDL (electrodo de trabajo) y la Ag (contraelectrodo). Entre los aditivos denominados aglomerantes de naturaleza plástica y cuya función es mantener en cohesión a todos los materiales del electrodo, podemos encontrar fluorpolímeros como el politetrafluoretileno (PTFE) o el floruoro de polivinilideno (PVDF), derivados del poliacrilonitrilo (PA) o de la carboximetil celulosa de sodio. El aglomerante utilizado en la preparación de los electrodos de este trabajo ha sido una disolución de fluoruro de polivinilideno (Solef S5130, Solvay) en N-metil pirrolidona (25 mg ml^{-1}). Entre la gran variedad de aditivos conductores generalmente derivados del petróleo, se optó por C65 carbon black (Timcal Super P C65) cuya función es mejorar la conductividad electrónica del material. Este aditivo induce además una porosidad adecuada al material activo que facilita la penetración del electrolito en el mismo. En determinadas ocasiones, cuando la cantidad de material activo por área es elevada, resulta importante la adición de una pequeña cantidad de grafito (Timcal SFG6) a la mezcla electródica para así aumentar la conductividad eléctrica. Las relaciones en peso de material activo (HDL o Ag): aglomerante: super p es un parámetro a tener en cuenta puesto que puede afectar en gran medida al comportamiento electroquímico. Mediante el uso de un dispersor Ultra-Turrax (ika) durante unos 30 minutos a 4000 r.p.m. se obtuvo la correspondiente suspensión constituida por una proporción en peso de 75:10:15:0 y 80:9:9:2 para el HDL y la Ag respectivamente. La metodología seguida para la preparación de los electrodos fue la conocida como “hand-painting” la cual se basa en extender la mezcla electródica, mediante el uso de un pincel, sobre la superficie de un colector de corriente. Este fue en todos los casos carbon cloth

(Fuel Cell Earth, Figura III.5. a y b), constituido por fibras de carbono (99.5 %) entrelazas formando un tejido conductor poroso (0.62 g m^{-2}), flexible (Tensile Strength = 192.5 kN cm^{-2}) y electroquímicamente estable en una amplia ventana de potencial. Dichos electrodos tienen aproximadamente 2.9 cm^2 de área y contienen aproximadamente 7 o 14 mg de HDL por cm^2. Para evitar la corrosión del conector (pinza observada en Figura III.6) que une el electrodo con el potenciostato, se aplica cera aislante bloqueando la capilaridad del carbon cloth, así todo el colector situado tras esta banda de cera permanece seco (Figura III.5. c). Previo a su uso, los electrodos se secaron en dos ocasiones a 60 ° C en estufa durante al menos 3 horas, la primera tras su impregnación con la suspensión y la segunda tras la adición de la cera aislante.

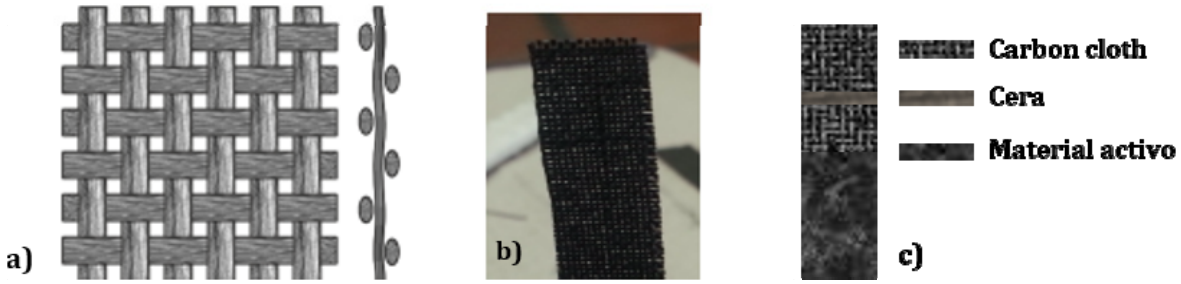

Figura III.5. Carbon cloth usado como colector de corriente (a y b) y composición de electrodo (c)

III.1.6. Tipo de celda electroquímica

El tipo de celda electroquímica donde se llevaron a cabo las deposiciones electroquímicas fue una celda de geometría cónica, la cual es conocida como "flooded three-electrode cell" (Figura III.6. a). Esta consta de 5 entradas (bocas), tres de ellas fueron empleadas para introducir el electrodo de trabajo (WE, por sus siglas en inglés), contraelectrodo (CE) y de referencia (RE). Otra entrada fue usada para acoplar un flujo de argón, el cual bloquea la entrada de oxígeno a la celda evitando el desarrollo de reacciones secundarias durante el proceso electroquímico. La última entrada esta provista de una jeringa, cuya función es retirar el volumen de electrolito correspondiente tras el proceso de deposición y de esta forma concentrar la disolución del metal. Esta misma configuración fue usada para el proceso de recuperación (oxidación del metal).

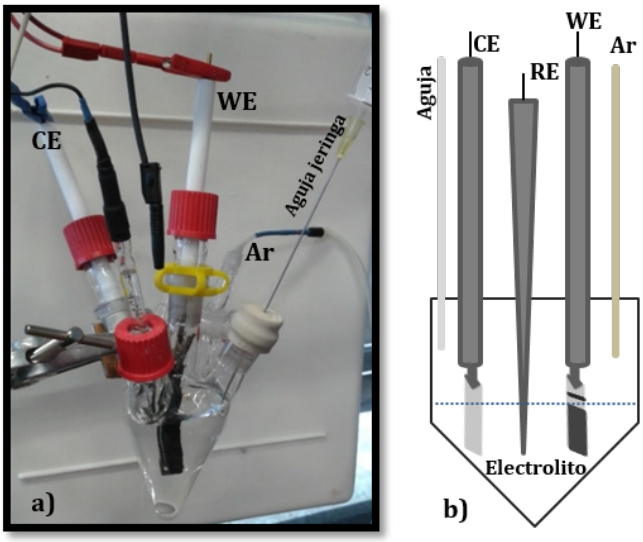

Figura III.6. a) Celda tres electrodos (Flooded three-electrode cell) y b) representación esquemática de la celda.

La disposición de los electrodos (Figura III.6. b) se basa en la confrontación con la menor separación posible entre el electrodo de trabajo (HDL) y el contraelectrodo (Ag) reduciendo así la resistencia óhmica, la cual aumenta directamente a mayor separación de los electrodos, quedando ubicado en medio de ambos el electrodo de referencia (Ag/AgCl 3 M KCl) que evita un posible cortocircuito. Este es preparado en el laboratorio y está constituido por un hilo de plata recubierto de AgCl sumergido en una disolución de KCl 3M y la exactitud de su potencial es evaluada mediante su comparación con un electrodo de referencia comercial Ag/AgCl 3 M. Su uso nos permite monitorizar la evolución del potencial en ambos electrodos durante el proceso electroquímico. El electrolito contiene disoluciones contaminantes de $PbCl_2$ (2.5mM/5mM) o $CdCl_2$ (5mM), las cuales son burbujeadas con un flujo de Ar durante 10 minutos.

Las reacciones que tienen lugar en la celda electroquímica se describen a continuación:

$$\boldsymbol{WE} \quad M^{2+}_{(aq)} + 2e^- \leftrightarrow M^{O}_{(e)} \tag{III.1}$$

$$\boldsymbol{CE} \quad Ag_{(e)} + Cl^-_{(aq)} \leftrightarrow AgCl_{(e)} + 1e^- \tag{III.2}$$

Reacción global: $M^{2+}_{(aq)} + 2Ag_{(e)} + 2Cl^-_{(aq)} \leftrightarrow M^{O}_{(e)} + 2AgCl_{(e)}$ (III.3)

Siendo: *M* (metal); *aq* (electrolito); *e* (electrodo); → (proceso de deposición o eliminación); ← (proceso de oxidación o recuperación)

Durante el proceso de eliminación, el catión metálico contaminante (Cd, Pb), proveniente del electrolito es reducido, depositándose en el electrodo de trabajo al mismo tiempo que la plata metálica es oxidada. Mientras que en el proceso de recuperación ocurre el proceso inverso, es decir, el metal proveniente del electrodo es oxidado liberándose a la disolución, y por consiguiente el AgCl se reduce a Ag metálica.

III.2. MÉTODOS EXPERIMENTALES

III.2.1. Control de pH

Se ha utilizado un medidor de pH Metrohm 691 conectado a un electrodo de combinado (con electrodo de referencia interno) de vidrio Metrohm tanto para registrar el pH como para el ajuste del mismo, para lo que se acopló el pH a una bureta automática Metrohm 725 Dosimat con disoluciones de base o ácido.

III.2.2. Difracción de Rayos X (DRX)

Esta técnica no destructiva suministra información acerca de la estructura cristalina del compuesto y permite determinar parámetros reticulares, posiciones atómicas, niveles de ocupación, tamaño de cristalito y microtensiones.

La interacción entre el vector eléctrico de la radiación X y los electrones de la materia que atraviesa da lugar a la dispersión de los rayos X por el entorno ordenado del cristal produciéndose interferencias, al ser las distancias entre los centros de dispersión del mismo orden de magnitud que la longitud de onda de la radiación se produce el fenómeno de la difracción (Figura III.7).

En la modalidad de difracción en polvo, un haz de rayos X se hace incidir sobre una muestra en polvo finamente dividida, de forma que tenga sus cristales orientados al azar en todas las direcciones del espacio y se produzcan todas las interacciones posibles. La difracción de los rayos X puede interpretarse mediante un modelo de reflexión de los fotones por los planos cristalográficos del material.

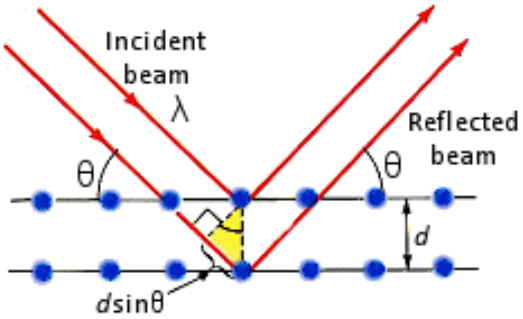

Figura III.7. Esquema del proceso de difracción

La condición para que los haces reflejados se encuentren en fase (interferencia constructiva) viene dada por la Ley de Bragg:

$$n \cdot \lambda = 2 \cdot d \cdot \operatorname{sen} \theta \qquad \text{(III.4)}$$

donde λ es la longitud de onda de la radiación incidente, d es el espaciado entre planos cristalográficos de la red cristalina, n un número entero y θ es el ángulo que forma el haz incidente y el plano de reflexión.

Los diagramas de difracción de rayos X de las distintas muestras se registraron en un difractómetro Siemens modelo D5000, controlado por el sistema informático DiffracPlus BASIC 4.0, provisto de un monocromador de grafito para el haz difractado y detector de tipo proporcional. La radiación utilizada fue Cu $K_{\alpha 1,2}$ (λ_1= 1.54056 Å y λ_2= 1.54439 Å) y las condiciones de registro fueron 40 kV y 30 mA en la modalidad de barrido por pasos entre 3° y 80° (2θ). Para fines de identificación de fases, el ancho de paso fue de 0.02° (2θ) y tiempo de registro 0.6 segundos por paso.

Esta técnica ha sido primordial para el análisis cualitativo de las fases cristalinas de los sustratos electroquímicos y los adsorbentes sintetizados.

III.2.3. Espectroscopia Infrarroja con Transformadas de Fourier (FTIR)

La espectroscopia infrarroja es un tipo de espectroscopia donde se analizan las vibraciones moleculares. Las bandas de un espectro corresponden a los modos de vibración activos en IR de los componentes de la muestra.

Una molécula que costa de N átomos puede vibrar de 3N – 6 formas distintas si es no lineal, y de 3N – 5 formas diferentes si sí lo es. Estas diversas vibraciones se llaman modos normales. Sólo los modos normales que corresponden a un

momento dipolar eléctrico cambiante pueden interactuar con la radiación infrarroja, de modo que únicamente esos modos son activos en la producción de un espectro IR.

La energía de la radiación infrarroja puede producir la excitación de los niveles vibracionales de las especies presentes en la muestra, dando lugar a una vibración. En moléculas complejas (poliatómicas), pueden encontrarse dos categorías básicas de vibraciones: *de tensión*, la cual supone un cambio continuo en la distancia interatómica a lo largo del eje del enlace entre dos átomos, y *de flexión*, que consisten en un cambio en el ángulo entre dos enlaces y son de cuatro tipos: de tijereteo, de balanceo, de aleteo y de torsión. Los distintos tipos de vibraciones se representan esquemáticamente en la Figura III.8. La energía implicada en estas transiciones es dependiente de las fuerzas interatómicas en la molécula o cristal, por lo que las posiciones, simetría e intensidades relativas de las bandas proporcionan información acerca de la estructura de la molécula.

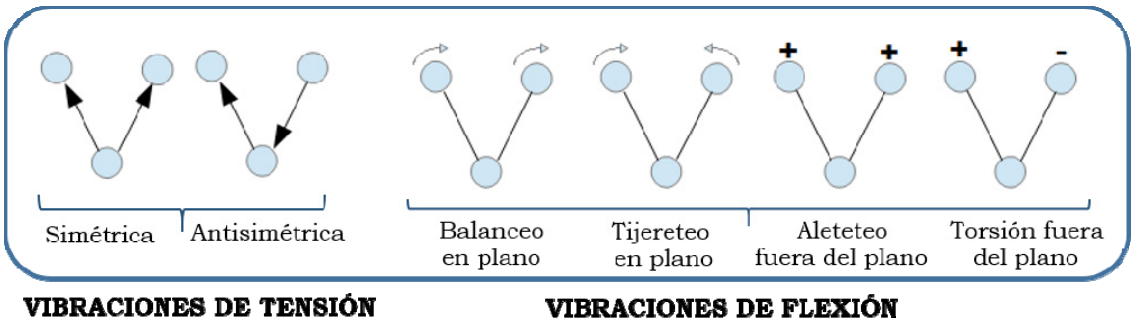

Figura III.8. Tipos de vibraciones moleculares

Los espectros de absorción de infrarrojo de las distintas muestras se registraron con un espectrofotómetro de infrarrojo con transformada de Fourier Perkin-Elmer Spectrum One. El barrido se realizó en el intervalo comprendido entre 400 y 4000 cm^{-1}. Los espectros obtenidos son el promedio de 40 registros (mejorando así la relación señal/ruido), con una resolución nominal de 4 cm^{-1}. Para realizar los registros de las muestras, se prepararon pastillas de 13 mm, prensadas a 8 Tm, de una mezcla homogénea elaborada a partir del compuesto 1% en bromuro potásico de calidad analítica para FT-IR. En el registro realizado a la muestra, se sustrajo el fondo producido por el KBr, restando al espectro de la muestra el espectro producido por una pastilla pura de dicha sal.

Esta técnica se ha empleado principalmente para identificar los aniones intercalados en las muestras y confirmar la presencia de compuestos orgánicos adsorbidos.

III.2.4. Análisis Térmico

El análisis térmico comprende el estudio de la evolución de las propiedades (físicas y químicas) de una muestra o compuesto mientras es sometido a una variación controlada de temperatura.

III.2.4.a. Análisis Termogravimértrico (ATG)

Esta técnica mide la variación de masa de un compuesto en función de la temperatura. Las variaciones de temperatura no siempre implican un cambio en la masa de la muestra. Existen sin embargo, cambios térmicos que sí se acompañan de un cambio de masa, como la descomposición, la sublimación, la reducción, la desorción, la absorción y la vaporización. Estos cambios pueden ser medidos con el analizador termogravimétrico. La gráfica resultante se denomina termograma o curva de descomposición térmica, y los principales tipos se representan en la Figura III.9.

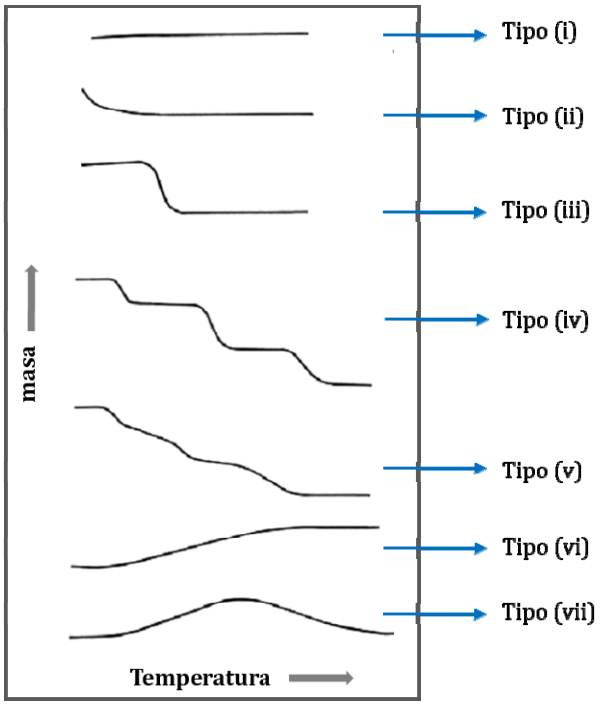

Figura III.9. Principales tipos de curvas termogravimétricas

III.2.4.b. Análisis Térmico Diferencial (ATD)

Es una técnica en la que se mide la diferencia de temperatura entre la muestra y un material de referencia, mientras que ambos se someten al mismo programa de calentamiento en una atmósfera controlada. Una configuración del ATD se muestra en la Figura III.10 donde S es la muestra y R el material de referencia. La diferencia de temperatura, ΔT, entre la muestra, Ts, y la referencia, Tr, se mide y se representa frente a la temperatura de la muestra para dar un termograma diferencial.

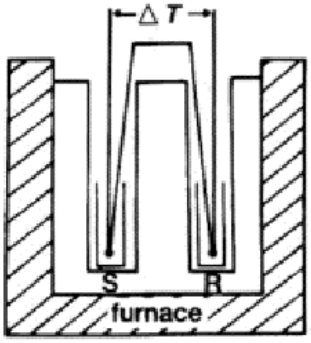

Figura III.10. Configuración clásica del ATD

Los picos de análisis térmico diferencial son el resultado tanto de cambios físicos como de reacciones químicas inducidas por los cambios de temperatura en la muestra. Existen dos tipos de reacciones: endotérmicas y exotérmicas. En la primera de ellas, el aporte de calor externo se gasta en mantener la reacción y la temperatura de la muestra no sube hasta que ésta acabe (Tm(s) < Tr). Sin embargo, en las reacciones exotérmicas el calor que se produce en la reacción hace que la temperatura de la muestra aumente más rápido que la de la referencia (Tm(s) > Tr). Entre los procesos físicos que son endotérmicos se incluyen la fusión, la vaporización, la sublimación, la absorción y la desorción. La adsorción y la cristalización son generalmente exotérmicas. Entre las reacciones químicas endotérmicas se encuentran la deshidratación, la reducción en una atmósfera gaseosa y la descomposición. Las reacciones exotérmicas incluyen la oxidación en aire u oxígeno, la polimerización y las reacciones catalíticas.

Ambos análisis (ATG y ATD) se han realizado simultáneamente empleando un equipo SETARAM SETSYS evolution, modelo 16/18 empleando un rango de temperatura entre 30-1000°C a una velocidad de calentamiento de 5°C min^{-1}.

Esta técnica ha sido útil para conocer a que temperatura tiene lugar la descomposición térmica de los adsorbentes y los efectos asociados (endotérmicos/ exotérmicos) a cambios producidos en la muestra. Es decir, mediante ATG se pudo conocer el rango de estabilidad térmica de los materiales estudiados, pero fundamentalmente el análisis térmico fue de gran utilidad para proponer una fórmula experimental de los mismos (cálculo de las moléculas de agua).

III.2.5. Microscopía Electrónica de Barrido (SEM)

Las técnicas de Microscopia Electrónica se basan en la interacción de un haz de electrones de alta energía con la materia para generar una imagen.

En un microscopio electrónico de barrido se recorre la superficie del sólido mediante un rastreo programado con un haz de electrones de energía elevada y, como consecuencia de ello se producen en la superficie diversos tipos de señales. Estas señales incluyen electrones retrodispersados, secundarios y Auger; fotones debidos a la Fluorescencia de Rayos X y otros fotones de diversas energías. Todas estas señales se han utilizado en estudios de superficies, pero las más usuales son las que corresponden a:

- electrones retrodispersados y secundarios, en los que se fundamenta el microscopio de barrido.
- la emisión de rayos X, que se utiliza en el análisis químico con microsonda de electrones.

Esta técnica nos permite observar y estudiar superficies de un área muy reducida de cualquier tipo de material, bien sea orgánico o inorgánico, sin necesidad de pasar por procesos de preparación muy complejos, ya que los requerimientos más importantes son que la muestra esté deshidratada y sea eléctricamente conductora. Por lo que esta técnica es de gran utilidad en el estudio de los rasgos morfológicos de las partículas sólidas (en nuestro caso de los HDLs).

Las muestras se prepararon por dispersión de los sólidos en tetracloruro de carbono y usando un baño de ultrasonido. Después, se depositó una pequeña cantidad sobre un portamuestras de cobre y se recubrieron con una fina capa de oro para hacer la muestra conductora y facilitar la visualización de la superficie de los compuestos.

Las imágenes electrónicas se obtuvieron con un microscopio JEOL JSM 6300 del Servicio Central de Apoyo a la Investigación (SCAI) de la UCO. El voltaje de aceleración utilizado fue de 20KV, con una distancia de muestra de 8mm.

III.2.6. Espectroscopia de Absorción Atómica (AA)

La técnica de absorción atómica de llama, es en la actualidad el método atómico más usado por su efectividad, sencillez y coste relativamente bajo. Por consiguiente, la técnica resulta casi insuperable como método de análisis elemental de metales.

Esta se basa en la medida de la radiación absorbida por los átomos libres en su estado fundamental. En este proceso, el átomo pasa desde un estado energético inferior a otro superior. Para que esto ocurra es necesario suministrar energía de una longitud de onda específica del elemento el cual se quiere excitar. Para conseguir un gas de partículas monoatómicas se utiliza un atomizador de llama que nebuliza la muestra mediante un flujo de gas oxidante que se mezcla con un gas combustible (llama). De esta manera, se suministra a las moléculas la energía necesaria para romper los enlaces y obtener átomos en estado fundamental. La fuente de radiación consiste en una lámpara de cátodo hueco del elemento que se pretende analizar. Este cátodo emite las radiaciones típicas de ese elemento. Por tanto, al hacer incidir esta radiación a través de la muestra, los átomos absorberán parte de la energía emitida. La diferencia entre la energía incidente y la transmitida se recoge en un detector, permitiendo realizar una determinación cuantitativa del elemento.

Las medidas fueron llevadas a cabo en un espectrómetro de absorción atómica AAnalyst 400 PerkinElmer controlado por el sistema informático WinLab32 7.1, provisto de un quemador, un nebulizador con bola de impacto, un sistema de drenaje, una fuente de radiación (lámparas de cátodo hueco de los diferentes elementos a analizar) y un detector fotomultiplicador que convierte la luz en señales eléctricas (Figura III.11).

Figura III.11. Espectrómetro de Absorción Atómica (AAnalyst 400)

La espectroscopia de AA fue empleada para la determinación de las concentraciones de metales pesados inicialmente (C_o) y en el equilibrio (C_e) y el porcentaje de Mg disuelto en el sobrenadante tras los experimentos de adsorción. Las disoluciones fueron diluidas con agua acidificada con HNO_3 hasta alcanzar concentraciones dentro del rango de la recta de calibrado. Durante mi estancia en la Universidad de Bochum (Alemania), se utilizó un espectrómetro Analytik Jena AAS 6 Vario para determinar las concentraciones de cadmio en el electrolito antes (Ci_{el}) y después (C_{el}) de los procesos electroquímicos.

III.2.7. Espectrometría de Masas con Plasma de Acoplamiento Inductivo (ICP-MS)

La espectrometría de masas con plasma de acoplamiento inductivo, es una variante de las técnicas de análisis por espectrometría de masas. Es una técnica capaz de determinar y cuantificar la mayoría de los elementos de la tabla periódica de forma simultánea en un rango dinámico lineal de 8 órdenes de magnitud (ng L^{-1} - mg L^{-1}) y con una gran precisión.

Combina dos propiedades analíticas que la convierten en un potente instrumento en el campo del análisis de trazas multielemental. Por una parte obtiene una matriz libre de interferencias debido a la eficiencia de ionización del plasma de Ar y por otra parte presenta una alta relación señal/ruido característica en las técnicas de espectrometría de masas. Es decir, la muestra, en forma líquida, es transportada por medio de una bomba peristáltica hasta el sistema nebulizador donde es transformada en aerosol gracias a la acción de gas argón. Dicho aerosol es

conducido a la zona de ionización que consiste en un plasma generado al someter un flujo de gas argón a la acción de un campo magnético oscilante inducido por una corriente de alta frecuencia. En el interior del plasma se pueden llegar a alcanzar temperaturas de hasta 8000 K. En estas condiciones, los átomos presentes en la muestra son ionizados. Los iones pasan al interior del filtro cuadrupolar a través de una interfase de vacío creciente, allí son separados según su relación carga/masa. Cada una de las masas sintonizadas llega al detector donde se evalúa su abundancia en la muestra.

El análisis químico elemental de los metales divalente/trivalente contenidos en los distintos sistemas de HDL fue llevada a cabo en un espectrómetro Perkin Elmer ELAN DRC-e, equipado de sistema de introducción de muestras con diluidor, ionización por plasma de argón y detección de iones tipo cuadrupolo. Dispone de celda DRC para la eliminación de interferencias. Las muestras fueron disueltas en la mínima cantidad posible de HNO_3 concentrado y posteriormente diluidas. Durante mi estancia en la Universidad de Bochum, las muestras del electrolito antes y después de los procesos electroquímicos fueron enviadas a la compañía Wessling GmbH para la determinación de su contenido en plomo.

III.2.8. Espectroscopia Ultravioleta-Visible (UV-Vis)

La espectroscopia ultravioleta visible se basa en la capacidad que tienen los átomos y moléculas para absorber energía en forma de fotones dando lugar a tránsitos electrónicos.

Se basa en la absorción de radiación UV/VIS (radiación con longitud de onda comprendida entre los 200 y 800 nm) por una molécula causando la promoción de un electrón de un estado basal a un estado excitado (de mayor energía), produciéndose una atenuación (I) en la intensidad de la radiación incidente (I_0) y denominándose Transmitancia (T) a la radiación que ha sido capaz de atravesar la muestra sin ser absorbida. Los electrones que se excitan al absorber radiación de esta frecuencia son los electrones de enlace de las moléculas, por lo que los picos de absorción se pueden correlacionar con los distintos tipos de enlaces presentes en el compuesto.

Este fenómeno es descrito por la ley de Lambert Beer, la cual relaciona la absorbancia medida con la concentración de la disolución.

$$A=-log\ T=\frac{I_O}{I}=\varepsilon \cdot c \cdot l \qquad \text{(III.5)}$$

Siendo ε el coeficiente de extinción molar, c la concentración de la especie absorbente y l el camino óptico.

Las medidas se llevaron a cabo en un espectrofotómetro Perkin-Elmer UV/VIS Lambda 11.

Esta técnica fue empleada para determinar las concentraciones iniciales (C_o) de los pesticidas estudiados así como las concentraciones en el equilibrio (C_e). Previo a la cuantificación, es necesario realizar un barrido para determinar la longitud de onda máxima a la cual absorbe el compuesto.

III.2.9. Técnicas Cronopotenciométricas

Este tipo de técnicas se fundamenta en la aplicación de uno o varios pulsos de corriente entre el electrodo de trabajo y contraelectrodo, mientras se mide la variación del potencial del electrodo de trabajo respecto a uno de referencia. Se denominan técnicas cronopotenciométricas porque el potencial viene determinado como una función del tiempo o también como técnicas galvanostáticas porque se aplica al electrodo de trabajo una corriente constante. La variación de voltaje real medida en la celda electroquímica, teniendo en cuenta las pérdidas por polarización existentes en la celda, viene dada por:

$$\Delta E_{celda} = \Delta E - \Delta E_{polarización} \qquad \text{(III.6)}$$

Donde:

$\Delta E_{polarización}$ = pérdidas por polarización debidas a la resistencia existente en la transferencia de carga en la interfase electrodo-electrolito y a la caída óhmica en la disolución electrolítica.

ΔE viene dado por la ecuación de Nernst:

$$\Delta E = \Delta E^o - \frac{RT}{nF} \cdot ln\ \frac{a_{productos}}{a_{reactivos}} \qquad \text{(III.7)}$$

$$\Delta E^o = E^o_{Cátodo} - E^o_{ánodo} \qquad \text{(III.8)}$$

La cual predice una caída lineal del potencial de la celda con el tiempo de descarga cuando la concentración de productos y reactivos varía con el transcurso de la reacción.

El número de electrones es medido en términos de carga total, Q, que pasa a través del circuito. La carga es expresada en unidades de culombios (C). La relación entre la carga y la cantidad de producto formado viene dada por la ley de Faraday, es decir, el paso de 96,485.4 C provoca 1 equivalente de reacción (por ejemplo, el consumo de 1 mol de reactivo o la producción de 1 mol de producto en una reacción de un electrón) y la intensidad de corriente, I, es la tasa de flujo de culombios (o electrones), donde una corriente de 1 amperio (A) es equivalente a 1 C s^{-1}. Por tanto, la intensidad de corriente que se aplica a la celda en cada experimento electroquímico puede determinarse a partir de la siguiente ecuación (III.10) deducida de las leyes de Faraday:

$$Q = \frac{F \cdot m \cdot n}{Pm \cdot 3600} \quad \text{(III.9)}$$

$$I = \frac{Q}{t} \quad \text{(III.10)}$$

Donde:

Q=carga total o densidad de corriente (mA h)
F= constante de Faraday (96500 C mol^{-1})
m= masa del material activo, en nuestro caso metal presente en la disolución (mg)
n=número de electrones que intervienen en la reacción
Pm= peso molecular del material activo (g mol^{-1})
I=intensidad de corriente (mA)
t= tiempo necesario en horas para reducir/oxidar toda la cantidad de catión metálico (en nuestro caso procedente del electrolito)

Una batería es generalmente utilizada para almacenar energía, la capacidad de almacenamiento depende del tipo y cantidad de material activo usado (electrodo de trabajo) de ahí que la corriente usada para su evaluación tradicionalmente se base en la masa del material activo. Sin embargo, en esta tesis las baterías son

usadas para eliminar metales de una disolución por lo que la corriente aplicada en dicho proceso se basa en la cantidad de contaminante presente en el electrolito y no en la masa de la hidrotalcita que constituye el electrodo de trabajo permitiendo comparar entre procesos de eliminación con diferente concentración de metal disuelto. La terminología usada para indicar la corriente aplicada (I) en los procesos de oxidación/reducción será C/h indicando que todo el metal presente será reducido u oxidado en h horas, por ejemplo una reducción a C/20 indica que la corriente aplicada es la necesaria para reducir todo el metal en 20 horas, así es posible relacionar el tiempo del proceso de reducción (equivalente a la corriente empleada) con la cantidad de metal eliminado.

Finalmente, otra propiedad que cabría destacar es la capacidad gravimétrica designada como Q ($Ahkg^{-1}$), y que equivale a la carga suministrada por la celda (capacidad de eliminar o recuperar metal) dividida por la masa del material (HDL) que constituye el electrodo de trabajo. Este parámetro permite comparar entre electrodos de diferente masa y obtener información sobre el efecto de la carga del HDL (mg/área) en la eliminación/recuperación de metales.

Las medidas electroquímicas fueron realizadas en un potenciostato Biologic VSP-300 provisto de 6 canales.

Esta técnica fue empleada para la determinación cualitativa de la cantidad eliminada y la cantidad liberada a la disolución del contaminante metálico, tras el proceso de deposición electroquímica (reducción del metal) y recuperación (oxidación del metal) respectivamente. Además, suministra información del mecanismo y cinética de la reacción, así como de la existencia de reacciones químicas acopladas, precediendo al proceso de transferencia electrónica.

Referencias

[1] http://sitem.herts.ac.uk/aeru/footprint/es/

[2] http://www.sigmaaldrich.com/

[3] R.K. Gautam, S.K. Sharma, M.C. Chattopadhyaya, 2015. Functionalized Magnetic Nanoparticles for Heavy Metals Removal from Aqueous Solutions, In: S.K. Sharma, (Ed.), Heavy Metals in Water: Presence, Removal and Safety, Royal Society of Chemistry.

[4] T. Tavares, C. Quintelas, 2015. Biosorption of Metals – From the Basics to High Value Catalysts Production, In: S.K. Sharma, (Ed.), Heavy Metals in Water: Presence, Removal and Safety, Royal Society of Chemistry.

[5] W. T. Reichle, Synthesis of anionic clay minerals (mixed metal hydroxides, hydrotalcite), Solid State Ionics 22 (1986) 135–141

[6] http://www.ncbi.nlm.nih.gov/pccompound

[7] http://www.chemspider.com/

[8] P. Vialat, F. Leroux, C. Taviot-Gueho, G. Villemure and C. Mousty, *Electrochim. Acta* 107 (2013) 599-610.

CAPÍTULO IV
Resultados y Discusión

Applied Clay Science 80–81 (2013) 76–84

CAPRYLATE INTERCALATED LAYERED DOUBLE HYDROXIDE AS ADSORBENT OF THE LINURON, 2,4-DB AND METAMITRON

I. Pavlovic*, M.A. González, F. Rodríguez-Rivas, M.A. Ulibarri, C. Barriga

Dpto. de Química Inorgánica e Ingeniería Química, Instituto Universitario de Química Fina y Nanoquímica (IUQFN), Universidad de Córdoba, Campus de Excelencia Internacional Agroalimentario, 14071 Córdoba, Spain

GRAPHICAL ABSTRACT

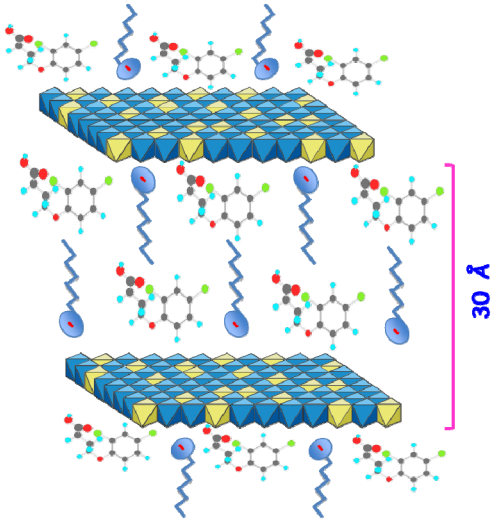

ABSTRACT

This study was carried out to elucidate the synthesis of organo-layer double hydroxide (LDH) and its capacity to adsorbs the widely applied pesticides linuron, 2,4-DB and metamitron from waters. The adsorbent (LDH-Cap) was synthesized by incorporating organic anion caprylate into magnesium aluminum layered double hydroxide with chloride as interlayer anion (LDH-Cl) via ion exchange. Characterization of the LDH-Cap adsorbent was carried out using powder X-ray diffraction (PXRD), infrared spectroscopy (FT-IR) and thermal analyses (TG and DTA). PXRD patterns indicate that caprylate anion was successfully intercalated in LDH according to the basal spacing d003 = 19.2 Å. Adsorption results indicated

that these three pesticides were adsorbed on LDH-Cap. The high percentage of initial pesticide amounts removed within the first 30 min (~90% of the total amount adsorbed) for linuron and 2,4-DB revealed a rapid adsorption process, while it was more gradual for metamitron. PXRD results suggest that adsorbed 2,4-DB and metamitron were intercalated in the LDH interlayers probably between caprylate chains and the brucite layers. Linuron was probably adsorbed on the external particle surface of LDH. Adsorption kinetic study revealed that the adsorption process followed pseudo-second-order equation. Adsorption data were well fitted to the Freundlich isotherm. The desorption of the pesticides from adsorption products were tested with three different solvents (distilled water, ethanol and acetone) and it was partial in all cases.

Keywords: LDH, Caprylate, Pesticides, Adsorption, Kinetics

1. Introduction

Contamination of natural waters is a current environmental problem and a lot of work has been done to find methods for its remediation and prevention. There is a great number and variety of water contaminants which reach the aqueous ecosystems in many ways. Therefore, different methods for their elimination from waters such as ionic exchange, adsorption, filtration, electrolysis, biodegradation, etc., exist (Bolto et al., 2002; Esplugas et al., 2002; LaPara et al., 2000; Tan et al., 2000; Zouboulis et al., 2002). The improvement of existing methods and development of new ones are a main objective for research. The adsorption on activated carbon is one of the most applied methods given its effectiveness and easy management, but due to its high cost there is a lot of interest in searching for alternatives.

Some adsorbents with good properties such as activated alumina (Kasprzyk-Hordern, 2004), zeolites (Misaelides, 2011), clays and clay minerals (Cornejo et al., 2008; Cruz-Guzmán et al., 2005) agricultural residues (Gámiz et al., 2012), etc., are suitable to substitute for activated carbon. One of the materials which have recently received considerable attention due to their good adsorptive properties is the layered double hydroxides (LDHs) or hydrotalcite-like

compounds which are scarce in nature, however inexpensive and easy to synthesize (Crepaldi et al., 2000; Newman and Jones, 1998; Rives, 2001).

The structure of LDH materials is based on hydrotalcite structure which is related to that of brucite, $Mg(OH)_2$, in which layers some of the Mg^{2+}cations in the layer structure were replaced by Al^{3+}. Thus generated excess of positive charge is balanced by intercalating of carbonate anions between layers (Cavani et al., 1991). The general formula for LDH could contain a variety of combinations of divalent and trivalent metal cations and can be written as $[M^{II}_{1-x}\, M^{II}_{x}(OH)_2 X_{x/q}] \cdot nH_2O$ where $[M^{II}_{1-x}\, M^{II}_{x}(OH)_2]^{x+}$ represents the layer, and the anions X^{q-} the interlayer together with H_2O molecules. LDHs have the ability to incorporate a variety of anions, and the intercalation chemistry and synthesis of LDHs have been the subjects of many previous studies (Braterman et al., 2004; Reichle, 1986). The adsorption properties of LDH in the case of anionic solutes (adsorbates) arise from their ability to interchange the interlayer anion with those present in the aqueous solution, as well as to reconstruct the LDH structure from their calcined product. Mixed oxides formed by calcining of LDH at 500 °C, when put in water, could recover again the LDH structure by incorporating anions present in aqueous solutions (Hermosín et al., 1996; Houri et al., 1998). In the case of non ionic adsorbate, the LDH adsorbent properties should be improved by modifying their interlayer through intercalating large organic anions (organo-LDHs) which could provide the media for the hydrophobic host– guest interactions (Bruna et al., 2006, 2008; Klumpp et al., 2004; Wang et al., 2005). LDHs can be also functionalized with the intercalation of ligands and the solids thus obtained showed uptake capacity for heavy metal cations such as Cu^{2+}, Cd^{2+}, and Pb^{2+} (Pavlovic et al., 2009; Perez et al., 2006).

On the other hand, the pesticides are compounds which could be considered emerging environmental contaminants. These chemicals are generally applied to agricultural soils in amounts which exceed those required to control plagues, weeds, etc., in order to compensate for the losses caused by leaching, run-off, degradation, etc., which is the reason why these compounds sometimes reach unacceptable levels in ground waters (Gerstl et al., 1998). The EC Drinking Water Directive (80/778/EC) stipulates the requirement that no single pesticide should exceed 0.1 mg/L and total pesticides should not exceed five-fold of this level in

drinking water from the tap. The aim of this work was to study the possibility of using the LDH intercalated with the organic anion caprylate, LDH-Cap, as a novel adsorbent for the removal of widely applied and toxic pesticides such as linuron, metamitron and 2,4-DB from aqueous solutions. To our knowledge there are no reported studies on caprylate-intercalated LDHs as adsorbents of water contaminants. We also tried to compare the adsorption capacity of LDH-Cap with other pesticide adsorbents, previously studied and reported by our research group, such as the uptake of linuron and metamitron by LDH intercalated by dodecyl sulfate or sebacate anions. The three pesticides studied here are actually widely used and they work by inhibiting photosynthesis in targeted weed plants in crops of cotton, potato, corn, bean, asparagus, carrot, and fruit (www.herts.ac.uk/aeru/projects/ppdb/). They have a toxic effect on human health and the environment (www.pesticideinfo.org). The effect of various parameters such as the pH of the solution, the contact time and the initial pesticide concentrations on the adsorption capacity of LDH-Cap were studied as well as the kinetics of the adsorption processes. Furthermore, in order to explore the type ofhost–guest interactions involved in the adsorption mechanism, the elution of pesticides from LDH-Cap with different solvents was also studied.

2. Materials and methods

2.1. Pesticides and other chemicals

The sodium caprylate (sodium octanoate) used in the preparation of the adsorbent, as well as linuron ([3-(3,4-dichlorophenyl)-1-methoxy-1-methylurea], 2,4-DB ([4-(2,4-dichlorophenoxy) butyric acid]) and metamitron ([4-Amino-3-methyl-6-phenyl-1,2,4-triazin-5-one)] pesticides were supplied by Sigma-Aldrich (Spain). The molecular structure and some characteristics of the studied pesticides are shown in Fig. 1 and Table 1. The concentration of the pesticides was measured using a PerkinElmer model Lambda 3B UV–visible spectrophotometer at λ_{max} corresponding to the maximum adsorption for each pesticide solution.

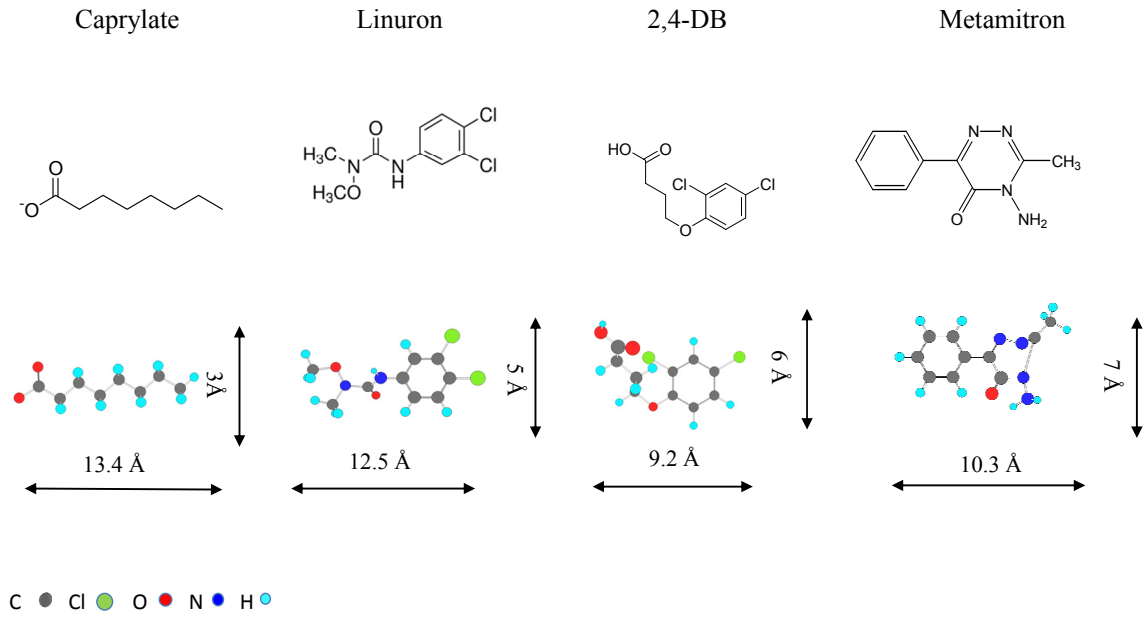

Fig. 1. Schematic representation of molecular structure of caprylate anion and pesticides.

Table 1
Characteristics of the pesticides studied.

Pesticide	Solubility[a] (mg/L)	pKa	Concentration[b] (mM)
Linuron	81	12.1	0.042-0.19
2,4-DB	46	4.1	0.05-0.12
Metamitron	1800	2.9	0.10-3.00

[a] Solubility in water
[b] Pesticide concentrations used in adsorption experiment

2.1.1. Synthesis of the adsorbents

The LDH with chloride as the interlayer anion $[Mg_3Al(OH)_8]Cl{\cdot}nH_2O$ (LDH-Cl),was prepared by the coprecipitation of 0.075 mol $MgCl_2{\cdot}6H_2O$ and 0.025 mol of $AlCl_3{\cdot}H_2O$, in 250 mL of the 0.025 mol of NaCl solution, under N_2 stream and using CO_2 free water. The pH was maintained at 8 using a 0.1 M NaOH solution. The suspension was hydrothermally treated at 80 °C for 24 h and then washed with distilled water and dried at 60 °C.

The adsorbent $[Mg_3Al(OH)_8]C_8H_{15}O_2$ (LDH-Cap) was obtained by the anion exchange method by suspending 1 g of previously obtained LDH-Cl in 500 mL of the 0.014 M sodium caprylate solution under N_2 stream at 75 °C and pH 8. The suspension was settled for 24 h and then washed, centrifuged and the precipitate was dried at 60 °C.

2.1.2. Adsorption–desorption experiments

The adsorption experiments were carried out by adding duplicate samples of 0.03 g of adsorbent LDH-Cap in 30 mL of aqueous solution of the pesticide. The initial concentration used in the pH and kinetic experiments were those of maximum solubility for linuron and 2,4-DB, C_o= 0.19 mM and C_o= 0.12 mM, respectively, and C_o= 1 mM for metamitron. The adsorption of pesticides on HT-Cap was measured by a batch equilibration technique and the proper solid/solution amounts were put into polypropylene centrifuge tubes. The suspensions were shaken at room temperature at 52 rpm (24h in the pH study and a range between 0.5 and 24 h in the kinetic study). The concentration range used in adsorption isotherm studies depended on the solubility (Table 1) of the pesticides whereas the contact times were determined by kinetic experiments (2 h for linuron and 2,4-DB and 5 h for metamitron).

The amount of pesticides adsorbed on LDH-Cap was calculated from the difference between the initial and equilibrium solution concentrations. The supernatants were filtered and used to determine the amount of remaining pesticides in the solutions after adsorption on LDH by UV–Vis spectrophotometry at 245, 228 and 305 nm for linuron, 2,4-DB and metamitron, respectively. A five-point calibration curve (a concentration range where the absorbance/concentration curve was lineal) was run before each analysis. The samples were diluted for its fitting to calibration curves, and measured. The blanks were also registered (only the adsorbent in distilled water under the same experimental conditions as the sample studied was used) but no interferences were found.

The suspensions were shaken at 52 rpm at room temperature and after suitable time were centrifuged. The resulting supernatants were filtered and used to determine the amount of pesticides adsorbed by the LDH, using UV– Vis

spectroscopy. The amounts of pesticides adsorbed per gram of adsorbent, q (mmol g^{-1}), were calculated as follows:

$$q = (C_o - C_e)\, V/W \quad (1)$$

where C_o and C_e are the initial and equilibrium solution concentrations (mmol L^{-1}), W is the weight of solids (g) and V is the pesticide solution volume (L). The experimental adsorption data were fitted to the Langmuir and Freundlich models, often used to describe adsorption processes and in which lineal forms are represented in Eqs. (2) and (3):

$$C_e/q = (1/q_m)C_e + 1/q_m K_L \quad (2)$$

where q_m is the maximum adsorption capacity at the monolayer coverage (mmol/g) and K_L (L/mmol) is a constant related to the adsorption energy.

$$\log q = \log Kf + Nf \log Ce \quad (3)$$

where K_f ($mmol^{1-Nf}\ L^{Nf}\ g^{-1}$) and N_f are Freundlich parameters, which are characteristic of the adsorbent-sorbate systems (Travis and Etnier, 1981).

In order to evaluate the possibility of regeneration of the adsorbent as well as to assess the adsorption mechanism, desorption experiments were also performed, as follows. The adsorption products LDH-Cap–pesticide (last isotherm points) were dried and 0.05 g of duplicate samples were treated with 7 mL of different solvents and shaken for 10 min. Water, ethanol or acetone was the solvent used in order to determine the best desorption conditions. Then, the supernatants were centrifuged for the pesticide quantification by UV–Vis spectrophotometry (ethanol and acetone were evaporated and the solid remains dissolved in water).

2.2. Characterization techniques

The adsorbent and the adsorption products were studied by different physical chemical techniques. Powder X-ray diffraction patterns were recorded at room temperature under air conditions using a Siemens D-5000 instrument with CuK α radiation (λ = 1.54050 Å), the step size and step counting time used were 0.02° (2 θ) and 0.65 s respectively. FT-IR spectra were recorded with a Perkin Elmer Spectrum One spectrophotometer using KBr disk method. TG and DTA

curves were recorded on a Setaram Setsys Evolution 16/18 apparatus, in air at the heating rate of 5 °C/min.

3. Results and discussion

3.1. Characterization of adsorbent precursor and adsorbent

The PXRD pattern of LDH-Cl confirmed the presence of chloride as an interlayer anion by the basal spacing d_{003} = 7.8 Å and its corresponding harmonics. Taking into account that this basal spacing is very similar to that of the carbonate anion, the presence of carbonate impurities in the interlayer is also possible. The PXRD pattern of LDH-Cap (Fig. 2a), with the basal spacing d_{003} = 19.2 Å, is very similar to that already reported for caprylate-intercalated into Mg–Al–LDH (Iyi and Sasaki, 2008). Taking into account 4.8 Å as the hydrotalcite-layer thickness, the gallery height is 14.4Å. Since the caprylate length is a proximately 13.4 Å (CSChem 3D 5.0 Program), this anion is probably oriented in a vertical position together with the water molecules in the interlayers.

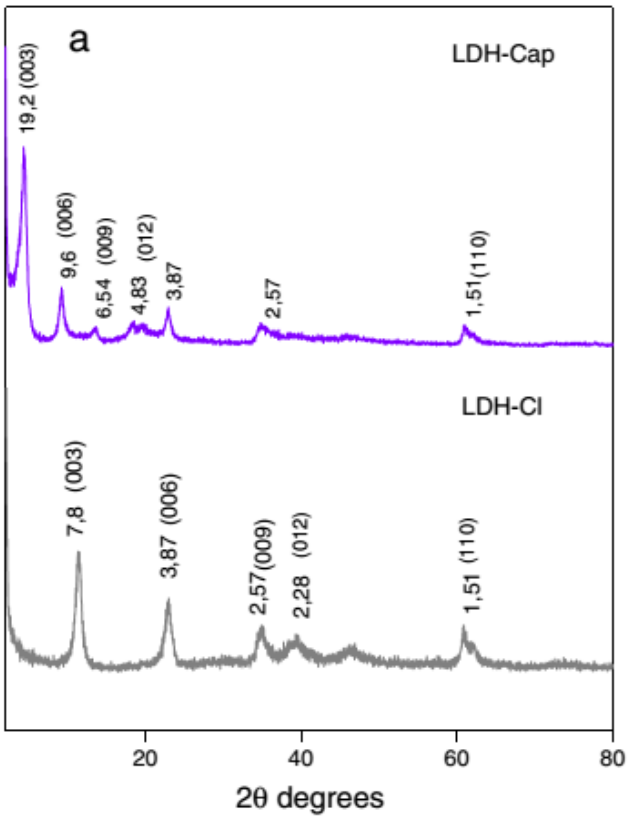

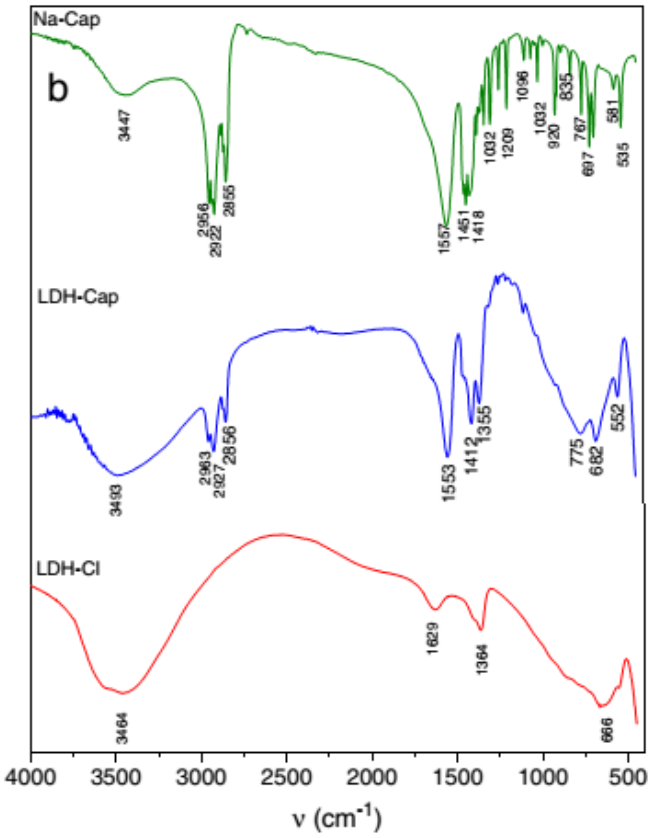

Fig. 2. PXRD patterns of a) LDH-Cl precursor and LDH-Cap adsorbent and b) FT-IR spectra of LDH-Cl precursor, LDH-Cap adsorbent and sodium caprylate (Na-Cap).

The FT-IR spectra (Fig. 2b) show the characteristic features of the hydrotalcite structure which are a broad band at around 3500 cm^{-1}, corresponding to the stretching vibration of OH^- groups of hydration water molecules and free OH^- groups of the brucite layers, and a band at 1629 cm^{-1}, corresponding to the bending vibration of water molecules. The band at 1364 cm^{-1} is attributed to the stretching vibration of carbonate anion which could also be present in the interlayer together with the chloride, due to the CO_2 contamination, difficult to avoid during the synthesis in spite of inert atmosphere maintained (Bellamy, 1978; Rives, 200). The most characteristic bands of caprylate in the LDH-Cap adsorbent are the bands at 1553 cm^{-1}, 1412 cm^{-1} and 1355 cm^{-1} due to carbonyl absorptions from carboxylate groups of caprylate, and the bands at 2963, 2927 and 2856 cm^{-1} which correspond to C–H stretching vibrations of the aliphatic chains.

The results of the thermal study of LDH-Cl and LDH-Cap samples are shown in Fig. 3. The DTA curve of the LDH-Cl precursor showed two endothermic effects, characteristic for hydrotalcite-like compounds, at 126 and 409 °C as well as their corresponding weigh losses. The first one is attributed to the loss of the physisorbed and interlayer water, and the second endothermic effect corresponds to a simultaneous loss of interlayer chloride, interlayer carbonate and the dehydroxylation of layers. In the DTA curve corresponding to LDH-Cap, the first endothermic peak related to physisorbed and interlayer water loss is not easy to quantify, because it is overlapped by a very high exothermic peak proceeding from the combustion of interlayer organic anion caprylate at 316 °C.

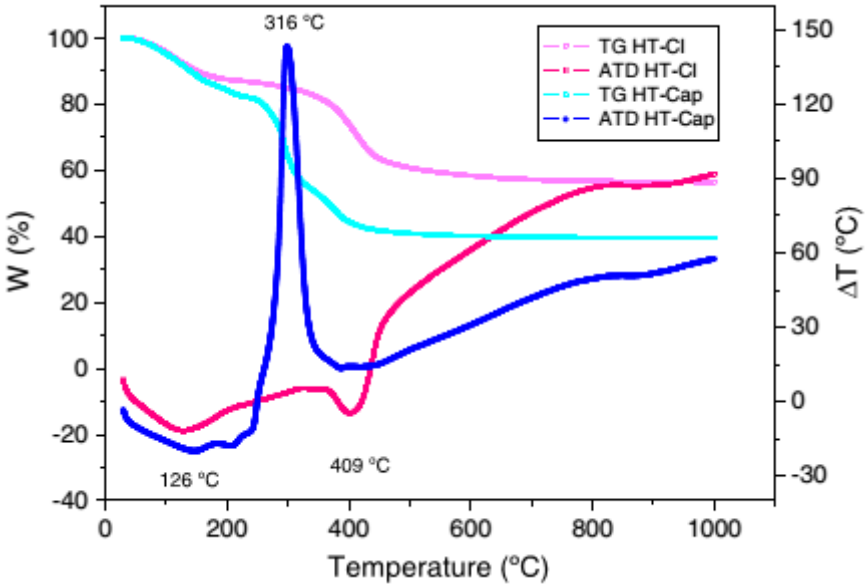

Fig. 3. TG and DTA curves of HT-Cl and LDH-Cap.

3.2. Adsorption and desorption experiments

3.2.1. pH influence and the contact time effect on pesticide adsorption

The pH experiments indicated that the variation of the initial pH of the solutions did not have influence on the amount of the pesticides removed by LDH-Cap (data not shown) and the final pHs were 7±0.5 for initial pH = 7 and 6±0.5 for initial pH = 5, due to the buffering property of hydrotalcite-like compounds. Therefore, the further adsorption experiments were carried out under the pH of

initial pesticide solutions which were all in the pH range between 6 and 7. These pH values are interesting because they are common for most of the natural waters.

The effect of contact time on the adsorption efficiency of LDH-Cap for the pesticides was also studied (Fig. 4). The results show that the adsorption of linuron and 2,4-DB was almost instantaneous while the adsorption of metamitron was more gradual. Although the main part of this pesticide (~90% of the total amount removed) was removed in 5 h, at 24 h the adsorption equilibrium had not been reached yet. This could be explained if we suppose that the diffusion is a limitation step in the adsorption of metamitron on LDH-Cap. It seems there should be enough time for bulky metamitron molecules to diffuse through the laminar layer and into pores to reach maximum adsorption, and 24 h is not enough to reach its full adsorption capacity as can be seen in Fig. 4.

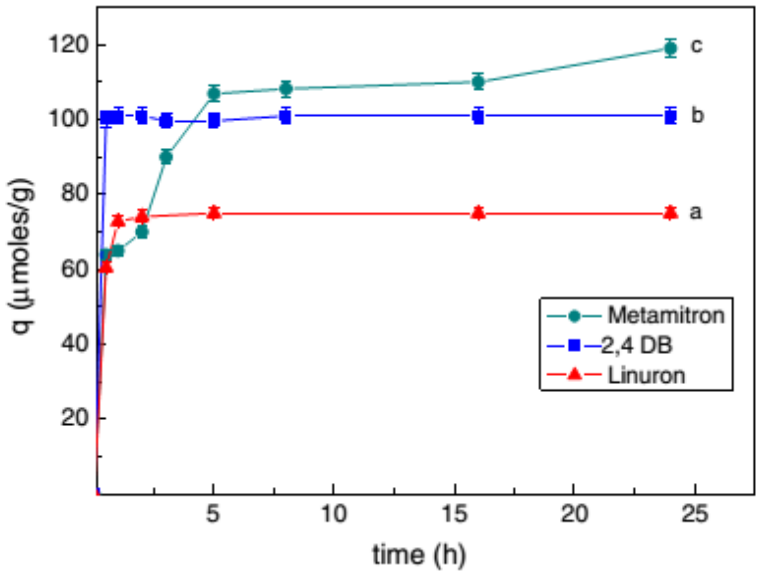

Fig. 4. Time evolution of the pesticide adsorption on LDH-Cap: a) linuron b) 2,4-DB and c) metamitron.

3.2.2. Kinetic modeling

The adsorption kinetic is an important aspect of the pollutant removal process control. The data in Fig. 4 were fitted using the two most widely used models in the literature to describe the adsorption process (i.e. pseudo-first-order Eq. (4), pseudo-second-order Eq. (5)) which can be expressed as follows:

$$\log (q_e - q_t) = \log q_e - (K_1/2.303)t \quad (4)$$

$$t/q_t = 1/(k_2 q_e^2) + (1/q_e)t \quad (5)$$

where q_e and q_t are the amounts of adsorbed pesticide at equilibrium and t time (mg g^{-1}), respectively, and k_1 (min^{-1}) is the pseudo-first order rate constant and k_2 (g (mg $min)^{-1}$) the pseudo-second-order rate constant.

The parameters of the kinetic models and the linear regression coefficients (R^2) were obtained and shown in Table 2. The kinetic data were fitted better to Eq. (5) for the three pesticides based on the correlation coefficient R^2 and the q_e values calculated from the pseudo-second-order rate model which are very consistent with the experimental q_e values (included in Table 2). This indicates that the experimental kinetic data for adsorption by LDH-Cap adsorbent work well with this model for the entire range time. These results suggested that the pseudo-second order adsorption mechanism was predominant, and that the overall rate of the pesticide adsorption process appeared to be controlled by a chemisorption process as was indicated by Ho (2006). The pseudo-second-order rate expression has been widely applied to the adsorption of pollutants from aqueous solutions (pesticides, dyes, metal ions, oils, and organic substances). In many cases the value of q_e is impossible to know from the experimental data because the adsorption process tends to become immeasurably slow and the amount adsorbed significantly smaller than the equilibrium amount. This model enables us to know the q_e equilibrium amount by simply using a lineal fitting of the experimental data (Ho, 2006). On the other hand, intra-particle diffusion model is commonly used for identifying the adsorption mechanism for design purposes. According to Weber and Morris (1963), for most adsorption processes, the uptake varies almost proportionally with $t^{1/2}$ rather than with the contact time and can be represented as follows:

$$q_t = K_p t^{1/2} + C \quad (6)$$

where k_p (mg g^{-1} $min^{-0.5}$) is the rate constant of intra-particle diffusion.

Table 2

Coefficients of pseudo-first-order, pseudo-second-order and intra-particle diffusion model for adsorption of linuron, 2,4-DB and metamitron by LDH-Cap.

Sample		*Pseudo-first-order model*			*Pseudo-second order model*			*Intra-particle diffusion model*		
	$q_{e\,Exp}$ *(mg.g^{-1})*	k_1 *min^{-1}*	q_e *(mg.g^{-1})*	R^2	k_2 *g(mg.min^{-1})*	q_e *(mg.g^{-1})*	R^2	k_p *(mg.g^{-1}min^{-1})*	C	R^2
Linuron	18.7±0.3	0.003±0.001	0.48±0.14	0.545	0.0191± 0.0003	18.59±0.001	0.999	0.062±0.08	17±1	0.329
2,4 DB	25.2±0.5	0.194±0.001	0.353±0.03	0.710	0.243± 0.002	25±0.006	1	0.063±0.003	24.990± 0.0008	0.331
Metamitron	22.3±0.4	0.0058±0.001	10.2±0.3	0.934	0.0009± 0.0005	23.25±0.006	0.997	0.430±0.09	11±3	0.802

According to Eq. (6), the plot of q_t versus $t^{1/2}$ should be a straight line with a slope k_p which is the intra-particle diffusion rate constant (mg g^{-1} $min^{-0.5}$) and intercept at C, when the adsorption mechanism follows the intra-particle diffusion process. The value of C gives an idea about the thickness of boundary layer i.e. the larger the intercept the greater is the boundary layer effect (Mall et al., 2006). The straight line deviation from the origin may be because of the difference in the rate of mass transfer in the initial and final stages of adsorption. In some cases the plot q_t versus square root time can show multilinearity which indicates that several steps occur in the process (Dawood and Sen, 2012; Dotto and Pinto, 2011; Mall et al., 2006). Each section of the curves represents the different stages in the adsorption process: the first part is due to surface adsorption and external diffusion (boundary layer diffusion). The second part is the gradual adsorption step where the intra-particle diffusion is rate controlled. The plateau (third part) is the final equilibrium step where the intra-particle diffusion starts to slow down due to the low solute concentration in the solution. In addition, if the regression passes through the origin, the intra-particle diffusion is the only rate-limiting step. The correlation coefficients for the intra-particle diffusion model included in Table 2 show that the adsorption plot is not linear over the whole time range for the three studied pesticides. However, the plot of Eq. (6) for metamitron adsorption, included in Fig. 5, shows three sections. In this case, the bulky molecule of metamitron has an important effect into the control of the rate at the initial time and the limiting step is the boundary layer diffusion or film diffusion. However, the 2,4-DB and linuron plots (Fig. 5) show two different stages: external mass transfer followed by intraparticle diffusion. The pesticide molecules seem to be transported to the external surface of the LDH-Cap through film diffusion and the k_{p1} (the rate constant corresponding to first section included in Fig. 5 as the slope of the line) was higher for linuron than for 2,4-DB where the value of C was lower and then the plateau was reached. This could be due to the different structures of the pesticides and their affinity for the adsorbent which are important to determine the mechanism of the adsorption. Moreover, from Fig. 5 it can be deduced that none of the plots show linear straight line sections that pass through the origin. This indicates that the intra-particle diffusion is involved in the adsorption process but it is not the only rate-limiting step. It can be concluded that the adsorptions of

these pesticides on the LDH-Cap were multi-step processes, involving adsorption on the external surface, intra-particle diffusion and chemical interaction (adsorption of the pesticide at the active site via hydrophobic and/or hydrophilic interaction).

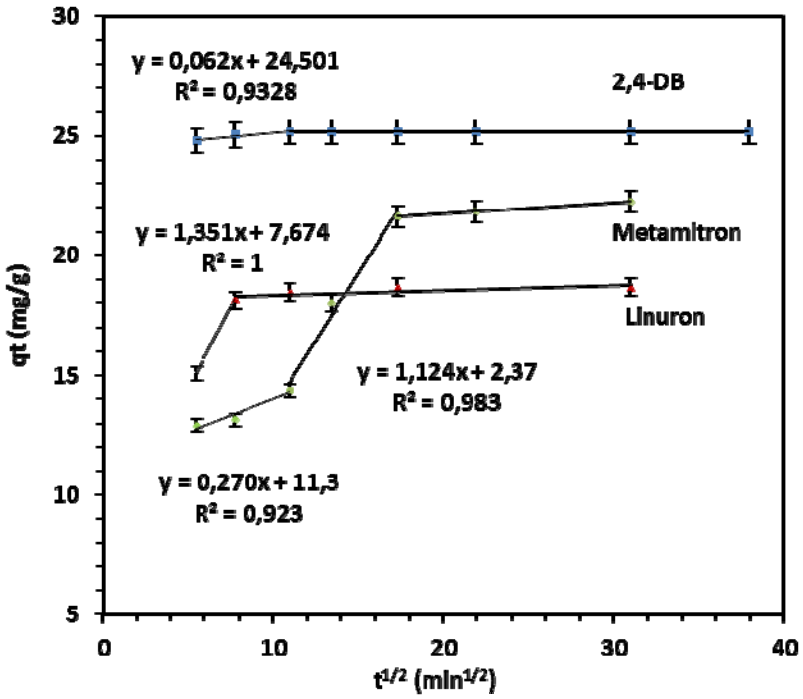

Fig. 5. Intra-particle diffusion model of pesticides adsorption on LDH-Cap.

3.2.3. Adsorption equilibrium isotherms

The adsorption isotherms of the three pesticides are given in Fig. 6. According to the classification of Giles et al., 1960, the shape of all adsorption isotherms was C-type. This type of isotherm indicates that there is a minimum or no competition of adsorbate molecules with other anions from the water solution for the adsorbent sites, i.e. there is a constant partition of adsorbate between the adsorbent and the solution.

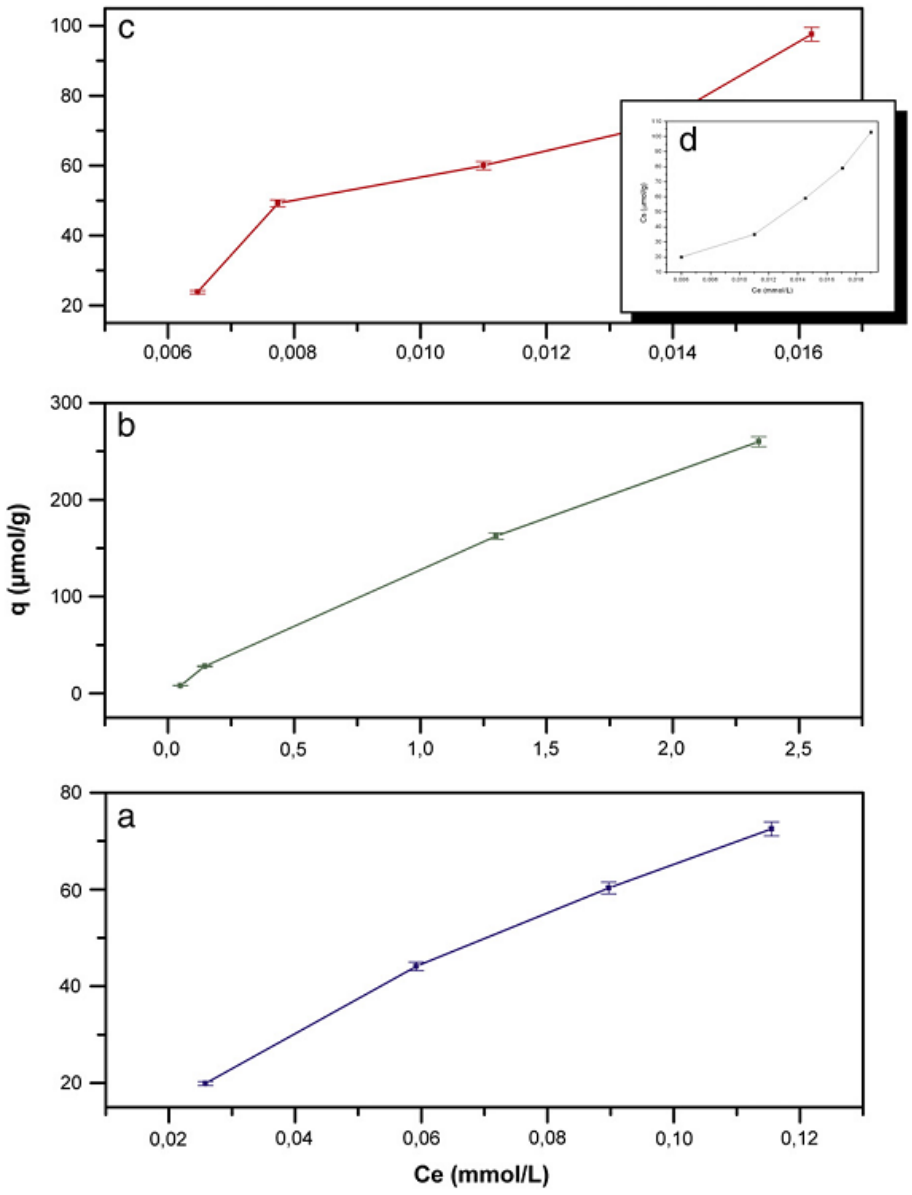

Fig. 6. Adsorption isotherms of a) linuron, b) metamitron, c) 2,4-DB on LDH-Cap and d) 2,4-DB on LDH-Cl.

The maximum amount of pesticide removed from the solution per gram of adsorbent was in the case of metamitron (q = 260 µmol/g vs. q = 72 µmol/g for linuron and q = 102 µmol/g for 2,4-DB), probably due to the higher initial concentrations used in the case of metamitron which was enabled by its higher solubility (Table 2). Notwithstanding, even in this case the isotherm "plateau" was not reached which indicates that under these conditions the maximum adsorption capacity of LDH-Cap was not saturated. However, the amounts of metamitron adsorbed here were higher than those reported for this pesticide on LDH intercalated with dodecyl sulfate, LDH– DDS, (100– 170 µmol/g) for the same

initial concentrations and under similar experimental conditions (Bruna et al., 2006). In the last case, the adsorption isotherm shape was different from that in the present study and indicated two different types of interactions between the adsorbent and the adsorbate (Giles et al., 1960). The authors suggested that the $-NH_2$ groups of metamitron could be involved in the hydrogen bonding with $SO4^{2-}$ groups of dodecyl sulfate (DDS), besides the hydrophobic adsorption of the pesticide on the alkyl chains of DDS. On the other hand, the amount of linuron adsorbed here, was similar to that reported for its adsorption on LDH intercalated by sebacate (LDH-SEB) q = 110 μmol/g, but it was lower than that of linuron adsorbed by LDH–DDS (q = 170 μmol/g) under similar experimental conditions (Chaara et al., 2012). Therefore, a different interlayer composition (functional groups and aliphatic tales) and/or the height of the interlayer gallery seems to have some influence in the interaction of metamitron and the hydrophobic part of interlayer anion.

In order to compare the adsorption behavior of the three pesticides studied here, the adsorption experiments were also performed on the inorganic layered double hydroxide, LDH-Cl, under the same experimental conditions. The adsorption of linuron and metamitron on LDH-Cl was negligible (under 5% of the initial concentration) while the adsorption of the 2,4-DB was close to that measured for LDH-Cap (q = 102 μmol/g). The anionic character of this pesticide probably provides more affinity between adsorbent and the adsorbate. Similar adsorption results were reported for the adsorption of herbicide 2,4-dichlorophenoxyacetate (2,4-D) (with similar structure to 2,4-DB) on LDH-Cl (Pavlovic et al., 2005). This suggests that the 2,4-DB pesticide could be adsorbed on organic and inorganic LDH on the first one by hydrophobic interactions through aromatic ring and on the second by ion–ion interactions between its carboxylic group and the positively charged layers.

The adsorption isotherm data were fitted to the Langmuir and Freundlich equations, but were mostly in agreement with the Freundlich equation where the regression coefficient (R^2) was in the range of 0.880–0.994 while that of Langmuir was ~0.4 (not shown). For the Langmuir model there is an important assumption that the adsorbate is adsorbed in monolayer, all surface sites are energetically equivalent and that the surface is homogeneous. The Freundlich isotherm can also

be used to model the adsorption processes on heterogeneous surfaces. In this model, due to its exponential character it is not possible to represent the maximum adsorption on surfaces. The agreement of the adsorption data with the Freundlich equation suggests the existence of heterogeneity of sites and different adsorption energies on the surface and this could be in accordance with the type of adsorbent here used which consists of different components (inorganic and organic) (Bruna et al., 2006; Dawood and Sen, 2012; Lazaridis and Asouhidou, 2003; Travis and Etnier, 1981). The Freundlich parameters are included in Table 3.

Table 3
Freundlich model parameters for pesticide adsorption on LDH-Cap

Sample	K_f ($\mu mol^{1-Nf}\ g\ L^{Nf}$)	N_f	R^2
Linurón	1.22±0.08	0.87±0.04	0.994
2.4-DB	2.6±0.9	1.29±0.30	0.880
Metamitrón	0.29±0.03	0.88±0.06	0.992

3.2.4. Desorption processes

Fig. 7 indicates that only a partial desorption of the studied pesticides occurs with three different solvents. Linuron desorption was quite low with the three solvents used, slightly higher with acetone in agreement with its low polarity. The lowest percentages of metamitron desorbed are in agreement with its high affinity for LDH-Cap together with the higher amounts of this pesticide adsorbed in LDH-Cap–pesticide complex compared to the two other pesticides (see adsorption values of the last isotherm points, Fig. 6). As it will beseen below the metamitron is well intercalated in the interlayer LDH-Cap space which makes it less accessible to the solvent under experimental conditions studied here. Higher percentages of 2,4-DB eluted by ethanol are probably related to the higher solvate–solvent affinity due to their similar polarities. The structure of 2,4-DB with two different entities could enable the adsorption of this pesticide on LDH-Cap by involving two different types of host–guest interactions: electrostatic interactions between the carboxylate groups of pesticide with the positive charge of the external particles surface and the hydrophobic ones between the aromatic ring of

2,4-DB and alkylic chains of caprylate, as will be confirmed below in the PXRD study.

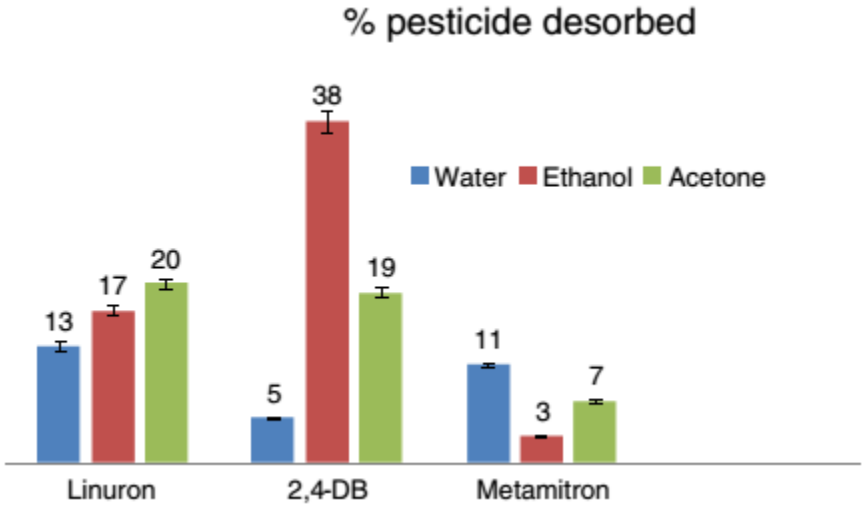

Fig. 7. Desorption percentage of the pesticides with different solvents.

3.3. Characterization of the adsorption products

When the PXRD pattern of LDH-Cap was compared to that of the adsorption products LDH-Cap–pesticide (Fig. 8), the appearance of a new peak d_{003} ~ 30 Å was observed in 2,4-DB and metamitron. Taking into account the layer thickness and the pesticides and caprylate lengths (Fig. 1), it could be concluded that these two pesticides are intercalated into the interlayer LDH space after adsorption. A decrease of the intensities of (00l) reflections in the patterns of the adsorption products LDH-Cap–pesticide has been observed. The incorporation of the pesticide molecules into the interlayer space could account for the decrease of the crystallinity in the adsorption products, due to the interlayer disorder caused by the presence of a new species. A shift to lower angles of the first basal reflection was also observed, giving a spacing that is greater than the original values (from 19.2 to 21.0Å in Fig. 8). These effects are typical for layered structures which contain stacking fault interstratification effects or other imperfections (Drits and Bookin, 2001). Some of these structural imperfections could be caused here by the adsorption process and the handling during the experiments (interaction with the pesticide, stirring of the suspension, LDH weathering…). In the LDH-Cap–2,4-DB

pattern, the presence of two phases could be observed despite their low crystallinity. Thus, there is a phase, with a basal spacing of $d_{003} \sim 30$ Å and its corresponding higher order reflections, in addition to a phase with a basal reflection of $d_{003} \sim 21$ Å, which suggests the co-existence of the LDH-Cap–2,4-DB complex phase and the adsorbent LDH-Cap phase. The difference between this pattern (Fig. 8c) and LDH-Cap–metamitron (Fig. 8d), is that there is only one adsorbent–pesticide complex phase observed in the latter ($d_{003} \sim 30$ Å), which is probably due to the higher amount of metamitron adsorbed (q = 260 μmol/g) compared to that of 2,4-DB (q=102 μmol/g). An important increase of the interlayer space found in the aforementioned metamitron adsorption, however, was not observed in its adsorption on LDH– DDS (Bruna el al., 2006), which is in accordance with higher amounts removed by LDH-Cap. The basal spacing of LDH-Cap–linuron PXRD (Fig. 8b) does not change significantly compared to the pure adsorbent pattern which suggests that this pesticide is probably adsorbed on the external surface of LDH particles. This was also observed in the adsorption of linuron on LDH intercalated with dodecyl sulfate and sebacate (Chaara et al., 2012).

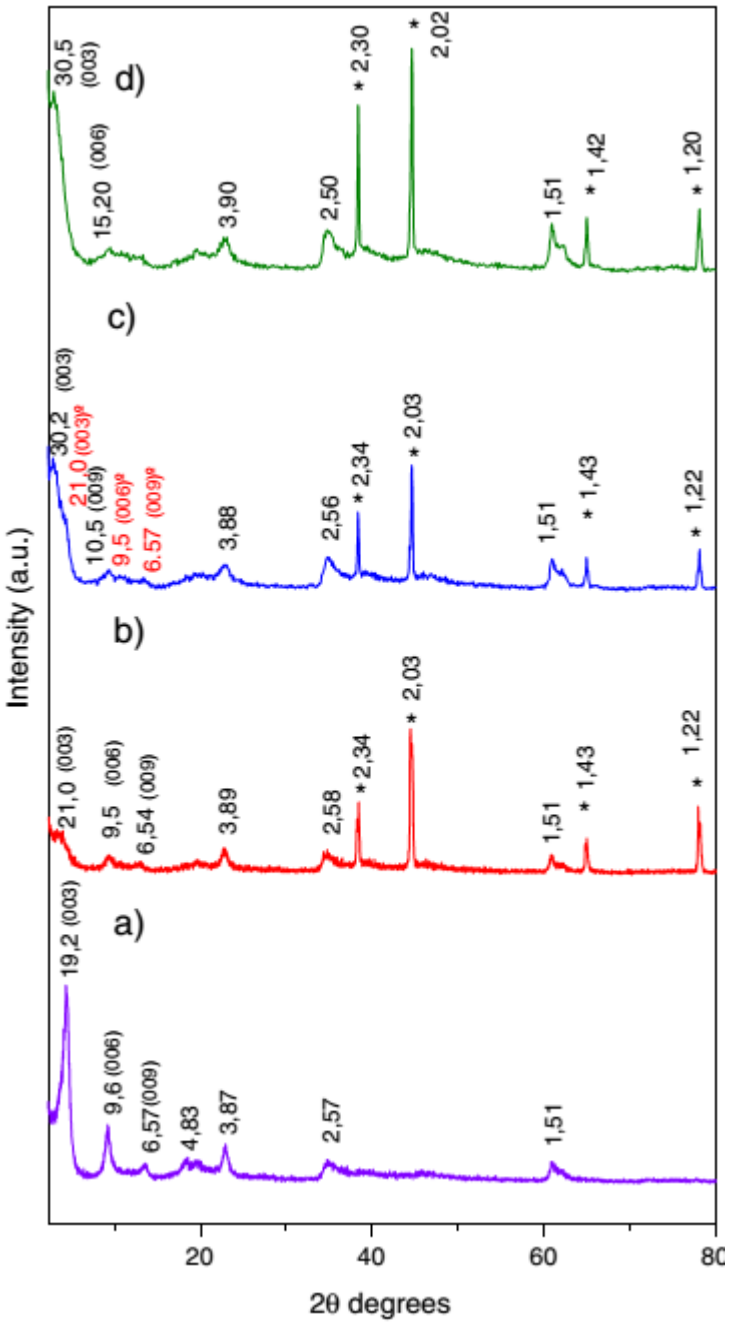

Fig. 8. PXRD patterns of the adsorbent and the adsorbent-pesticide complexes corresponding to the last isotherm point (°LDH-Cap phase, *Al sample holder): a) LDH-Cap, b) LDH-Cap–linuron, c) LDH-Cap-2,4-DB and d) LDH-Cap-metamitron.

4. Conclusions

The fast adsorption of pesticides studied here and the shapes of their adsorption isotherms on LDH-Cap suggest a great adsorbent/adsorbate affinity.

Comparative study of the adsorption of these pesticides on inorganic LDH-Cl suggests that the organophilic LDH modification improves the uptake of linuron and metamitron, whereas the adsorption of 2,4-DB was almost the same, probably due to the presence of carboxylate group together with the organic entity. Metamitron and linuron uptake by LDH-Cap was also compared to their uptake reported in our previous papers for LDHs with similar organic interlayer anions dodecyl sulfate (DDS) and sebacate (SEB) under similar experimental conditions.

There was no clear relationship observed between pesticide amounts adsorbed and the nature of organic interlayer anions. However, isotherm shapes and d003 reflections suggest that a different combination of hydrophobic–electrostatic interactions probably determines the amounts of these pesticides on different organically-tuned LDHs. PXRD results suggest that adsorbed 2,4-DB and metamitron were intercalated in the LDH interlayers while linuron was probably adsorbed on the external particle surface of LDH. The desorption experiments were performed with different solvents but pesticides were desorbed only partially.

Consequently, LDH-Cap could be a suitable water decontaminant with these pesticides, judging by the high percentage of the initial pesticide concentrations removed by it. Notwithstanding, more exhaustive investigations should be carried out in order to study adsorbent behavior in natural conditions, recycling optimization, etc.

Acknowledgments

This work was partially funded by the MCI (CTM 2011-25325) and the Junta de Andalucía through Research Group FQM-214. Fredy González acknowledges a grant from the Fundación Carolina to research at the University of Córdoba (Spain).

References

- Bellamy, L.J., 1978. The Infrared Spectra of Complex Molecules. Chapman and Hall, London.

- Bolto, B., Dixon, D., Eldridge, R., King, S., Linge, K., 2002. Removal of natural organic matter by ion exchange. Water Research 36, 5057–5065.

- Bratermann, P.S., Xu, Z.P., Yarberry, F., 2004. Layered double hydroxides (LDHs). In: Auerbach, S.M., Carrado, K.A., Dutta, P.K. (Eds.), Handbook of Layered Materials. Marcel Decker, Inc., New York, pp. 373–474.

- Bruna, F., Pavlovic, I., Barriga, C., Cornejo, J., Ulibarri, M.A., 2006. Adsorption of pesticides carbetamide and metamitron on organohydrotalcite. Applied Clay Science 33, 116–124.

- Bruna, F., Pavlovic, I., Celis, R., Barriga, C., Cornejo, J., Ulibarri, M.A., 2008. Organohydrotalcites as novel supports for the slow release of the herbicide terbuthylazine. Applied Clay Science 42, 194–200.

- Cavani, F., Trifiro, F., Vaccari, A., 1991. Hydrotalcite-type anionic clay: preparation, properties and application. Catalysis Today 11, 173–301.

- Chaara, D., Bruna, F., Draoui, K., Ulibarri, M.A., Barriga, C., Pavlovic, I., 2012. Study of key parameters affecting sorption of the herbicide linuron by organohydrotalcites. Applied Clay Science 58, 34–38.

- Cornejo, J., Celis, R., Pavlovic, I., Ulibarri, M.A., 2008. Interactions of pesticides with clays and layered double hydroxides: a review. Clay Minerals 43, 155–176.

- Crepaldi, E.L., Pavan, P.C., Valim, J.B., 2000. Anion exchange in layered double hydroxides by surfactant salt formation. Journal of Materials Chemistry 10, 1337-1343.

- Cruz-Guzmán, M., Celis, R., Hermosín, M.C., Koskinen, W., Cornejo, J., 2005. Adsorption of pesticides from water by functionalized organobentonites. Journal of Agricultural and Food Chemistry 53, 7502–7511.

- Dawood, S., Sen, I.K., 2012. Removal of anionic dye Congo from aqueous solution by raw pine and acid-treated pine cone powder as adsorbents: equilibrium, thermodynamic, kinetic, mechanism and process design. Water Research 461, 1933–1946.

- Dotto, G.L., Pinto, L.A.A., 2011. Adsorption of food dyes acid blue 9 and food yellow 3 onto chitosan: stirring rate effect in kinetics and mechanism. Journal of Hazardous Materials 87, 164–170.
- Drits, V.A., Bookin, A.S., 2001. Layered double hydroxides: present and future. (Chapter 2) In: Rives, V. (Ed.), Nova Science Publishers, N.Y. Esplugas, S., Gimenez, J., Contreras, S., Pascual, E., Rodriguez, M., 2002. Comparison of different advanced oxidation processes for phenol degradation. Water Research 36, 1034–1042.
- Gámiz, B., Celis, R., Cox, L., Hermosín, M.C., Cornejo, J., 2012. Effect of olive-mill waste addition to soil on sorption, persistence and mobility of herbicides used in Mediterranean olive groves. Science of the Total Environment 429, 292–299.
- Gerstl, Z., Nasser, A., Mingelgrin, U., 1998. Controlled release of pesticides into soils from clay–polymer formulations. Journal of Agricultural and Food Chemistry 46, 3797–3809.
- Giles, C.H., MacEwan, T.H., Nakhwa, S.N., 1960. Studies in adsorption. Part XI. A system of classification of solution adsorption isotherms and its use in diagnosis of adsorption mechanisms and in measurement specific surface of solids. Journal of the Chemical Society 3973–3993.
- Hermosín, M.C., Pavlovic, I., Ulibarri, M.A., Cornejo, J., 1996. Hydrotalcite as sorbent for trinitrophenol: sorption capacity and mechanism. Water Research 30, 171–177.
- Ho, Y.S., 2006. Review of second-order models for adsorption system. Journal of Hazardous Materials 136, 681–689.
- Houri, B., Legrouri, A., Barroug, A., Forano, C., Besse, J.P., 1998. Use of the ion-exchange properties of layered double hydroxides for water purification. Collection of Czechoslovak Chemical Communications 63, 732–740.
- Iyi, N., Sasaki, T., 2008. Deintercalation of carbonate ions and anion exchange of an Al-rich MgAl–LDH (layered double hydroxide). Applied Clay Science 42, 246-251.
- Kasprzyk-Hordern, B., 2004. Chemistry of alumina reactions in aqueous solution and its application in water treatment. Advances in Colloid and Interface Science 110, 19–48.

- Klumpp, E., Contreras-Ortega, C., Klahre, P., Tino, F.J., Yapar, S., Portillo, C., Stegen, S., Queirolo, F., Schwuger, M.J., 2004. Sorption of 2,4-dichlorophenol on modified hydrotalcites. Colloid Surface 230, 111 –116.

- LaPara, T.M., Konopka, A., Nakatsu, C.H., Alleman, J.E., 2000. Thermophilic aerobic waste water treatment in continuous-flow bioreactors. Journal of Environmental Engineering 126, 739–744.

- Lazaridis, N.K., Asouhidou, D.D., 2003. Kinetics of sorptive removal of chromium (VI) from aqueous solutions by calcined Mg–Al–CO_3 hydrotalcite. Water Research 37, 2875–2882.

- Mall, J.I., Srivastava, V.C., Agarwall, R., 2006. Removal of Orange-G and methyl violet dyes study by adsorption onto bagasse fly ash-kinetic study and equilibrium isotherm analyses. Dyes and Pigments 69, 210–223.

- Misaelides, P., 2011. Application of natural zeolites in environmental remediation. (A short review) Microporous and Mesoporous Materials 144, 15–18.

- Newman, S.P., Jones, W., 1998. Synthesis, characterization and applications of layered double hydroxides containing organic guests. New Journal of Chemistry 22,105–115.

- Pavlovic, I., Barriga, C., Hermosín, M.C., Cornejo, J., Ulibarri, M.A., 2005. Adsorption of acidic pesticides 2,4-D, clopyralid and picloram on calcined hydrotalcite. Applied Clay Science 30, 125–133.

- Pavlovic, I., Pérez, M.R., Barriga, C., Ulibarri, M.A., 2009. Adsorption of Cu^{2+}, Cd^{2+} and Pb^{2+} ions by layered double hydroxides intercalated with the chelating agents diethylenetriaminepentaacetate and meso-2,3-dimercaptosuccinate. Applied Clay Science 43, 125–129.

- Pérez, M.R., Pavlovic, I., Barriga, C., Cornejo, J., Hermosín, M.C., Ulibarri, M.A., 2006. Uptake of Cu^{2+}, Cd^{2+} and Pb^{2+} on Zn–Al layered double hydroxide intercalated with EDTA. Applied Clay Science 32, 245–251.

- Reichle, W.T., 1986. Synthesis of anionic clay minerals (mixed metal hydroxides, hydrotalcite). Solid State Ionics 22, 135–141.

- Rives, V., 2001. Layered Double Hydroxides: Present and Future. Nova Science Publishers, Inc., New York.

- Tan, B.H., Teng, T.T., Omar, A.K.M., 2000. Removal of dyes and industrial dye wastes by magnesium chloride. Water Research 34, 597–601.

- Travis, C.C., Etnier, E., 1981. A survey of sorption relationships for reactive solutes in soil. Journal of Environmental Quality 10, 8–17.
- Wang, B., Zhang, H., Evans, D., Duan, X., 2005. Surface modification of layered double hydroxides and incorporation of hydrophobic organic compounds. Materials Chemistry and Physics 92, 190–196.
- Weber Jr., W.J., Morris, J.C., 1963. Kinetics of adsorption on carbon from solution. Journal of the Sanitary Engineering Division American Society of Civil Engineers 89, 31–60.
- Zouboulis, A.I., Lazaridis, N.K., Grohmann, A., 2002. Toxic metals removal from waste waters by up flow filtration with floating filter medium. I. The case of zinc. Separation Science and Technology 37, 403–416.

Chemical Engineering Journal 254 (2014) 605–611

REMOVAL OF Cu^{2+}, Pb^{2+} AND Cd^{2+} BY LAYERED DOUBLE HYDROXIDE– HUMATE HYBRID. SORBATE AND SORBENT COMPARATIVE STUDIES

M.A. González[a] , I. Pavlovic[a,*], R. Rojas-Delgado[b] , C. Barriga[a]

[a] Dpto. de Química Inorgánica e Ingeniería Química, Instituto Universitario de Química Fina y Nanoquímica (IUQFN), Universidad de Córdoba, Campus de Excelencia Internacional Agroalimentario, 14071 Córdoba, Spain

[b] INFQC, Departamento de Fisicoquímica, Facultad de Ciencias Químicas, Universidad Nacional de Córdoba, Ciudad Universitaria, 5000 Córdoba, Argentina

GRAPHICAL ABSTRACT

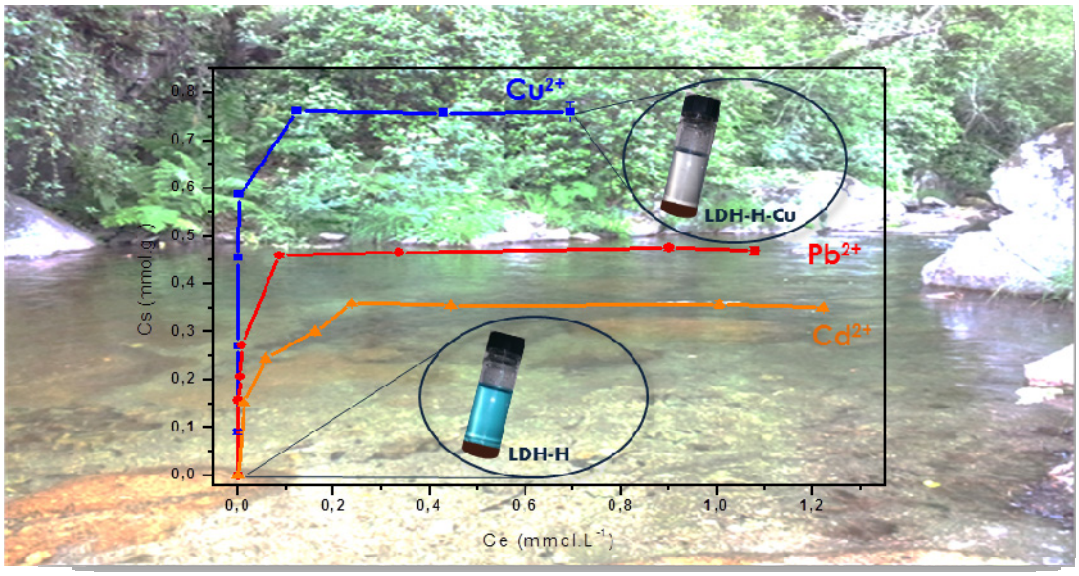

ABSTRACT

The synthesis of a layered double hydroxide-humate (LDH–H) hybrid was purposed for the removal of Cu^{2+}, Pb^{2+} and Cd^{2+} from aqueous solutions. This sorbent has been synthesized by incorporating humate anion into magnesium aluminum layered double hydroxide with chloride as an interlayer anion (LDH–Cl) via ion exchange. The effects of various physic-chemical factors such as pH influence, contact time, initial metal concentration and the simultaneous sorption

of the three heavy metal ions onto LDH–H were investigated. The sorption capacities of humic acid (HA), LDH–Cl and LDH–H were compared under the same experimental conditions. The hybrid LDH–H presented better properties, such as greater stability and less pH increase throughout the sorption process. A high affinity and large removal capacity of Cu^{2+}, Pb^{2+} and Cd^{2+} were obtained by complexation and hydroxide precipitation mechanism, being this major for the case of Cu^{2+}, according to its low hydroxide solubility product value. The sorption isotherms were well described by the Langmuir equation. The metal removal efficiency was lower when the three cations were competing for the available adsorbent sites, compared to monocomponent solutions.

Highlights

- Layered double hydroxide–humate hybrid was synthetized by ionic exchange method.
- Inorganic matrix was stabilized by humate incorporation.
- High capacity for the Cu^{2+}, Pb^{2+} and Cd^{2+} removal by different mechanisms.
- The simultaneous heavy metal sorption increased the total metal amount sorbed.

Keywords: Layered double hydroxides, Humic acid, Heavy metals, Sorption

1. Introduction

Heavy metals are important pollutants that reach the soils and waters due to natural processes and human activities such as mining, metal plating, batteries and fertilizing industry among many others. They are not biodegradable and their toxicity lies in their bioacumulativity. For humans, extended exposure to heavy metals can result in damage to mental and central nervous function, blood composition, lungs, liver and other vital organs. World Health Organization drinking water guideline values for Cu, Cd and Pb are 2, 0.003 and 0.01 mg/l respectively [1]. Therefore, there is a great interest in the development of processes for heavy metals removal from wastewater ground water and sediments. Methods applied in heavy metal removal from aquifers are chemical precipitation as sulfides or hydroxides, filtration, coagulation, inverse osmosis, electrolysis, etc. [2–5]. However, some of them are expensive or unsuitable and

there is an increasing interest in the research of low-cost and non-toxic alternatives adsorbents such as zeolites [6], clays and clay minerals [7,8], as well as agricultural and municipal wastes [9].

Thus, heavy metals are immobilized by humic substances (HS), which are the product of decomposed organic matter in soils and waters. Their sorbent properties arise from the presence of humic acid (HA) which is the most abundant fraction of HS. HA are large colloidal molecules with variable composition, but they have a high content of oxygen-containing (carboxylic, phenolic) functional groups [10]. These functional groups exist in anionic form in a large pH range and in bond metal ions through electrostatic interactions and coordinate bonding [11–13]. HA could provoke problems in water treatments for many reasons such as the alteration of color, taste, odor, forming of carcinogenic by-products during the chlorination etc. Consequently, different materials such as activated carbon, alumina, zeolites, clays and clay minerals were proposed for the uptake of HA from waters [14–17]. Moreover, humic acids affect the removal capacity of pollutants such as heavy metal ions by other sorbents, such as carbon nanotubes and zero valent iron nanoparticles [18].

A class of minerals, which are also reported to be good sorbents of both heavy metals and HA, are the layered double hydroxides (LDHs) [16,19]. The structure of LDHs, also known as hydrotalcite-like compounds, are derived from that of brucite ($Mg(OH)_2$) by isomorphic substitution of Mg^{2+} by Al^{3+} ions. The charge excess generated is balanced by intercalation of anions between the layers [20]. The general LDH formula can be represented as $[M^{II}_{1-x}\, M^{II}_{x}(OH)_2 X_{x/q}]\, X^{n-}_{x/n} \cdot mH_2O$ where M^{II}, M^{III}, and X represent a divalent and trivalent cation and the interlayer anion, respectively. All of them may vary over a wide range and X is quite easy to exchange with other anions [21, 22]. These materials are receiving increasing attention due to interesting specific properties such as anion exchange capacity, acid–base buffering capacity, reconstruction from their calcination products, and high customization possibilities. Therefore, LDHs have been studied for their potential applications in diverse areas [23–25], their low toxicity making them suitable for environmental applications [26–30]. Thus, LDHs were used to remove heavy metal by precipitation of the corresponding hydroxides due to their pH buffering capacity and when LDHs are functionalized with chelating ligands

such as ethylenediaminetetraacetic acid, diethylenetriaminepentaacetate or meso-(2,3)-dimercaptosuccinate etc., the solids thus obtained showed sorption capacity for heavy metal cations such as Cu^{2+}, Cd^{2+}, Pb^{2+} [31–33]. The objective of this work was to obtain a layered double hydroxide–humate hybrid (LDH–H) and explore its capacity to remove Cu^{2+}, Cd^{2+}, Pb^{2+} from water. Firstly, the sorption capacity of this hybrid was compared to those of chloride intercalated LDH and humic acid. Afterwards, the effect of pH, the contact time and initial metal concentration on LDH–H sorption capacity was assessed and the competition between the three heavy metal ions was evaluated.

2. Experimental

All reagents were reagent grade and purchased from Aldrich. Water was distilled and previously boiled and purged with N_2 to prevent CO_2 presence.

2.1. Synthesis and characterization

The synthesis of the layered double hydroxide–humate hybrid (LDH–H) was carried out in two steps: the preparation of a chloride intercalated precursor (LDH–Cl), obtained by the coprecipitation method [21], which was afterwards dispersed in a sodium humate solution.

LDH–Cl was prepared by drop-wise addition of a 200 mL aqueous solution of 0.75 M of $MgCl_2 \cdot 6H_2O$ and 0.25 M of $AlCl_3 \cdot 6H_2O$ to a 0.25 M of NaCl solution under vigorous agitation and constant pH = 8, set by addition of 1M NaOH solution. The synthesis was performed in N_2 atmosphere in order to avoid atmospheric CO_2 dissolution and consequently carbonate incorporation to the solid. The suspension obtained was hydrothermally treated at 80 °C for 24 h, separated by centrifugation and washed. A portion of the precipitate was dried at 60 °C to obtain LDH–Cl, while the remaining slurry was suspended in a 0.13 M sodium humate solution under vigorous stirring and a constant pH = 8 for 24 h. The resulting dispersion (LDH–H) was separated by centrifugation, washed and dried as previously described.

Mg and Al elemental chemical analyses were performed by Inductively Coupled Plasma Mass Spectrometry (ICP-MS) in a Perkin Elmer ELAN DRC-e instrument. The samples were dissolved in concentrated HNO_3 and diluted to meet the calibration range. Powder X-ray diffraction (PXRD) patterns were recorded

using a Siemens D-5000 diffractometer with Cu K_α a radiation (k = 1.54050). Fourier-transform infrared (FT-IR) spectra were registered using the KBr disk method on a Perkin Elmer Spectrum One spectrophotometer. TG and DTA curves were recorded on a Setaram Setsys Evolution 16/18 apparatus in an oxidizing atmosphere and at the heating rate of 5 °C/min. Finally, SEM images were recorded in a JEOL JSM 6300 instrument on samples covered with an Au layer.

2.2. Sorption experiments

The optimal sorption conditions (initial pH, contact time) were determined in the sorption experiments performed. 0.05 g of the adsorbent (LDH–Cl or LDH–H) was dispersed in 30 mL, 1 mM aqueous solutions of Cu^{2+}, Pb^{2+} and Cd^{2+} nitrate salts. Sorption isotherms were performed in 30 mL dispersions containing 0.05 g sorbent with increasing initial concentration (C_0) of the corresponding heavy metal ion (C_0 = 0–2 mM). Finally, the competence between the three heavy metals for LDH–H sorbent was studied by dispersing 0.05 g of sorbent in 30 mL solutions containing all three heavy metal ions (C_0 = 1 mM and initial pH 5, each). The initial pH 5 was selected to be sure that the all of the metal ions were dissolved in all cases.

The experiments were performed by duplicate in all cases. The dispersions were shaken at 52 rpm at room temperature, centrifuged and finally filtered on Nylon filters (pore size 0.22 μm). The heavy metal concentration of the resulting supernatants was determined by atomic absorption spectrometry (AAS) in a Perkin Elmer AAnalyst400 instrument, the samples being dissolved in concentrated HNO_3 and diluted to meet the calibration range. These concentrations were used to determine the amount of each metal adsorbed by the sorbents (C_S, mmol g^{-1}):

$$C_s = (C_o - C_e)\, V/W \quad (1)$$

where C_o and C_e are the initial and equilibrium solution concentrations (mmol L^{-1}), W is the weight of solid (g) and V is the solution volume (L). The adsorption isotherm data were fitted to the Langmuir model (Eq. (2))

$$C_e/C_s = (1/C_m)C_e + 1/C_m K_L \quad (2)$$

where C_m is the maximum sorption capacity at the monolayer coverage (mmol g^{-1}) and K_L (L $mmol^{-1}$) is a constant related to the adsorption energy.

3. Results and discussion

3.1. Characterization of the LDH-Cl and LDH-H

The XRD patterns of LDH–Cl and LDH–H (Fig. 1) portrayed characteristic peaks of hydrotalcite-like compounds [34], sharp, high intensity (00l) peaks at 2 θ values below 30° , and broad, low intensity (hkl) peaks above this value. The basal spacing obtained for LDH–Cl (7.7 Å) was typical of chloride-intercalated hydrotalcites [34]. LDH–H basal spacing was slightly higher (7.9 Å) and similar to other HA containing LDHs previously reported.

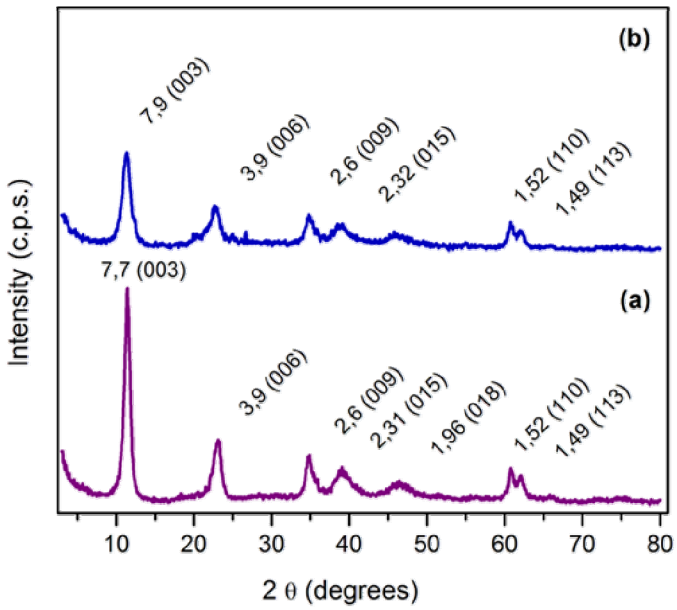

Fig. 1. XRD patterns of (a) LDH–Cl and (b) LDH–H.

Thus, Seida and Nakano [35] suggest that LDH weathering provokes a coagulation of a part of humic acid which is adsorbed on LDH surface, while a small part is bonded by ionic exchange with LDHs interlayer carbonates. Also, Vreysen and Maes [16] propose a ligand exchange between HA and Al-OH groups of the brucite layers as a main mechanism of humic acid bonding to LDH. We consider that the incorporation of HA anions were produced mainly at the surface of the LDH particles, and that a partial intercalation of the humate near the LDH particle edges

was concurrent. Humate anions were disposed in a parallel position to the layers, which could explain the slight basal spacing increase.

The FT-IR spectra of LDH–Cl (Fig. 2a) presented bands corresponding to the hydroxylated layers (below 900 cm $^{-1}$), hydroxyl stretching (above 3000 cm-^{1}), and bending mode of the interlayer water (1630 cm $^{-1}$) while the bands at 1358 and 1408 cm $^{-1}$ were assigned to the presence of a small fraction of carbonate anions. On the other hand, LDH–H (Fig. 2b) presented characteristic bands of the humate anion (Fig. 2c): 1603 and 1387 cm $^{-1}$ were attributed to antisymmetric and symmetric carboxylate vibration while those at 1105 and 1041 cm $^{-1}$ were assigned to bending =CH vibration of HA [36].

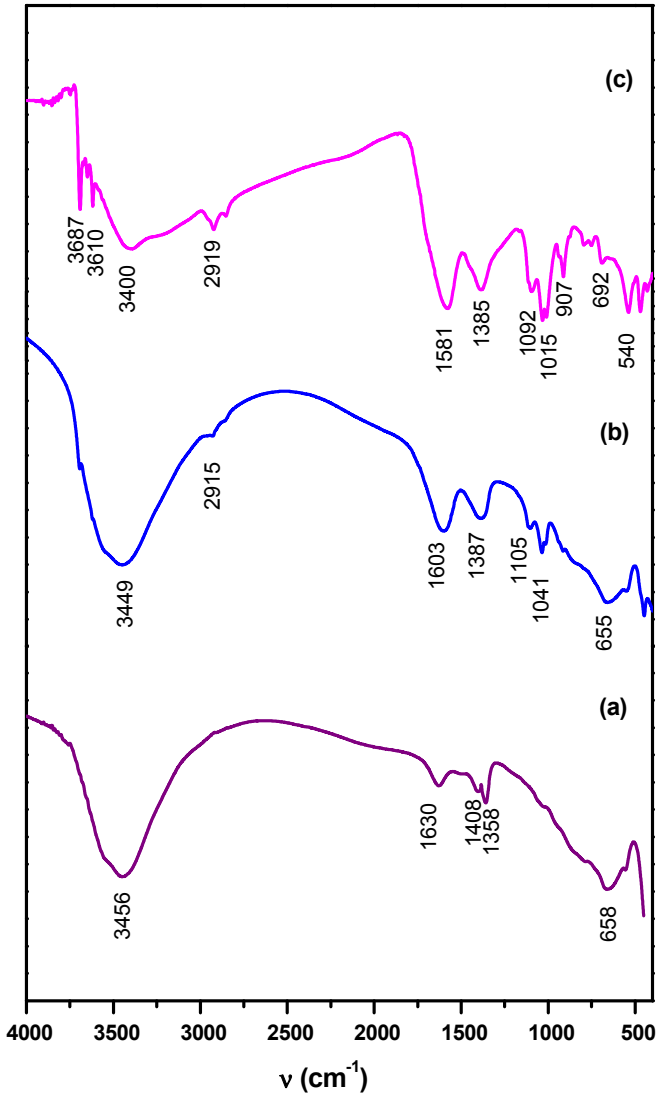

Fig. 2. FT-IR spectra of (a) LDH–Cl, (b) LDH–H and (c) sodium humate (NaH).

The SEM images of LDH–Cl (Supplementary data, Fig. S1) showed that the sample consisted of well-shaped, regular particles (Fig. S1a and S1b) formed by aggregation of small plate-like units. LDH–H particles (Fig. S1c) presented a broader size range and more irregular edges (Fig. S1d). The increased particle size was assigned to a larger agglomeration of the LDHs platelets related to a higher hydrophobicity and lower particle charge expected for LDH–H particle surface due to the intercalation of an organic anion [37] thus increasing the particle–particle interactions. On the other hand, the irregular shape of LDH–H particles is similar to that obtained for other LDHs that incorporate organic anions at their surface [38].

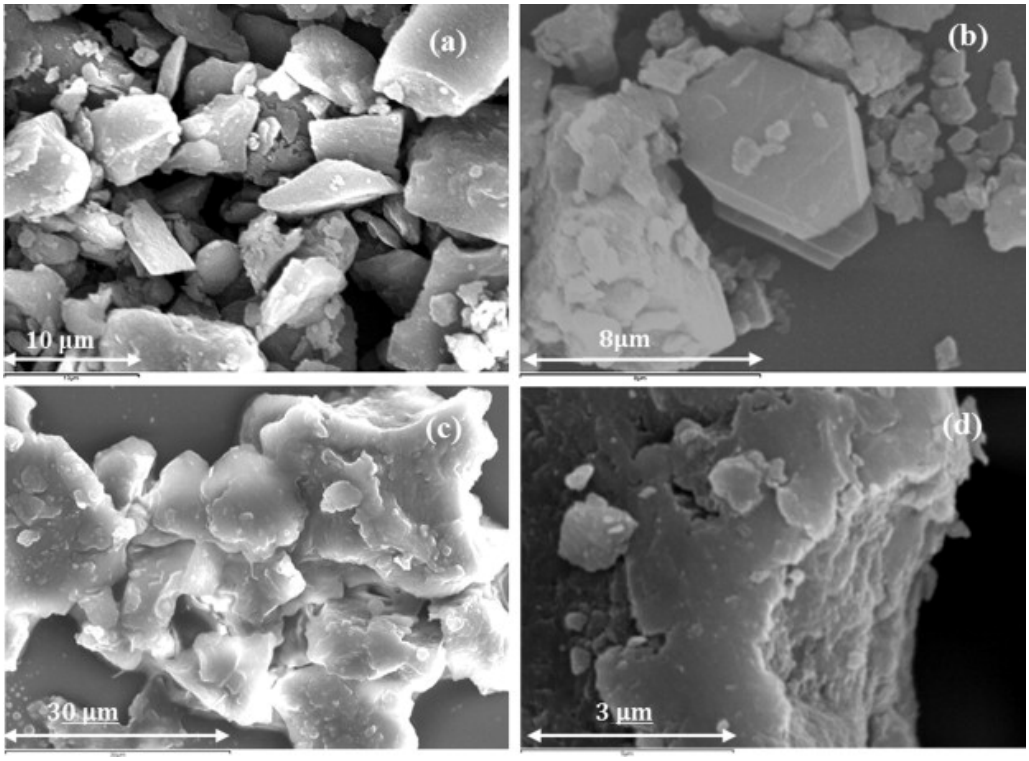

Supplementary Fig. S1.
SEM images at different magnification of (a) and (b) LDH–Cl sample, (c) and (d) LDH–H sample.

DTA curves of LDH–Cl and LDH–H and HA are included in Fig. 3. Three endothermic effects at 83, 371 and 421 °C were observed during the thermal treatment of LDH–Cl (Fig. 3a). These thermal effects and their corresponding weight losses were assigned to (1) interlayer water loss, (2) dehydroxylation of the layers and (3) interlayer chloride loss [34]. The DTA curve of the LDH–H hybrid

(Fig. 3b) showed the endothermic peak corresponding to the interlayer water, while the endothermic peaks corresponding to the last two effects were overlapped by an exothermic process of HA oxidation (Fig. 3c). The metal analysis of the LDH–Cl and LDH–H and their proposed formulae are represented in the Table 1.

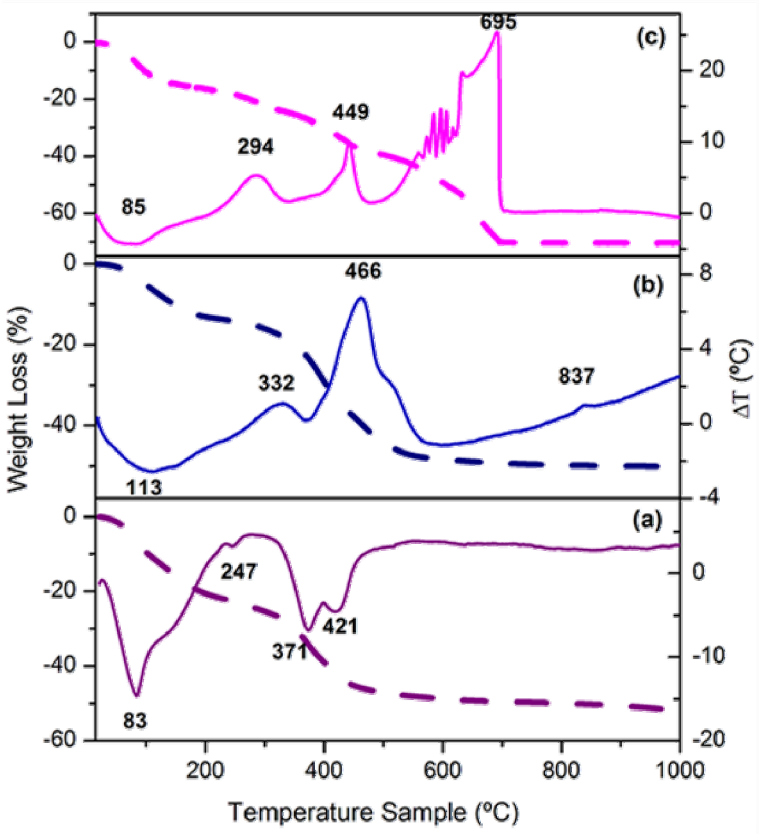

Fig. 3. TG and DTA curves of (a) LDH–Cl, (b) LDH–H and (c) NaH.

Table 1
Chemical analysis results of LDH-Cl and LDH-H.

	% wt		Atomic ratio	Proposed Formula
	Mg	Al	Mg/Al	
LDH-Cl	20	8	2.8	$[Mg_{0.74}Al_{0.26}(OH)_2](Cl)_{0.26}.0.83H_2O$
LDH-H	15	7	2.4	$[Mg_{0.71}Al_{0.29}(OH)_2](X)_{0.29/n}.mH_2O$

X= Cl and/or H (n= 1 and/or 2; m= 0.58-0.71)

The results indicated that the molar ratio Mg:Al of the sample LDH–Cl was very close to that in the starting solution, while a decrease had been observed on the sample LDH–H because of a Mg partial dissolution during the HA exchange.

According to the Mg/Al ratio and considering that the charge of the layer is only balanced by humate or chloride anion, a formula with a range of substitution was proposed for the LDH–H sample. The number of water molecules has been calculated from the first weight loss in the TG curve and the range has been obtained in accordance to the degree of the anionic substitution. The total weight loss for the proposed formula is consistent with the experimental value obtained by the TG curve, which is 50% considering a total substitution of chloride by humate. This result confirmed that the HA incorporation was probably produced at the surface of LDH particles along with an important intercalation at the edges of the particles.

3.2. Sorbents comparison

The sorption capacity of LDH–Cl, LDH–H (0.05 g/30 mL, C_i = 1 mM, pH initial = 5, 48 h,) and HA (0.014 g/30 mL, amount equivalent to the total amount of humate adsorbed on 0.05 g of the LDH) was compared and the results are shown in Table 2. Copper was completely removed by LDH–Cl and LDH–H, both sorbents being more effective than HA. In the case of Pb^{2+}, LDH–Cl and LDH–H were capable of producing an almost complete removal, while HA presented lower sorption values. Finally, HA produced the highest Cd^{2+} removal, followed by LDH–H and LDH–Cl, respectively. On the other hand, equilibrium (final) pH values (pH_f) were highly dependent on the sorbent. The buffering capacity of LDH–Cl [39] produced the highest pH values, while the least important pH variation with respect to pHi was produced for HA. The amounts of Mg and Al released from the solids after metal sorption experiments were also determined. Al^{3+} concentration was negligible in all cases, which was consistent with the low solubility of $Al(OH)_3$ ($K_{SP}(Al(OH)_3) = 5 \times 10^{-33}$). On the other hand, the Mg was detected in all supernatants and it increased upon heavy metal sorption. These results were related to the different sorption mechanisms of the sorbents: in the case of HA heavy metals were bounded by complex formation. Consequently, the heavy metals affinity for HA being determined by the stability of these complexes and the sorption process produced only minor pH variations. In the case of LDH–Cl, its buffering capacity leaded to an important pH increase and heavy metal precipitation as hydroxides was the main sorption mechanism [40]. These

hydroxides precipitate either as part of a LDH structure, in a mechanism known as ''diadochy'' [41] or in a separate phase [42, 43]. LDH–Cl affinity for heavy metal was then determined by the solubility products of the their hydroxides ($K_{SP}(Cu(OH)_2)$ = 1 x 10^{-20}, $K_{SP}(Cd(OH)_2)$ = 3.2 x 10^{-14} and $K_{SP}(Pb(OH)_2)$ = 2.5 x 10^{-16}). Finally, both mechanisms were concurrent in the LDH–H hybrid, humate anions stabilizing and adding complexation capacity to the inorganic matrix. All pH_f values for the heavy metal sorption on LDH–H were lower compared to those of LDH–Cl (Table 2) due to the stabilizing effect of humate anions [44]. Although the pHf was sufficient to produce an almost complete precipitation of $Cu(OH)_2$, they were not enough for Pb^{2+} and Cd^{2+} due to the higher solubility of the corresponding hydroxides. Nevertheless, LDH–H showed higher Cd^{2+} sorption than LDH–Cl, which confirmed the contribution of the HA complexation mechanism [45].

Table 2
Metals sorption capacity on different sorbents

Sample	Metal	pH_{final}	% Mg	% sorbed
AH	Cu^{2+}	5.4	-	78
	Pb^{2+}	5.0	-	79
	Cd^{2+}	6.8	-	64
LDH-Cl	-	9.3	5.9	-
	Cu^{2+}	9.0	10.0	100
	Pb^{2+}	9.1	9.4	87
	Cd^{2+}	8.2	6.7	37
LDH-H	-	8.9	5.7	-
	Cu^{2+}	8.3	8.9	100
	Pb^{2+}	7.6	7.8	95
	Cd^{2+}	7.8	7.4	56

According to the results obtained, LDH–H presents interesting properties due to (1) the stabilization of LDH matrix, diminishing the layers weathering and the final pH of the supernatants, which in turn, also decrease the environmental impact of the treated effluents and (2) the addition of a complexation mechanism,

extending LDH functionalities. Also, due to the recurring presence of HA in the effluents, their interactions with LDHs and the effect on their sorptive behavior are of primary importance. As a consequence, the sorption behavior of the hybrid will be studied in the next section.

3.3. Heavy metal cations sorption by LDH–H

Table 3 shows the effect of pH on the heavy metal sorption capacity of LDH–H. Both C_s and pH_f slightly decreased with decreasing pH_i, as the buffering capacity of LDH–H is exhausted by both heavy metal sorption and proton consumption. It could be noted here that, as Cs decreases from Cu^{2+} to Cd^{2+}, the influence of pH_i in pH_f also decreased, which confirmed that the buffering capacity of LDHs was not consumed, i.e. lower pH_s (higher acid concentrations) are necessary to displace the final pH from 7 to 8 range.

Table 3
pH influence on the metals sorption on LDH-H.

Sample	pH initial	pH final	Cs (mmol g^{-1})
Cu^{2+}	3	6.1	0.51
	5	8.3	0.57
Pb^{2+}	3	7.4	0.34
	5	7.6	0.40
	7	8.0	0.36
Cd^{2+}	3	7.7	0.23
	5	7.8	0.26
	7	8.0	0.27

The kinetic study results (Fig. 4) showed that sorption was produced into two steps. The first step was fast and produced half of the final sorption within the first 2 h, and the second gradually approached to equilibrium, reaching it within 48 h in the cases of Pb and Cd, and 24 h for the case of Cu. 100%, 95% and 56% of the initial metal concentration were removed for Cu, Pb and Cd, respectively, and the time to reach equilibrium increased in the same sequence as well. A similar kinetic behavior was previously observed for Cu^{2+} on LDH modified by edta [46]: the first,

fast step being assigned to the hydroxide precipitation mechanism and the second step to a cation exchange mechanism at edta complexes located at the interlayer. The only difference here was substitution of edta by HA. The presence of the second mechanism was confirmed by Fig. 4b, which indicated that the main pH variation, associated with the hydroxide precipitation mechanism, was produced within the first minutes of the experiment in all cases.

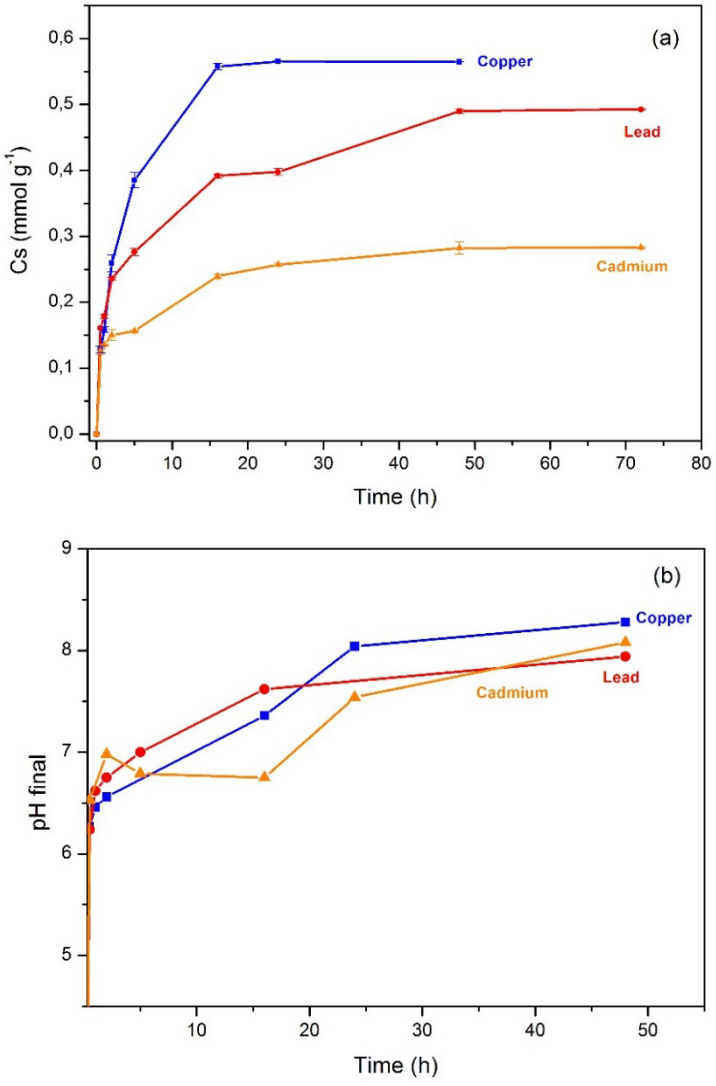

Fig. 4. The evolution of: (a) heavy metals uptake by LDH–H and (b) pH evolution (C_i = 1 mM, pH initial 5).

The time of 48 h was considered enough to reach equilibrium for the sorption isotherm (Fig. 5). A steep Cs increase was registered in all cases, indicating the high effectiveness of LDH–H as sorbent, the metal ions being completely adsorbed at lower initial concentrations. As determined by the

Langmuir model fitting (Table 4), the maximum sorption increased in the sequence Cd (C_m = 0.35 mmol g^{-1}) Pb (C_m =0.48 mmol g^{-1}) and Cu (C_m = 0.75 mmol g^{-1}). These values were comparable to those obtained for similar Mg–Al–LDHs: between 0.01 and 0.15 mmol g^{-1} for Cd^{2+} sorption by Mg–Al–LDHs containing carbonate and edta, respectively [47], 0.33 and 0.86 mmol g^{-1} for Pb^{2+} sorption by chloride-containing Mg–Al–LDHs [48, 49] and between 0.78 and 2.50 mmol g^{-1} for Cu^{2+} sorption by chloride intercalated LDHs either [42, 50]. In all cases sorption was assigned to a hydroxide precipitation mechanism, except for the case of Cd^{2+}, which only reaches significant sorption capacity when complexation mechanism is incorporated by intercalating the solid with edta. Similarly, LDH–H showed higher sorption capacity than LDH–Cl or even than the edta intercalated Mg–Al–LDHs.

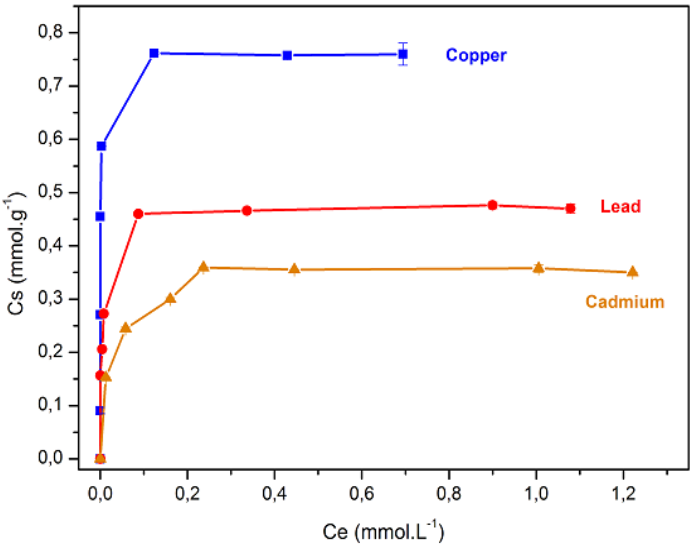

Fig. 5. Sorption isotherms of heavy metals on LDH–H at pH = 5.

Table 4
Langmuir model parameters for heavy metals sorption on LDH-H.

Sample	C_m (mmol g^{-1})	K_L	R^2
Cu^{2+}	0.75	69	0.993
Pb^{2+}	0.48	187	0.999
Cd^{2+}	0.35	114	0.998

The sorption products were studied by PXRD and FT-IR (Fig. 6) and there were no important changes observed compared to the pure sorbent pattern (Fig. 1). PDRX of LDH–H–Metal complexes patterns (Fig. 6a) indicated that the crystallinity of the sorption product decreased but the LDH structure was maintained and there was no additional precipitates observed. This is probably due to the low mass of hydroxide formed respect the amount of sorbent in the experiments (less than 10% w/w in all cases, as calculated from C_m values and the formula weight of the corresponding heavy metal hydroxide). The FT-IR spectrum (Fig. 6b) of sorbent after the sorption experiments showed slight displacements of the bands in the 1600–1000 cm^{-1} zone, which is likely to be due to the interaction of the functional groups of the HA with metal ions.

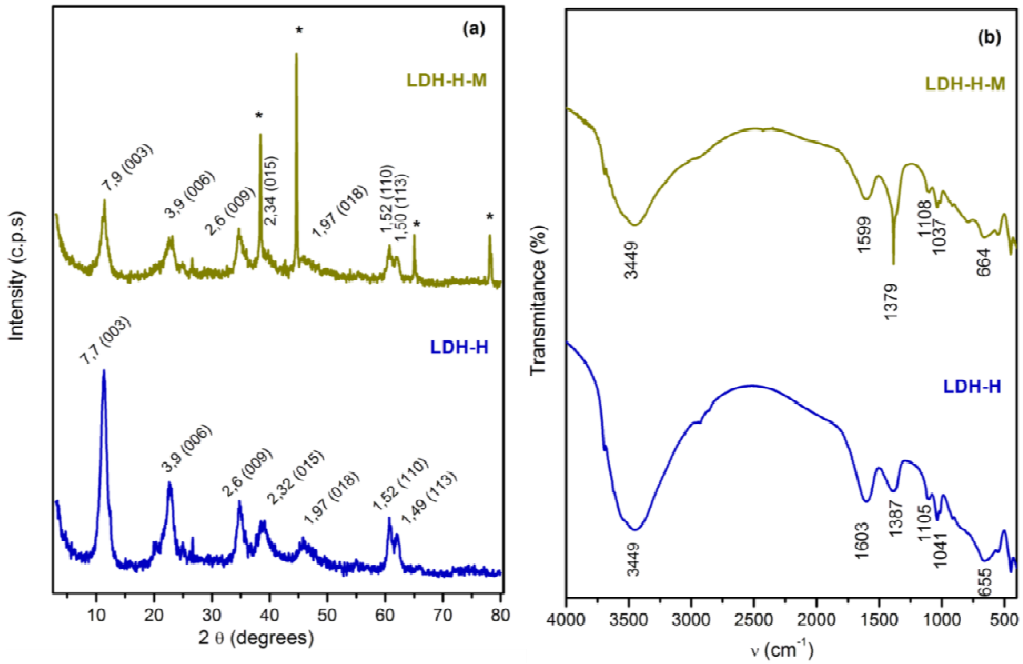

Fig. 6. XRD patterns (a) and FT-IR spectra (b) of the sorption products (M = Cu, Pb and Cd) corresponding to the last isotherm point (/Al sample holder).

The simultaneous sorption of the three heavy metal ions is represented in Fig. 7. The sorption was slower and the amounts of metal uptaken were lower compared to the monocomponent solutions. The maximum amounts sorbed at the equilibrium time for the multicomponent system were C_s = 0.46 mmol g^{-1}, C_s =0.21 mmol g^{-1}, C_s = 0.00 mmol g^{-1} for Cu, Pb and Cd respectively, vs. C_s = 0.57 mmol g^{-1}, Cs = 0.49 mmol g^{-1}, C_s = 0.28 mmol g^{-1} obtained for the corresponding experiments

with a single heavy metal ion. The highest amounts of the metal cations sorbed on LDH–H were reached for copper in both cases, while the sorption of Cd was completely inhibited by the presence of the other two cations probably due to sorption occupation sites by the species with more affinity and/or precipitation of the hydroxides. This behavior was concordant with the sequence of stability of the corresponding metal hydroxides (decreasing K_{SP}) and correlated with the stability constants of M–humate complexes [45], decreasing in the order of Cu > Pb > Cd. Moreover, the sum of C_s for the multicomponent system (0.67 mmol g^{-1}) was larger than the maximum C_s value obtained for the single metal experiments (Cu^{2+} ion, 0.57 mmol g^{-1}), indicating that both precipitation and complexation mechanisms are concurrent and that the different ions were incorporated to different sites. According to this result, Cd^{2+} and Pb^{2+} were competing preferentially for humate complexation sites.

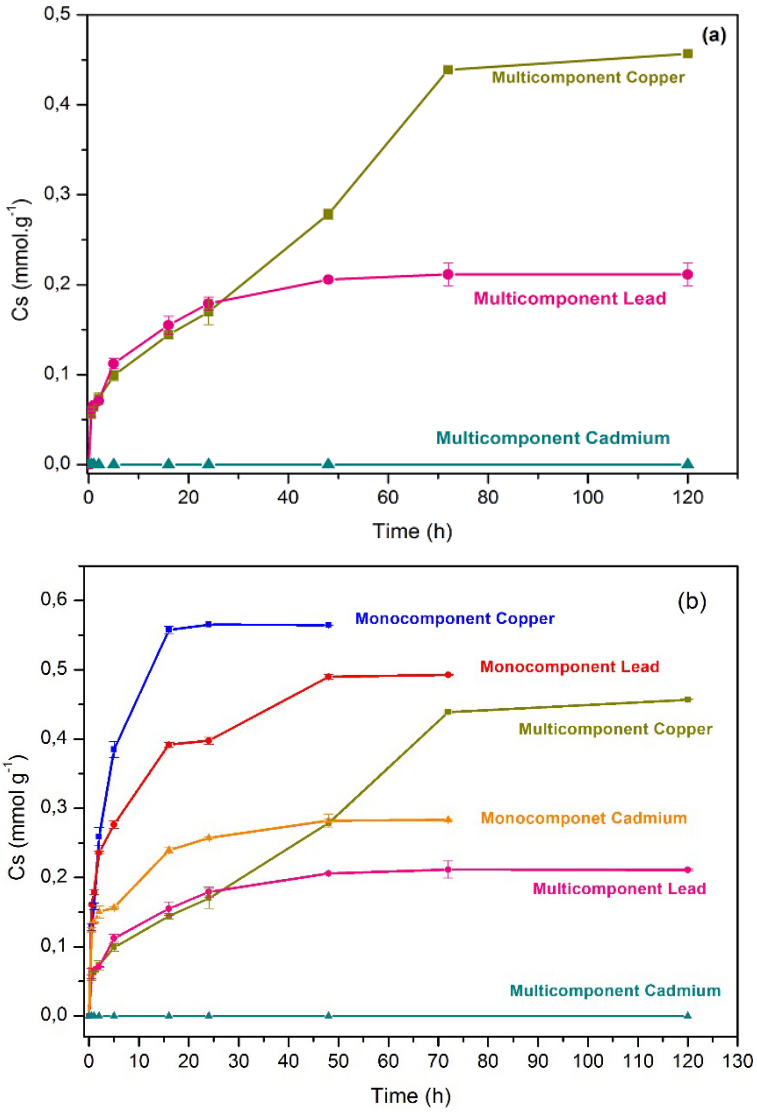

Fig. 7. The evolution of sorption of heavy metals on LDH–H: (a) metal cations coexisting in the solution (multicomponent) and (b) comparing with the monocomponent solution sorption behavior.

4. Conclusions

Layered double hydroxide–humate hybrid (LDH–H) was synthesized by dispersing chloride containing LDH in a humate solution. Humate incorporation was produced at the surface of the particles but also some intercalation at the particles edges was inferred. Humate incorporation produced a stabilization of the inorganic matrix and the resulting hybrid showed sorption capacity of Cu^{2+}, Pb^{2+} and Cd^{2+} due to precipitation and complexation mechanism. As a consequence, LDH–H presented an intermediate behavior compared to LDH–Cl and HA

separately. Moreover, LDH–H presents a better stability, resulting in less pH increase during the experiments, which moderates the environmental impact of the sorption process. Also, LDH–H avoids the separation and dewatering problems associated with humic acids. The LDH–H sorption process was fast and was produced in two steps, the first fast step was exclusively associated with hydroxide precipitation, while in the second, slower step, the complexation mechanism was involved. LDH–H presented high affinity for heavy metal ions, leading to low pollutant concentrations at equilibrium while the sorption capacities were similar to other sorbents with similar characteristics. Finally, the presence of more than one heavy metal even increased the overall sorption capacity, indicating that different heavy metals were sorbed by different mechanisms, Pb^{2+} and Cd^{2+} competing for the humate complexation sites.

Acknowledgments

This work was partially funded by the Ministerio de Ciencia e Innovación (CTM 2011-25325) and Junta de Andalucía through Research Group FQM-214. We appreciate the technical assistance received in the SCAI (Universidad de Córdoba) for Electron Microscopy and Elemental Analysis Units (ICP-MS).

References

[1] World Health Organization, Guidelines for Drinking-water Quality, Health Criteria and Other Supporting Information, vol. 2, Second ed., WHO, Geneva, 1996.

[2] J.B. Brower, R.L. Ryan, M. Pazirandeh, Comparison of ion-exchange resins and biosorbents for the removal of heavy metals from plating factory wastewater, Sci. Technol. 31 (1997) 2910–2914.

[3] K.G. Karthikeyan, H.A. Elliott, F.S. Cannon, Adsorption and coprecipitation of copper with the hydrous oxides of iron and aluminum, Environ. Sci. Technol. 31 (1997) 2721–2725.

[4] A.T. Heijne, F. Liu, R. Weijden, J. Weijma, C.J.N. Buisman, H.V.M. Hamelers, Copper recovery combined with electricity production in a microbial fuel cell, Environ. Sci. Technol. 44 (2010) 4376–4381.

[5] M.A. Hashim, S. Mukhopadhyay, J.N. Sahu, B.J. Sengupta, J. Environ. Manage. 92 (2011)2355–2388.

[6] P. Misaelides, Application of natural zeolites in environmental remediation: a short review, Microporous Mesoporous Mater. 144 (2011) 15–18.

[7] M. Cruz-Guzmán, R. Celis, M.C. Hermosín, W. Koskinen, J. Cornejo, Adsorption of pesticides from water by functionalized organobentonites, J. Agric. Food Chem. 53 (2005) 7502–7511.

[8] J. Cornejo, R. Celis, I. Pavlovic, M.A. Ulibarri, Interactions of pesticides with clays and layered double hydroxides: a review, Clay Miner. 43 (2008) 155–176.

[9] A. Bhatnagar, M. Sillanpaa, Utilization of agro-industrial and municipal waste materials as potential adsorbents for water treatment: a review, Chem. Ing. J. 157 (2010) 277–296.

[10] G.W. vanLoon, S.L. Duffy, Environmental Chemistry (a global perspective), Oxford University Press Inc., New York, 2000.

[11] C.A. Coles, R.N. Yong, Humic acid preparation, properties and interactions with metals lead and cadmium, Eng. Geol. 85 (2006) 26–32.

[12] M. Havelcová, J. Mizera, I. Sy´korová, M. Pekar, Sorption of metal ions on lignite and the derived humic substances, J. Hazard. Mater. 161 (2009) 559–564.

[13] Y. Li, Q. Yue, B. Gao, Adsorption kinetics and desorption of Cu(II) and Zn(II) from aqueous solution onto humic acid, J. Hazard. Mater. 178 (2010) 455–461.

[14] B. Bolto, D. Dixon, R. Eldridge, S. King, K. Linge, Removal of natural organic matter by ion exchange, Water Res. 36 (2002) 5057–5065.

[15] A.A.M. Daifullah, B.S. Girgis, H.M.H. Gad, A study of the factors affecting the removal of humic acid by activated carbon prepared from biomass material, Colloids Surf., A 235 (2004) 1–10.

[16] S. Vreysen, A. Maes, Adsorption mechanism of humic and fulvic acid onto Mg/Al layered double hydroxides, Appl. Clay Sci. 38 (2008) 237–249.

[17] Y. Zhan, Z. Zhu, J. Lin, Y. Qiu, J. Zhao, Removal of humic acid from aqueous solution by cetylpyridinium bromide modified zeolite, J. Environ. Sci. 22 (2010) 1327–1334.

[18] W.W. Tang, G.M. Zeng, J.L. Gong, J. Liang, P. Xu, C. Zhang, B.B. Huang, Impact of humic/fulvic acid on the removal of heavy metals from aqueous solutions using nanomaterials: a review, Sci. Total Environ. 468–469 (2014)

1014–1027.

[19] G. Onkal-Engin, R. Wibulswas, D.A. White, Humic acid uptake from aqueous media using hydrotalcites and modified montmorillonite, Environ. Technol. 21 (2000) 167–175.

[20] F. Cavani, F. Trifiro, A. Vaccari, Hydrotalcite-type anionic clays: preparation, properties and applications, Catal. Today 11 (1991) 173–301.

[21] W.T. Reichle, Synthesis of anionic clay-minerals (Mixed metal-hydroxides, hydrotalcite), Solid State Ionics 22 (1986) 135–141.

[22] P.S. Braterman, Z.P. Xu, F. Yarberry, Layered double hydroxides (LDHs), in: S.M.

Auerbach, K.A. Carrado, P.K. Dutta (Eds.), Handbook of Layered Materials, Marcel Decker Inc, New York, 2004, pp. 373–474.

[23] J.H. Choy, S.Y. Kwak, J.S. Park, Y.J. Jeong, Cellular uptake behavior of [32P] labeled ATP–LDH nanohybrids, J. Mater. Chem. 11 (2001) 1671–1674.

[24] D.G. Evans, X. Duan, Preparation of layered double hidroxides and their applications as aditive in polymers, as precursors to magnetic materials and in biology and medicine, Chem. Commun. (2006) 485–496.

[25] J.H. Choy, S.J. Choi, J.M. Oh, T. Park, Clay minerals and layered double hydroxides for novel biological applications, Appl. Clay Sci. 36 (2007) 122–132.

[26] J. Serrano, V. Bertín, S. Bulbulian, Mo-99 sorption by thermally treated hydrotalcites, Langmuir 16 (2000) 3355–3360.

[27] I. Pavlovic, C. Barriga, M.C. Hermosín, J. Cornejo, M.A. Ulibarri, Adsorption of acidic pesticides 2,4-D, clopyralid and picloram on calcined hydrotalcite, Appl. Clay Sci. 30 (2005) 125–133.

[28] F. Bruna, I. Pavlovic, C. Barriga, J. Cornejo, M.A. Ulibarri, Adsorption of pesticides Carbetamide and Metamitron on organohydrotalcite, Appl. Clay Sci. 33 (2006) 116–124.

[29] F. Bruna, I. Pavlovic, R. Celis, C. Barriga, J. Cornejo, M.A. Ulibarri, Organohydrotalcites as novel supports for the slow release of the herbicide terbuthylazine, Appl. Clay Sci. 42 (2008) 194–200.

[30] R. Extremera, I. Pavlovic, M.R. Pérez, C. Barriga, Removal of acid orange 10 by calcined Mg/Al layered double hydroxides from water and recovery of the adsorbed dye, Chem. Eng. J. 213 (2012) 392–400.

[31] M.R. Pérez, I. Pavlovic, C. Barriga, J. Cornejo, M.C. Hermosín, M.A. Ulibarrri, Uptake of Cu^{2+}, Cd^{2+} and Pb^{2+} on Zn–Al layered double hydroxide intercalated with edta, Appl. Clay Sci. 32 (2006) 245–251.

[32] T. Kameda, H. Takeuchi, T. Yoshioka, Uptake of heavy metal ions from aqueous solution using Mg–Al layered double hydroxides intercalated with citrate, malate, and tartrate, Sep. Purif. Technol. 62 (2008) 330–336.

[33] I. Pavlovic, M.R. Pérez, C. Barriga, M.A. Ulibarri, Adsorption of Cu^{2+}, Cd^{2+} and Pb^{2+} ions by layered double hydroxides intercalated with the chelating agents diethylenetriaminepentaacetate and meso-2,3-dimercaptosuccinate, Appl. Clay Sci. 43 (2009) 125–129.

[34] V. Rives, Layered Double Hydroxides: Present and Future, Nova Science Publishers Inc, New York, 2001.

[35] Y. Seida, Y. Nakano, Removal of humic substances by layered double hydroxide containing iron, Water Res. 34 (2000) 1487–1494.

[36] L.J. Bellamy, The Infrared Spectra of Complex Molecules, vol. 1, third ed., Chapman and Hall, London, 1975.

[37] R. Rojas, F. Bruna, C.P. de Pauli, M.A. Ulibarri, C.E. Giacomelli, The effect of interlayer anion on the reactivity of Mg–Al layered double hydroxides: improving and extending the customization capacity of anionic clays, J. Colloid Interface Sci. 359 (2011) 136–141.

[38] Z.P. Xu, P.S. Braterman, Synthesis, structure and morphology of organic layered double hydroxide (LDH) hybrids: comparison between aliphatic anions and their oxygenated analogs, Appl. Clay Sci. 48 (2010) 235–242.

[39] M.L. Parello, R. Rojas, C.E. Giacomelli, Dissolution kinetics and mechanism of Mg–Al layered double hydroxides: a simple approach to describe drug release in acid media, J. Colloid Interface Sci. 351 (2010) 134–139.

[40] X. Liang, Y. Zang, Y. Xu, X. Tan, W. Hou, L. Wang, Y. Sun, Sorption of metal cations on layered double hydroxides: a review, Colloids Surf., A 433 (2013) 122–131.

[41] S. Komarneni, N. Kozai, R. Roy, Novel function for anionic clays: selective

transition metal cation uptake by diadocky, J. Mater. Chem. 8 (1998) 1329–1331.

[42] M. Park, C.L. Choi, Y.J. Seo, S.K. Yeo, J. Choi, S. Komarneni, J.H. Lee, Reactions of Cu^{2+} and Pb^{2+} with Mg/Al layered double hydroxide, Appl. Clay Sci. 37 (2007) 143–148.

[43] R. Rojas, Cooper, lead and cadmium removal by CaAl layered double hydroxides, Appl. Clay Sci. 87 (2014) 254–259.

[44] Y. Kameshima, H. Yoshizaki, A. Nakajima, K. Okada, Preparation of sodium oleate/layered double hydroxide composites with acid-resistant properties, J. Colloid Interface Sci. 298 (2006) 624–628.

[45] A.K. Pandey, S.D. Pandey, V. Misra, Stability constants of metal–humic acid complexes and its role in environmental detoxification, Ecotox. Environ. Safe. 47 (2000) 195–200.

[46] R. Rojas, M.R. Pérez, P. Eustaquio, M. Erro, I. Ortiz, M.A. Ulibarri, C.E. Giacomelli, Edta modified LDHs as Cu2+ scavengers: removal kinetics and sorbent stability, J. Colloid Interface Sci. 331 (2009) 425–431.

[47] T. Kameda, S. Saito, Y. Umetsu, Mg–Al layered double hydroxide intercalated with ethylene-diaminetetraacetate anion: synthesis and application to the uptake of heavy metal ions from an aqueous solution, Sep. Purif. Technol. 47 (2005) 20–26.

[48] X. Liang, W. Hou, Y. Xu, G. Sun, L. Wang, Y. Sun, X. Quin, Sorption of lead ion by layered double hydroxide intercalated with diethylenetriaminepentaacetic acid, Colloids Surf., A 366 (2010) 50–57.

[49] D. Zhao, G. Sheng, J. Hu, C. Chen, X. Wang, The adsorption of Pb(II) on Mg_2Al layered double hydroxide, Chem. Eng. J. 171 (2011) 167–174.

[50] Y. Zang, W. Hou, J. Xu, Removal of Cu(II) from CuSO4 aqueous solution by Mg–Al hydrotalcite-like compounds, Chin. J. Chem. 29 (2011) 847–852.

Chemical Engineering Journal 269 (2015) 221–228

Cu(II), Pb(II) AND Cd(II) SORPTION ON DIFFERENT LAYERED DOUBLE HYDROXIDES. A KINETIC AND THERMODYNAMIC STUDY AND COMPETING FACTORS

I. Pavlovic, M.A. González, C. Barriga*

Dpto. de Química Inorgánica e Ingeniería Química, Instituto Universitario de Química Fina y Nanoquímica (IUQFN), Campus de Excelencia Internacional Agroalimentario (CeiA3), Universidad de Córdoba, Córdoba, Spain

GRAPHICAL ABSTRACT

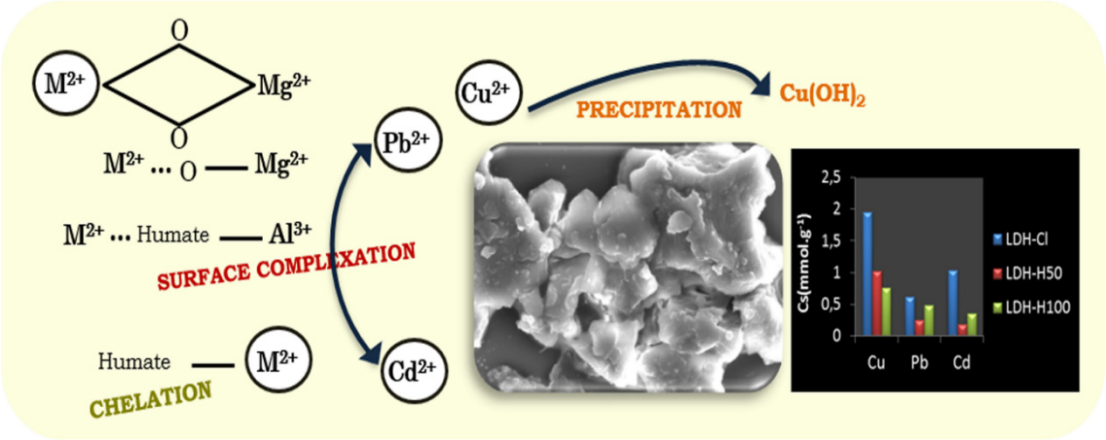

ABSTRACT

Layered double hydroxide-humate hybrids containing different amounts of humate anions (LDH-H100 and LDH-H50) were synthesized by an ion exchange mechanism from layered double hydroxides intercalated by chloride (LDH-C l). These LDH-base d compounds (LDH-Cl, LDH-H100 and LDH-H50) were proposed as sorbents of Cu^{2+}, Pb^{2+} and Cd^{2+} from aqueous solutions. The study of the influence of the initial metal concentration on sorption capacity of LDHs showed that LDH-Cl achieved the best sorption capacity for the potentially toxic metals studied, which is quite unexpected given that humate functional groups have a high affinity for metal cations. The thermodynamic and kinetic studies were

carried out and the results confirmed that all sorption processes were spontaneous and thermodynamically favourable, fitting to pseudo second kinetic order. The sorption competition of the metals from binary and ternary metal solutions was also studied in order to obtain a better understanding of metal sorption behaviour on this material

Highlights

- Higher amount s of metals were sorbed on original LDH-Cl than on humate-modified LDH.
- Kinetics of all sorption systems fitted well to a pseudo second-order model.
- The presence of humate in the solution competes and diminishes metals sorption.
- Copper was sorbed in greater amounts in all cases.
- LDH composition determines order of metal sorption from multicomponent solutions.

Keywords: Metal sorption, Layered double hydroxides, Kinetic, Humate anion

1. Introduction

The presence of metal cations in water could cause serious environmental and human health problems because of their potentially high toxicity. They reach aquifers as the result of both natural processes and human activities such as agriculture or industrial waste discharge.

As a consequence, this concern generates great interest in the development of methods to remedy the presence of potentially toxic metals in water. Among the different techniques applied with this aim in mind, the most extended one is the precipitation of metals as insoluble metal hydroxides, by increasing the pH [1]. However this could produce large volumes of low density sludge, which make the disposal process difficult. This is one of the reasons why adsorption and ion-exchange methods have been studied recently as alternatives for the removal of metallic elements from water.

Layered double hydroxides (LDHs) or hydrotalcite-like compounds form part of a family of natural or synthetic materials with the general formula $[M^{II}_{1-x}\, M^{II}_{x}(OH)_2 X_{x/q}]^{x+}\, X^{m-}_{x/m} \cdot \mathrm{n}H_2O$, where M^{II} and M^{III} are a divalent and a

trivalent cations, and A is the interlayer anion. In the last few decades, LDHs have received considerable attention for their potential applications in many fields, due to their interesting and unique properties. Low-cost and simple preparation, high sorption efficiency and many other advantages makes these materials suitable for the application in the field of wastewater treatment [2-4].

Although LDH is known to be a good sorbent for anionic pollutants through the ionic exchange of interlayer anions, in recent years these materials were also studied as possible sorbents and scavengers of metal cations from waters [5–9].

On the other hand, humic acids (HA) which are natural polymers formed by the decomposition of biological organisms, could be bonded to metal cations thus affecting their retention and mobility. Their functional groups such as carboxylate, hydroxyl and phenolate could interact with both metals cations and LDHs.

The kinetic and thermodynamic parameters of the metal sorption on different natural substrates as well as their competition with the naturally occurring anions, such as humate, for the sorption sites could be important for understanding the behaviour and fate of these contaminants in the environment.

Therefore, the aim of this work was the study of the kinetic and thermodynamic parameters of the sorption of Cu^{2+}, Cd^{2+} and Pb^{2+} on layered double hydroxides intercalated by (i) chloride (LDHCl), (ii) high amounts of the humate anion (LDH-H100) and (iii) low amounts of the humate anion (LDH-H50). Also, the factors affecting the metal sorption such as the competition of the three metals for the sorption sites, as well as their competition with the humate anion from the solution, were studied.

2. Experimental

All the reagents were of analytical grade products and purchased from Aldrich (Spain).

2.1. Synthesis of the sorbents

Three LDHs were synthesized for study as sorbents of potentially toxic metals Cu^{2+}, Cd^{2+} and Pb^{2+}. A layered double hydroxide with chloride as the interlayer inorganic anion (LDH-Cl), was obtained by co-precipitation method and two layered double hydroxide-humate hybrids (LDH-H100 and LDH-H50) were

prepared as we have previously described [8] by incorporating of 100% and 50% of humate stoichiometric concentration required to compensate the layer charge (estimated by elemental analysis and TG–DTA study) to the slurry of the sample LDH-Cl.

2.2. Metal sorption experiments

The optimal sorption conditions (initial pH, contact time) were determined in the sorption experiments performed. 0.05 g of the sorbent (LDH-H100, LDH-H50 or LDH-Cl) was dispersed in 30 mL aqueous solutions of Cu^{2+}, Pb^{2+} and Cd^{2+} nitrate salts (initial concentrations C_0= 1 mM). Sorption isotherms were performed in 30 mL dispersions containing 0.05 g sorbent with corresponding metal ion. Initial metal concentrations ranged in all cases between C_0 = 0 and 2.5 mM, except in the case of Cu sorption on LDH-Cl, where the initial concentration was increased up to 4.4 mM in order to reach the sorption isotherm plateau. Finally, the competition between two and three metals simultaneously present in the solution (each C_0 = 1mM at pH = 5), was studied by dispersing 0.05 g of sorbent in 30 mL of the metal solutions. Also, the influence of humate presence in the solution (C_0 = 1 mM) on sorption for metals on LDH-Cl was studied only for the ternary system (three heavy metals simultaneously present in the solution, each C_0 = 1 mM, 0.05 g/30 mL).

The suspensions were shaken and after a suitable time, were centrifuged and the supernatants were filtered and used to determine the amounts of metals by atomic absorption spectrometry (AAS) in a Perkin Elmer AAnalyst 400 instrument. The amounts of metal sorbed per gram of sorbent, Cs (mmol g^{-1}), were calculated as follows:

$$C_s = (C_o - C_e)\, V/W \quad (1)$$

where C_0 and C_e are the initial and equilibrium solution concentrations (mmol L^{-1}), W is the weight of solids (g) and V is the metal solution volume (L). The experimental sorption data were fitted to the Langmuir and Freundlich models, represented in Eqs. (2) and (3), respectively:

$$C_e/C_s = (1/C_m)\, C_e + 1/C_m K_L \quad (2)$$

where C_m is the maximum sorption capacity at the monolayer coverage (mmol g^{-1}) and K_L (L $mmol^{-1}$) is a constant related to the sorption energy:

$$\log C_e = \log K_f + N_f \log C_0 \quad (3)$$

where K_f ($mmol^{1-Nf}$ L^{Nf} g^{-1}) and N_f are Freundlich parameters, whose are characteristic of the sorbent–sorbate systems [10].

2.3. Kinetic models

The kinetic models of pseudo-first order and pseudo-second order assume that sorption is a pseudo-chemical reaction, and the sorption rate can be determined for the equations of pseudofirst (Eq. (4)) and pseudo-second order (Eq. (5)) respectively:

$$\log (q_e - q_t) = \log q_e - (K_1 / 2.303)t \quad (4)$$

$$t/q_t = 1/(k_2 q_e^2) + (1/q_e)t \quad (5)$$

where q_t and q_e are the metal amount sorbed at time t (min) and at equilibrium (mg g^{-1}), respectively, k_1 and k_2 are the rate constants of pseudo-first and pseudo second-order models, in (min^{-1}) and (g mg^{-1} min^{-1}), respectively.

2.4. Characterization techniques

Mg and Al elemental chemical analyses were performed by Inductively Coupled Plasma Mass Spectrometry (ICP-MS) in a Perkin Elmer ELAN DRC-e instrument. The samples were dissolved in concentrated HNO_3. Powder X-ray diffraction patterns (XRD) were recorded using a Siemens D-5000 instrument with CuK_α radiation. FT-IR spectra were recorded with a Perkin Elmer Spectrum One spectrphotometer using KBr disk method.

3. Results and discussion

3.1. Characterization of the sorbents

XRD patterns corresponding to the three sorbents (Supplementary data, Figure S1) showed that the synthesized samples are hydrotalcite type compounds and the presence of humate anions was confirmed by FT-IR spectrum on the LDH-H100 and LDHH50 samples (Supplementary data, Figure S2). The elemental

analysis indicated that the molar ratio Mg:Al for both hybrids was 2.4, with a content of magnesium and aluminium of 15% and 7%, respectively. This result shows that the relation of divalent and trivalent cations obtained was close to the LDH-Cl precursor indicating a slight Mg dissolution during the humate incorporation in the synthesis process [8].

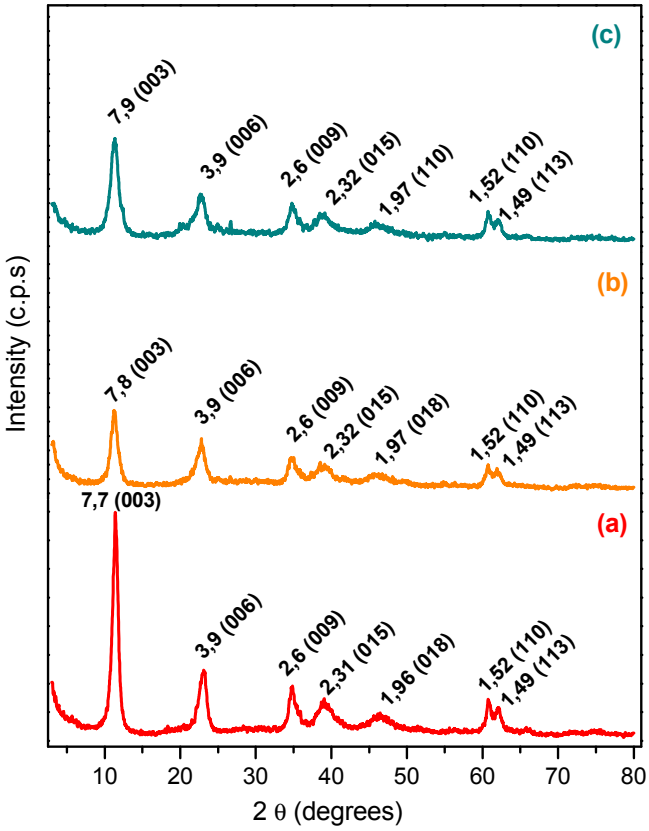

Supplementary Figure S1.

XRD patterns of (a) LDH-Cl, (b) LDH-H 50 and (c) LDH-H 100.

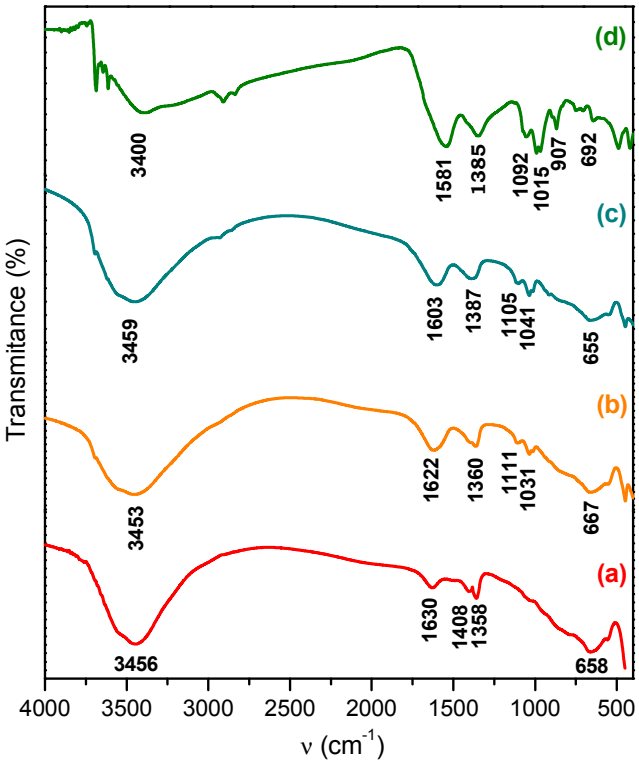

Supplementary Figure S2.

FT-IR spectra of (a) LDH-Cl, (b) LDH-H 50, (c) LDH-H 100 and (d) sodium Humate (NaH).

3.2. Sorption equilibrium studies

3.2.1. Influence of the initial metal concentration (sorption isotherms)

The Cu^{2+}, Pb^{2+} and Cd^{2+} sorption isotherms on LDH-H100, LDHH50 and LDH-Cl are included in Fig. 1. The shape of the sorption isotherm was very similar for each metal sorption in the three sorbents and they correspond to type L or H according to the Giles classification [11]. The results showed that the maximum uptake of Cu^{2+} on LDH-H100, LDH-H50 and LDH-Cl was 0.76, 1.02 and 1.95mmol g^{-1}, respectively. The amounts sorbed of Pb^{2+} were 0.48, 0.25 and 0.61 mmol g^{-1}, and finally for Cd^{2+} were 0.35, 0.18 and 1.03 mmol g^{-1} on LDH-H100, LDH-H50 and LDH-Cl, respectively. In all cases, the removal of the three metals was higher on LDH-Cl. The final pH 8.2–9 values achieved after sorption processes on LDH-Cl, suggest that the main mechanism of uptake of metals is probably their precipitation as metal hydroxides. These hydroxides can precipitate either as part

of the LDH structure by a mechanism known as diadochy or in a separate phase [12]. The higher amounts of metals sorbed on LDH-Cl could be caused by the precipitation of $M(OH)_2$ determined by its solubility product (K_{SP} $(Cu(OH)_2)$ = 1 x 10^{-20}, K_{SP} $(Pb(OH)_2)$ = 2.5 x 10^{-16}, K_{SP} $(Cd(OH)_2)$ = 3.2 x 10^{-14}. The isomorphic substitution in the layer of magnesium for copper due to their similar cation radio (r_{Mg2+} = 86 pm and r_{Cu2+} = 87 pm [13] could also contribute to the removal of this metal cation. However, the lowest sorption percentage of Pb^{2+} may be due to the large size of its cation (r_{Pb2+} = 133 pm), which would cause greater steric hindrance than the other two metal cations which would hinder the cation exchange in the layers. Also, it should be noted here that for LDH-Cl and C_0 = 0–2 mM, the metal elimination percentages were 98%, 80% and 53% for Cu^{2+}, Cd^{2+} and Pb^{2+}, respectively. In the hybrids (LDH-H100 and LDH-H50), the metal sorption behavior was different, due to an additional bonding mechanism between the metal ions and the humate. The sorption was higher on LDHH100 than on LDH-H50 for metal cations Pb^{2+} and Cd^{2+}, which is consistent with the additional sorption mechanisms (complexation) of these metals with the functional groups of the hybrid LDHs [14]. Conversely, the Cu^{2+} is sorbed in higher amounts on LDH-H50 than on LDH-H100. One could conclude from this that the precipitation mechanism is the most important for the metal uptake on LDH non-hybrid, since there is a greater proportion of inorganic components on LDH-H50 than on LDH-H100. These results could be comparable and are quite competitive (under similar experimental conditions) with those obtained by other authors; i.e. the maximum amounts of studied metal sorbed on LDHs could be grouped into the following ranges: 0.01–0.5 mmol g^{-1} for Cd^{2+}, 0.03–1.78 mmol g^{-1} for Cu^{2+} and 0.03–0.5 mmol g^{-1} for Pb^{2+} [5, 6, 12, 15–20].

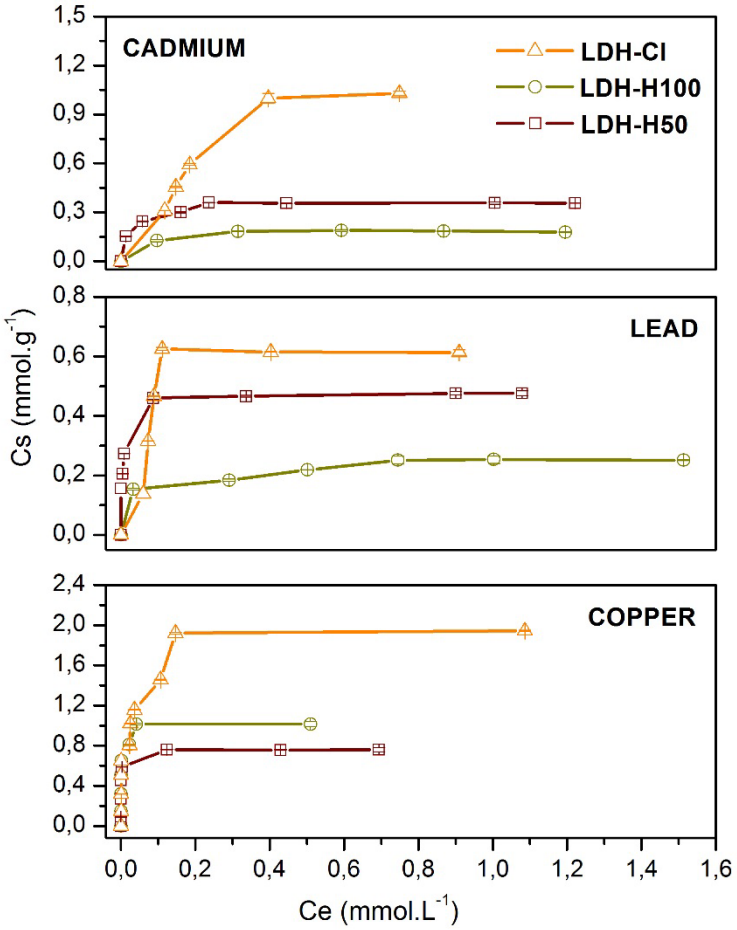

Fig. 1. Sorption isotherms of Cu^{2+}, Pb^{2+} and Cd^{2+} on the sorbents: LDH-H50, LDH-H100 and LDH-Cl.

3.2.2. Sorption equilibrium models

In order to correlate the experimental data adequately, Langmuir and Freundlich isotherm equations were tested (Eqs. (2) and (3)) to find the best fit using a linear regression coefficient. The results have been included in Table 1 and have shown that the best fit of Cu^{2+}, Pb^{2+} and Cd^{2+} sorption founded on LDH-H100 was the Langmuir model with a R^2 = 0.998–0.999, on LDH-Cl with R^2 = 0.980–0.999 and on LDH-H50 with R^2 = 0.997–0.999. This fact confirms that the sorption processes occur in a monolayer and that the distribution of active sites on the sorbents is homogeneous.

Table 1
Langmuir model parameters for heavy metals sorption on the LDH-H100, LDH-H50 and LDH-Cl sorbents.

Sample	Pollutant	T (K)	C_m (mmol g^{-1})	K_L	R^2
LDH-H100	Cu^{2+}	288	2.109	227	0.998
		298	1.326	260	0.999
		308	1.168	570	0,999
	Pb^{2+}	288	0.286	63	0.999
		298	0.48	187	0.999
		308	0.619	249	0.999
	Cd^{2+}	288	0.177	70	0.999
		298	0.180	123	0.999
		308	0.177	122	0.999
LDH-Cl	Cu^{2+}	288	0.80	41	0,995
		298	0.61	64	0.999
		308	0.57	125	0.980
	Pb^{2+}	288	0.531	9	0.999
		298	0.633	41	0.999
		308	1.209	43	0.999
	Cd^{2+}	288	0.466	5.9	0.996
		298	1.264	6	0.980
		308	2.680	11	0.991
LDH-H50	Cu^{2+}	298	1.02	250	0.999
	Pb^{2+}	298	0.265	14	0.997
	Cd^{2+}	298	0.188	48	0.998

3.2.3. Thermodynamics of sorption

The effect of the temperature on the sorption of metal on LDH-H and LDH-Cl was studied in the temperature range 288–308 K (Fig. 2). The thermodynamic parameters, such as enthalpy (ΔH°), entropy (ΔS°) and Gibb's free energy (ΔG°) were estimated using the relation:

$$\Delta G° = -RT \ln K_L \quad (6)$$

where K_L is the equilibrium constant obtained from Langmuir equation (Table 1).

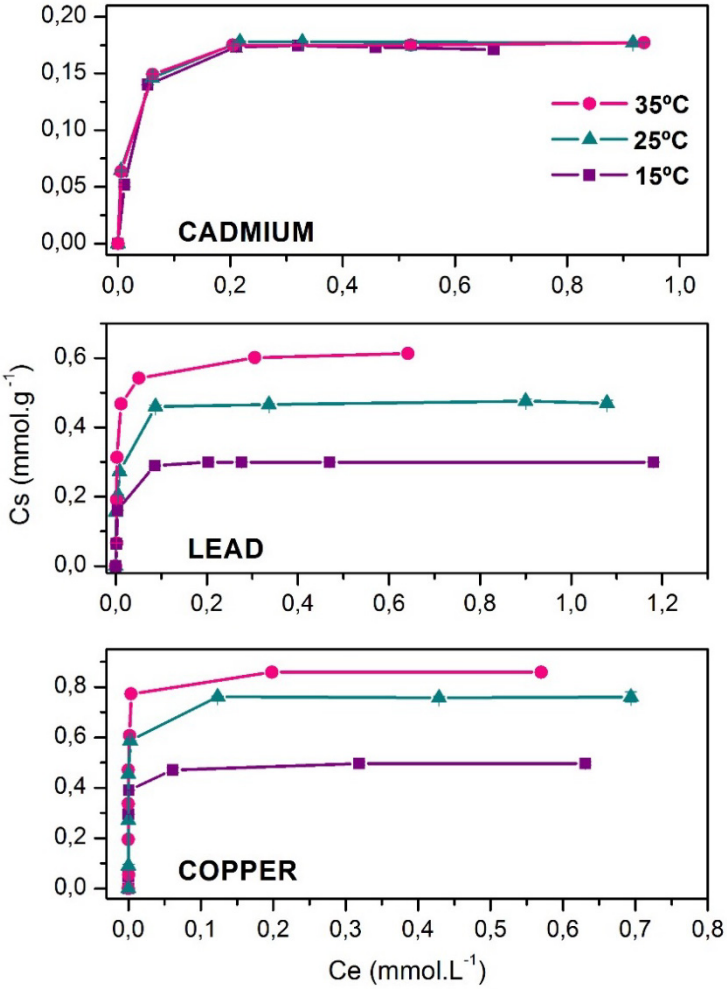

Fig. 2. Sorption isotherms of Cu^{2+}, Pb^{2+} and Cd^{2+} on LDH-H 100 at several temperatures.

The standard enthalpy (ΔH°) and entropy (ΔS°) were determined from Van't Hoff equation:

$$\ln K_L = \Delta S°/R - \Delta H°/RT \quad (7)$$

the values of ΔH° and ΔS° were obtained from the slope and intersection of the plot of $\ln K_L$ versus 1/T, and the results are shown in Table 2. The ΔG° values for the temperatures at a range of 288–308 K were obtained between 4.06 and 16.25 kJ/mol. Negative values of free energy changes indicated that the sorption of metal on the LDHs is a spontaneous and a thermodynamically favourable process. These values were in the middle of physisorption (20–0 kJ/mol) and chemisorption (80–400 kJ/mol) [21] and it may be concluded that the process was a physical–

chemical effect. Positive values of ΔS° indicate the increasing randomness in the sorption process. The positive value of ΔH° indicated that the sorption processes were endothermic in all cases.

Table 2
Thermodynamic data for the sorption of Cu^{2+}, Pb^{2+} and Cd^{2+} on the LDH-H100 and LDH-Cl sorbents.

Sample	Pollutant	T (K)	ΔG (kJ.mol^{-1})	ΔH (kJ mol^{-1})	ΔS (kJ mol^{-1})
LDH-H100	Cu^{2+}	288	-12.99	33.70	0.161
		298	-13.78		
		308	-16.25		
	Pb^{2+}	288	- 9.92	50.97	0.212
		298	-12.96		
		308	-14.13		
	Cd^{2+}	288	-10.17	20,7	0.108
		298	-11.92		
		308	-12.30		
LDH-Cl	Cu^{2+}	288	- 8.89	69.7	0,274
		298	-10.30		
		308	-14.38		
	Pb^{2+}	288	- 6.34	95.90	0.360
		298	- 9.89		
		308	-13.44		
	Cd^{2+}	288	- 4.06	18.40	0.078
		298	- 4.84		
		308	- 5.62		

3.3. Sorption kinetics

The kinetic of the sorption describes the rate of the removal metal ions on the layered double hydroxides and it is an important aspect of the pollutant removal process control. The kinetic of metal ions uptake is required for selecting optimum operating conditions for the full-scale bath process and gives notable information for designing and modelling the process.

3.3.1. The effect of contact time

The studies of the influence of time on the sorption have been included in Fig. 3, showing that the amount of metal sorbed increased with time. In the case of sorption of Cu^{2+} on LDH-Cl, the plateau was reached at 2 h; however, it took 24 h for the LDH-H100 and LDH-H50 sorbents. The removal rates of Pb^{2+} and Cd^{2+} were slower than that corresponding to Cu^{2+}. The equilibrium was reached at 24 h (for LDH-Cl and LDH-H50) and 48 h (for LDH-100) for Pb^{2+} while the equilibrium for sorption of Cd^{2+} occurred at 48 h for the three sorbents. The precipitation process could be less significant in these last cases due to the fact that $Pb(OH)_2$ and $Cd(OH)_2$ have higher Ks than $Cu(OH)_2$ and a higher concentration of metal in these cases produced a greater interaction between carboxylate groups from the humate anions and the metals ions.

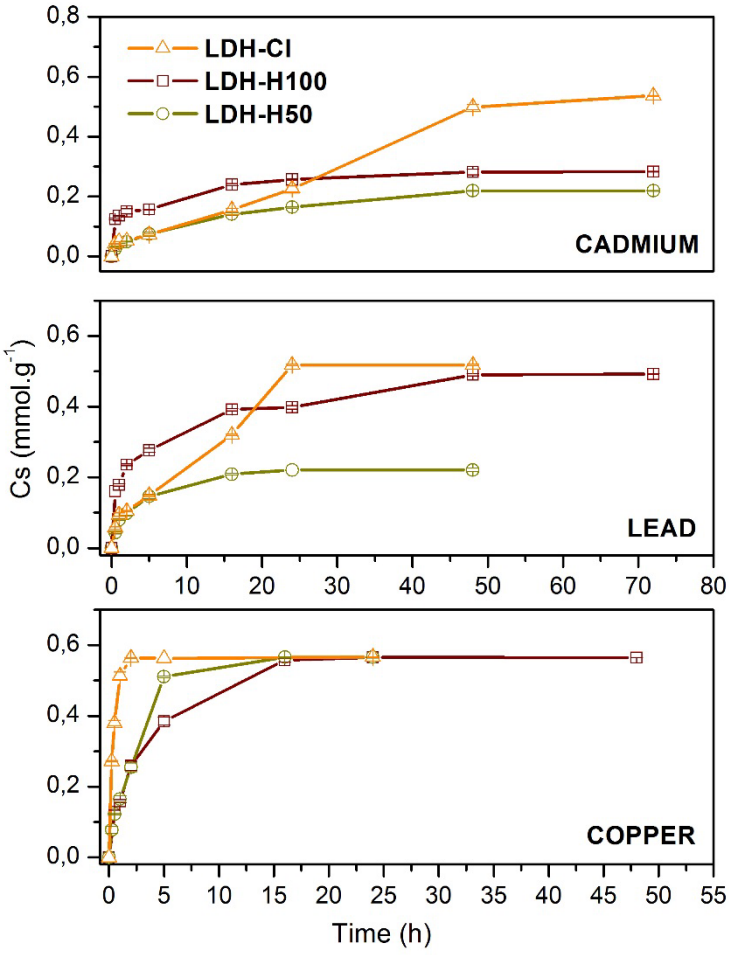

Fig. 3. The evolution of sorption of Cu^{2+}, Pb^{2+} and Cd^{2+} on different sorbents: LDH-H50, LDH-H100 and LDH-Cl at pH = 5.

3.3.2. Kinetic models

The kinetic was analysed using different kinetic models such as pseudo-primer-order and pseudo-second-order (Eqs. (4) and (5)).

The parameters of the kinetic models and the linear regression coefficients (R^2) were obtained and shown in Table 3. The kinetic data were fitted better to Eq. (5) for the three sorbents and the three metals based on the correlation coefficient R^2. The q_e values calculated from the pseudo-second-order rate model are very consistent with the experimental qe values. This indicates that the experimental kinetic data for sorption by this type of LDH sorbents work well with this model for the entire time range. These results suggested that the pseudo-second order sorption mechanism was predominant, and that the overall rate of the metal uptake appeared to be controlled by a chemisorption process as was indicated by Ho [22]. The pseudo-second-order rate expression has been widely applied in the description of the sorption of the pollutants from aqueous solutions (pesticides, dyes, metal ions, and organic substances) on different sorbents [23–26]. The advantage of using this model is that there is no need to know the equilibrium capacity (q_e) from the experiments as it can be calculated from the model [22]. The rate k_2 for metals sorption process on LDH-Cl and LDH-H50 presented the following sequence: $Cu^{2+} > Pb^{2+} > Cd^{2+}$ and for LDH-H100; $Cd^{2+} \sim Cu^{2+} > Pb^{2+}$. Given the variety of possibilities of different types and/or degrees of specific interaction between the solute and the sorbent (precipitation of hydroxide, diadochy and/or complexation) [7], it is difficult to identify which has a greater influence on the sequence of the apparent rate constant for the different sorbents used.

Table3

Coefficients of pseudo-first-order, pseudo-second-order and intra-particle diffusion model for sorption of Cu^{2+}, Pb^{2+} and Cd^{2+} on LDH-H100, LDH-H50 and LDH-Cl.

Metal/adsorbent	qe Exp (mg/g)	Pseudo-first-order model			Pseudo-second-order model			Intra-particle diffusion model		
		$K_1 \times 10^3$ (min^{-1})	q_e (mg/g)	R^2	$K_2 \times 10^3$ (g/mg.min)	q_e (mg/g)	R^2	K_{ip} (mg/g $min^{0.5}$)	C	R^2
Cu/LDH-H 100	36	1.3	17	0.811	0.20	38.5	0.998	0.62	9	0.827
Cu/LDH-H 50	36	4.6	50	0.896	0.19	40.0	0.995	0.93	25	0.803
Cu/LDH-Cl	36	4.0	8	0.840	0.05	36.3	0.999	0.38	24	0.385
Pb/LDH-H 100	102	1.8	83	0.909	0.05	105.0	0.995	1.20	34	0.936
Pb/LDH-H 50	46	2.1	25	0.840	0.16	47.6	0.999	0.78	12	0.849
Cd/LDH-Cl	108	2.5	114	0.795	0.01	124.0	0.935	2.11	-2	0.845
Cd/LDH-H 100	32	1.6	21	0.993	0.22	32.3	0.998	0.33	13	0.916
Cd/LDH-H 50	24	2.3	39	0.864	0.08	27.0	0.985	0.38	2	0.996
Cd/LDH-Cl	61	1.4	89	0.914	0.006	83.0	0.673	1.00	-5.64	0.938

3.3.3. Intraparticle diffusion model

The overall rate of the sorption process is explored by plotting of q_t versus $t^{1/2}$. According to Weber and Morris [27], for most sorption processes the uptake varies almost proportionally with $t^{1/2}$ rather than with the contact time and can be represented as follows:

$$q_t = K_{ip} t^{1/2} + C \quad (8)$$

where k_{ip} (mg/g $min^{0.5}$) is the rate constant of intra-particle diffusion.

According to Eq. (8), the plot of qt versus $t^{1/2}$ should be a straight line with a slope k_p, which is the intra-particle diffusion rate constant (mg/g $min^{0.5}$), and with an intercept C, when the sorption mechanism follows the intra-particle diffusion process. The value of C gives an idea about the thickness of the boundary layer i.e. the larger the intersection, the greater the boundary layer effect [28].

If the plot shows multilinearity, this would indicate further complexity of the sorption process; each section representing a distinct mechanism. The first section is the external surface sorption or instantaneous sorption step. The second section is the gradual sorption step where the intra-particle diffusion can be rate controlling. The third section is the final equilibrium step where the intra-particle diffusion starts to slow down due to the extremely low solute concentration in the solution [29].

In our case, Fig. 4 shows the Weber and Morris plots for Cu^{2+}, Pb^{2+} and Cd^{2+}, respectively, on the three sorbents used. It was observed that the plots were not linear in any case and they did not pass through the origin, which indicated that intraparticle diffusion is involved in the sorption process, but it is not the only rate limiting mechanism as some other mechanisms also appeared to play an important role. Surface sorption and intraparticle diffusion probably took place simultaneously, both processes controlling the kinetics of sorbate–sorbent interaction. Moreover, the diffusion rate constants in every stage (k_{pi} where i = 1, 2, . . .) follow the order of $k_{p1} > k_{p2} > k_{p3}$. Therefore the changes of k_{p1}, k_{p2}, and k_{p3} could be attributed to the sorption stages of the exterior surface, interior surface and equilibrium, respectively. This can be illustrated as follows: the first section with a steep slope represents the instantaneous diffusion stage, in which large numbers of metal ions from the bulk phase were sorbed rapidly by the surface of

the LDH. After almost all the exterior active sites were occupied, the entry of the sorbate into the pores of the sorbents was enhanced [30] and was then sorbed by the interior surface of the pores, which arose in the second stage. In the third section, the intra-particle diffusion rate constants were close to zero, indicating that the equilibrium state had finally been reached. Furthermore, the diffusion rate constant k_{p1} for the sorption of Cu^{2+} on LDH-Cl is much higher than that of LDH-H100, which might be attributed to more active sites on the surface of LDH-Cl or that the high final pH on the process can induce rapid precipitation of Cu^{2+} [8]. The value of the diffusion rate constant kp1 for sorption of Pb^{2+} on LDH-H100 is higher than that on LDH-Cl due to the presence of more active sites on the surface of LDH-H100, thus attracting metal ions and enhancing the diffusion rate.

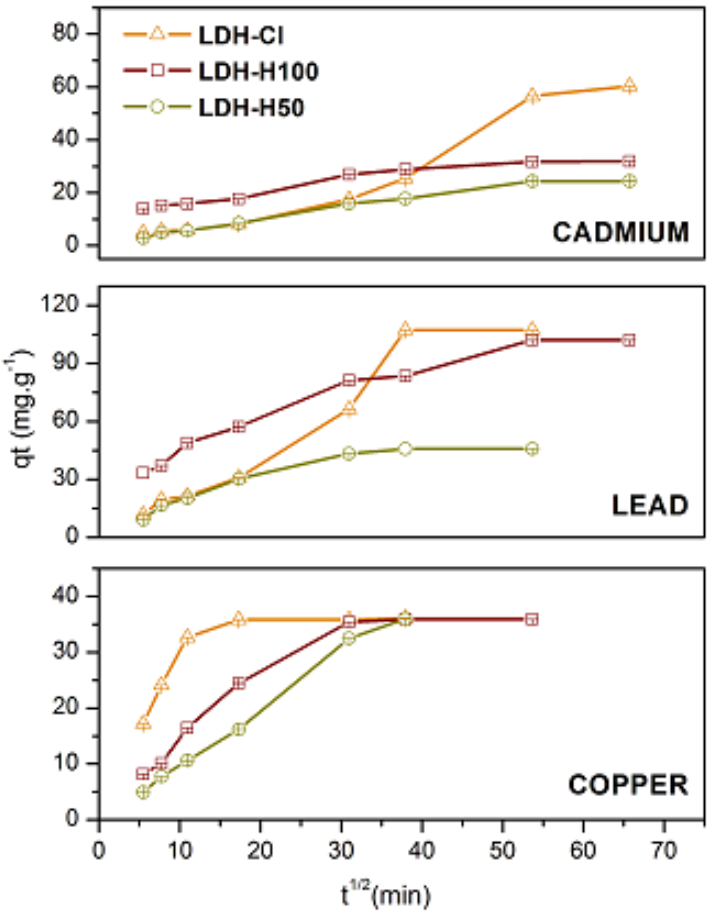

Fig. 4. Intraparticule diffusion plot for the sorption of Cu^{2+}, Pb^{2+} and Cd^{2+} on LDH-H50, LDH-H100 and LDH-Cl.

3.4. Competition experiments

3.4.1. Competition of metal sorption in a multicomponent solution in LDH-Cl

The competitive effects that the metals exert on each other in multicomponent (binary and ternary) solutions and the removal efficiencies of LDH-Cl for each metal in a monocomponent (single metal) and in multicomponent solutions, were studied and included in Figs. 5 and 6.

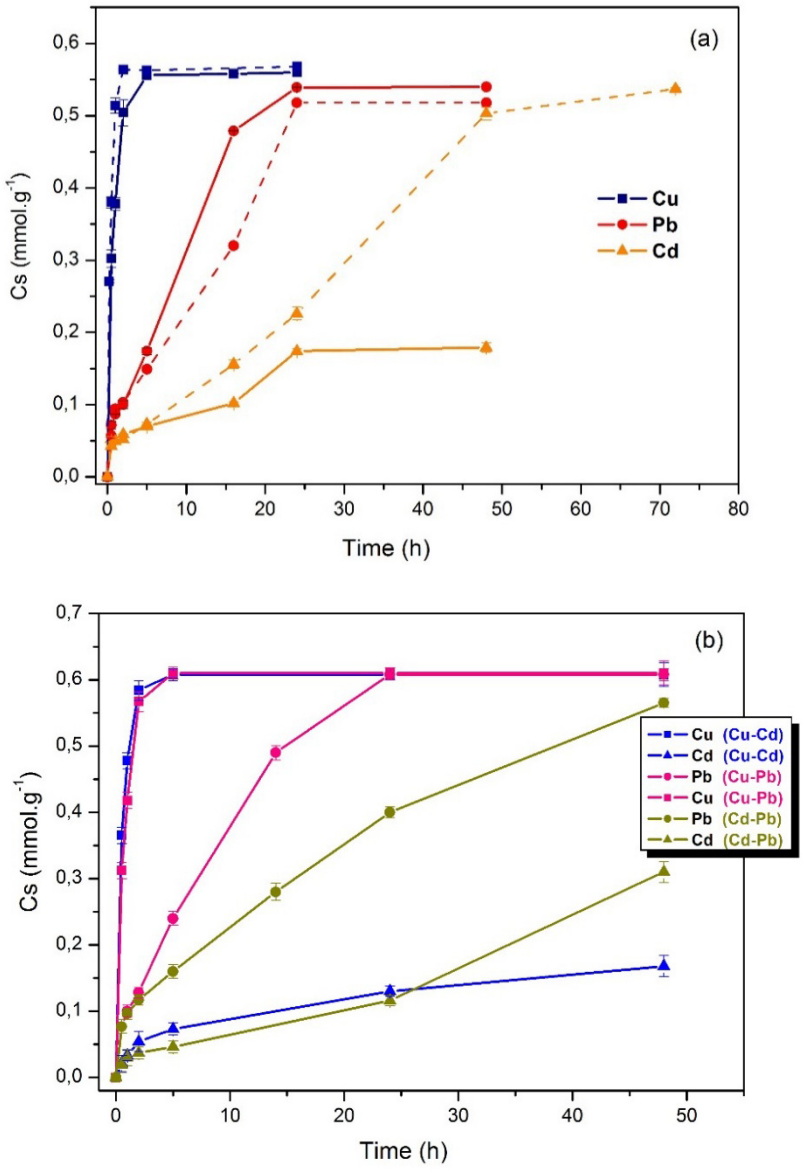

Fig. 5. The evolution of removal of Cu^{2+}, Pb^{2+} and Cd^{2+} on LDH-Cl at pH = 5 and $Ci_{(Cu,Pb,Cd)}$ = 1 mM. (a) From ternary solution (solid line) and single solution (dash line). (b) From binary system.

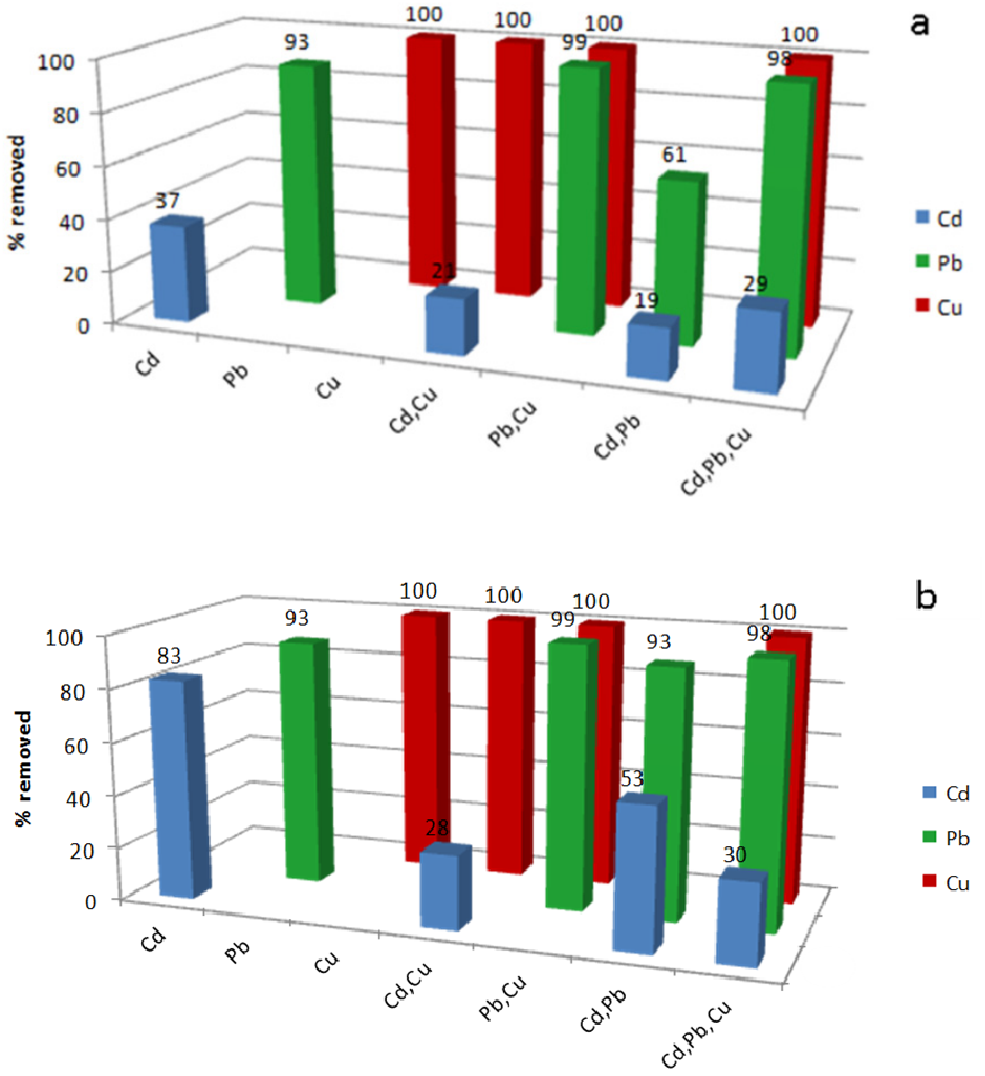

Fig. 6. The evolution of sorption of Cu^{2+}, Pb^{2+} and Cd^{2+} on LDH-Cl from ternary and binary systems (a) at 24 h, and (b) at 48 h.

Comparing the binary and the ternary systems, it could be observed that the Pb^{2+} and Cd^{2+} present in the solution do not affect the high percentage of Cu^{2+} sorption in any case. The referred reaction between Cu^{2+} and LDH hydroxyl groups (greater stability constant) cause a fast surface sorption. The precipitation of Cu^{2+} on LDH-Cl takes place (Fig. 5) which makes it difficult for other metals to reach the sorption sites and/or causes its posterior precipitation in different sheets. The results for the multicomponent systems show that the presence of Cd^{2+} has a negligible influence on the sorption of Cu^{2+} and Pb^{2+} on the LDH-Cl, whereas the sorption of Cd^{2+} is significantly reduced but only if the contact time is 48 h.

The results for the binary solution show that the sorption of Cu^{2+} achieved 100% in both the Cu–Cd and Cu–Pb systems. However, the percentage of the removal of Pb2+ decreases in the presence of Cd^{2+} in respect to the Cu–Pb system and this value for Cd^{2+} is lower in the presence of Pb^{2+} (Cd–Pb system) than in Cu^{2+} (Cu–Cd system), showing competition between Pb^{2+} and Cd^{2+} during a 24 h period. The decrease in percentage of the removal of the metals on LDH-Cl from the multicomponent solutions in respect to the single solution (non competitive system), may be ascribed to less availability of binding sites. In the multicomponent solutions where metals compete for the same sorption sites of the sorbent metals with a greater affinity, for example; Cu^{2+} could displace others such as Pb^{2+} and/or Cd^{2+} with a weaker affinity [31].

Hence, the order of removal efficiencies of LDH-Cl for the three metal ions was $Cu^{2+} > Pb^{2+} > Cd^{2+}$, implying a stronger affinity of the sorbent for Cu^{2+} than for Pb^{2+} and Cd^{2+}, which agrees with the precipitation of metals as hydroxides and confirms it as the predominant mechanism on LDH-Cl precipitation [8].

3.4.2. Influence of the presence of humate anion on the solution

In order to study the influence of the presence of humate anion on the solution over the metal sorption, some experiments were performed. A simultaneous sorption of these three metals on LDH-Cl in the presence of a humate solution (Fig. 7) was carried out. The maximum amount sorbed of Cu^{2+} at the equilibrium time (in the presence and absence of humate) was the same (C_s = 0.56 mmol g^{-1}). For Pb^{2+} sorption the maximum C_s was 0.54 mmol g^{-1} (in the absence of humate) and 0.49 mmol g^{-1} (in the presence of humate). It could be due to a small part of the metal being complexed with the humate anions present in the solution and remaining there. The Cd^{2+} sorption follows a similar tendency, the C_s values were 0.18 mmol g^{-1} (in the absence of humate) vs 0.12 mmol g^{-1} (in the presence of humate). This could be due to the formation of $Cd(OH)_2$ starting at a higher pH value, the complexation possibly being more favoured (in the presence of NaH) than in the Pb system. This behaviour could indicate that the affinity sequence of metal cations by the humate anion varies, in accordance with the following order: $Cd^{2+} > Pb^{2+} > Cu^{2+}$ (Supplementary data, S3).

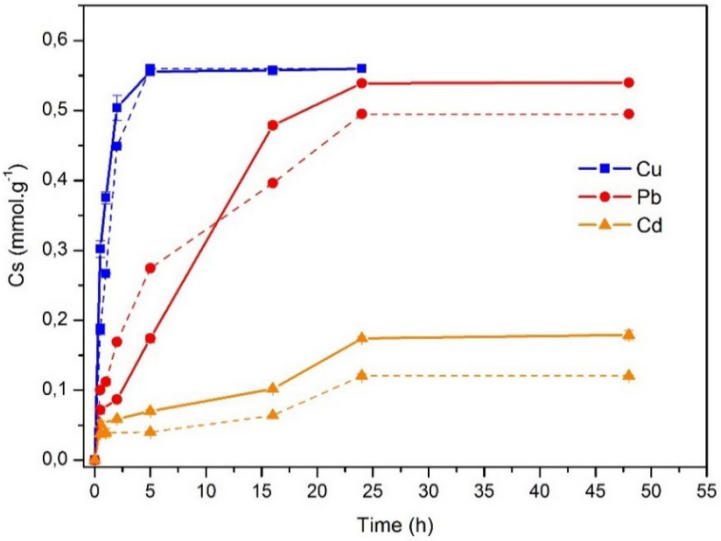

Fig. 7. The evolution of sorption of Cu^{2+}, Pb^{2+} and Cd^{2+} on LDH-Cl from ternary system (solid line) and from ternary solution of metals in presence of humic acid solution (C_i = 1 mM at pH = 5) (dash line).

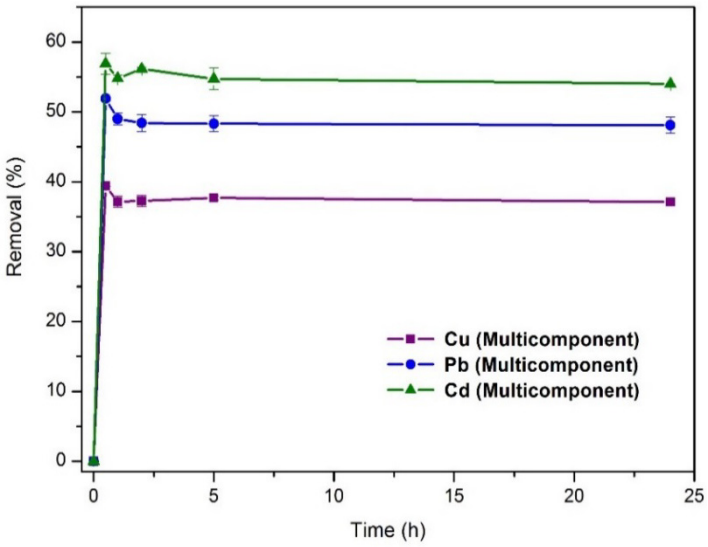

Supplementary Figure S3.

The evolution of sorption of Cu^{2+}, Pb^{2+} and Cd^{2+} on NaH from ternary system of metals

4.Conclusions

LDHs could uptake metal cations by two mechanisms: (i) chemical precipitation by LDH weathering reactions which lead to a pH increase and precipitation of metal hydroxides and (ii) chelation, if LDH is previously functionalized with a chelating agent. Thus we synthesised LDH intercalated by chloride (LDH-Cl) and two LDHhumate hybrids with different humate loadings (LDH-H50 and LDH-H100) for their study as sorbents of potentially toxic metals from a water solution. LDH-humate is a novel material which we had believed could be very efficient, possibly even more so than LDH-Cl in the metal captions, due to the humate functional groups which could bond metal cations.

However, even though all the sorbents presented high efficiency for the studied metals, maximum sorption was achieved for LDH-Cl, and decreased in the following order: Cu^{2+}, Cd^{2+} and Pb^{2+}. Higher metal amounts sorbed on LDH-Cl suggest that the LDH buffer properties play an important role here, where a slight dissolution of LDH took place, thus inducing precipitation of the metals as hydroxides. In the cases of LDH-H, the LDH moiety is covered by humate, as indicated by characterization analysis, which makes it more stable against dissolution. In this case, humate functional groups are also responsible for the metal uptake.

The thermodynamic parameters indicate that the sorption process is endothermic, feasible and thermodynamically favoured. The pseudo second-order model was found to be more adequate to describe the kinetic of the sorption system in each case. The competitive metal sorption (both in the presence and the absence of humate anions) from binary and ternary solutions for LDH-Cl showed the following sorption order: $Cu^{2+} > Pb^{2+} > Cd^{2+}$. This competing behaviour was related to different factors such as the solubility product constants, complex formation stabilities and/or contact time.

The results suggest that the LDHs studied here are efficient sorbents of potentially toxic metals. Nevertheless, a more detailed research, such as sorbent recyclability and the influence of other ions currently present in water, is needed to optimize this application. Notwithstanding, the novel LDH-humate materials provide an effective solid matrix for immobilizing metals without substantially

altering environmental pH values, and could be suitable, as well as LDH-Cl, in the decontamination of water of toxic metallic elements.

Acknowledgements

The financial support from the Spanish Junta de Andalucía (research group FQM214) and MCYT (Project CTM2011-25325) is gratefully acknowledged. We appreciate the technical assistance received in the SCAI (Universidad de Córdoba) for Elemental Analysis Units (ICP-MS).

References

[1] M.A. Hashim, S. Mukhopadhyay, J.N. Sahu, B. Sengupta, Remediation technologies for heavy metal contaminated groundwater: a review, J. Environ. Manage. 92 (2011) 2355–2388.

[2] C. Forano, T. Hibino, F. Leroux, C. Taviot-Guého, Layered double hydroxides, in: F. Bergaya, B.K.G. Theng, G. Lagaly (Eds.), Handbook of Clay Science, Elsevier Ltd., 2006, pp. 1021–1095.

[3] U. Costantino, M. Noccheti, M. Sisani, R. Vivani, Recent progress in the synthesis and application of organically modified hydrotalcites, Z. Kristallogr. 224 (2009) 273–281.

[4] J.H. Choy, S.J. Choi, J.M. Oh, T. Park, Clay minerals and layered double hydroxides for novel biological applications, Appl. Clay Sci. 36 (2007) 122–132.

[5] M.R. Pérez, I. Pavlovic, C. Barriga, J. Cornejo, M.C. Hermosín, M.A. Ulibarrri, Uptake of Cu^{2+}, Cd^{2+} and Pb^{2+} on Zn–Al layered double hydroxide intercalated with EDTA, Appl. Clay Sci. 32 (2006) 245–251.

[6] I. Pavlovic, M.R. Pérez, C. Barriga, M.A. Ulibarri, Adsorption of Cu^{2+}, Cd^{2+} and Pb^{2+} ions by layered double hydroxides intercalated with the chelating agents diethylenetriaminepentaacetate and meso-2,3-dimercaptosuccinate, Appl. Clay Sci. 43 (2009) 125–129.

[7] X. Liang, Y. Zang, Y. Xu, X. Tan, W. Hou, L. Wang, Y. Sun, Sorption of metal cations on layered double hydroxides: a review, Colloids Surf., A. 433 (2013) 122–131.

[8] M.A. González, I. Pavlovic, R. Rojas-Delgado, C. Barriga, Removal of Cu^{2+}, Pb^{2+}

and Cd^{2+} by layered double hydroxide-humate hybrid. Sorbate and sorbent comparative studies, Chem. Eng. J. 254 (2014) 605–611.

[9] R. Rojas, Copper, lead and cadmium removal by Ca Al layered double hydroxides, Appl. Clay Sci. 87 (2014) 254–259.

[10] C.C. Travis, E.L. Etnier, A survey of sorption relationships for reactive solutes in soil, J. Environ. Qual. 10 (1981) 8–17.

[11] C.H. Giles, T.H. MacEwan, S.N. Nakhwa, D. Smith, Studies in adsorption. Part XI. A system of classification of solution adsorption isotherms and its use in diagnosis of adsorption mechanisms and in measurement of specific surface areas of solids, J. Chem. Soc. (1960) 3973–3993.

[12] S. Komarneni, N. Kozai, R. Roy, Novel function for anionic clays: selective transition metal cation uptake by diadochy, J. Mater. Chem. 8 (1998) 1329–1331.

[13] J.E. Huheey, E.A. Keiter, R.L. Keiter, Inorganic Chemistry: Principles of Structure and Reactivity, fourth ed., Harper Collins College Publishers, New York, 1993.

[14] S. Vreysen, A. Maes, Adsorption mechanism of humic and fulvic acid onto Mg/Al layered double hydroxides, Appl. Clay Sci. 38 (2008) 237–249.

[15] T.S. Anirudhan, P.S. Suchithra, Synthesis and characterization of tannin immobilized hydrotalcite as a potential adsorbent of heavy metal ions in effluent treatments, Appl. Clay Sci. 42 (2008) 214–223.

[16] R. Rojas, M.R. Perez, E.M. Erro, P.I. Ortiz, M.A. Ulibarri, C.E. Giacomelli, EDTA modified LDHs as Cu2+ scavengers: removal kinetics and sorbent stability, J. Colloid Interface Sci. 331 (2009) 425–431.

[17] T. Kameda, S. Saito, Y. Umetsu, Mg–Al layered double hydroxide intercalated with ethylene-diaminetetraacetate anion: synthesis and application to the uptake of heavy metal ions from an aqueous solution, Sep. Purif. Technol. 47 (2005) 20–26.

[18] H. Nakayama, S. Hirami, M. Tsuhako, Selective adsorption of mercury ion by mercaptocarboxylic acid intercalated Mg–Al layered double hydroxide, J. Colloid Interface Sci. 315 (2007) 177–183.

[19] X. Liang, W. Hou, Y. Xu, G. Sun, L. Wang, Y. Sun, X. Qin, Sorption of lead ion by layered double hydroxide intercalated with diethylenetriaminepentaacetic acid, Colloids Surf., A 366 (2010) 50–57.

[20] D. Zhao, G. Sheng, J. Hu, C. Chen, X. Wang, The adsorption of Pb(II) on Mg_2Al layered double hydroxide, Chem. Eng. J. 171 (2011) 167–174.

[21] F. Renault, N. Morin-Crini, F. Gimbert, P. Badot, G. Crini, Cationized starchbased material as a new ion-exchanger adsorbent for the removal of C. I. Acid Blue 25 from aqueous solutions, Bioresour. Technol. 99 (2008) 7573–7586.

[22] Y.S. Ho, Review of second-order models for adsorption system, J. Hazard. Mater. B136 (2006) 681–689.

[23] A. Bhatnagar, M. Sillanpää, Utilization of agro-industrial and municipal waste materials as potential adsorbents for water treatment: a review, Chem. Eng. J. 157 (2010) 277–296.

[24] L.D.L. Miranda, C.R. Bellato, M.P.F. Fontes, M.F. de Almeida, J.L. Milagres, L.A. Minim, Preparation and evaluation of hydrotalcite–iron oxide magnetic organocomposite intercalated with surfactants for cationic methylene blue dye removal, Chem. Eng. J. 254 (2014) 88–97.

[25] J. Febrianto, A.N. Kosasih, J. Sunarso, Y.H. Ju, N. Indraswati, S. Ismadji, Equilibrium and kinetic studies in adsorption of heavy metals using biosorbent: a summary of recent studies, J. Hazard. Mater. 162 (2009) 616–645.

[26] T.S. Anirudhan, P.S. Suchithra, Heavy metals uptake from aqueous solutions and industrial wastewaters by humic acid-immobilized polymer/bentonite composite: kinetics and equilibrium modeling, Chem. Eng. J. 156 (2010) 146–156.

[27] W.J. Weber, J.C. Morris, Kinetics of adsorption on carbon solution, J. Sanit. Eng. Div. ASCE 89 (1963) 31–59.

[28] J.I. Mall, V.C. Srivastava, N.K. Agarwall, Removal of Orange-G and Methyl Violet dyes study by adsorption onto bagasse fly ash-kinetic study and equilibrium isotherm analyses, Dyes Pigments 69 (2006) 210–223.

[29] G.L. Dotto, L.A.A. Pinto, Adsorption of food dyes acid blue 9 and food yellow 3 onto chitosan: stirring rate effect in kinetics and mechanism, J. Hazard. Mater. 87 (2011) 164–170.

[30] Y. Ren, H.A. Abbood, F. He, H. Peng, K. Huang, Magnetic EDTA-modified chitosan/SiO2/Fe3O4 adsorbent: preparation, characterization, and application in heavy metal adsorption, Chem. Eng. J. 226 (2013) 300–311.

[31] F. Qin, B. Wen, X.Q. Shan, Y.N. Xie, T. Liu, S.Z. Zhang, S.U. Khan, Mechanisms of competitive adsorption of Pb, Cu, and Cd on peat, Environ. Pollut. 144 (2006) 669–680.

Physical Chemistry Chemical Physics 18 (2016) 1838-1845

CAPTURING Cd(II) AND Pb(II) FROM CONTAMINATED WATER SOURCES BY ELECTRO-DEPOSITION ON HYDROTALCITE-LIKE COMPOUNDS

M.A. González[a], R. Trócoli*[b], I. Pavlovic[a] C. Barriga[a] and F. La Mantia*[bc]

[a] Dpto de Quiímica Inorgánica e Ingeniería Química, Campus de Excelencia Internacional Agroalimentaio (CeiA3), Universidad de Córdoba, Córdoba, Spain

[b] Semiconductor and Energy Conversion, Zentrum für Elektrochemie – CES, Ruhr-Universität Bochum, Germany. E-mail: rafael.trocolijimenez@rub.de

[c] Energiespeicher- und Energiewandlersysteme, Universita¨t Bremen, Germany

GRAPHICAL ABSTRACT

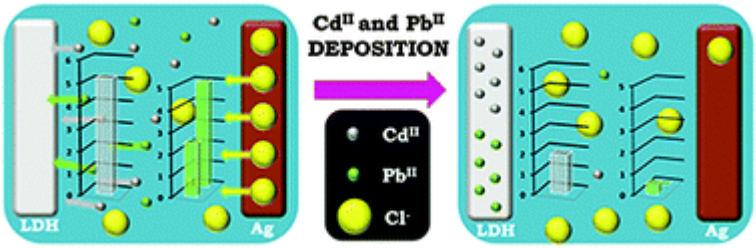

ABSTRACT

Two different hydrotalcite-like compounds were prepared and used as substrates for the electrochemical removal of extremely toxic pollutant cations, such as Cd(II) and Pb(II), from aqueous solutions, and their subsequent recovery for further potential applications. By deposition on the hydrotalcite electrode, it was possible to remove 75% of Cd(II) contained in a starting 5.2 mM solution of $CdCl_2$, which was subsequently recovered and concentrated up to 14.3 mM in a single step. A removal of almost 100% was obtained in the case of Pb(II). Its recovery was largely hindered by the formation of several inert phases, among which is some stable formation of hydroxycarbonate. Our results suggest that the removal of these contaminants by hydrotalcite-like compounds occurs by the combination of two parallel processes: electro-deposition and adsorption. It was possible to achieve a removal capacity for Cd(II) and Pb(II) equal to 763 mg $g_{a.m.}^{-1}$ and 1039 mg $g_{a.m.}^{-1}$, respectively. These removal capacities, accompanied by an excellent

posterior eluent-free recovery of Cd(II), suggest that this new method could be an environmentally friendly alternative to the conventional adsorption wastewater treatment.

1. Introduction

Heavy metals are extremely toxic pollutants, which are directly or indirectly discharged into natural water from different sources, such as metal plating, mining operations, pesticides, textile and dyeing, paper industries, and battery manufacturing, as well as natural rock mineralization processes. Many of them are soluble in water and therefore become more available for living organisms. Their toxicity lies in their bio-accumulation characteristics, i.e. they are not biodegradable and thus accumulate in living systems. Lead and cadmium are recognized to be the most hazardous pollutants to various ecosystems and human health[1] since they bind to soft tissues and bones,[2] thus inducing complex changes in plants at genetic, biochemical and physiological levels and leading to phytotoxicity.[3] World Health Organization drinking water guideline values for Cd and Pb are 0.003 and 0.01 mg l^{-1} respectively. Therefore, several remediation technologies such as adsorption by complex formation,[4] co-precipitation,[5] flotation,[6] ion exchange,[7] coagulation[8] inverse osmosis, nanofiltration,[9] electrolysis,[10] biosorption,[11] etc. have been applied to remove the pollutants from contaminated water. Notwithstanding that in many places two or more techniques can work synergistically for better results, new processes can improve the efficiency and functionality of waste water treatment. Among the different techniques applied with this aim in mind, the most extensively used is the precipitation of metals as insoluble metal hydroxides, obtained by increasing the pH of the solution. However, this process consumes a large amount of chemicals and produces large volumes of low density sludge, which is difficult to dispose. One of the most promising emerging technologies in this field is the biological or biochemical techniques but there are several challenges related to the extreme complexity of soil chemistry.[12] Even active carbons, which have been widely used as an adsorbent, present several disadvantages, among which are its high cost and difficulty to be separated from the aquatic system after utilization.[13]

Electro-deposition is an attractive technology due to its high efficiency. The electrochemical treatment techniques offer good removal yields, rapidity, lower volume of sludge, eco-friendly processing, and the possibility of obtaining excellent removal capacities even at high concentration of pollutants.[14] The substrate used to deposit heavy metals from wastewaters plays an important role during the electrochemical process, affecting the formation of dendrites, the occurrence of side reactions (H_2 evolution), and the stability of the process. So, it is necessary to find a low-cost and non-toxic material as a substrate with the purpose to get good electrochemical performance. To this aim, some of the most promising materials are the hydrotalcite-like compounds (layered double hydroxides, LDHs). These materials have attracted attention because of their interesting applications in many fields, and their singular structural characteristics and properties.[15–19] The LDHs exist as minerals, as well as synthetic phases, and their structure could be derived from those of brucite by Al-for-Mg substitution, which results in an excess of positive layer charge that is balanced by interlayer carbonate anions. LDHs have the general chemical formula $[M^{II}_{1-X}M^{III}_{X}(OH)_2]X^{n-}_{x/n} \cdot mH_2O$, where M(II), M(III) and X^{n-} are divalent (Mg^{2+}, Zn^{2+}, Ni^{2+}, etc.), trivalent (Al^{3+}, Fe^{3+}, Cr^{3+}, etc.) cations, and the interlayer anion, respectively.[20,21] Thus, it is possible to obtain a huge variety of LDH compounds by modifying the nature of these three components.

Recently, these materials have found increasing interest also in electrochemistry because of their layered structure[22] and many attractive properties, such as magnetic, redox, and catalytic functions.[23] The LDHs have been used as an anode material in Zn–Ni secondary batteries, showing lower corrosion, better reversibility and superior electrochemical stability in galvanostatic charge/discharge processes.[24]

For these multiple reasons, this work deals with the incorporation of LDH materials as a substrate component of the electrodes used in the electrochemical deposition of heavy metals. The control of secondary reactions, the metal concentration in the electrolyte, the amount of LDHs, current rate, etc. are crucial parameters during the removal process, which should be optimized. Therefore, the first aim of this work was to find out an effective removal method based on the electrochemical deposition of Pb(II) and Cd(II) and using LDH compounds as a substrate. Based on the previously developed mixed entropy, desalination and

lithium recovery technologies,[25–28] the second objective of this study was to investigate the possibility of recovering and concentrating the removed metals in a recovery water stream, which could be used for other industrial purposes, such as the production of Pb and Ni–Cd batteries, metallic coatings, dyes, stabilizers for plastics, alloys, fertilizers, etc. To this aim, two different hydrotalcite-like materials where prepared: one consisting of Zn/Al layers with carbonate as the balancing anion (ZnAl-CO_3), and another with an organic anion humate (H) between the Mg/Al layers (MgAl-H).

2. Materials and methods

All the reagents were of analytical grade products and purchased from Sigma-Aldrich. To synthesize Mg–Al-H, distilled water previously boiled and purged with N_2 to prevent CO_2 presence was used.

2.1. Preparation of ZnAl-CO_3 and MgAl-H

The hydrotalcite $[Zn_4Al(OH)_{10}]_2(CO_3)\cdot mH_2O$, named ZnAl-$CO_3$, was synthesized using the previously reported coprecipitation method at room temperature.[29] A mixed aqueous solution of 0.40 M $Zn(NO_3)_2\cdot 6H_2O$ and 0.10 M $Al(NO_3)_3\cdot 3H_2O$ was dropped from a funnel into 50 mL of water solution of 1.5 M NaOH and 0.2 M Na_2CO_3, under vigorous agitation and maintaining the basic pH. The suspension obtained was hydrothermally treated at 85 °C for 24 h, separated by centrifugation, washed with distilled water, and dried overnight at 60 °C. The hydrotalcite $[Mg_3Al(OH)_8]_2(H)\ mH_2O$, named MgAl-H, was prepared in two steps: a chloride intercalated precursor (Mg_3Al-Cl) was synthesized using the coprecipitation method, which was afterwards dispersed (second step) in a sodium humate solution obtaining the final product by anion exchange. Mg_3Al-Cl was prepared by the dropwise addition of a 200 mL aqueous solution of 0.75 M of $MgCl_2\cdot 6H_2O$ and 0.25 M of $AlCl_3\cdot 6H_2O$ to a 0.25 M of NaCl solution under vigorous agitation and constant pH = 8, set by the addition of 1 M NaOH solution. The synthesis was performed in a N_2 atmosphere in order to avoid atmospheric CO_2 dissolution and consequently carbonate incorporation into the solid. The suspension obtained was hydrothermally treated at 80 °C for 24 h, separated by centrifugation, and washed. A portion of the precipitate was dried at 60 °C to

obtain Mg_3Al-Cl, while the remaining slurry was suspended in a 0.13M sodium humate solution under vigorous stirring and a constant pH = 8 for 24 h.

2.2. Characterization of Zn/Mg-Al hydrotalcites

X-ray diffraction patterns (XRD) of powder samples were recorded using a Siemens D-500 diffractometer under CuK_α radiation (λ = 1.54050 Å). The Fourier-transform infrared (FT-IR) spectra were registered on a Perkin Elmer Spectrum One Spectrometer using the KBr disc method. Elemental chemical analyses for Zn, Mg and Al were carried out by inductively coupled plasma mass spectrometry (ICP-MS) using a Perkin Elmer ELAN DRC-e instrument. The samples were dissolved in concentrated HNO_3. Thermogravimetric (TG) and differential thermal analysis (DTA) curves were recorded on a Setaram Setsys Evolution 16/18 apparatus in an oxidizing atmosphere under the heating rate of 5°C/min. Scanning electron microscopy (SEM) images were recorded using a Quanta 3D FEG instrument equipped with an energy dispersive X-ray analyser (EDAX). Cadmium concentrations were determined by atomic absorption spectroscopy (AAS) on an Analytik Jena AAS 6 Vario instrument and lead concentrations were analyzed by inductively coupled plasma mass spectrometry (ICP-MS) by Wessling GmbH according to the ISO 11885A standard.

2.3. Preparation of electrodes based on Zn/Mg-Al hydrotalcites

To prepare the electrodes, a slurry consisting of an active material (LDH or Ag), C65 carbon black (Timcal Super P C60), polyvinylidene fluoride (Solef S5130, Solvay) binder solution in N-methyl pyrrolidone (25 mg mL^{-1}), and graphite (Timcal SFG6) in a 75: 10: 15 and 80: 9: 9: 2 by weight proportion for LDH and Ag respectively were mixed thoroughly for 30 min at 4000 rpm using an ultra-turrax disperser (Ika). The electrodes, with an approximate area of 2.9 cm^2, were prepared by handpainting on a carbon cloth (Fuel Cell Earth) current collector with a mass loading of 7 mg of LDH per cm^2 for the removal process from a 5.2 mM solution of $CdCl_2$, and 7 and 14 mg of LDH per cm^2 when 2.5 mM and 5 mM solutions of $PbCl_2$ were respectively used. Prior to use, the electrodes were dried at 60 °C.

2.4. Electrochemical measurements

Electrochemical deposition of metals was performed on a flooded three-electrode cell containing 40 mL of the respective solution (5.2 mM $CdCl_2$, 2.5 mM $PbCl_2$ or 5 mM $PbCl_2$), the LDH-based electrode as the working electrode, Ag as the counter electrode, and Ag/AgCl (3 M KCl) as the reference electrode. Prior to the electro-deposition process, argon was bubbled for 10 minutes in solution, and a slow flow was kept during the measurements to avoid the presence of oxygen. After the deposition process, the volume of the cell was reduced to 10 mL and the same configuration described above was used for the recovery process. For the calculation of the current density, the amount of cations in the starting solution was used. Current rates of C/5.2 and C/20.8 were applied for the reduction/oxidation of cadmium and C/20 in the case of lead, where a rate of C/ n represents a complete reduction (deposition step) or oxidation (recovery step) of all the amount of cations in n hours. Electrochemical measurements were performed using a Biologic VSP-300 instrument.

3. Results and discussion

3.1. Structural characterization of the hydrotalcites

The ZnAl-CO_3, MgAl-Cl and MgAl-H samples were characterized using the XRD powder method. Their XRD patterns, included in Fig. 1, correspond to hydrotalcite-like compounds with a rhombohedral symmetry and a basal spacing of 7.6 Å for $ZnAlCO_3$, 7.7 Å for MgAl-Cl and 7.9 Å for MgAl-H samples. The XRD reflections of ZnAl-CO_3 were sharper and more symmetric than MgAl-H, showing a good crystallized system. The modification of the hydrotalcite with organic anions (humate) caused a broadening of the diffraction lines and a decrease of the intensities in the hydrotalcite-system. The basal spacing, d_{003} obtained for ZnAl-CO_3 (7.6 Å) corresponds to carbonate containing hydrotalcite,[30] for MgAl-H the basal spacing was 7.9 Å, close to MgAl-Cl used as a precursor.[31] The slight modification of the interlayer spacing during the exchange was consistent with others LDHs containing humic acid.[32–34]

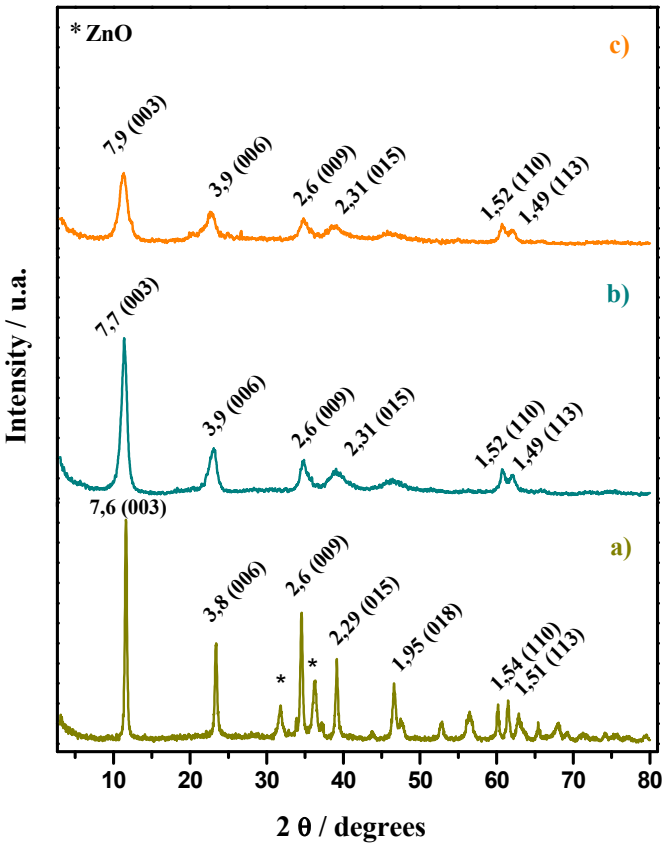

Fig. 1. X-ray patterns of ZnAl-CO_3 (a), MgAl-Cl (precursor of MgAl-H) (b) and MgAl-H (c) hydrotalcites.

The FT-IR spectra of the ZnAl-CO_3, and MgAl-H samples are given in Fig. 2. The broad absorption peak in both spectra between 3600 and 3300 cm^{-1} is due to the υ(OH) mode of the hydroxy groups, both from the brucite-like layers and from interlayer water molecules. Interlayer water also gives rise to the broad, medium-intensity, absorption between 1600 and 1500 cm^{-1}, δ(H_2O). Hydrogen bonding of water with interlayer carbonate anions also shows a shoulder at 3038 cm^{-1} in the spectrum of the ZnAl-CO_3 sample. The very intense absorption band at 1362 cm^{-1} in the spectrum of Fig. 2a corresponds to the υ_3 mode of the carbonate species. Absorption below 800 cm^{-1} is due to lattice vibrations, involving metal–oxygen stretching modes and, in the case of the ZnAl-CO_3 sample, also modes υ_2 (out-of-plane deformation) and n4 (in plane bending) of carbonate at 868 and 670 cm^{-1} respectively.[35] In the case of MgAl-H, the bands at 1114 and 1035 cm^{-1} confirmed the presence of humate anions in the hydrotalcite and the bands at 1603 cm^{-1} and 1387 cm^{-1} were associated with antisymmetric and symmetric vibration of the carboxylate groups.[31,36]

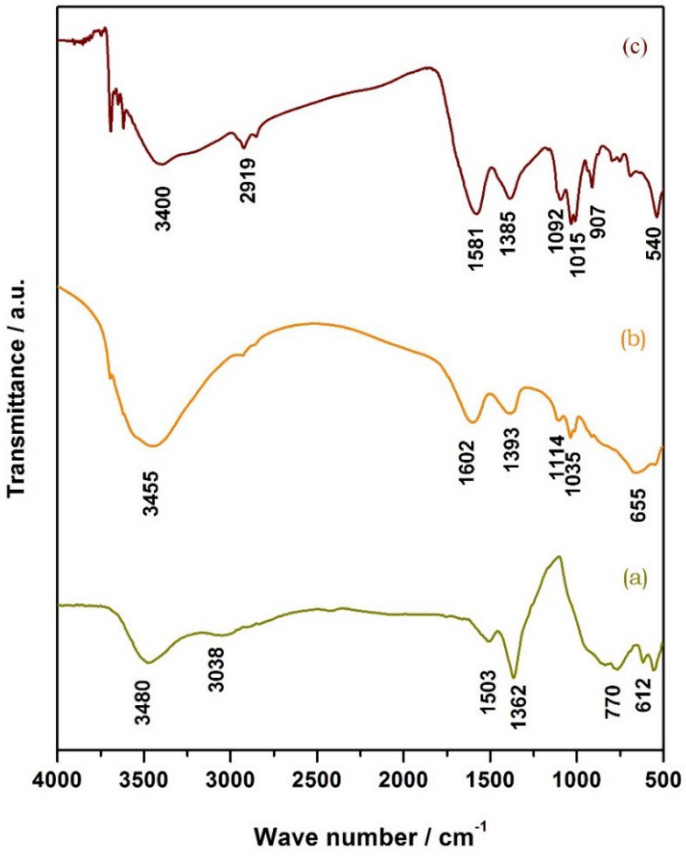

Fig. 2. FT-IR spectra of ZnAl-CO_3 (a) and MgAl-H (b) hydrotalcites. A pattern of humic acid solution salt was added for comparison (c).

The chemical analysis of the ZnAl-CO_3 and MgAl-H hydrotalcites is shown in Table 1. The molar ratio of Zn:Al was approximately 4, close to the one of the starting solutions used to prepare the sample, which evidenced that co-precipitation was practically complete. The results for MgAl-H indicated that a partial dissolution of Mg^{2+} could have occurred in the sample with respect to the composition of the precursor MgAl-Cl used during the synthesis.[31]

Table 1
Chemical analysis results of ZnAl-CO_3, MgAl-Cl and MgAl-H hydrotalcites.

Sample	% wt		Atomic ratio	Proposed formula
	M(II)[a]	Al	M(II)/Al	
ZnAl-CO_3	50	5.4	3.8	$[Mg_{0.79}Al_{0.21}(OH)_2](Cl)_{0.105}\cdot 0.33H_2O$
MgAl-Cl	20	8	2.8	$[Mg_{0.74}Al_{0.26}(OH)_2](Cl)_{0.26}\cdot 0.83H_2O$
MgAl-H	15	7	2.4	$[Mg_{0.79}Al_{0.29}(OH)_2](Cl)_{0.29/n}\cdot mH_2O$

[a]M= Zn or Mg. [b]X= Cl and/or H (n= 1 and/or 2; m=0.58-0.71).

The number of water molecules has been calculated from the total weight loss in the TG curves (Appendix 1 ESI, Fig. S1) attributed to the loss of physically adsorbed and interlayer water, dehydroxylation and decarbonation of the sample ZnAl-CO_3, and for the MgAl-H hydrotalcite was calculated from the first water loss, in the TG curves. In the latter case, two assumptions were used to define the extreme value of the hydration range: all humate molecules are substituting the chlorides in the interlayer; humate is sitting only on the surface.[31,37]

The SEM images of the substrates containing different matrix of LDHs are included in Fig. 3.

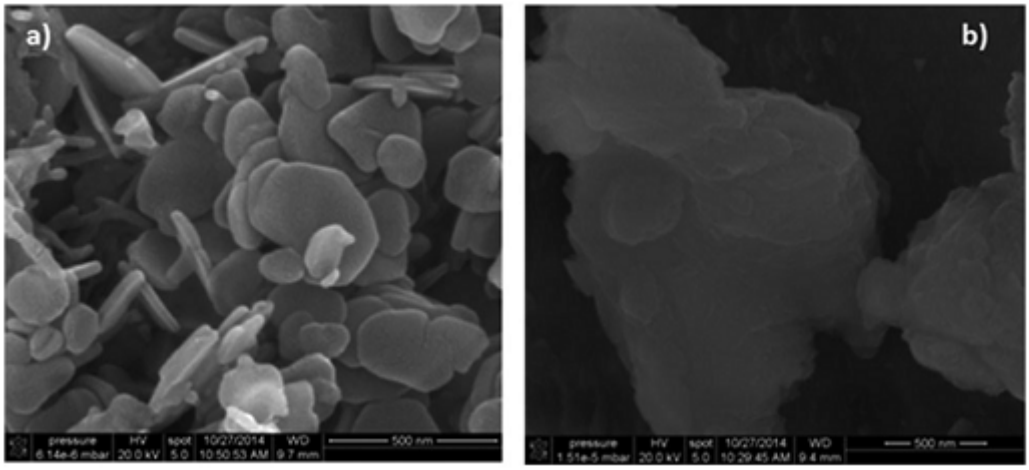

Fig. 3. SEM images of ZnAl-CO_3 (a) and MgAl-H (b) hydrotalcites.

ZnAl-CO_3 showed thin platelets and a regular shape, which is consistent with a good crystallized structure. The primary particle size was in the range 85–250 nm. The morphology of the MgAl-H sample kept the structural homogeneity after the incorporation of humate anions but a loss of crystallinity and aggregation of the

layered particles were observed (SEM image of MgAl-Cl, a precursor of MgAl-H is included in Appendix 2 ESI, Fig. S2).

Finally, the aggregation of the primary particles can reach a size of more than 300 nm, likely due to the presence of humate anions.

3.2. Electrochemical removal of cadmium

Fig. 4 shows the electrochemical deposition of Cd(II) on both ZnAl-CO_3 and MgAl-H, at two different current densities. The process can be described by the following reaction:

$$CdCl_{2(el)} + LDH_{(e)} + 2Ag \leftrightarrow Cd_{(e)}\text{–}LDH + 2AgCl \quad (1)$$

where subscripts (el) and (e) indicate the electrolyte and electrode phases respectively. When a negative current was applied, Cd^{2+} was reduced on the LDH to Cd^0 (from left to right in the reaction (1)) and simultaneously 2 Ag were oxidized
in the counter electrode.

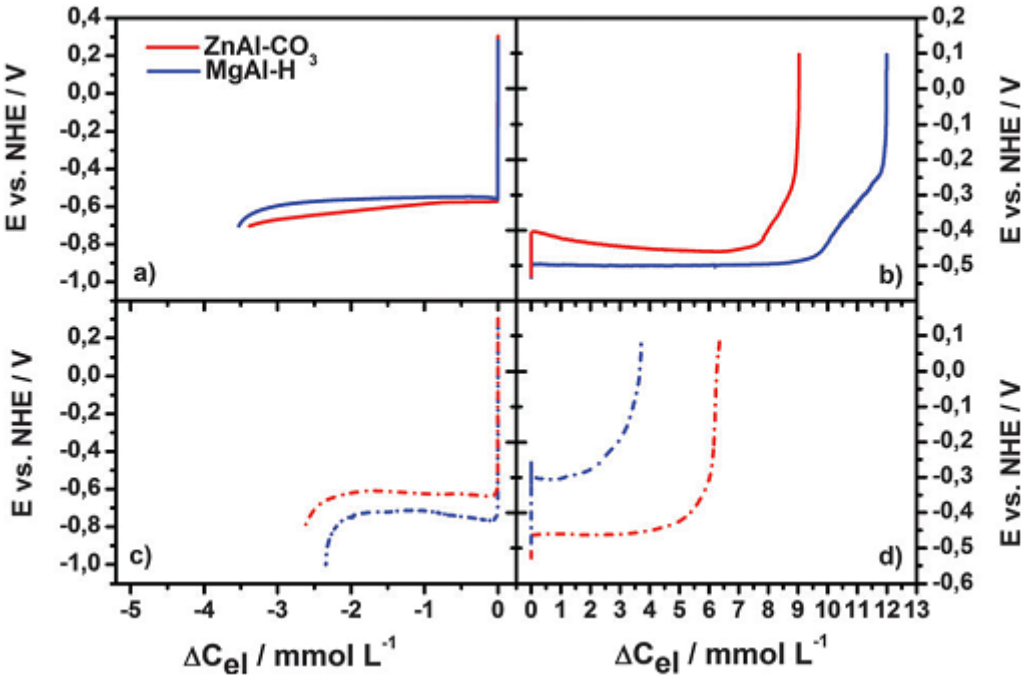

Fig. 4. Electrochemical removal of cadmium at C/20.8 (a) and C/5.2 (c) and their posterior recovery (b and d).

Under the experimental conditions used in this study, the limiting diffusion current is 3.73 mA (more details in Appendix 3 ESI). The current applied for electro-deposition under C/5.2 was close to this value and equal to 2.14 mA, which implies that a high concentration overpotential is required to reduce Cd^{2+} in these measurements. This effect was evidenced in Fig. 4, where the initial overvoltage was 43 mV (E_{eq} = 0.471 V vs. NHE) for both double layered hydroxides when a rate of C/20.8 was used, but it increased to 119 mV and 248 mV when the current rate was increased to C/5.2, for ZnAl-CO_3 and MgAl-H, respectively.

Table 2 summarizes the modifications in the concentration of cadmium after the electro-removal process (ΔC_{el}). The value of ΔC_{el} was calculated from the charge flow using the Faraday law. The amounts of cadmium in solution of 3.38 and 3.53 mM decreased when ZnAl-CO_3 and MgAl-H were respectively used at C/20.8. These values indicate the reduction of the pollutant ions of 65.0% and 67.8% respectively. Upon increasing the current rate, the percentage of the cadmium removal decreased to 50.3% (ZnAl-CO_3) and 45% (MgAl-H), respectively. These lower values are in agreement with the fact that the electrodeposition process was controlled by diffusion limitation at this current rate. It is noteworthy to mention that the duration required in the faster experiments was 4 times shorter compared to when a rate of C/20.8 was used. Therefore, it is possible to select the current rate in order to reach the desired objective, i.e. shorter times or higher removal fraction. Additionally, the combination of different current densities permits achieving multiple targets, for example, a high initial current to decrease the concentration of the pollutant very fast, followed by a lowncurrent to increase the total amount of removed metal ions.

Table 2
Analysis of variation of the concentrations of cadmium (ΔC) in the electrolyte after deposition and recovery processes on ZnAl-CO_3 and MgAl-H at different rates, (Ci_{el} = 5.20 mM)

Sample	Rate	Deposition ΔC_{el} (mM)	Recovery ΔC_{el} (mM)	Deposition ΔC_A (mM)	Recovery ΔC_A (mM)
ZnAl-CO_3	C/5.2	-2.62	6.37	-3.18	6.65
ZnAl-CO_3	C/20.8	-3.38	9.04	-3.84	10.55
MgAl-H	C/5.2	-2.34	3.72	-2.65	2.75
MgAl-H	C/20.8	-3.53	11.99	-3.91	14.33

Furthermore, if higher percentages of removal are desired, it is enough that a lower current density is applied. It would be possible also to combine this technology with the previously reported adsorption process based on similar LHDs,[31,37] whose effectiveness is limited to the concentration of pollutants lower than 2.5 mM. Therefore, after the electro-deposition step it could be possible to use an adsorption step, to remove all the remaining pollutants from the solution. To measure the real variation of the concentration in the electrolyte, the solutions after and before the electrochemical processes were analysed by AAS. In all the cases, the values of cadmium elimination observed by means of AAS (ΔC_A, Table 2) were higher than the value of ΔC_{el}. It would have been expected that the value of ΔC_{el} would be larger than DCA, due to a non-unitary efficiency in the electrochemical process, maybe caused by hydrogen evolution. The observed differences were associated with the adsorption properties of the double layered hydroxides, able to remove a fraction of cadmium by a simple contact of the electrode with the electrolyte. An estimation of the contribution of the adsorption process to the total removal of metal is described in Appendix 4 ESI. When this effect is taken into account, an efficiency lower than 1 was obtained for the electrochemical process. The electrochemical removal capacities were equal to 622 mg $g_{a.m.}^{-1}$ ($g_{a.m}$ = gram of active material) and 518 mg $g_{a.m.}^{-1}$ when ZnAl-CO_3 and MgAl-H were respectively used as a substrate with a current rate of C/5.2. These values increased to 749 mg $g_{a.m.}^{-1}$ and 763 mg $g_{a.m.}^{-1}$ when the current rate was equal to C/20.8. These removal capacities are considerably higher than the

traditional values obtained by the adsorption process alone, which generally ranges from 10^{-3} mg g^{-1} to 270 mg g^{-1} of the adsorbent.[38] The presence of a pollutant was reduced by 61.2% and 73.8% for ZnAl-CO_3, and 50.9% and 75.2% for MgAl-H, when the current rate was equal to C/5.2 and C/20.8, respectively. To confirm the critical role of the LDHs in the electrochemical deposition of Cd and to evaluate the contribution of the current collector (carbon cloth) and additives used to prepare the electrodes (carbon black, polyvinylidene fluoride, and graphite), a removal process was performed using an electrode composed only by carbon black, graphite, and a binder at a current rate of C/20.8 (Appendix 5 ESI, Fig. S3a). The electro-deposition of Cd using such a substrate was limited to just 6.5% of the initial amount, confirming that the LDH plays a critical role (Table 2).

After the removal process, the volume of the cell was reduced to 10 mL and the cadmium was recovered by applying a positive current (from right to left in the reaction (1), Fig. 5). A recovery of 60.7% and 39.7% of the cadmium deposited was obtained when ZnAl-CO_3 and MgAl-H were used at C/5.2, respectively. When the current applied was decreased to C/20.8, the values of 84.2% and 66.8% were achieved. These percentages are greater than the recovery obtained (close to 38%) using adsorption methods that have removal capacities similar to the ones of this work.[39] This methodology permitted us to increase the concentration of cadmium up to 14.33 mM, 4.5 times higher than that obtained by other effective absorbents, and without the need to use any eluent.[40] The recovery solution could be used for other applications, such as the reactant in flow cadmium batteries; this technology permits us to convert wastewater into an added-value product. Additionally, the reduction of the volume used for the recovery process and the possibility of reusing the same solution would permit us to increase the concentration of cadmium to the desired values, as we previously demonstrated in an equivalent method for lithium recovery from brines.[27,28]

3.3. Electrochemical removal of lead

Fig. 5 shows the electrochemical deposition of Pb(II) on both ZnAl-CO_3 and MgAl-H hydrotalcites, at two different concentrations of the electrolyte. Similar to the one reported previously in the case of cadmium, the process can be described by the following reaction:

$$PbCl_{2(el)} + LDH_{(e)} + 2Ag \leftrightarrow Pb_{(e)}\text{-}LDH + 2AgCl \quad (2)$$

where subscripts (el) and (e) indicate the electrolyte and electrode phases respectively.

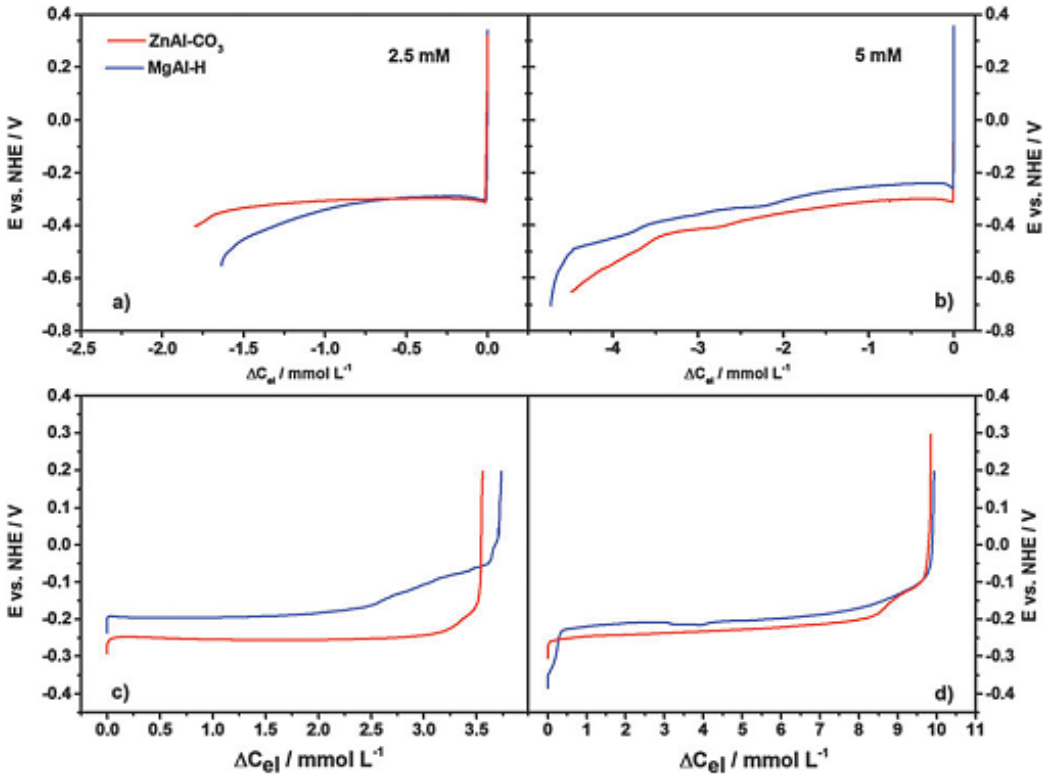

Fig. 5. Electrochemical removal of lead from 2.5 mM (a) and 5 mM $PbCl_2$ (b) and their posterior recovery (c and d).

When a negative current was applied Pb^{2+} was reduced on the LDH to Pb^0 (from left to right in the reaction (2)) and simultaneously 2 Ag were oxidized in the opposite electrode. In the case of lead, the applied current was always far from the diffusion limiting current, thus polarization observed at lower concentrations of Pb(II) can be attributed to the deposition mechanism itself, which is kinetically slow.The variations of lead concentration are summarize in Table 3.

Table 3
Analysis of the variation of the concentrations of lead (ΔC) after the deposition and recovery process on ZnAl-CO_3 and MgAl-H at different concentrations of electrolyte (Ci_{el})

Sample	Ci_{el}	Deposition ΔC_{el} (mM)	Recovery ΔC_{el} (mM)	Deposition ΔC_A (mM)	Recovery ΔC_A (mM)
ZnAl-CO_3	2.5	-1.80	3.56	-2.09	1.31
ZnAl-CO_3	5	-4.48	9.85	-4.60	0
MgAl-H	2.5	-1.64	3.73	-1.95	2.16
MgAl-H	5	-4.73	9.93	-5.07	3.32

The Pb(II) concentration was reduced by 1.8 mM and 1.64 mM when ZnAl-CO_3 and MgAl-H were respectively used a solution containing an initial concentration of 2.5 mM of $PbCl_2$, decreasing the starting amount of Pb(II) by 72% and 65.6%, respectively.

When a solution with initial concentration equal to 5 mM was used, it was possible to decrease the concentration of the pollutant by 4.48 mM (ZnAl-CO_3) and 4.73 mM (MgAl-H), reaching percentages of removal equal to 89.6% and 94.6%. The concentration of Pb(II) in the solution after the removal process was analyzed by ICP-MS. Again, higher values of ΔC_A were obtained with respect to the values of ΔC_{el} calculated from the Faraday law. These differences were in the same range of the one observed for Cd, and it was verified that they were due to the inevitable adsorption process occurring during the contact of the hydrotalcite with the solution containing the pollutant (more details in Appendix 4 ESI). Considering the combination of the electrochemical removal process and the adsorption effect, the percentages of Pb eliminated from a 2.5 mM solution the reached values of 83% and 78% for ZnAlCO_3 and MgAl-H respectively, these values increased up to 92% and 100% when a 5 mM solution was used, achieving a nearly total removal of Pb(II). The highest removal capacity was obtained by the sample MgAl-H from a 5 mM Pb(II) solution, reaching 1039 mg $g_{a.m.}^{-1}$, 2.7 times higher than the best adsorption method.[41] As in the case of the electro-deposition of Cd, the presence of LDH in the electrode was vital to the process. Without LDH in the electrode a removal of Pb(II) equal to just 4.4% was achieved when a 5 mM $PbCl_2$ solution was treated with a current rate of C/20. This clearly shows that LDHs play a critical role

in the electro-deposition of these highly toxic metals. After the removal process, the volume of the cell was reduced to 10 mL and lead was recovered by applying a positive current (from right to left in reaction (2), Fig. 5). Although from Fig. 5c and d, it could be supposed that the recovery of the deposited lead was successful, the ICP analysis (Table 3) showed that there was no or little recovered lead, so that the final solution after recovery had a lower concentration than the initial one. With the aim to clarify the mechanism of lead depletion during the recovery process, the electrodes were analyzed by X-ray diffraction (Fig. 6).

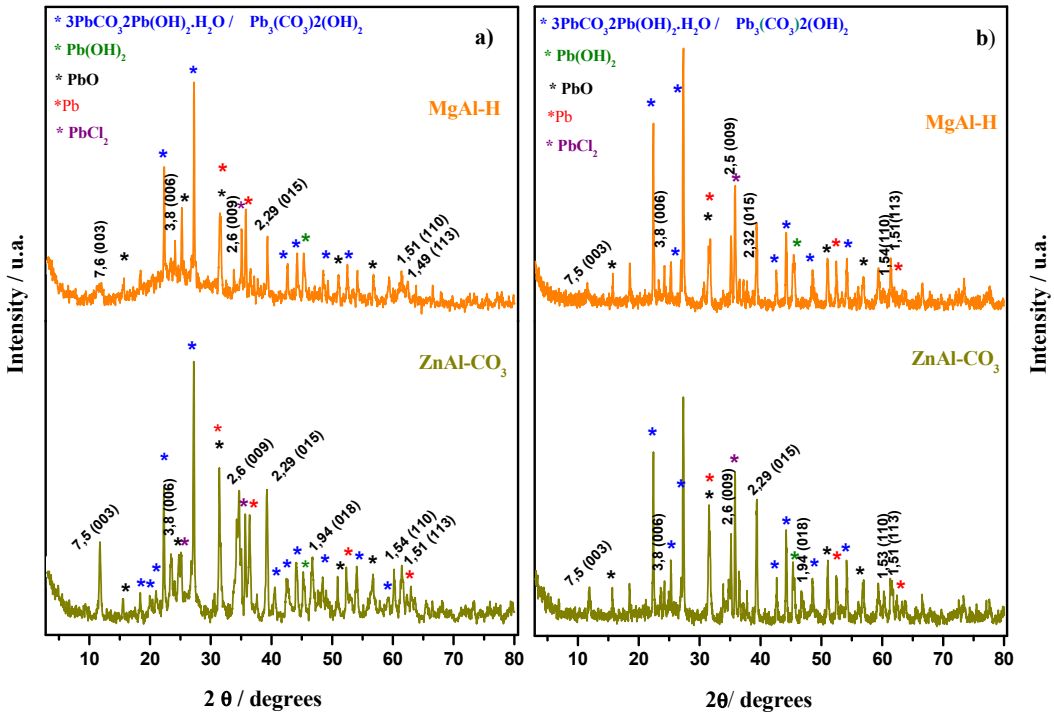

Fig. 6. X-ray diffractograms of the substrates after the recovery process from 2.5 mM (a) and 5 mM (b) lead solutions as electrolytes.

The XRD patterns showed a complex system containing several phases: lead metal, oxide, hydroxide, hydroxycarbonate, and chloride of lead. Three possible mechanisms of re-adsorption of Pb(II) on LDHs during the recovery process, or their combination, could explain the differences observed between the electrochemical and ICP-MS data, as they are schematically shown in Fig. 7.

$$\xrightarrow[mechanism\ 1]{} Pb_x(CO_3)_y(OH)_Z \downarrow$$

$$Pb_{(e)}\text{\_LDH} \rightarrow Pb^{2+}_{(el)} + LDH_e \xrightarrow[mechanism\ 2]{} Pb(OH)_2 \leftarrow 2OH^- + H_2 \leftarrow 2H_2O$$

$$\xrightarrow[mechanism\ 3]{} PbCl_2 \leftarrow 2Cl^-_{(el)}$$

Fig. 7. Possible mechanisms of lead depletion during the recovery process.

The first mechanism is given by precipitation as hydroxycarbonate of lead. The presence of carbonate as an interlayer anion in the structure of the hydrotalcite helps in producing this compound. The lower values of recovery obtained using ZnAl-CO_3 (Table 3) and comparing with MgAl-H are in agreement with the higher amount of carbonate inside ZnAl-CO_3, so the possibility of removing this anion to form hydroxycarbonate of lead is plausible. This assumption was confirmed by the blank measurements, which showed higher removal values of this HT (more details in Table S2, ESI). Pavlovic et al. also found $PbCO_3$ precipitated in ZnAl-LDH intercalated with DMSA ligands and Park et al. in Mg/Al-LDH.[21,42] The humate anion contained in MgAl-H could contribute to the sorption process via complexation/chelation between the metallic cation and the functional groups of humate. This mechanism was confirmed by XRD, several peaks associated with this phase are shown in Fig. 6. The uptake of lead by precipitation as hydroxide on the LDH is the second mechanism proposed. The local increase of pH caused by possible H_2 evolution during the deposition process could induce its precipitation. Finally, the third mechanism involves the formation of $PbCl_2$. During the recovery process the concentration of Pb(II) in the surrounding of the electrode increases and simultaneously Cl anions are attracted from the bulk owing to the positive current applied, generating locally an oversaturated solution and the precipitation of $PbCl_2$. However, there was neither a clear evidence of the presence of hydroxide nor chloride of lead, which could occur in a negligible amount or could be rebalanced very rapidly, once the current is interrupted. The identification of both phases could also be complicated by the fact that the main peaks of the XRD pattern are overlapping with the diffraction lines of different species of hydroxycarbonate, whose phase is the majority. In any case the XRD patterns

indicate the high complexity of these systems that hinder the recovery of lead and its concentration to values higher than 3.3 mM.

Due to the nature of the reactions involved in the removal process investigated in this study (reactions (1) and (2)), the integrity of the LDHs is not compromised by oxidation/reduction of their components or structural stress. Thereforewe expect a long cycle life and good stability of the LDHs, similar to that reported by Huang et al. [24] The authors demonstrated that LDH-based electrodes had a cycle life superior to 500 cycles. The silver electrode showed a good stability, and was cycled at least 30 times in 5.2 mM $CdCl_2$ and 5 mM $PbCl_2$ at least 30 times (Appendix 6 ESI, Fig. S4), reaching a capacity close to 60 mA h g^{-1}.

4. Conclusions

The electrochemical method for the removal of Cd(II) and Pb(II) developed in this article is based on the use of ZnAl-CO_3 and MgAl-H hydrotalcites as substrates. The structural characterization of these compounds confirms the hydrotalcite-like structure with a good crystallization of the samples. The utilization of these materials permits the elimination of pollutants by two simultaneous processes; electrochemical reduction of M^{2+} to M^0, and adsorption. This combined methodology shows the removal values of 763 mg $g_{a.m.}^{-1}$, and 1039 mg $g_{a.m.}^{-1}$ of Cd(II) and Pb(II), respectively, removing 75% and 100% of the heavy metals from the water stream. These values are considerably higher than the traditional values obtained by using other materials as adsorbents. We have shown that the presence of the LDH is vital to the electro-deposition process, and only negligible removal is reached in electrodes that do not contain the hydrotalcite-like compounds. Additionally, it was possible to recover 27% of the removed lead in a separate solution; in the case of cadmium it was possible to reach a recovery value of 84.2%, thus obtaining a solution with a concentration of 14.3 mM, 4.5 times higher than the best cadmium recovery method using adsorbents and without the need to use any eluent. This recovery solution could be used for other applications, such as a reactant in flow cadmium batteries, without further treatment. The lower amount of lead recovered was attributed to the formation of different species of this metal resorbed on the LDH. This was also confirmed by XRD. Future work

should focus on replacing silver as the counter electrode with more suitable materials, in terms of cost and effectiveness.

Acknowledgements

The financial support from the Spanish Junta de Andalucía (research group FQM214) and MCYT (Project CTM2011-25325), the Federal Ministry of Education, Research (BMBF) in the framework of the project ''Energiespeicher'' (FKZ 03K3005), and the Cluster of Excellence RESOLV (EXC 1069) funded by the Deutsche Forschungsgemeinschaft (DFG) are gratefully acknowledged.

References

1 S. Mol, *Biol. Trace Elem. Res.*, 2011, 143, 974.

2 G. Yuan, S. Dai, Z. Yin, H. Lu, R. Jia, J. Xu, X. Song, L. Li,
Y. Shu and X. Zhao, *Food Chem. Toxicol.*, 2014, 65, 260.

3 G. Drazic and N. Mihailovic, *Plant Sci.*, 2005, 168, 511.

4 M. R. Pérez, I. Pavlovic, C. Barriga, J. Cornejo, M. C. Hermosin and M. A. Ulibarri, *Appl. Clay Sci.*, 2006, 32, 245.

5 K. G. Karthikeyan, H. A. Elliot and F. S. Cannon, *Environ. Sci. Technol.*, 1997, 31, 2721.

6 J. Rubio, M. L. Souza and R. W. Smith, *Miner. Eng.*, 2002, 15, 139.

7 S. Y. Kanga, J. U. Leeb, S. H. Moona and K. W. Kima, *Chemosphere*, 2004, 56, 141.

8 Q. Chang and G. Wang, *Chem. Eng. Sci*., 2007, 62, 4636.

9 H. A. Qdais and H. Moussa, *Desalination*, 2004, 164, 105.

10 A. T. Heijne, F. Liu, R. Weijden, J. Weijma, C. J. N. Buisman and H. V. M. Hamelers, *Environ. Sci. Technol.*, 2010, 44, 4376.

11 N. Ahalya, T. V. Ramachandra and R. D. Kanamadi, *Res. J. Chem. Environ.*, 2003, 7, 71.

12 M. A. Hashim, S. Mukhopadhyay, J. N. Sahu and B. Sengupta, *J. Environ. Manage.*, 2011, 92, 2355.

13 Q. Jiuhui, *J. Environ. Sci.*, 2008, 20, 1.

14 F. Fu and Q. Wang, *J. Environ. Manage.*, 2011, 92, 407.

15 A. E. Palomares, J.-M. Lo´ pez-Nieto, F. J. Lazaro, A. Lopez and A. Corma, *Appl. Catal., B*, 1999, 20, 257.

16 D. G. Evans and X. Duan, *Chem. Commun.* , 2006, 485.

17 J.-H. Choy, S.-J. Choi, J.-M. Oh and T. Park, *Appl. Clay Sci.*, 2007, 36, 122.

18 F. Bruna, I. Pavlovic, R. Celis, C. Barriga, J. Cornejo and M. A. Ulibarri, *Appl. Clay Sci.*, 2008, 42, 194.

19 R. Extremera, I. Pavlovic, M. R. Pérez and C. Barriga, *Chem. Eng. J.*, 2012, 213, 392.

20 P. S. Braterman, in *Handbook of Layered Materials*, ed. S. M. Auerbach, et al., Marcel Dekker, Inc., New York, Basel, 2004, pp. 373–474.

21 I. Pavlovic, M. R. Pérez, C. Barriga and M. A. Ulibarri, *Appl. Clay Sci.*, 2009, 43, 125.

22 P. Vialat, F. Leroux, C. Taviot-Gueho, G. Villemure and C. Mousty, *Electrochim. Acta*, 2013, 107, 599.

23 C. Obayashi, M. Ishizaka, T. Konishi, H. Yamada and K. Katakura, *Electrochemistry*, 2012, 80, 879.

24 T. Wang, Z. Yang, B. Yang, R. Wang and J. Huang, *J. Power Sources*, 2014, 257, 174.

25 F. La Mantia, M. Pasta, H. D. Deshazer, B. E. Logan and Y. Cui, *Nano Lett.*, 2011, 11, 1810.

26 M. Pasta, C. D. Wessells, Y. Cui and F. La Mantia, *Nano Lett.*, 2012, 12, 839.

27 M. Pasta, A. Battistel and F. La Mantia, *Energy Environ. Sci.*, 2012, 5, 9487.

28 R. Trócoli, A. Battistel and F. La Mantia, *Chem. – Eur. J.*, 2014, 20, 9888.

29 W. T. Riechle, *Solid State Ionics*, 1986, 22, 135.

30 I. Crespo, C. Barriga, V. Rives and M. A. Ulibarri, *Solid State Ionics*, 1997, 729, 101.

31 M. A. González, I. Pavlovic, R. Rojas-Delgado and C. Barriga, *Chem. Eng. J.*, 2014, 254, 605.

32 Y. Seida and Y. Nakano, *Water Res.*, 2000, 34, 1487.

33 S. J. Santosa, E. S. Kunarti and Kamato, *Appl. Surf. Sci.*, 2008, 254, 7612.

34 S. Vreysen and A. Maes, *Appl. Clay Sci.*, 2008, 38, 237.

35 V. Rives, *Layered Double Hydroxides: Present and Future*, Nova Science Publishers, Inc., New York, 2001.

36 L. J. Bellamy, *The Infrared Spectra of Complex Molecules*, Chapman and Hall, London, 1975.

37 M. A. González, I. Pavlovic and C. Barriga, *Chem. Eng. J.*, 2015, 269, 221.
38 D. Purkayastha, U. Mishra and S. A. Biswas, *Journal of Water Process Engineering journal*, 2014, 2, 105.
39 V. Singh, A. K. Sharma and S. Maurya, *Ind. Eng. Chem. Res.*, 2009, 4, 4688.
40 K. C. Justi, V. T. Fávere, M. C. M. Laranjeira, A. Neves and R. A. Peralta, *J. Colloid Interface Sci.*, 2005, 291, 369.
41 K. Kesenci, R. Say and A. Denizli, *Eur. Polym. J.*, 2002, 38, 1443.
42 M. Park, C. L. Choi, Y. J. Seo, S. K. Yeo, J. Choi, S. Komarneni and J. H. Lee, *Appl. Clay Sci.*, 2007, 37, 143.

Supplementary information

This supporting information contains 6 appendixes:

Appendix 1: Thermogravimetric and Differential Thermal analysis.
Appendix 2: Scanning electron images (SEM) of MgAl-Cl.
Appendix 3: Calculation limiting currents.
Appendix 4: Estimation of the removal by adsorption (blank).
Appendix 5: Electrochemical removal of Cd(II) and Pb(II), electrodes without LDH.
Appendix 6: Stability of Ag in $CdCl_2$ and $PbCl_2$ solutions.

1. Thermogravimetric and Differential Thermal Analysis.

Thermogravimetric and Differential Thermal analysis were performed to calculate the content of water molecules to propose an experimental formula of the LDHs. Fig. S1 shows the thermograms obtained.

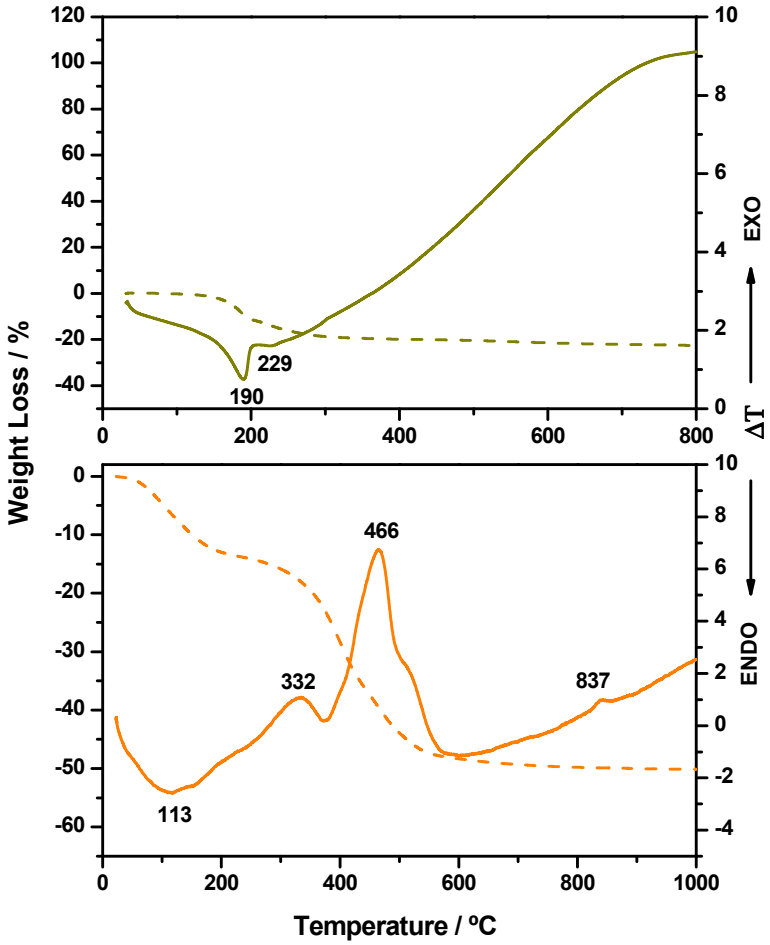

Fig. S1. Thermogravimetric and Differential Thermal analysis of ZnAl-CO_3 (top), and MgAl-Cl (bottom).

2. Scanning Electron Image (SEM) of MgAl-Cl.

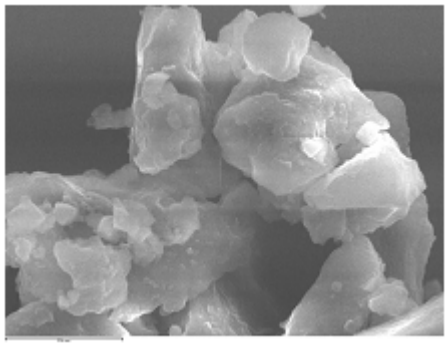

Fig. S2. Scanning Electron Image (SEM) of MgAl-Cl.

3. Calculation limiting currents.

As we indicated in the main article, the diffusion limiting current affects considerably the removal process. In order to evaluate such effect, the diffusion limiting currents (Il) of the Cd(II) and Pb(II) were calculated according to the following equation:

$$I_l = nFAD\frac{C_b}{\delta} \quad \text{(S1)}$$

where A is the geometrical surface area, D the diffusion coefficient of Cd(II) or Pb(II), cb the concentration of Cd(II) or Pb(II) in the bulk of the solution, and δ the diffusion layer thickness (estimated around 100 μm for systems subject only to natural convection). The values of D are 4.6224 x 10^{-6} m^2 h^{-1} and 5.29 x 10-6 m^2 h^{-1} for Cd and Pb respectively. [S1]

The table S1 shows the diffusion limiting current obtained for the respective concentration of metal, and the currents used in the deposition step in every case.

Table S1. Diffusion current under the experimental conditions, and currents applied during the deposition step.

Concentration (mA)	**Difussion limiting current (mA)**		**Current used (mA)**		
	Cd	Pb	Cd (5.20)	Cd (C/20.8)	Pb (C/20)
2.5	-	2.06	-	-	0.26
5	3.73	4.11	2.14	0.53	0.52

The current applied for the removal of Pb(II) was 790 times smaller than the diffusion limiting current what permitted its elimination in a potential close to the predicted by the Nernst equation and obtaining higher percentages of removal than in the case of Cd(II). For this metal, the current used was 58 % and 14.2 % of the diffusion limiting current what is in agreement with the polarization observed in deposition process (Fig. 4 main article) and the lower eliminations of pollutant reached.

[S1] Ana C.F. Ribeiro, Joselaine C.S. Gomes, Luís M.P. Veríssimo, Carmen Romero, Luis H. Blanco, Miguel A. Esteso. *J. Chem. Thermodynamics*, 2013, **57**, 404–407.

4. Estimation of the removal by adsorption (blank).

The differences observed in the concentrations predicted by electrochemistry and the one measured by AAS and ICP-MS were attributed in the main article to the metal adsorption capacity of the substrate employed, the adsorption property of the LDHs is well known. The Table S2 shows the variations in the concentration of a 5.2 mM $CdCl_2$ solution by the immersion of the electrodes for a time equivalent to the one employed in the electrodeposition process. It is important to consider that the experimental conditions during the electro-deposition step could be quite different with respect to the one existing during these measurements of removal by immersion, because the applied current could generate strong modifications in the chemical composition of the solution in the surrounding of the electrode. In any case, there is a good correlation between the removal values observed in the adsorption process and the difference between electrochemical data and chemical analysis (Table 2 main article).

Table S2. Analysis of concentrations of cadmium (mmol L^{-1}) in the electrolyte after the adsorption process by ZnAl-CO_3 and MgAl-H under different contact times (Ci_{el} = 5.20 mM).

BLANKS	CONTACT TIME (h)	ΔC_A (mM)
ZnAl-CO_3	5	-0.16
	20	-0.32
MgAl-H	5	-0.5
	20	-0.71

Similar results were obtained when the electrodes were submerged in 2.5 mM and 5 mM $PbCl_2$ solutions for 20 hours (Table S3). Higher removed amounts were obtained for higher concentrations of pollutant. The high values observed in the case of ZnAl-CO_3 are in agreement with the low concentrations reached during the recovery process. As we described in the main article, the Pb(II) generated was re-

adsorbed by the hydrotalcite following three possible mechanisms. The data obtained with these blank measurements confirm the high affinity of the LDHs towards lead and its precipitation as hydroxycarbonate that can be observed as majority phase in the X-ray analysis (Fig. 6 main article).

Table S3. Analysis of concentrations of cadmium (mmol L^{-1}) in the electrolyte after the adsorption process by ZnAl-CO_3 and MgAl-H hydrotalcites. Ci_{el} indicates the initial concentration of the electrolyte. Contact time = 20 h.

BLANKS	$C_{i_{el}}$ **(mM)**	ΔC_A **(mM)**
ZnAl-CO_3	2.5	-1.45
	5	-3.24
MgAl-H	2.5	-0.83
	5	-1.02

5. Electrochemical removal of Cd(II) and Pb(II), blank without LDH.

To confirm the critical role of the LDHs on the electrochemical deposition of Cd and Pb and to evaluate the contribution of the current collector (carbon cloth) and additives used to prepare the electrodes (carbon black, polyvinylidene fluoride, and graphite), a removal process was done using an electrode formed by these components but without the presence of LDH (Figure S3 a) at a slow current rate, namely C/20. The deposition of Cd showed a decrement of the concentration of 0.34 mM starting from a solution of 5.20 mM of $CdCl_2$, reducing the initial concentration of just 6.5%. For the electro-deposition of Pb from a 5mM $PbCl_2$ solution, the decrease of its concentration using an electrode without LDH was 0.22 mM, equal to just 4.4 % removal. This removal capacities obtained in absence of LDHs clearly manifests the critical role of the LDH as substrate for the electrochemical removal of these highly toxic metals.

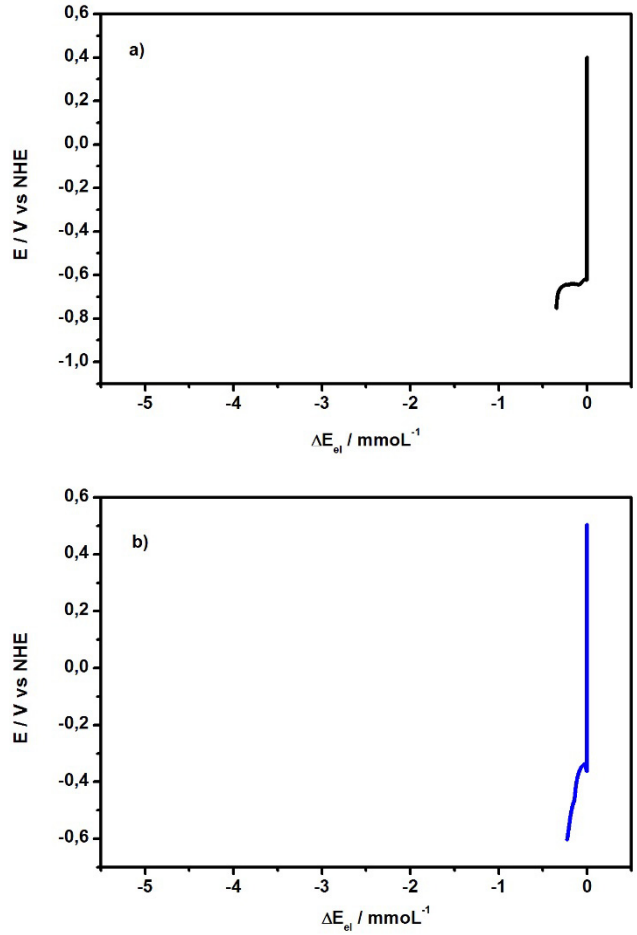

Fig. S3. Electrochemical removal of Cd (a) and Pb (b) using electrodes without LDH.

6. Stability of Ag in $CdCl_2$ and $PbCl_2$ solutions.

The stability of silver in 5.2 mM $CdCl_2$ and 5 mM $PbCl_2$ was analysed. Figure S4 shows that the capacity was stabilized after 25 cycles to around 60 mAh g^{-1} in the case of use $PbCl_2$ as electrolyte, when $CdCl_2$ was used, a similar capacity was obtained immediately from the 1 st cycle. In both cases it was possible to reuse the silver electrode at least 30 times, that proves its possible utilization as chloride capturing electrode during the electrochemical removal of metals. Its electrochemical performance and low voltage reaction makes Ag an ideal candidate as counter electrode for the electrochemical removal process, however the possible commercial applicability of this technique required undoubtedly the substitution of silver by another materials due to the elevate cost of this noble metal.

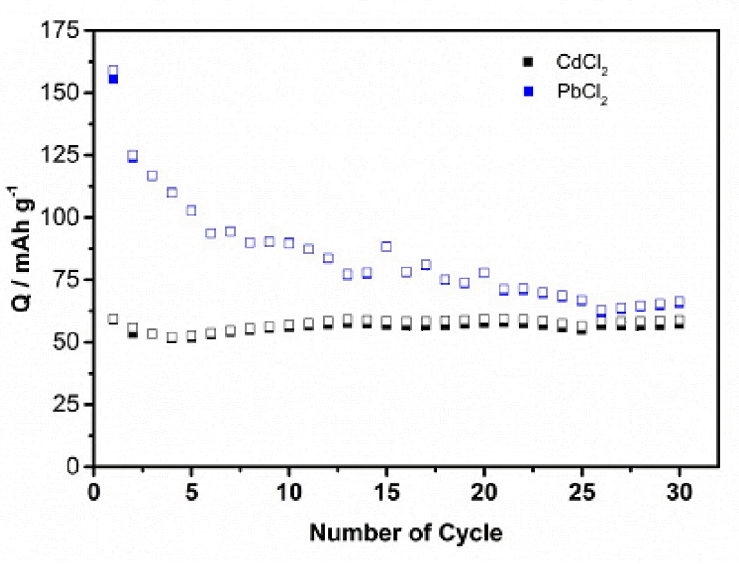

Fig. S4. Electrochemical stability of Ag in $CdCl_2$ (black) and $PbCl_2$ (blue).

CAPÍTULO V
Resumen Global / Summary

RESUMEN GLOBAL

La contaminación de las aguas naturales producida por el uso cada vez más extendido de sustancias tóxicas, tanto inorgánicas (metales pesados) como orgánicas (herbicidas) puede causar problemas ambientales graves, particularmente relacionados con la calidad del agua potable. Esto ha dado lugar a la necesidad de desarrollar nuevas estrategias de remediación más eficaces. Entre las técnicas fisicoquímicas más utilizadas para la recuperación rápida de aguas afectadas por altas concentraciones de contaminantes destaca la adsorción, la cual se considera superior a otras técnicas de tratamiento de aguas en términos de coste inicial, simplicidad de diseño y fácil preparación. También los métodos electroquímicos han sido objeto de creciente interés en los últimos años, ya que es una técnica innovadora, versátil y altamente eficaz. Se les podrían denominar "tecnologías verdes" porque se necesitan poco o nada de productos químicos para facilitar el tratamiento de agua y tienen la ventaja de que podrían ser usados como pretratamiento en combinación con otras tecnologías de purificación de aguas logrando introducir menos efectos nocivos al medio ambiente y abriendo una nueva perspectiva de remediación.

Los hidróxidos dobles laminares (HDLs) también denominados compuestos tipo Hidrotalcita cuyas características estructurales y superficiales hacen de ellos materiales muy interesantes y adecuados para múltiples aplicaciones, entre ellas su uso como adsorbente de contaminantes de diferente naturaleza, son compuestos fáciles y económicos de sintetizar, presentan una gran estabilidad en un amplio rango de pH y no son tóxicos para el medio ambiente.

Los HDLs presentan la posibilidad de funcionalización lo que permite mejorar sus propiedades de adsorción para una amplia variedad de adsorbatos. **Los primeros resultados que se publicaron (primer artículo)** trataron sobre la adsorción de herbicidas de baja polaridad tales como como linurón, 2,4-DB y metamitrón, todos ellos con propiedades fisicoquímicas diferentes, mediante el uso de un adsorbente HDL intercalado con el anión orgánico caprilato (LDH-Cap). El HDL modificado se caracterizó mediante DRX y se confirmó que el anión caprilato estaba intercalado en el espacio interlaminar, posiblemente orientado en posición vertical respecto a las láminas de hidróxido. Técnicas como FT-IR y ATG-

ATD también confirmaron la presencia de dicho anión en el sólido. Las bandas más características en el espectro de FT-IR fueron las correspondientes a los modos de vibración de los grupos carboxilato del anión caprilato y a los de tensión C-H de las cadenas alifáticas. La presencia de un efecto exotérmico bastante notable procedente de la combustión del anión orgánico interlaminar fue el resultado más destacado del estudio térmico. Los experimentos de adsorción y desorción se realizaron a un pH de trabajo entre 6-7 ya que previamente se confirmó éste no tenía influencia en la cantidad de pesticida eliminado. El estudio de la cinética mostró que la adsorción del linurón y del 2,4-DB fue casi instantánea. Sin embargo, para el caso del metamitrón la adsorción tuvo lugar de forma más gradual aunque a las 24h aún no se había alcanzado el equilibrio. Dado que la cinética es un aspecto importante en el control del proceso de eliminación de los contaminantes, los datos se ajustaron a una serie de modelos muy ampliamente usados en la literatura. Para los tres pesticidas los datos cinéticos se ajustaron mejor al modelo de pseudo-segundo orden, teniendo en cuenta los valores de los coeficientes de correlación obtenidos y dado que las cantidades de pesticida adsorbidas calculadas (q_e) fueron muy consistentes con los valores experimentales. Por tanto, los resultados sugirieron que el proceso de adsorción estaba controlado por quimisorción. Los datos cinéticos también se ajustaron al modelo propuesto por Weber y Morris (difusión intraparticula). De los resultados se dedujeron que la difusión intraparticula está involucrada en el proceso de adsorción pero no era el único paso determinante de la velocidad. En todos los casos tiene lugar un proceso en multietapas, aunque para el metamitrón se observa con mayor claridad. Por tanto, el proceso implicaba adsorción del adsorbato en la superficie externa del adsorbente, difusión intraparticula e interacción química adsorbato/adsorbente. Las isotermas de adsorción para los tres pesticidas fueron de tipo C y la cantidad máxima eliminada fue para el caso del metamitrón (q=260 μmol/g vs. q= 72 μmol/g para linurón y q= 102 μmol/g para 2,4-DB). Tras comparar las cantidades adsorbidas con trabajos con otros aniones orgánicos intercalados y bajo condiciones experimentales similares se dedujo que tanto la composición del anión interlaminar (grupos funcionales) como la altura de la galería pudieron influir en la interacción del metamitrón con la la parte hidrofóbica del anion interlaminar. Con objeto de comparar el comportamiento de la adsorción de los tres pesticidas

estudiados, también se llevó a cabo un estudio de adsorción en una hidrotalcita con anión inorgánico (LDH-Cl). La adsorción de linurón y metamitrón en LDH-Cl fue despreciable mientras que la adsorción de 2,4-DB fue similar a la obtenida en LDH-Cap. Esto sugirió que el 2,4-DB pudo adsorberse en la HT inorgánica a través de interacciones ion-ion entre su grupo carboxílico y las láminas cargadas positivamente del HDL. Los datos de las isotermas de adsorción en LDH-Cap se ajustaron a la ecuación de Freundlich, lo que sugiere una heterogeneidad de los sitios de adsorción en la superficie y diferentes energías de adsorción. Tras la adsorción, se llevó a cabo el proceso de desorción de los pesticidas usando disolventes de distinta polaridad pero todos ellos se desorbieron tan solo parcialmente. Los porcentajes más bajos se obtuvieron para el metamitrón lo que está de acuerdo con la alta afinidad presentada por LDH-Cap junto con las mayores cantidades adsorbidas en comparación con el 2,4-DB y linurón. Sin embargo, el 2,4-DB se desorbió con mayor facilidad en etanol, probablemente debido a la mayor afinidad por este disolvente por similitud de polaridades. Finalmente, los productos de adsorción se caracterizaron mediante DRX y se comparó con el diagrama de LDH-Cap pura. El desplazamiento de la posición de las líneas de difracción correspondientes a los planos (00l), a ángulos 2Θ más bajos con valores de $d_{(003)} \sim 30$Å en LDH-Cap-2,4DB y LDH-Cap-metamitrón confirmaron que ambos pesticidas fueron intercalados en el espacio interlaminar tras el proceso de adsorción. También, se observó una disminución en la intensidad de las reflexiones (00l). En el caso del diagrama de DRX de LDH-Cap-2,4DB se observaron dos fases, lo que sugiere la coexistencia de la fase de dicho complejo y la fase del adsorbente LDH-Cap. Por el contrario, el diagrama de LDH-Cap-linuron no cambió significativamente con respecto al adsorbente puro, lo que indicó que posiblemente fuese adsorbido en la superficie externa de las partículas del HDL.

Los metales pesados también son contaminantes altamente peligrosos que podrían causar problemas ambientales y de salud bastantes graves debido a su alta toxicidad, la cual deriva de su bioacumulación. Por tanto, en un **segundo y tercer artículo,** se estudió la síntesis y caracterización de adsorbentes basados en HDLs (inalterados y modificados por la incorporación de un anión orgánico en sus espacio interlaminar) y se evaluaron sus propiedades adsorbentes para cationes metálicos pesados, tales como cobre, plomo y cadmio. En primer lugar, se obtuvo

una hidrotalcita modificada con el anión orgánico humato (LDH-H o también llamada LDH-H100), preparada por el método de intercambio iónico a partir de una hidrotalcita inorgánica que contenía cloruro como anión interlaminar (LDH-Cl). Este ácido orgánico es la fracción más abundante de las sustancias húmicas, de composición muy variable pero con un alto contenido de grupos funcionales existentes en forma aniónica en un amplio rango de pH, lo cual permite la unión con los cationes metálicos mediante interacciones electrostáticas y mediante enlaces de coordinación. La caracterización de la muestra LDH-H mediante difracción de rayos X mostró un diagrama típico de estructura tipo hdrotalcita con un ligero aumento del espaciado basal (003) de LDH-H con respecto a LDH-Cl, por lo que los aniones humato pudieron alojarse en la superficie de las partículas del HDL y/o intercalados en posición paralela a las láminas de hidróxidos. Las bandas más características obtenidas mediante espectroscopia FT-IR fueron las atribuidas a los modos de vibración simétrica y antisimetrica de los grupos carboxilato y las correspondientes al modo de vibración de flexión =CH del humato, ambas confirman la presencia de humato en el sólido. Mediante análisis termogravimétrico (ATG/ATD) se observó la presencia de un efecto exotérmico debido a la oxidación del ácido húmico. Mediante análisis elemental se calcularon los porcentajes de Mg y Al y por tanto la relación (M^{2+}/M^{3+}) para ambas muestras. Para el caso del LDH-Cl esta relación fue muy similar a la de los metales en la disolución de partida. Sin embargo, para LDH-H se observó una ligera disminución de la relación de metales respecto al precursor debido al proceso de síntesis. A partir de esta relación de metales para la muestra LDH-H se estableció un rango de composición suponiendo que toda la carga de la lámina podría estar compensada por los aniones humato o bien por los aniones cloruros y se propuso una fórmula aproximada para la hidrotalcita preparada LDH-H, el número de moléculas de agua en cada una de las muestras se calculó a partir de la primera pérdida de peso en las curvas de TG. La capacidad de adsorción del adsorbente híbrido (LDH-H) fue comparada con la del LDH-Cl y con el ácido húmico en su forma disociada (H). Este último produjo una eliminación má alta para el Cd^{2+}, seguida por LDH-H y LDH-Cl. Sin embargo, ambos LDHs fueron excelentes adsorbentes para la eliminación del Cu^{2+}, lográndose una eliminación completa y casi completa de Pb^{2+}. Un cierto porcentaje de Mg^{2+} fue detectado en dichos sobrenadantes, lo cual hizo aumentar

la adsorción por los metales pesados. Por tanto, los resultados obtenidos estaban relacionados con los distintos mecanismos de adsorción que concurren, es decir, para las experiencias realizadas usando H como adsorbente los metales pesados se adsorbieron mediante formación de complejos produciéndose variaciones mínimas en el pH final. Para LDH-Cl, se produjo un importante aumento del pH con respecto al inicial, por lo que la precipitación de hidróxidos en la estructura o bien como fase separada podría ser el principal mecanismo. La afinidad del LDH-Cl por los metales pesados viene determinada por los productos de solubilidad de los hidróxidos metálicos ($K_{SP}(Cu(OH)_2$=1. 10^{-20}, $K_{SP}(Cd(OH)_2$=1 . 10^{-14} y $K_{SP}(Pb(OH)_2$= 1 . 10^{-16}). Ambos mecanismos podrían darse en el proceso de adsorción con el híbrido LDH-H, donde los aniones humato aportarían estabilidad y añadirían capacidad de complejación a la matriz inorgánica. Además, la adsorción de Cd^{2+} fue mayor en el LDH-H que en LDH-Cl, lo que corrobora la contribución del mecanismo de complejación. Como consecuencia, se estudió en primer lugar la adsorción de estos metales en este híbrido así como el efecto de una serie de parámetros en el proceso. El pH seleccionado para los experimentos de adsorción fue 5 y el estudio cinético reveló que la adsorción tuvo lugar en dos etapas, una rápida donde a las 2h se había adsorbido el 50% de la adsorción final y otra más gradual hasta que se alcanzó el equilibrio. Para el Cu^{2+} este se alcanzó a las 24h eliminándose el 100% de su concentración inicial (C_o=1 mM) y a las 48h para el Pb^{2+} y Cd^{2+} eliminándose 96% y 56% respectivamente. Las isotermas de adsorción mostraron una alta efectividad del adsorbente híbrido, siendo adsorbidos completamente a bajas concentraciones todos los cationes metálicos. Tal y como se determinó mediante el ajuste de Langmuir la adsorción máxima aumentó en el siguiente orden Cd (C_m= 0.35mmol g^{-1}), Pb (C_m= 0.48mmol g^{-1}) y Cu (C_m= 0.75mmol g^{-1}). La caracterización estructural de los productos de adsorción reveló que no había cambios importantes, tan solo una pérdida de cristalinidad pero sin la aparición de fases de hidróxidos adicionales (detectada mediante DRX) y un ligero desplazamiento de algunas bandas características en los espectros FT-IR causado probablemente por la interacción de los grupos funcionales del humato con los iones metálicos. Finalmente, se realizó una experiencia de adsorción simultánea de los tres metales estudiados (disolución multicomponente). Las cantidades más altas adsorbidas fueron para el caso del Cu^{2+} siendo 0.46mmol g^{-1} (cinética multicomponente) y

0.57mmol g^{-1} (cinética monocomponente) mientras que la adsorción de Cd^{2+} fue completamente inhibida por la presencia de otros cationes metálicos en la disolución. Este comportamiento estaba de acuerdo a la secuencia de estabilidad de los hidróxidos metálicos y también con las constantes de estabilidad de los complejos metal-humato, disminuyendo en el siguiente orden: Cu>Pb>Cd.

Dada la alta afinidad que presentaron los iones de metales pesados (Cu^{2+}, Pb^{2+} y Cd^{2+}) por LDH-Cl se hizo un estudio más exhaustivo de este adsorbente **(artículo 3)**, el cual se comparó con dos híbridos con diferentes cantidades de aniones humato (100% y 50% de la concentración de humato requerida para compensar la carga laminar), los cuales se denominaron LDH-H100 o LDH-H y LDH-H50 respectivamente. Fundamentalmente, el estudio se basó en el cálculo de los parámetros cinéticos y termodinámicos además de otros factores que afectan al proceso de adsorción. El análisis estructural de ambos híbridos mostró las mismas características dada la similitud de su composición y método de síntesis. Para el estudio de la influencia de la concentración inicial de los iones metálicos en el proceso de adsorción (isotermas de adsorción) el rango de concentración seleccionado inicialmente fue C_o=0-2.5 mM, excepto para el caso del Cu^{2+} que se incrementó hasta 4.4 mM en LDH-Cl. Los resultados mostraron que la captación máxima para el Cu^{2+} en LDH-H100, LDH-H50 y LDH-Cl fue 0.76, 1.02 y 1.95 mmol g^{-1} respectivamente. Las cantidades adsorbidas de Pb^{2+} fueron 0.48, 0.25 y 0.61 mmol g^{-1}, y finalmente para Cd^{2+} fueron 0.35, 0.18 y 1.03 mmol g^{-1}. En todos los casos las cantidades adsorbidas mayores se lograron usando LDH-Cl como adsorbente, y dado que los valores de pH finales fueron bastante elevados (~8.2-9), cabe pensar que el principal mecanismo involucrado podía ser la precipitación como hidróxidos metálicos, bien mediante la incorporación de los iones metálicos en la estructura de la hidrotalcita (diadochy) o como una fase separada. También merece destacar que para LDH-Cl los porcentajes de adsorción fueron 98%, 80% y 53% para Cu^{2+}, Cd^{2+} y Pb^{2+} respectivamente en el rango de concentración inicial de 0-2mM. En los adsorbentes híbridos, el Pb^{2+} y Cd^{2+} se adsorbieron en mayor cantidad en el híbrido con mayor contenido de humato, LDH-H100, lo que es consecuente con un mecanismo adicional de adsorción (complejación). Por el contrario, el Cu^{2+} fue adsorbido en mayor medida en LDH-H50, el cual contiene más componente inorgánico. Esto permite concluir que la precipitación es el

mecanismo fundamental en la captación de metales por un HDL no híbrido. Para correlacionar los datos experimentales se realizó el ajuste a las isotermas de Langmuir y Freunlich, los resultados indicaron que todos los procesos de adsorción se ajustaron perfectamente a la ecuación de Langmuir. También se estudió el efecto de la temperatura en el rango de 288-308 K para LDH-Cl y LDH-H100, Los valores de ΔH° indicaron que el proceso fue endotérmico en todos los casos y los valores de ΔG° se situaron entre -4.06 y 16.25KJ/mol (valores intermedios correspondientes a quimisorción y fisisorción), siendo todos los procesos de adsorción espontáneos y termodinámicamente favorables. Posteriormente, se estudió la cinética de adsorción de los iones metálicos en los distintos HDLs usando diferentes modelos. Para el caso del Cu^{2+} en LDH-Cl a las 2h ya se había alcanzado el equilibrio y en el resto de adsorbentes se alcanzó a las 24h. Las velocidades de eliminación fueron más lentas tanto para el Pb^{2+} como para el Cd^{2+}. El equilibrio se alcanzó a las 24h (LDH-Cl y LDH-H50) y a las 48h para (LDH-H100) para el Pb^{2+}, y para el Cd^{2+} a las 48h en todos los casos. Los datos cinéticos se ajustaron al modelo de pseudo-segundo orden para los tres adsorbentes. La representación de las cinéticas mediante el modelo de difusión intraparticula mostró multilinealidad en todos los casos, probablemente la adsorción en la superficie y difusión intraparticula controlan la interacción adsorbente-adsorbato de forma simultánea. Las constantes de velocidad en cada etapa siguieron el siguiente orden: $K_{p1}>K_{p2}>K_{p3}$ siendo el valor de la K_{p1} para el Cu^{2+} mayor en LDH-Cl que LDH-H100, y viceversa para el Pb^{2+}, lo que es indicativo de la mayor disponibilidad de sitios en el adsorbente en cada caso. Debido a la alta capacidad de adsorción observada para el LDH-Cl de naturaleza inorgánica se llevaron a cabo varios experimentos de competición adsortiva en disoluciones binarias y ternarias de los metales. La presencia de Pb^{2+} y/o Cd^{2+} no afectó al porcentaje de Cu^{2+} adsorbido en ningún caso. Tampoco la presencia de Cd^{2+} (disolución multicomponente) afectó prácticamente a la adsorción de Cu^{2+} y Pb^{2+} aunque la adsorción de Cd^{2+} si fue inhibida, sobre todo de forma significativa transcurridas 48h. En los sistemas bicomponentes, el porcentaje de eliminación de Pb^{2+} en Cd-Pb disminuyó con respecto al sistema Cu-Pb (a las 24h), y el porcentaje de Cd^{2+} eliminado fué mucho menor en presencia de Cu^{2+} que en presencia de Pb^{2+} (a las 48h), lo cual confirmó cierta competición entre estos cationes durante estos

periodos de tiempo. Por consiguiente, la disminución en el porcentaje de Cd^{2+} adsorbido en el sistema bicomponente y multicomponente con respecto al monocomponente, pudo ser debido a la menor disponibilidad de sitios de adsorción, de manera que iones con mayor afinidad por el LDH-Cl pueden desplazar a los de menor afinidad. Finalmente, se llevó a cabo un estudio sobre la influencia en el proceso de adsorción de la presencia del anión humato en la disolución de los contaminantes. La cantidad de Cu^{2+} no se vio afectada por la presencia de humato. Sin embargo, la cantidad de Pb^{2+} y Cd^{2+} disminuyó en presencia de dicho anión, lo que lleva a pensar que parte de esa metal se compleja con los aniones humato presentes en disolución. Además, la secuencia de afinidad que presentan los cationes metálicos por este anión varía según el siguiente orden: Cd>Pb>Cu.

En un **cuarto artículo,** se prepararon HDLs de distinta composición y se usaron como sustratos para la eliminación cationes metálicos de elevada toxicidad como Pb^{2+} y Cd^{2+}, mediante electrodeposición. Las hidrotalcitas utilizadas fueron MgAl-H y ZnAl-CO_3. Esta última fue caracterizada mediante DRX, IR y SEM al igual que la muestra MgAl-H caracterizada en trabajos anteriores. Mediante difracción de rayos X se confirmó la estructura tipo-HT de la muestra ZnAl-CO_3 la cual presentó una elevada cristalinidad, mediante SEM se observó la morfología laminar de las partículas. El espectro FT-IR de la muestra obtenido, típico de hidrotalcita con carbonato en el espacio interlaminar, mostró las bandas correspondientes a los modos de vibración de las especies carbonato junto con las de agua y grupos hidróxidos. Mediante análisis elemental y las curvas de TG se propuso una fórmula aproximada y la relación molar Zn:Al fue de ≈ 4, muy similar a la de las disoluciones de partida. Previo al proceso electroquímico, fue necesario optimizar una serie de parámetros en la celda, tales como control de reacciones secundarias, cantidad de HDL, concentración del metal en el electrolito, densidad de corriente, entre otros. El proceso de deposición electroquímica de los metales se describe mediante la siguiente reacción: $MCl_{2(el)} + LDH_{(e)} + 2Ag \leftrightarrow M\text{-}LDH_{(e)} + 2AgCl_{(e)}$; donde M= Cd y/o Pb, la Ag es el contraelectrodo y los subíndices (el) y (e) indican electrolito y electrodo respectivamente. Para el cadmio se usaron dos densidades de corriente diferentes (C/5.2 y C/20.8) y se partió de una disolución

de 5.20 mM $CdCl_2$. Tras aplicar una intensidad de corriente negativa, la concentración de Cd^{2+} (electrolito) se logró disminuir 3.38 mM y 3.53 mM usando ZnAl-CO_3 y MgAl-H respectivamente, a C/20.8. Al aumentar la densidad de corriente, las cantidades eliminadas fueron un poco inferiores, lo cual se debió a que el proceso estaba controlado por difusión dado que se trabajaba muy cerca de la corriente de difusión límite. La concentración de los iones M^{2+} en el electrolito (antes y después del proceso electroquímico) fue analizada mediante AA y la variación de la concentración en todos los casos fue mayor que la obtenida por los datos electroquímicos, lo que probablemente era debido a la contribución de un proceso de adsorción en la hidrotalcita simultáneo a la electrodeposición. Las capacidades de eliminación (mg por gramo de material activo) fueron 622 mg $g_{a.m.}^{-1}$ y 518 mg $g_{a.m.}^{-1}$ cuando se usó ZnAl-CO_3 y MgAl-H a C/5.20. Estos valores fueron superiores (749 mg $g_{a.m.}^{-1}$ y 763 mg $g_{a.m.}^{-1}$) cuando se trabajaba a C/20.8. Es decir, se redujo hasta un 75.2% la presencia de este contaminante en el medio. Finalizado el proceso de eliminación, fue posible recuperar gran parte del metal electroquímicamente depositado mediante la aplicación de una intensidad de corriente positiva. A C/5.20 se consiguió recuperar un 60.7% y un 39.7% y a C/20.8 un 84.2% y un 66.8% cuando ZnAl-CO_3 y MgAl-H se usaron como sustratos respectivamente. Esta metodología permitió concentrar el metal hasta 14.4 mM, pudiendo usarse para otras aplicaciones. La electrodeposición de Pb se llevó a cabo usando dos concentraciones distintas de electrolito (Ci_{el}= 2.5 mM y 5 mM) y a una densidad de corriente equivalente a C/20. La concentración de Pb^{2+} se redujo 1.8 mM y 1.64 mM (Ci_{el}= 2.5 mM), usando ZnAl-CO_3 y MgAl-H respectivamente. Para Ci_{el}= 5 mM los porcentajes de eliminación fueron superiores, alcanzándose el 89.6% y hasta 94.6% (equivalente a 4.48mM y 4.73mM). Al igual que ocurrió en el cadmio, tras analizar la concentración de Pb^{2+} en el electrolito (mediante ICP) se observaron diferencias notables, los porcentajes eliminados eran más altos que los obtenidos mediante la ley de Faraday, para la disolución Ci_{el}=2.5mM se había conseguido eliminar un 83% y 78% usando ZnAl-CO_3 y MgAl-H respectivamente, y valores superiores se alcanzaron para la disolución de 5mM, 92% y 100%. La capacidad más alta obtenida fue 1039 mg $g_{a.m.}^{-1}$ para la muestra MgAl-H partiendo de una Ci_{el}= 5mM. En último lugar, el proceso inverso se realizó para recuperar el metal y según los datos electroquímicos parte del metal fue posible concentrarlo,

sin embargo los datos de ICP revelaron lo contrario, no se había recuperado plomo y en algunos casos tan solo una pequeña parte. Esto se atribuyó a la formación de diferentes especies de plomo re-adsorbidas en la hidrotalcita, lo cual se confirmó mediante el análisis de DRX de los sustratos una vez finalizado el proceso electroquímico. A partir de los resultados obtenidos, se propusieron tres mecanismos que pudieron tener lugar durante el proceso, tales como la precipitación de plomo en forma de hidroxicarbonato, la precipitación como hidróxido de plomo y/o la formación de $PbCl_2$ aunque la identificación de todas las fases fue complicada debido a posibles solapamientos con la fase mayoritaria (hidroxicarbonato de plomo).

SUMMARY

The contamination of natural water by the widespread use of toxic substances, such as inorganic (heavy metals) and organic (herbicides) can cause serious environmental problems, particularly related to the quality of drinking water. This fact has given rise to the need to develop new remediation strategies more effectives. Among the physicochemical techniques used for fast recovery of waters affected by high concentrations of contaminants, is the adsorption, which is considered superior to other water treatments techniques in terms of initial cost, simplicity of design and ease of preparation. Also electrochemical methods have received increasing attention in recent years because it is an innovative, versatile and highly effective technique. They are could be called "green technologies" because little or no chemicals are needed to facilitate the treatment of water and have the advantage that could be used as pre-treatment in combination with other technologies of water purification managing to introduce less harmful to environment and opening a new perspective of remediation.

Layered double hydroxides (LDHs) or Hydrotalcite-like compounds (HT) whose structural and surface characteristics make them very interesting materials and suitable for multiple applications, including use as adsorbent for pollutants of different nature, are easy and economical to synthesize, exhibit great stability in a wide range of pH and are nontoxic to the environment.

LDHs have the potential for functionalization which allow for improving their adsorptive properties for a wide variety of adsorbates. **The first results which were published (first article)** dealt with the adsorption of low polarity herbicides, such as Linuron, 2,4-DB and metamitron, all of them with different physicochemical properties, by using an adsorbent LDH intercalated with the organic anion caprylate (LDH-Cap). The modified LDH was characterized by XRD and was confirmed that caprylate anion was intercalated in the interlayer space, possibly oriented in a vertical position against the hydroxide layers. Techniques like FT-IR spectra and thermal study also confirmed the presence of that anion on the solid. The most characteristic bands in the FT-IR spectra were corresponding to the vibration modes of the carboxylate groups of caprylate, and C-H stretching vibrations of the aliphatic chains. The presence of a quite noticeable exothermic effect from the combustion of interlayer organic anion was the most outstanding result of thermal study. The adsorption and desorption experiments were performed at pH range between 6 and 7 since was confirmed previously it had no influence on the amount of pesticide removed. The kinetic study showed that the adsorption of linuron and 2,4-DB was almost instantaneous while the adsorption of metamitron was more gradual, however, at 24h the adsorption equilibrium had not been reached yet. Since the adsorption kinetic is an important aspect of the pollutant removal process control, the data was fitted to a series of very widely used models in the literature. The kinetic data were fitted better to pseudo-second-order equation for the three pesticides taking into account the values of the correlation coefficients obtained, and given that the amounts of adsorbed pesticide calculated (q_e) were very consistent with the experimental q_e values. Therefore, the results suggested that the adsorption process was controlled by chemisorption. Kinetic data were also fitted to the model proposed by Weber and Morris (intra-particle diffusion model). From the results were deduced that the intra-particle diffusion is involved in the adsorption process but it is not the only rate-limiting step. In all cases the adsorptions were multi-step processes, although in the case of metamitron was observed more clearly. Therefore, the process involved adsorption of the adsorbate on the external surface, intra-particle diffusion, and chemical interaction adsorbate /adsorbent. The adsorption isotherms of the three pesticides were C-type and the maximum amount removed from the solution was

in the case of metamitron (q = 260 mol g^{-1} vs. q = 72 mol g^{-1} for linuron and q = 102 mol g^{-1} to 2,4-DB). After comparing the amounts adsorbed with previous reports with other organic anions intercalated and under similar experimental conditions, it was concluded that either interlayer composition (functional groups) and/or the height of the interlayer gallery could influence the interaction of the metamitron with the hydrophobic part of the interlayer anion. In order to compare the adsoption behavior of the three pesticides studied, also it was carried out a study of adsorption on an inorganic layered double hydroxide (LDH-Cl). The adsorption of linuron and metamitron on LDH-Cl was negligible while the adsorption of 2,4-DB was similar to that measured for LDH-Cap. This suggested that the 2,4-DB could be adsorbed on inorganic HT by ion-ion interactions between the carboxylic group and the positively charged layers of LDH. The adsorption isotherm data on LDH-Cap were fitted to the Freundlich equation, suggesting heterogeneity of the adsorption sites and different adsorption energies on the surface. After adsorption, it was carried out a desorption process of the pesticides using solvents of different polarities but all of them were partially desorbed. The lowest percentages were obtained for metamitron, which is in agreement with its high affinity by LDH-Cap together with the higher amounts of this pesticide adsorbed compared to those obtained with 2,4-DB and linuron. However, 2,4-DB was desorbed more readily in ethanol, probably due to the higher solvate-solvent affinity by similarity polarities. Finally, the adsorption products were characterized by XRD and were compared with the XRD pattern of LDH-Cap pure. The displacement of the diffraction lines corresponding to the (00l) lattice planes to lower 2Θ angles with values of $d_{(003)} \sim$ 30Å in LDH-Cap-2,4-DB and LDH-Cap-metamitron confirmed that both pesticides were intercalated in the interlayer space after the adsorption process. A decrease of the intensities of (00l) reflections had been also observed. For the XRD pattern of LDH-Cap-2,4-DB two phases were observed, suggesting the co-existence of the LDH-Cap-2,4-DB complex phase and the adsorbent LDH-Cap phase. On the other hand, the LDH-Cap-linuron XRD pattern did not change significantly compared to the pure adsorbent pattern, indicating that was possibly adsorbed on the external surface of the LDH particles.

Heavy metals are also highly hazardous pollutants that may cause environmental and many serious health problems due to its high toxicity, which

derives from its bio-accumulation. Therefore, in a **second and third article,** the synthesis and characterization of adsorbents based on LDHs (unchanged and modified by the incorporation of an organic anion in its interlayer space) and the adsorbent properties for heavy metal cations such as copper, lead and cadmium were studied. Firstly, a hydrotalcite modified with the organic anion humate (LDH-H, also called LDH-H100) was prepared by the method of ion exchange from an inorganic hydrotalcite containing chloride as interlayer anion (LDH-Cl). This organic acid is the most abundant fraction of humic substances, with a very variable composition, but with a high content of functional groups in anionic form in a large pH range, which allows binding with metal cations by electrostatic interactions and coordination bonds. The characterization of the LDH-H sample by X-ray diffraction showed characteristic peaks of hydrotalcite-like compounds with a slight increase of the basal spacing (003) of LDH-H with respect to LDH-Cl, so the humate anions could be disposed at the surface of the LDH particles and/or intercalated in a parallel position to the layers. The most characteristic bands obtained by FT-IR spectroscopy were attributed to the symmetric and antisymmetric carboxylate vibration, and those assigned to bending = CH vibration of humate, both confirm the presence of humate on the solid. By thermogravimetric analysis (TGA / DTA) the presence of an exothermic effect of humic acid oxidation was observed. The percentages of Mg and Al in addtion to the atomic ratio for both samples were calculated by elemental analysis. The molar ratio Mg:Al of the sample LDH-Cl was very close to that in the starting solution, while a slight decrease had been observed on the sample LDH-H compared to the precursor due to the synthesis process. In accordance with the Mg/Al ratio for the sample LDH-H a composition range was established assuming that the entire charge of the layer could be balanced by humate and/or chlorides anions and an approximated formula was proposed for the LDH-H sample. The number of water molecules in each of the samples was calculated from the first weight loss in TG curves. The adsorption capacity of the LDH-H hybrid was compared with the LDH-Cl and the dissociated form of humic acid (H). The latter produced the highest Cd^{2+} removal, followed by LDH-H and LDH-Cl, respectively. Both LDHs were excellent adsorbents, achieving a complete removal of Cu^{2+}, and almost complete of Pb^{2+}. A certain percentage of Mg^{2+} was detected in these supernatants, which caused an

increase on the adsorption of heavy metals. Therefore, the results obtained were related to the different adsorption mechanisms which take place, i.e., for the experiments carried out using H as adsorbent, the heavy metals were adsorbed by a complex formation producing minimal variations in the final pH. In the case of LDH-Cl, there was a significant pH increase compared to the initial pH, so the precipitation of hydroxides as part of the structure or in a separate phase could be the main mechanism involved. LDH-Cl affinity for heavy metals was then determined by the solubility products of their hydroxides (K_{SP} ($Cu(OH)_2$ = 1 10^{-20}, K_{SP} ($Cd(OH)_2$ = 1. 10^{-14} and K_{SP} ($Pb(OH)_2$ = 1. 10^{-16}). Both mechanisms were concurrent in the adsorption process with LDH-H hybrid, where the humate anions provide stability and complexing ability to the inorganic matrix. Furthermore, the higher adsorption of Cd^{2+} on LDH-H than on LDH-Cl confirmed the contribution of the mechanism of complexation As a consequence, the adsorption of these metals cations on the hybrid and the effect of a series of parameters in the process were studied first. The selected pH for the adsorption experiments was 5 and the kinetic study results revealed that the adsorption took place in two steps. The first step was fast and produced half of the final adsorption within the first 2h, and the second approached an equilibrium more gradually, reaching it within 48h in the case of Pb and Cd, and 24h for the case of Cu. 100%, 95% and 56% of the initial metal concentration (C_o=1 mM) was removed for Cu, Pb and Cd, respectively. The adsorption isotherms showed high effectiveness of LDH-H hybrid as an adsorbent, where the metals ions were completely adsorbed at lower initial concentrations. By the Langmuir model fitting, the maximum adsorption increased in the following order Cd (C_m = 0.35mmol g^{-1}), Pb (C_m = 0.48mmol g^{-1}) and Cu (C_m = 0.75mmol g^{-1}). The structural characterization of the adsorption products showed that there were no important changes. XRD patterns indicated a loss of crystallinity but there were no additional precipitates observed. The FT-IR spectra showed slight displacements of some characteristics bands, which are likely to be due to the interaction of the functional groups of humate with metal ions. Finally, the simultaneous adsorption of the three metals ions (multicomponent solution) was studied. The highest amount of the metal cations adsorbed on LDH-H was reached for Cu, in both cases, C_s= 0.46 mmol g^{-1} (multicomponent kinetic) and C_s= 0.57 mmol g^{-1} (monocomponent kinetic), while the adsorption of Cd was completely

inhibited by the presence of the other cations in solution. This behavior was concordant with the sequence of stability of the corresponding metal hydroxides and the stability constants of the metal-humate complexes, decreasing in the order of Cu> Pb> Cd.

Given the high affinity of heavy metal ions (Cu^{2+}, Pb^{2+} and Cd^{2+}) for LDH-Cl, a more comprehensive study of this adsorbent was carried out **(third article)**, comparing it with two hybrids (LDH-H100 so-called LDH-H and LDH-H50) containing different amounts of humate anions (100% and 50% of humate stoichiometric concentration required to compensate the laminar charge). Basically, the study was based on the calculation of the kinetic and thermodynamic parameters as well as other factors affecting the adsorption process. The structural analysis of both hybrids showed the same characteristics given the similarity of their composition and synthesis method. Initial metal concentrations ranging in all cases between C_o=0-2.5mM, except in the case of Cu sorption on LDH-Cl where the initial concentration increased to 4.4mM, were selected to study the influence of the initial concentration in the metal adsorption (isotherms). The results showed that the maximum uptake for Cu^{2+} in LDH-H100, LDH-H50 and LDH-Cl was 0.76, 1.02 and 1.95 mmol g^{-1} respectively. The amounts of Pb^{2+} adsorbed were 0.48, 0.25 and 0.61 mmol g^{-1}, and finally for Cd^{2+} were 0.35, 0.18 and 1.03 mmol g^{-1}. In all cases higher adsorption was achieved using LDH-Cl as the adsorbent. Therefore, the main mechanism involved could be precipitation as metal hydroxides, either by incorporation of the metal ions in the structure of the hydrotalcite (diadochy) or as a separate phase, given the very high values of final pH reached (~8.2-9). Also, it should be noted here that for LDH-Cl and C_o=0-2mM, the metal elimination percentages were 98%, 80% and 53% for Cu^{2+}, Cd^{2+} and Pb^{2+} respectively. In the hybrids adsorbents, higher amounts of Pb^{2+} and Cd^{2+} were adsorbed on the hybrid containing a higher proportion of humate (LDH-H100), which is consistent with an additional adsorption mechanism (complexation). On the contrary, a higher amount of Cu^{2+} was adsorbed on LDH-H50, which contained a greater proportion of inorganic components. This leads to the conclusion that precipitation is the fundamental mechanism in metal uptake by a non-hybrid LDH. In order to correlate the experimental data adequately, Langmuir and Freunlich isotherms were tested, the results indicating that all adsorption processes were perfectly

fitted to the Langmuir equation. The effect of temperature was also studied in the range of 288-308°K to LDH-Cl and LDH-H100. The ΔH° values indicated that the adsorption process was endothermic in all cases and the ΔG° values (-4.06 and 16.25KJ/mol) were in the middle of physisorption and chemisorption, all adsorption processes being spontaneous and thermodynamically favorable. Subsequently, the kinetic of metal ions uptake on the LDHs was analyzed using different kinetic models. In the case of adsorption of Cu^{2+} on LDH-Cl the plateau was reached at 2h; however, it took 24h for the LDH-H100 and LDH-H50 adsorbents. The removal rates of Pb^{2+} and Cd^{2+} were slower than that corresponding to Cu^{2+}. The equilibrium was reached at 24h (LDH-Cl and LDH-H50) and 48h (LDH-H100) for Pb^{2+}, and at 48h for Cd^{2+} in all cases. The kinetic data were fitted better to the of pseudo-second order model for the three adsorbents. The plot of the kinetics by the intra-particle diffusion model showed multilinearity in all cases. The surface adsorption and intra-particle diffusion probably took place simultaneously, both processes controlling the kinetic of adsorbate-adsorbent interactions. The rate constants at each step followed the order of $K_{p1} > K_{p2} > K_{p3}$, being the diffusion rate constant K_{p1} for the adsorption of Cu^{2+} on LDH-Cl higher than that of LDH-H100 and vice versa for Pb^{2+}, which might be attributed to more active sites on the surface in each case. Due to the high adsorption capacity observed for the inorganic LDH, several competition experiments of adsorption were carried out in a binary and ternary solutions. The presence of Pb^{2+} and/or Cd^{2+} did not affect the percentage of Cu^{2+} adsorption in any case. The presence of Cd^{2+} (multicomponent solution) hardly affected the adsorption of Cu^{2+} and Pb^{2+}, although the adsorption of Cd^{2+} was significally reduced, especially after 48h. For the binary systems, the percentage of removal of Pb^{2+} decreased in the presence of Cd^{2+} (Cd-Pb system) in respect to the Cu-Pb system at 24h, and the percentage of Cd^{2+} removed was much lower in presence of Cu^{2+} than in the presence of Pb^{2+} at 48h. This fact confirmed some competition between these cations during these periods of time. Therefore, the decrease in percentage of the removal of Cd^{2+} in all systems, may be ascribed to less availability of binding sites, so that ions with greater affinity for LDH-Cl could displace others with a weaker affinity. Finally, a study of the influence of the presence of humate anion on the solution over the metal sorption was carried out. The amount of Cu^{2+} adsorbed was the same (in the

presence and absence of humate) although the amount of Pb^{2+} and Cd^{2+} adsorbed decreased in the presence of this anion. It could be due to a small part of the metal being complexed with the humate anions present in solution and remaining there. Furthermore, the affinity sequence of metal cations by the humate anion varies, in accordance with the following order: Cd> Pb> Cu.

In a **fourth article**, different LDHs were prepared and used as substrates for the removal of extremely toxic metal cations, such as as Pb^{2+} and Cd^{2+} from aqueous solution , by electro-deposition. These hydrotalcites were named MgAl-H and ZnAl-CO_3. This latter was characterized by XRD, SEM and IR just as the MgAl-H sample which was characterized in a previous work. By X-ray diffraction the HT-type structure of the ZnAl-CO_3 was confirmed, showing a high crystallinity. By SEM the laminar morphology of the particles was observed. The FT-IR spectra of the sample, typical of a hydrotalcite with carbonate in the interlayer space, showed bands corresponding to the vibration modes of the carbonate species together with the absorption peaks due to the water molecules and hydroxy groups. By elemental analysis and TG curves an approximate formula was proposed and the molar ratio Zn: Al was ≈ 4, close to the one of the starting solutions. Prior to the electrochemical process, it was necessary to optimize a number of parameters in the cell, such as control of side reactions, the amount of LDH, metal concentration in the electrolyte and current density among others. The process of electrochemical deposition of metals is described by the following reaction: $MCl_{2(el)}$ + $LDH_{(e)}$ ⇄ 2 $Ag_{(e)}$ + M-$LDH_{(e)}$ + 2$AgCl_{(e)}$; where M = Cd and/or Pb, Ag is the counter electrode and the subscripts (el) and (e) indicate the electrolyte and electrode phases respectively. For the electrochemical deposition of cadmium two different current densities (C/5.2 and C/20.8) and 5.20 mM solution of $CdCl_2$ were used. When a negative current was applied, the concentration of Cd^{2+} (electrolyte) was reduced by 3.38 mM and 3.53 mM when ZnAl-CO_3 and MgAl-H were respectively used at C/20.8. On increasing the current rate, the amounts of Cd^{2+} removed decreased. These lower values are in agreement with the fact that the electro-deposition process was controlled by diffusion since the current applied was close to the value of the diffusion limit current. The concentration of metal ions in the electrolyte (before and after the electrochemical process) was analyzed by AA and the variation of the concentration in all cases was higher than the value obtained

by the electrochemical data. This was probably due to the contribution of an adsorption process in the hydrotalcite simultaneous to the electro-deposition. The electrochemical removal capacities were 622 mg $g_{a.m.}^{-1}$ (mg per gram of active material) and 518 mg $g_{a.m.}^{-1}$ when ZnAl-CO_3 and MgAl-H were respectively used as substrates with a current rate of C/5.20. These values increased to 749 mg $g_{a.m.}^{-1}$ and 763 mg $g_{a.m.}^{-1}$ when the current rate was equal to C/20.8, so the presence of this pollutant can be reduced to 75.2%. After the removal process the metal electrochemically deposited was recovered to a large extent by applying a positive current. At C/5.20 a recovery of 60.7% and 39.7% was obtained when ZnAl-CO_3 and MgAl-H were used respectively, and values of recovery of 84.2% and 66.8% were achieved when the current rate was C/20.8. This methodology permitted us to increase the concentration of cadmium up to 14.4 mM, so the recovery solutions could possibly be used for other applications. The electro-deposition of Pb^{2+} was carried out at using a current density equal to C/20 and two different concentrations of electrolyte (Ci_{el} = 2.5 mM and 5 mM). The concentration of Pb^{2+} was reduced by 1.8 mM and 1.64 mM when ZnAl-MgAl-CO_3 and MgAl-H were used respectively in a solution containing an initial concentration of 2.5 mM of $PbCl_2$. When a solution with an initial concentration equal to 5 mM was used, higher percentages of elimination were achieved, reaching 89.6% and 94.6% (equivalent to 4.48mM and 4.73mM). The analysis of the concentration of Pb^{2+} in the electrolyte (by ICP) revealed significant differences (with the same range of those observed for Cd). The percentages of removal were higher with respect to the values calculated from Faraday law. The percentages of Pb^{2+} eliminated from a 2.5mM solution were 83% and 78% for ZnAl-CO_3 and MgAl-H respectively and values of 92% and 100% were achieved when a 5mM solution was used. The highest removal capacity was obtained by the sample MgAl-H from a 5mM solution, reaching 1039 mg. $g_{a.m.}^{-1}$. Finally, the reverse process was carried out to recover the metal, and by electrochemical data this recovery of lead deposited was successful. However, ICP analysis revealed that there was little or no recovered lead. This fact was attributed to the formation of different lead species re-adsorbed on the hydrotalcite, which was confirmed by the analysis of the electrodes by X-Ray diffraction (after recovery process). From these results, three possible mechanisms that could have occurred during the process were proposed, such as

precipitation as hydroxycarbonate of lead, precipitation as hydroxide of lead and/or formation of lead chloride. The identification of all phases could be complicated by the overlapping with the predominating phase (hydroxycarbonate of lead).

CAPÍTULO VI
Conclusiones Generales / General Conclusions

Las conclusiones más relevantes obtenidas en cada uno de los artículos desarrollados y discutidos en esta memoria doctoral se indican a continuación:

"Caprylate intercalated layered double hydroxide as adsorbent of the linuron, 2,4-DB and metamitron pesticides from aqueous solution"

1. El anión caprilato fue intercalado como anión interlminar en una hidrotalcita con cloruro (LDH-Cl) obteniéndose LDH-Cap. Este adsorbente mostró mediante DRX un aumento del espaciado basal con respecto al de LDH-Cl, lo que indica que el anión probablemente se encuentre orientado en posición vertical respecto a las láminas de hidróxidos junto con las moléculas de agua en el espacio interlaminar.

2. El estudio del efecto del tiempo de contacto en la adsorción de 2,4-DB y linurón en LDH-Cap indicó que el proceso fue casi instantáneo mientras que la adsorción del metamitrón fue más gradual. Al cabo de las 5h se alcanzó la eliminación del ~90% de la cantidad inicial (C_o=0.19; 0.12 y 1mM para linurón, 2,4-DB y metamitrón respectivamente).

3. Los datos cinéticos para la adsorción de los tres presticidas en LDH-Cap se ajustaron a la ecuación de pseudo segundo orden. Esto sugiere que el proceso de adsorción está controlado preferentemente por quimisorción.

4. Las isotermas de adsorción de los tres pesticidas en LDH-Cap fueron de tipo C en todos los casos. Las máximas cantidades adsorbidas por gramo de adsorbente fueron 260 μmol g^{-1}, 72 μmol g^{-1} y 102 μmol g^{-1} de metamitrón, linurón y 2,4-DB respectivamente.

5. La adsorción de linurón y metamitrón en LDH-Cl fue despreciable, sin embargo, el 2,4-DB se adsorbió en la misma proporción que lo hizo en LDH-Cap, probablemente debido al carácter aniónico de este pesticida con mayor afinidad hacia las láminas del adsorbente.

6. Los datos de las isotermas de adsorción de los tres pesticidads en LDH-Cap se ajustaron mejor a la ecuación de Freundlich sugiriendo heterogeneidad de los sitios de adsorción

7. El estudio de la desorción se realizó con agua, etanol y acetona obteniéndose una desorción parcial con los tres disolventes (13%, 17% y 20% para linurón; 5%, 38% y 19% para el 2,4-DB; y 11%, 3% y 7% para el metamitrón). El porcentaje de desorción más alto se obtuvo para el 2,4-DB eludido con etanol, debido posiblemente a la similitud de polaridades del pesticida y del disolvente.

8. Los resultados obtenidos de la caracterización estructural de los productos de adsorción sugirieron que el 2,4-DB y el metamitrón se intercalaron en el espacio interlaminar mientras que el linurón se adsorbía en la superficie externa de las partículas de HDL.

"Removal of Cu^{2+}, Pb^{2+} and Cd^{2+} by layered double hydroxide–humate hybrid. Sorbate and sorbent comparative studies"

1. Se ha sintetizado una hidrotalcita modificada con el anión orgánico humato (LDH-H), mediante intercambio iónico en LDH-Cl para su utilización como adsorbente para eliminar Cu^{2+}, Pb^{2+} y Cd^{2+} procedentes de disoluciones acuosas.

2. De acuerdo con los resultados de DRX y espectroscopia FT-IR los aniones humatos posiblemente se encuentran alojados en la superficie de las partículas de HDL, y también probablemente una parte se haya intercalado en los extremos de las mismas.

3. Los resultados de la adsorción de los metales pesados estudiados mostraron que los adsorbentes tipo hidrotalcita LDH-Cl, LDH-H son mas efectivos que el humato sódico. Los altos valores de pH final obtenido para la adsorción de los metales en LDH-Cl indicaron que el principal

mecanismo pudo ser la precipitación como hidróxidos. Mientras que en el híbrido LDH-H, además de la precipitación, es probable que se produciese la captura de metales a través de los grupos funcionales del anión humato mediante formación de complejos, de esta forma los aniones humato estabilizaban la matriz de HDL (menor incremento de pH).

4. El estudio de la influencia de pH en la adsorción de los metales pesados mostró que los valores de C_s y pH_f disminuyeron ligeramente al disminuir el pH.

5. El estudio cinético reveló que la adsorción tuvo lugar en dos etapas: una rápida, probablemente asociada con la precipitación de los hidróxidos y otra más gradual debido a la complejación.

6. Las isotermas de adsorción en todos los casos se ajustaron al modelo de Langmuir, sugiriendo alta afinidad adsorbato-adsorbente. Los valores de capacidad de adsorción obtenidos fueron: Cd^{2+} (C_m= 0.35mmol g^{-1}), Pb^{2+} (C_m= 0.48mmol g^{-1}) y Cu^{2+} (C_m= 0.75mmol g^{-1}).

7. El estudio de sistemas multicomponente mostró que la eficiencia de eliminación de cada metal fue más baja cuando varios metales compiten por ocupar los sitios disponibles en el adsorbente en comparación con las disoluciones monocomponentes. Sin embargo, la presencia de más de un ion metálico llegó a aumentar la capacidad total del adsorbente.

"Cu(II), Pb(II)and Cd(II) sorption on different layered double hydroxides. A kinetic and thermodynamic study and competing factors"

1. Se ha realizado el estudio de adsorción de cationes metálicos (Cu^{2+}, Pb^{2+} y Cd^{2+}) utilizando como adsorbentes híbridos que contenían distinta cantidad de aniones humato (50 y 100% de la cantidad estequiometrica

calculada), LDH-H50 y LDH-H100 y el precursor utilizado para ambas síntesis (LDH-Cl).

2. La forma de las isotermas de adsorción fue similar para cada metal en los tres adsorbentes, y se corresponde con tipo L o H (fuerte afinidad adsorbato/adsorbente).

3. Los porcentajes de metales eliminados fueron mayores en LDH-Cl que en LDH-H100 y LDH-H50. Los valores de pH final obtenidos después de la adsorción sugirieron que el principal mecanismo fue la precipitación como hidróxidos metálicos, aunque probablemete puede producirse simultáneamente la incorporación de los cationes metálicos en la estructura de la hidrotalcita (diadochy) o formando una fase separada. Los porcentajes de eliminación fueron 98%, 80% y 53% (Cu^{2+}, Cd^{2+} y Pb^{2+} respectivamente) para C_o= 0-2 mM.

4. Para los adsorbentes híbridos, la cantidad adsorbida en el equlibrio fue mayor en LDH-H100 que en LDH-H50 para los cationes metálicos Pb^{2+} y Cd^{2+}, lo que confirma la existencia de un mecanismo adicional a la precipitación, probablemente la formación de complejos con los grupos funcionales del humato del adsorbente.

5. El Cu^{2+} se adsorbió en mayores cantidades en el híbrido LDH-H50 que en LDH-H100. Una mayor fracción de componente inorgánico favoreció la precipitación en este caso frente a la formación de complejo.

6. El cálculo de los parámetros termodinámicos reveló que todos los procesos de adsorción en el rango de temperatura estudiado (288-308°K) fueron endotérmicos y termodinámicamente favorables. Los valores obtenidos de $\Delta G°$ indicaron que el proceso estaba controlado por fisisorción y quimisorción.

7. El estudio de la influencia del tiempo de contacto mostró que las velocidades de adsorción del Pb^{2+} y el Cd^{2+} fueron más lentas que las del Cu^{2+}.

8. El estudio cinético mostró que el proceso de adsorción de los tres metales sobre los adsorbentes utilizados (LDH-Cl, LDH-H100 y LDH-H50) se ajustó a la ecuación de pseudo segundo orden. Los valores de la constante de velocidad k_2 presentó la siguiente secuencia: Cu^{2+}> Pb^{2+}> Cd^{2+} para la adsorción en LDH-Cl y LDH-H50, mientras que para LDH-H100 fue Cd^{2+}∼Cu^{2+}> Pb^{2+}.

9. La representación de Weber y Morris mostró multilinealidad. La adsorción en la superficie y la difusión intraparticula probablemente ocurrieron simultáneamente. El valor de la constante de difusión, k_{p1} para el Cu^{2+} en LDH-Cl fue mucho mayor que en LDH-H100, lo que se puede atribuir a la precipitación Por el contrario, para el caso del Pb^{2+} k_{p1} fue mayor en LDH-H100.

10. En las disoluciones multicomponentes (binarias y ternarias) y monocomponentes el porcentaje adsorbido de Cu^{2+} fue del 100%, por lo que la adsorción de este metal no se vio afectada en ningún caso por otros iones presentes en la disolución. Los porcentajes de Pb^{2+} y Cd^{2+} en los sistemas bicomponentes variaron de forma notable con respecto a las disoluciones monocomponentes, lo cual confirmaría que existe cierta competición entre ambos cationes metálicos. La secuencia de adsorción competitiva en todos los casos siguió el siguiente orden: Cu^{2+}> Pb^{2+}>Cd^{2+}. Este comportamiento puede estar determinado por varios factores, tales como constantes de productos de solubilidad, constantes de estabilidad de formación de complejos y/o tiempo de contacto.

11. El estudio de la influencia del anión humato en la disolución multicomponente, reveló la mayor afinidad de este anión por los iones Pb^{2+} y Cd^{2+}, ya que la cantidad adsorbida de Cu^{2+} fue la misma en ausencia

y en presencia de humato. Sin embargo, los iones Pb^{2+} y el Cd^{2+} se adsorbieron en menor cantidad en presencia del ácido húmico en disolución, lo cual confirmó que una parte del metal fue complejado con los aniones humato presentes en la disolución.

"Capturing Cd(II) and Pb(II) from contaminated water sources by electro-deposition on Hydrotalcites-like Compounds"

1. Se han utilizado dos compuestos tipo hidrotalcita de distinta composición (ZnAl-CO_3 y MgAl-H) como sustratos electroquímicos para la eliminación electroquímica de metales pesados (Pb^{2+} y Cd^{2+}) procedentes de medios acuosos, y para su posterior recuperación y concentración.

2. Los diagramas de DRX de las muestra ZnAl-CO_3 y MgAl-H se corresponden con el de un compuesto con estructura tipo hidrotalcita, destacando la elevada cristalinidad del ZnAl-CO_3, lo cual fue consistente con la imagen de SEM obtenida. Por otro lado, mediante espectroscopia FT-IR se confirmó la presencia de humato en la muestra MgAl-H.

3. Durante el proceso electroquímico fue posible eliminar el 65% y el 67.8% del Cd^{2+} (Ci_{el}= 5.20 mM) cuando se usó ZnAl-CO_3 y MgAl-H respectivamente, a una corriente equivalente C/20.8. Aumentando la densidad de corriente a C/5.2, los porcentajes de eliminación disminuyeron ya que el proceso queda controlado por la difusión de las especies al electrodo.

4. El análisis de la variación real de la concentración en el electrolito reveló que la cantidad de Cd^{2+} eliminada fue mayor que la obtenida mediante electroquímica, lo que implica posiblemente la contribución de un proceso de adsorción simultáneo dado las propiedades adsortivas de los HDLs. La presencia de este contaminante se redujo un 61.2% y 73.8% para

ZnAl-CO_3, y 50.9% y 75.2% para MgAl-H trabajando a C/5.2 y C/20.8 respectivamente y la cantidad máxima eliminada por gramo de material activo fue 763 mg g^{-1}.

5. Los porcentajes de recuperación del cadmio electroquímicamente depositado fueron: 60.7% y 39.7% a C/5.20. Sin embargo, se obtuvieron valores más altos cuando se disminuyó la corriente; 84.2% y 66.8% para ZnAl-CO_3 y MgAl-H respectivamente. Esta metodología permitió aumentar la concentración de Cd^{2+} hasta 14.33 mM, el cual puede ser posteriormente empleado con fines industriales.

6. Mediante la electrodeposición de Pb^{2+} a C/20 se logró eliminar un 72% y 65.6% para ZnAl-CO_3 y MgAl-H cuando se usó una concentración inicial de 2.5mM. Cuando la concentración de la disolución de partida fue mayor (Ci_{el}= 5 mM), se alcanzaron porcentajes de eliminación de 89.6% y 94.6%.

7. El análisis de la cantidad de Pb^{2+} eliminada en el electrolito mostró valores superiores a los calculados mediante la ley de Faraday. Por tanto, considerando la combinación de la deposición electroquímica y el efecto de la adsorción se obtuvieron porcentajes de eliminación de 83% y 78% para ZnAl-CO_3 y MgAl-H respectivamente (Ci_{el}= 2.5 mM) y estos aumentaron hasta 92% y 100% cuando se partió de una concentración inicial de 5 mM. El valor de capacidad de eliminación más alto que se obtuvo fue de 1039 mg g^{-1}.

8. El análisis del plomo recuperado tras el proceso electrodeposición mostró grandes divergencias con el aumento de concentración predicho por las medidas galvanostaticas Este hecho, indicó que varios mecanismos de re-adsorción limitaron la recuperación de dicho contaminante.

9. Los diagramas de DRX de los electrodos tras el proceso de recuperación mostraron un sistema muy complejo constituido por varias fases. Por lo que tres posibles mecanismos de re-adsorción de Pb^{2+} en los HDLs o la combinación de ellos pudieron explicar las diferencias mencionadas

anteriormente. Estos mecanismos son: la formación de hidroxicarbonato (fase mayoritaria), de hidróxido de plomo y de cloruro de plomo.

The most relevant conclusions obtained in each of the papers developed and discussed in this doctoral thesis are detailed below:

"Caprylate intercalated layered double hydroxide as adsorbent of the linuron, 2,4-DB and metamitron pesticides from aqueous solution"

1. The caprylate anion was intercalated into hydrotalcite with chloride as an interlayer anion (LDH-Cl) obtaining LDH-Cap. By XRD, this adsorbent showed an increase of the basal spacing with respect to LDH-Cl, indicating that the anion could probably be oriented in a vertical position with respect to the hydroxides layers together with the water molecules in the interlayer space.

2. The study of the contact time effect on the adsorption of linuron and 2,4-DB on LDH-Cap indicated that the process was almost instantaneous whereas the adsorption of metamitron was more gradual. ~90% of the initial amount removed was done so in 5h (C_o= 0.19; 0.12 and 1mM for linuron, 2,4-DB and metamitron respectively).

3. The kinetic data for the adsorption of the three pesticides on LDH-Cap was fitted to the equation of pseudo-second order. This suggests that the adsorption process was preferably controlled by chemisorption.

4. The adsorption isotherms of the three pesticides on LDH-Cap were type C in all cases. The maximum amounts adsorbed per gram of adsorbent were 260 μmol g^{-1}, 72 μmol g^{-1} and 102 μmol g^{-1} for metamitron, linuron and 2,4-DB respectively.

5. The adsorption of linuron and metamitron on LDH-Cl was negligible, although the adsorption of 2,4-DB was close to that measured for LDH-Cap, probably due to the anionic character of this pesticide with a higher affinity to the adsorbent layers.

6. The adsorption isotherms data were fitted to the Freundlich equation for the three pesticides on LDH-Cap, suggesting a heterogeneity of the adsorption sites.

7. The desorption study was performed with water, ethanol and acetone, obtaining a partial desorption with the three solvents (13%, 17% and 20% for linuron; 5%, 38% and 19% for 2,4-DB; and 11%, 3% and 7% for metamitron). The highest desorption percentage was achieved for 2,4-DB eluded with ethanol, possibly related to the similarity of the polarities solvate-solvent.

8. The results obtained from the structural characterization of the adsorption products suggested that the 2,4-DB and metamitron were intercalated in the interlaminar space, while linuron was probably adsorbed on the external surface of LDH particles.

"Removal of Cu^{2+}, Pb^{2+} and Cd^{2+} by layered double hydroxide–humate hybrid. Sorbate and sorbent comparative studies"

1. A modified hydrotalcite has been synthetized by incorporating humate anion into the LDH-Cl via ion exchange to be used as an adsorbent for the removal of Cu^{2+}, Pb^{2+} and Cd^{2+} from aqueous solutions.

2. According to the results obtained by XRD analysis and FT-IR spectroscopy, the humate anions were disposed on the surface of the LDH particles, with a part intercalated probably at the edges of the particles.

3. The results of the heavy metals adsorption showed that the hydrotalcite-type adsorbents, LDH-Cl and LDH-H are more effective than sodium humate. The high final pH values obtained for the adsorption of metals on LDH-Cl indicated that the main mechanism may be ascribed to the precipitation as hydroxides, while in the hybrid LDH-H the capturing of metals via the functional groups of humate anions by complexation is likely, in addition to the precipitation. In this way, the humate anions stabilize the LDH matrix (lower pH increase).

4. The study of the pH influence on the heavy metals adsorption showed that C_s and pH_f values decreased slightly with a decreasing pH.

5. The kinetic study revealed that adsorption was produced into two steps: the first, fast step being associated with the precipitation of hydroxides and the second, more gradual due to complexation.

6. The adsorption isotherms in all cases were fitted to the Langmuir model, suggesting a high affinity between the adsorbate and the adsorbent. The adsorption capacity values were: Cd^{2+} (C_m = 0.35 mmol g^{-1}), Pb^{2+} (C_m = 0.48 mmol g^{-1}) and Cu^{2+} (C_m = 0.75 mmol g^{-1}).

7. The study of the multicomponent systems showed that the efficiency removal of each metal was less when several metals compete to occupy the available sites on the adsorbent compared to the monocomponent solutions. However, the presence of the other cations managed to increase the total capacity of the adsorbent.

"Cu(II), Pb(II)and Cd(II) sorption on different layered double hydroxides. A kinetic and thermodynamic study and competing factors"

1. A study of metallic cation adsorption (Cu^{2+}, Pb^{2+} and Cd^{2+}) using LDH hybrids as adsorbents containing different amount of humate anions (50 and 100% of the stoichiometric amount calculated), LDH-H50 and LDH-H100, and the precursor used for both synthesis (LDH-Cl).

2. The shape of the adsorption isotherms was similar for each metal in the three adsorbents, and they corresponds to type L or H (strong affinity adsorbate/adsorbent).

3. The percentages of metals removed were higher in LDH-Cl than in LDH-H100 and LDH-H50. The values of final pH obtained after adsorption suggested that the main mechanism was precipitation as metal hydroxides, although the incorporation of metal cations on the HT structure (diadochy) or in a separate phase might have occurred simultaneously. The percentages of removal were 98%, 80% and 53% (Cu^{2+}, Cd^{2+} and Pb^{2+} respectively) to C_o= 0-2mM.

4. For the hybrids adsorbents, the amount adsorbed on the equilibrium was higher on LDH-H100 than on LDH-H50 for metal cations Pb^{2+} and Cd^{2+}, confirming the existence of an additional adsorption mechanism, probably by complexing with the functional groups of the hybrid LDHs .

5. The Cu^{2+} was adsorbed in higher amounts on the hybrid LDH-H50 than on LDH-H100. A larger fraction of the inorganic component favored the precipitation in this case against the complexation.

6. The calculation of thermodynamic parameters revealed that all adsorption processes were endothermic and thermodynamically favorable in the temperature range 288-308°K. The $\Delta G°$ values obtained indicated that the process was controlled by physisorption and chemisorption.

7. The study of the influence of contact time showed that the adsorption rates of Pb^{2+} and Cd^{2+} were slower than that corresponding to Cu^{2+}.

8. The kinetic study suggested that the adsorption process of the three metals on the adsorbents (LDH-Cl, LDH-H100 and LDH-H50) was fitted to the pseudo-second order equation. The values of the constant rate k_2 presented the following sequence: $Cu^{2+} > Pb^{2+} > Cd^{2+}$ for the adsorption on LDH-Cl and LDH-H50, and $Cd^{2+} \sim Cu^{2+} > Pb^{2+}$ for the LDH-H100.

9. The plotting of Weber and Morris showed multilinearity. The surface adsorption and intra-particle diffusion probably took place simultaneously. The value of the diffusion constant, k_{p1} for the adsorption of Cu^{2+} on LDH-Cl was much higher than on LDH-H100, which can be attributed to the precipitation. On the contrary, k_{p1} for the adsorption of Pb^{2+} was higher on LDH-H100.

10. In multicomponent (binary and ternary) and monocomponent solutions the percentage of Cu^{2+} adsorbed was 100%, so the adsorption of this metal was not affected in any case by other ions present in the solution. The percentages of Pb^{2+} and Cd^{2+} in the binary systems varied considerably with respect to the monocomponent solutions, which would confirm that there was some competition between metal cations. The sequence of competitive adsorption in all cases was: $Cu^{2+} > Pb^{2+} > Cd^{2+}$. This behavior can be determined by several factors, such as the solubility product constant, stability constants of complex formation and/or contact time.

11. The study of the influence of the humate anion on the multicomponent solution, exhibited the highest affinity of this anion by Pb^{2+} and Cd^{2+} ions, as the amount of Cu^{2+} adsorbed was the same in both the absence and presence of humate. However, the Pb^{2+} and Cd^{2+} ions were adsorbed in lower amounts in the presence of humic acid in the solution, which confirmed that a small part of the metal being complexed with the humate anions was present in the solution.

"Capturing Cd(II) and Pb(II) from contaminated water sources by electro-deposition on Hydrotalcites-like Compounds"

1. Two different hydrotalcites-like compounds (ZnAl-CO_3 and MgAl-H) were used as substrates for the electrochemical removal of heavy metals (Pb^{2+} and Cd^{2+}) from aqueous solutions, and their subsequent recovery and concentration.

2. The XRD patterns of the ZnAl-CO_3 and MgAl-H correspond to a compound with a HT-type structure, emphasizing the high crystallinity of ZnAl-CO_3, which was consistent with the SEM image obtained. On the other hand, FT-IR spectroscopy confirmed the presence of humate in the sample MgAl-H.

3. During the electrochemical process it was possible to remove 65% and 67.8% of Cd^{2+} (Ci_{el}= 5.20 mM) when ZnAl-CO_3 and MgAl-H were used respectively at C/20.8. Increasing the current rate to C/5.2, the percentages of removal decreased since the process was controlled by the diffusion limitation of the species to the electrode.

4. The analysis of the real variation of the concentration in the electrolyte revealed that the amount of Cd^{2+} removed was higher than the value obtained by electrochemistry, which possibly implying the contribution of a simultaneous adsorption process given the adsorptive properties of the LDHs. The presence of this pollutant was reduced by 61.2% and 73.8% for ZnAl-CO_3, and 50.9% and 75.2% for MgAl-H, when the current rate was equal to C/5.2 and C/20.8 respectively, and the maximum amount removed per gram of active material was 763 mg g^{-1}.

5. The percentages of recovery of cadmium electrochemically deposited were 60.7% and 39.7% at C/5.20. However, higher values were obtained when the current density was decreased; 84.2% and 66.8% for ZnAl-CO_3 and MgAl-H, respectively. This methodology permitted the concentration of

Cd^{2+} to be increased to 14.33 mM, which can be used for industrial purposes.

6. By the electro-deposition of Pb^{2+} at a current rate equal to C/20, it was possible to eliminate 72% and 65.6% for ZnAl-CO_3 and MgAl-H, when a solution containing an initial concentration of 2.5 mM was used. Percentages of 89.6% and 94.6% were achieved when the concentration of the starting solution was higher (Ci_{el} = 5 mM).

7. The analysis of the amount of Pb^{2+} eliminated in the electrolyte showed higher values than those calculated from the Faraday law. Therefore, considering the combination of electrochemical deposition and the effect of the adsorption, percentages of removal of 83% and 78% for ZnAl-CO_3 and MgAl-H respectively (Ci_{el} = 2.5 mM) were obtained and these values increased up to 92% and 100% when the 5mM solution was used. The highest value of removal capacity was 1039 mg g^{-1}.

8. The analysis of lead recovered after the electro-deposition process, showed wide divergences with the increase of the concentration predicted by the galvanostatic measurements. This fact indicated that several re-adsorption mechanisms limited the recovery of that pollutant.

9. The XRD patterns of the electrodes after the recovery process showed a very complex system consisting of several phases. Therefore, three possible mechanisms of re-adsorption of Pb^{2+} on the LDH or the combination of them could explain the above-mentioned differences. These mechanisms are: the formation of hydroxycarbonate (predominant phase), lead hydroxide and lead chloride.

CAPÍTULO VII
Informes

VII.1. INDICIOS DE CALIDAD

Los artículos que se exponen en esta memoria han sido publicados en revistas de primer cuartil y cuyos factores de impacto del Journal Citation Reports, asi como la categoría a la que pertencen, se muestran a continuación.

-Título: **"Caprylate intercalated layered double hydroxide as adsorbent of the linuron, 2,4-DB and metamitron pesticides from aqueous solution"**

-Autores: I. Pavlovic, M.A. González, F. Rodríguez-Rivas, M.A. Ulibarri, C. Barriga
-Revista: Applied Clay Science 80–81 (2013) 76–84
-Editorial: Elsevier Science BV
-Índice de impacto (año publicación, 2013): 2.703
-Categoría: Materials Science, Multidisciplinary (Q1)
-Ranking en la categoría/ Número de revistas en la categoría: 51/251
-Citas: 4

-Título: **"Removal of Cu^{2+}, Pb^{2+} and Cd^{2+} by layered double hydroxide–humate hybrid. Sorbate and sorbent comparative studies"**
-Autores: M.A. González, I. Pavlovic, R. Rojas-Delgado, C. Barriga
-Revista: Chemical Engineering Journal 254 (2014) 605–611
-Editorial: Elsevier Science SA
-Índice de impacto (año publicación, 2014): 4.321
-Categoría: Engineering, Chemical (Q1)
-Ranking en la categoría/ Número de revistas en la categoría: 9/135
-Citas: 11

-Título: **"Cu(II), Pb(II) and Cd(II) sorption on different layered double hydroxides. A kinetic and thermodynamic study and competing factors"**
-Autores: M.A. González, I. Pavlovic, C. Barriga
-Revista: Chemical Engineering Journal 269 (2015) 221–228
-Editorial: Elsevier Science SA
-Índice de impacto (año 2014): 4.321
-Categoría: Engineering, Chemical (Q1)
-Ranking en la categoría/ Número de revistas en la categoría: 9/135

-Citas: 4

-Titulo: **"Capturing Cd(II) and Pb(II) from contaminated water sources by electro-deposition on Hydrotalcites-like Compounds"**

-Autores: M. A. González a, R. Trócoli, I. Pavlovic, C. Barriga, F. La Mantia

-Revista: Physical Chemistry Chemical Physics 18 (2016) 1838-1845

-Editorial: Royal Society of Chemistry

-Índice de impacto (año 2014): 4.493

-Categoría: Physics, Atomic, Molecular & Chemical (Q1)

-Ranking en la categoría/ Número de revistas en la categoría: 6/34

-Citas: 0

VII.2. APORTACIONES CIENTÍFICAS DERIVADAS DIRECTAMENTE DE LA TESIS DOCTORAL

COMUNICACIONES A CONGRESOS

-Título: **A sorption study of Cu(II), Pb(II) and Cd(II) by layered double hydroxide hybrids with humate anion**

-Autores: M.A. González, I. Pavlovic, C. Barriga

-Tipo participación: Póster

-Congreso: Fourth International Conference on on Multifunctional, Hybrid and Nanomaterials, Sitges, España, 2015

-Título: **Adsorción de metales pesados mediante el uso de hidrotalcitas de cloruro y humato**

-Autores: M.A. González, I. Pavlovic, C. Barriga

-Tipo de participación: Póster

-Congreso: V Encuentro sobre Nanociencia y Nanotecnología de Investigadores y Tecnólogos Andaluces, Córdoba, España, 2015

-Título: **Eliminación de Cu^{2+}, Pb^{2+} y Cd^{2+} mediante el híbrido Hidróxido Doble Laminar Humato**

-Autores: M.A. González, I. Pavlovic, C. Barriga

-Tipo participación: Póster

-Congreso: QUIES-2014, Almería, España, 2014

-Título: **Caprylate intercalated layered double hydroxide as adsorbent of pesticides from aqueous solution**

-Autores: M.A. González, F. Rodríguez-Rivas, I. Pavlovic, M.A. Ulibarri, C. Barriga

-Tipo de participación: Comunicación oral

-Congreso: Nanouco IV, Encuentro sobre Nanociencia y Nanotecnología de Investigadores Andaluces, Córdoba, España, 2013

CAPÍTULO VIII
Otras Aportaciones Científicas

Estas aportaciones científicas no forman parte de la memoria doctoral aquí presentada.

PUBLICACIONES

-Título: **"Pesticides adsorption–desorption on Mg–Al mixed oxides. Kinetic modeling, competing factors and recyclability"**

-Autores: R. Otero, J.M. Fernández, M.A. González, I. Pavlovic, M.A. Ulibarri

-Revista: Chemical Engineering Journal 221 (2013) 214–221

-Editorial: Elsevier

-Índice de impacto (año publicación, 2013): 4.058

-Categoría: Engineering, Chemical (Q1)

-Ranking en la categoría/ Número de revistas en la categoría: 8/133

-Citas: 6

-Título: **"Layered Double Hydroxides as suitable substrate to improve the efficiency of Zn anode in neutral pH Zn-ion batteries"**

-Autores: M.A. González, R. Trócoli, I. Pavlovic, C. Barriga, F. La Mantia

-Manuscrito en prensa

COMUNICACIÓN A CONGRESO

-Título: **Sorption of pesticides nicosulfuron and mecoprop-p by layered double hydroxides**

-Autores: R. Otero, M.A. González, M.A. Ulibarri, C. Barriga, I. Pavlovic, J.M. Fernández

-Tipo participación: Póster

-Congreso: HybridMaterials 2011, Estrasburgo, Francia

OTRAS PUBLICACIONES DE TIPO DIVULGATIVO

- Noticia en el gabinete de comunicación de la UCO

Titular: **La UCO explora un compuesto capaz de retener metales pesados para reducir la contaminación en ríos y suelos**

Publicado en UCO Ciencia el 29 de Junio de 2015 [1]

- Noticia en el Diario CÓRDOBA

Titular: **La UCO estudia la forma de reducir la contaminación**

Publicado el 8 de Julio de 2015 [2]

- Articulo en SaberUniversidad

Titular: **Un componente del antiácido Almax, utilizado como descontaminante**

Publicado en el periódico de las universidades públicas de Andalucia en Diciembre de 2015 [3]

Referencias

[1] http://www.uco.es/uconews/es/article/la-uco-explora-un-compuesto-capaz-de-retener-metales-pesados-para-reducir-l/

[2] http://www.diariocordoba.com/noticias/cordobalocal/uco-estudia-forma-reducir-contaminacion_974237.html

[3]http://www.saberuniversidad.es/article/INVESTIGACION/2166208/componente/antiacido/almax/utilizado/como/descontaminante.html

ANEXO 1
PUBLICACIONES

Applied Clay Science 80–81 (2013) 76–84

Contents lists available at ScienceDirect

Applied Clay Science

journal homepage: www.elsevier.com/locate/clay

Research paper

Caprylate intercalated layered double hydroxide as adsorbent of the linuron, 2,4-DB and metamitron pesticides from aqueous solution

I. Pavlovic *, M.A. González, F. Rodríguez-Rivas, M.A. Ulibarri, C. Barriga

Dpto. de Química Inorgánica e Ingeniería Química, Instituto Universitario de Química Fina y Nanoquímica (IUQFN), Universidad de Córdoba, Campus de Excelencia Internacional Agroalimentario, 14071 Córdoba, Spain

ARTICLE INFO

Article history:
Received 25 January 2013
Received in revised form 2 May 2013
Accepted 1 June 2013
Available online 9 July 2013

Keywords:
LDH
Caprylate
Pesticides
Adsorption
Kinetics

ABSTRACT

This study was carried out to elucidate the synthesis of organo-layer double hydroxide (LDH) and its capacity to adsorbs the widely applied pesticides linuron, 2,4-DB and metamitron from waters. The adsorbent (LDH-Cap) was synthesized by incorporating organic anion caprylate into magnesium aluminum layered double hydroxide with chloride as interlayer anion (LDH-Cl) via ion exchange. Characterization of the LDH-Cap adsorbent was carried out using powder X-ray diffraction (PXRD), infrared spectroscopy (FT-IR) and thermal analyses (TG and DTA). PXRD patterns indicate that caprylate anion was successfully intercalated in LDH according to the basal spacing $d_{003} = 19.2$ Å. Adsorption results indicated that these three pesticides were adsorbed on LDH-Cap. The high percentage of initial pesticide amounts removed within the first 30 min (~90% of the total amount adsorbed) for linuron and 2,4-DB revealed a rapid adsorption process, while it was more gradual for metamitron. PXRD results suggest that adsorbed 2,4-DB and metamitron were intercalated in the LDH interlayers probably between caprylate chains and the brucite layers. Linuron was probably adsorbed on the external particle surface of LDH. Adsorption kinetic study revealed that the adsorption process followed pseudo-second-order equation. Adsorption data were well fitted to the Freundlich isotherm. The desorption of the pesticides from adsorption products were tested with three different solvents (distilled water, ethanol and acetone) and it was partial in all cases.

1. Introduction

Contamination of natural waters is a current environmental problem and a lot of work has been done to find methods for its remediation and prevention. There is a great number and variety of water contaminants which reach the aqueous ecosystems in many ways. Therefore, different methods for their elimination from waters such as ionic exchange, adsorption, filtration, electrolysis, biodegradation, etc., exist (Bolto et al., 2002; Esplugas et al., 2002; LaPara et al., 2000; Tan et al., 2000; Zouboulis et al., 2002). The improvement of existing methods and development of new ones are a main objective for research. The adsorption on activated carbon is one of the most applied methods given its effectiveness and easy management, but due to its high cost there is a lot of interest in searching for alternatives.

Some adsorbents with good properties such as activated alumina (Kasprzyk-Hordern, 2004), zeolites (Misaelides, 2011), clays and clay minerals (Cornejo et al., 2008; Cruz-Guzmán et al., 2005) agricultural residues (Gámiz et al., 2012), etc., are suitable to substitute for activated carbon. One of the materials which have recently received considerable attention due to their good adsorptive properties is the layered double hydroxides (LDHs) or hydrotalcite-like compounds which are scarce in nature, however inexpensive and easy to synthesize (Crepaldi et al., 2000; Newman and Jones, 1998; Rives, 2001).

The structure of LDH materials is based on hydrotalcite structure which is related to that of brucite, $Mg(OH)_2$, in which layers some of the Mg^{2+}cations in the layer structure were replaced by Al^{3+}. Thus generated excess of positive charge is balanced by intercalating of carbonate anions between layers (Cavani et al., 1991). The general formula for LDH could contain a variety of combinations of divalent and trivalent metal cations and can be written as $[M^{II}_{1-x}M^{III}_{x}(OH)_2]X_{x/q}\cdot nH_2O$ where $[M^{II}_{1-x}M^{III}_{x}(OH)_2]^{x+}$ represents the layer, and the anions X^{q-} the interlayer together with H_2O molecules. LDHs have the ability to incorporate a variety of anions, and the intercalation chemistry and synthesis of LDHs have been the subjects of many previous studies (Braterman et al., 2004; Reichle, 1986). The adsorption properties of LDH in the case of anionic solutes (adsorbates) arise from their ability to interchange the interlayer anion with those present in the aqueous solution, as well as to reconstruct the LDH structure from their calcined product. Mixed oxides formed by calcining of LDH at 500 °C, when put in water, could recover again the LDH structure by incorporating anions present in aqueous solutions (Hermosín et al., 1996; Houri et al., 1998). In the case of non ionic adsorbate, the LDH adsorbent properties should be improved by modifying their interlayer through intercalating large organic anions (organo-LDHs) which could provide the media for the hydrophobic

* Corresponding author. Tel.: +34 957 218648; fax: +34 957 218621.
E-mail address: iq2pauli@uco.es (I. Pavlovic).

0169-1317/$ – see front matter © 2013 Elsevier B.V. All rights reserved.
http://dx.doi.org/10.1016/j.clay.2013.06.008

host–guest interactions (Bruna et al., 2006, 2008; Klumpp et al., 2004; Wang et al., 2005). LDHs can be also functionalized with the intercalation of ligands and the solids thus obtained showed uptake capacity for heavy metal cations such as Cu^{2+}, Cd^{2+}, and Pb^{2+} (Pavlovic et al., 2009; Perez et al., 2006).

On the other hand, the pesticides are compounds which could be considered emerging environmental contaminants. These chemicals are generally applied to agricultural soils in amounts which exceed those required to control plagues, weeds, etc., in order to compensate for the losses caused by leaching, run-off, degradation, etc., which is the reason why these compounds sometimes reach unacceptable levels in ground waters (Gerstl et al., 1998). The EC Drinking Water Directive (80/778/EC) stipulates the requirement that no single pesticide should exceed 0.1 mg/L and total pesticides should not exceed five-fold of this level in drinking water from the tap.

The aim of this work was to study the possibility of using the LDH intercalated with the organic anion caprylate, LDH-Cap, as a novel adsorbent for the removal of widely applied and toxic pesticides such as linuron, metamitron and 2,4-DB from aqueous solutions. To our knowledge there are no reported studies on caprylate-intercalated LDHs as adsorbents of water contaminants. We also tried to compare the adsorption capacity of LDH-Cap with other pesticide adsorbents, previously studied and reported by our research group, such as the uptake of linuron and metamitron by LDH intercalated by dodecyl sulfate or sebacate anions. The three pesticides studied here are actually widely used and they work by inhibiting photosynthesis in targeted weed plants in crops of cotton, potato, corn, bean, asparagus, carrot, and fruit (www.herts.ac.uk/aeru/projects/ppdb/). They have a toxic effect on human health and the environment (www.pesticideinfo.org).

The effect of various parameters such as the pH of the solution, the contact time and the initial pesticide concentrations on the adsorption capacity of LDH-Cap were studied as well as the kinetics of the adsorption processes. Furthermore, in order to explore the type of host–guest interactions involved in the adsorption mechanism, the elution of pesticides from LDH-Cap with different solvents was also studied.

2. Materials and methods

2.1. Pesticides and other chemicals

The sodium caprylate (sodium octanoate) used in the preparation of the adsorbent, as well as linuron ([3-(3,4-dichlorophenyl)-1-methoxy-1-methylurea], 2,4-DB ([4-(2,4-dichlorophenoxy) butyric acid]) and metamitron ([4-Amino-3-methyl-6-phenyl-1,2,4-triazin-5-one)] pesticides were supplied by Sigma-Aldrich (Spain). The molecular structure and some characteristics of the studied pesticides are shown in Fig. 1 and Table 1.

The concentration of the pesticides was measured using a Perkin-Elmer model Lambda 3B UV–visible spectrophotometer at λ_{max} corresponding to the maximum adsorption for each pesticide solution.

2.1.1. Synthesis of the adsorbents

The LDH with chloride as the interlayer anion $[Mg_3Al(OH)_8]Cl\cdot nH_2O$ (LDH-Cl),was prepared by the coprecipitation of 0.075 mol $MgCl_2\cdot 6H_2O$ and 0.025 mol of $AlCl_3\cdot H_2O$, in 250 mL of the 0.025 mol of NaCl solution, under N_2 stream and using CO_2 free water. The pH was maintained at 8 using a 0.1 M NaOH solution. The suspension was hydrothermally treated at 80 °C for 24 h and then washed with distilled water and dried at 60 °C.

The adsorbent $[Mg_3Al(OH)_8]C_8H_{15}O_2$ (LDH-Cap) was obtained by the anion exchange method by suspending 1 g of previously obtained LDH-Cl in 500 mL of the 0.014 M sodium caprylate solution under N_2 stream at 75 °C and pH 8. The suspension was settled for 24 h and then washed, centrifuged and the precipitate was dried at 60 °C.

2.1.2. Adsorption–desorption experiments

The adsorption experiments were carried out by adding duplicate samples of 0.03 g of adsorbent LDH-Cap in 30 mL of aqueous solution of the pesticide. The initial concentration used in the pH and kinetic experiments were those of maximum solubility for linuron and 2,4-DB, $C_o = 0.19$ mM and $C_o = 0.12$ mM, respectively, and $C_o =$ 1 mM for metamitron. The adsorption of pesticides on HT-Cap was measured by a batch equilibration technique and the proper solid/solution amounts were put into polypropylene centrifuge tubes. The suspensions were shaken at room temperature at 52 rpm (24 h in the pH study and a range between 0.5 and 24 h in the kinetic study). The concentration range used in adsorption isotherm studies depended on the solubility (Table 1) of the pesticides whereas the contact times were determined by kinetic experiments (2 h for linuron and 2,4-DB and 5 h for metamitron).

The amount of pesticides adsorbed on LDH-Cap was calculated from the difference between the initial and equilibrium solution concentrations. The supernatants were filtered and used to determine the amount of remaining pesticides in the solutions after adsorption on LDH by UV–Vis spectrophotometry at 245, 228 and 305 nm for linuron, 2,4-DB and metamitron, respectively. A five-point calibration curve (a concentration range where the absorbance/concentration

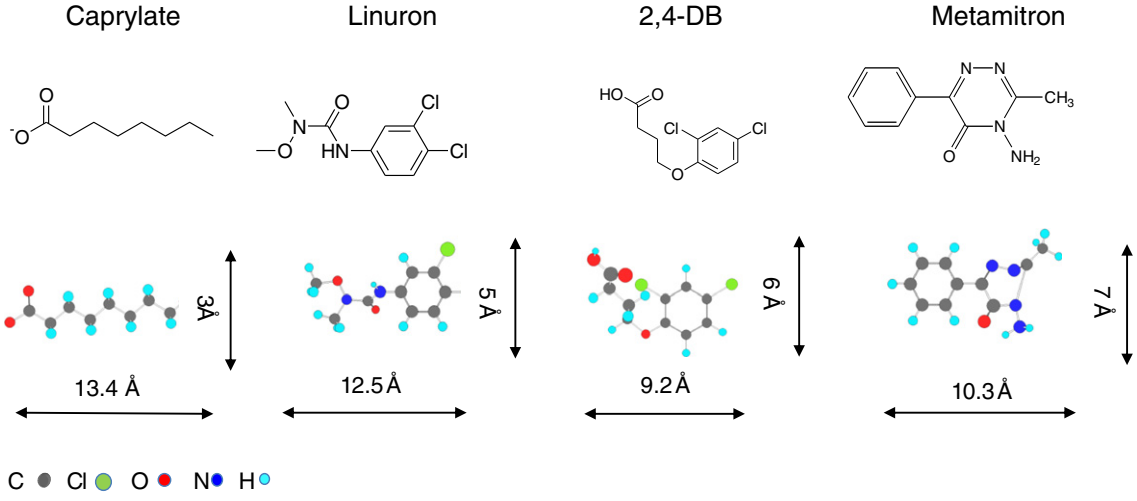

Fig. 1. Schematic representation of molecular structure of caprylate anion and pesticides.

Table 1
Characteristics of the pesticides studied.

Pesticide	Solubility[a](mg/L)	pKa	Concentration[b](mM)
Linuron	81	12.1	0.042–0.19
2,4-DB	46	4.1	0.05–0.12
Metamitron	1800	2.9	0.10–3.00

[a] Solubility in water.
[b] Pesticide concentrations used in adsorption experiments.

curve was lineal) was run before each analysis. The samples were diluted for its fitting to calibration curves, and measured. The blanks were also registered (only the adsorbent in distilled water under the same experimental conditions as the sample studied was used) but no interferences were found.

The suspensions were shaken at 52 rpm at room temperature and after suitable time were centrifuged. The resulting supernatants were filtered and used to determine the amount of pesticides adsorbed by the LDH, using UV–Vis spectroscopy. The amounts of pesticides adsorbed per gram of adsorbent, q (mmol g^{-1}), were calculated as follows:

$$q = (C_o - C_e)V/W \quad (1)$$

where C_o and C_e are the initial and equilibrium solution concentrations (mmol L^{-1}), W is the weight of solids (g) and V is the pesticide solution volume (L).

The experimental adsorption data were fitted to the Langmuir and Freundlich models, often used to describe adsorption processes and in which lineal forms are represented in Eqs. (2) and (3):

$$C_e/q = (1/q_m)C_e + 1/(q_m K_L) \quad (2)$$

where q_m is the maximum adsorption capacity at the monolayer coverage (mmol/g) and K_L (L/mmol) is a constant related to the adsorption energy.

$$\log\ q = \log K_f + N_f \log C_e \quad (3)$$

where K_f ($mmol^{1-Nf}\ L^{Nf}\ g^{-1}$) and N_f are Freundlich parameters, which are characteristic of the adsorbent-sorbate systems (Travis and Etnier, 1981).

In order to evaluate the possibility of regeneration of the adsorbent as well as to assess the adsorption mechanism, desorption experiments were also performed, as follows. The adsorption products LDH-Cap–pesticide (last isotherm points) were dried and 0.05 g of duplicate samples were treated with 7 mL of different solvents and shaken for 10 min. Water, ethanol or acetone was the solvent used in order to determine the best desorption conditions. Then, the supernatants were centrifuged for the pesticide quantification by UV–Vis spectrophotometry (ethanol and acetone were evaporated and the solid remains dissolved in water).

2.2. Characterization techniques

The adsorbent and the adsorption products were studied by different physical chemical techniques. Powder X-ray diffraction patterns were recorded at room temperature under air conditions using a Siemens D-5000 instrument with CuKα radiation (λ = 1.54050 Å), the step size and step counting time used were 0.02° (2θ) and 0.65 s respectively. FT-IR spectra were recorded with a Perkin Elmer Spectrum One spectrophotometer using KBr disk method. TG and DTA curves were recorded on a Setaram Setsys Evolution 16/18 apparatus, in air at the heating rate of 5 °C/min.

3. Results and discussion

3.1. Characterization of adsorbent precursor and adsorbent

The PXRD pattern of LDH-Cl confirmed the presence of chloride as an interlayer anion by the basal spacing d_{003} = 7.8 Å and its corresponding harmonics. Taking into account that this basal spacing is very similar to that of the carbonate anion, the presence of carbonate impurities in the interlayer is also possible. The PXRD pattern of LDH-Cap (Fig. 2a), with the basal spacing d_{003} = 19.2 Å, is very similar to that already reported for caprylate-intercalated into Mg–Al–LDH (Iyi and Sasaki, 2008). Taking into account 4.8 Å as the

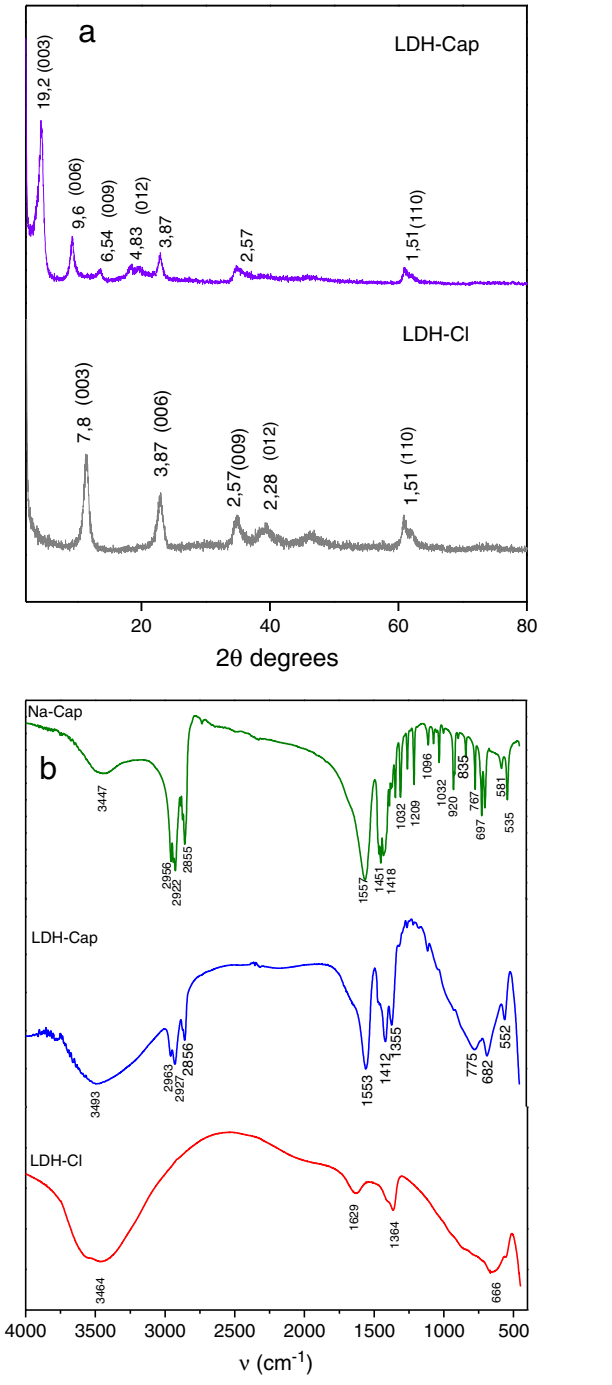

Fig. 2. PXRD patterns of a) LDH-Cl precursor and LDH-Cap adsorbent and b) FT-IR spectra of LDH-Cl precursor, LDH-Cap adsorbent and sodium caprylate (Na-Cap).

hydrotalcite-layer thickness, the gallery height is 14.4 Å. Since the caprylate length is approximately 13.4 Å (CS Chem 3D 5.0 Program), this anion is probably oriented in a vertical position together with the water molecules in the interlayers.

The FT-IR spectra (Fig. 2b) show the characteristic features of the hydrotalcite structure which are a broad band at around 3500 cm^{-1}, corresponding to the stretching vibration of OH^- groups of hydration water molecules and free OH^- groups of the brucite layers, and a band at 1629 cm^{-1}, corresponding to the bending vibration of water molecules. The band at 1364 cm^{-1} is attributed to the stretching vibration of carbonate anion which could also be present in the interlayer together with the chloride, due to the CO_2 contamination, difficult to avoid during the synthesis in spite of inert atmosphere maintained (Bellamy, 1978; Rives, 2001). The most characteristic bands of caprylate in the LDH-Cap adsorbent are the bands at 1553 cm^{-1}, 1412 $cm^{-1}$and 1355 cm^{-1} due to carbonyl absorptions from carboxylate groups of caprylate, and the bands at 2963, 2927 and 2856 cm^{-1} which correspond to C–H stretching vibrations of the aliphatic chains.

The results of the thermal study of LDH-Cl and LDH-Cap samples are shown in Fig. 3. The DTA curve of the LDH-Cl precursor showed two endothermic effects, characteristic for hydrotalcite-like compounds, at 126 and 409 °C as well as their corresponding weight losses. The first one is attributed to the loss of the physisorbed and interlayer water, and the second endothermic effect corresponds to a simultaneous loss of interlayer chloride, interlayer carbonate and the dehydroxylation of layers. In the DTA curve corresponding to LDH-Cap, the first endothermic peak related to physisorbed and interlayer water loss is not easy to quantify, because it is overlapped by a very high exothermic peak proceeding from the combustion of interlayer organic anion caprylate at 316 °C.

3.2. Adsorption and desorption experiments

3.2.1. pH influence and the contact time effect on pesticide adsorption

The pH experiments indicated that the variation of the initial pH of the solutions did not have influence on the amount of the pesticides removed by LDH-Cap (data not shown) and the final pHs were 7 ± 0.5for initial pH = 7 and 6 ± 0.5 for initial pH = 5, due to the buffering property of hydrotalcite-like compounds. Therefore, the further adsorption experiments were carried out under the pH of initial pesticide solutions which were all in the pH range between 6 and 7. These pH values are interesting because they are common for most of the natural waters.

The effect of contact time on the adsorption efficiency of LDH-Cap for the pesticides was also studied (Fig. 4). The results show that the

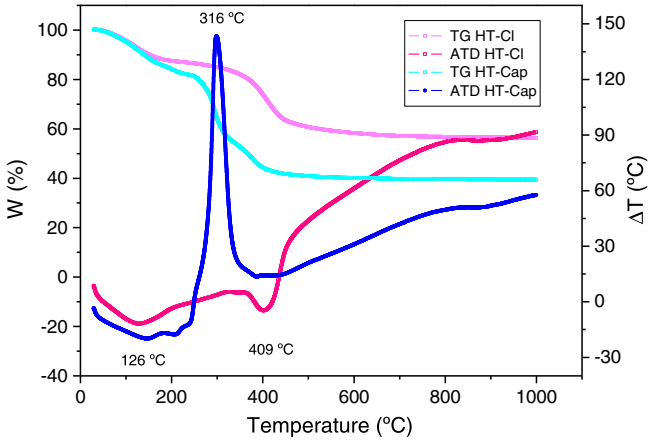

Fig. 3. TG and DTA curves of HT-Cl and LDH-Cap.

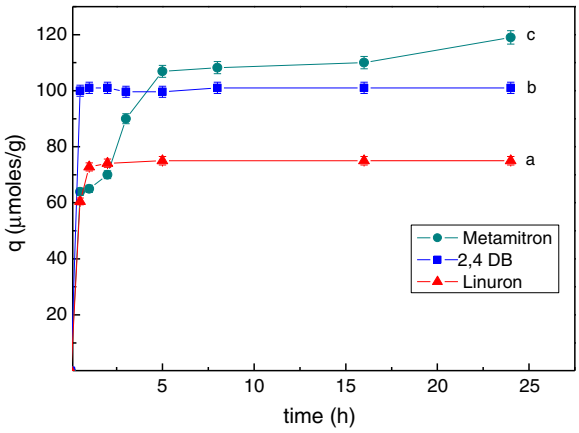

Fig. 4. Time evolution of the pesticide adsorption on LDH-Cap: a) linuron b) 2,4-DB and c) metamitron.

adsorption of linuron and 2,4-DB was almost instantaneous while the adsorption of metamitron was more gradual. Although the main part of this pesticide (~90% of the total amount removed) was removed in 5 h, at 24 h the adsorption equilibrium had not been reached yet. This could be explained if we suppose that the diffusion is a limitation step in the adsorption of metamitron on LDH-Cap. It seems there should be enough time for bulky metamitron molecules to diffuse through the laminar layer and into pores to reach maximum adsorption, and 24 h is not enough to reach its full adsorption capacity as can be seen in Fig. 4.

3.2.2. Kinetic modeling

The adsorption kinetic is an important aspect of the pollutant removal process control. The data in Fig. 4 were fitted using the two most widely used models in the literature to describe the adsorption process (i.e. pseudo-first-order Eq. (4), pseudo-second-order Eq. (5)) which can be expressed as follows:

$$\log(q_e - q_t) = \log\ q_e - (k_1/2.303)t \quad (4)$$

$$t/q_t = 1/\left(k_2 q_e^{\ 2}\right) + (1/q_e)t \quad (5)$$

where q_e and q_t are the amounts of adsorbed pesticide at equilibrium and t time (mg g^{-1}), respectively, and k_1 (min^{-1}) is the pseudo-first-order rate constant and k_2 (g (mg min)$^{-1}$) the pseudo-second-order rate constant.

The parameters of the kinetic models and the linear regression coefficients (R^2) were obtained and shown in Table 2. The kinetic data were fitted better to Eq. (5) for the three pesticides based on the correlation coefficient R^2 and the q_e values calculated from the pseudo-second-order rate model which are very consistent with the experimental q_e values (included in Table 2). This indicates that the experimental kinetic data for adsorption by LDH-Cap adsorbent work well with this model for the entire range time. These results suggested that the pseudo-second order adsorption mechanism was predominant, and that the overall rate of the pesticide adsorption process appeared to be controlled by a chemisorption process as was indicated by Ho (2006). The pseudo-second-order rate expression has been widely applied to the adsorption of pollutants from aqueous solutions (pesticides, dyes, metal ions, oils, and organic substances). In many cases the value of q_e is impossible to know from the experimental data because the adsorption process tends to become immeasurably slow and the amount adsorbed significantly smaller than the equilibrium amount. This model enables us to know the q_e equilibrium amount by simply using a lineal fitting of

Table 2
Coefficients of pseudo-first-order, pseudo-second-order and intra-particle diffusion model for adsorption of linuron, 2,4DB and metamitron by LDH-Cap.

Sample	Pseudo-first-order model				Pseudo-second order model			Intra-particle diffusion model		
	$q_{e\ Exp}$ (mg/g)	k_1 min^{-1}	q_e (mg/g)	R^2	k_2 (g/mg min)	q_e (mg/g)	R^2	k_p (mg/g $min^{0.5}$)	C	R^2
Linuron	18.7 ± 0.3	0.003 ± 0.001	0.48 ± 0.14	0.545	0.0191 ± 0.0003	18.59 ± 0.001	0.999	0.06 ± 0.08	17 ± 1	0.329
2,4-DB	25.2 ± 0.5	0.194 ± 0.001	0.35 ± 0.03	0.710	0.243 ± 0.002	25.125 ± 0.006	1	0.063 ± 0.003	24.990 ± 0.008	0.331
Metamitron	22.3 ± 0.4	0.006 ± 0.001	10.2 ± 0.3	0.934	0.0009 ± 0.0005	23.25 ± 0.006	0.997	0.43 ± 0.09	11 ± 3	0.802

the experimental data (Ho, 2006). On the other hand, intra-particle diffusion model is commonly used for identifying the adsorption mechanism for design purposes. According to Weber and Morris (1963), for most adsorption processes, the uptake varies almost proportionally with $t^{1/2}$ rather than with the contact time and can be represented as follows:

$$q_t = k_p t^{1/2} + C \quad (6)$$

where k_p (mg g^{-1} $min^{-0.5}$) is the rate constant of intra-particle diffusion.

According to Eq. (6), the plot of q_t versus $t^{1/2}$ should be a straight line with a slope k_p which is the intra-particle diffusion rate constant (mg g^{-1} $min^{-0.5}$) and intercept at C, when the adsorption mechanism follows the intra-particle diffusion process. The value of C gives an idea about the thickness of boundary layer i.e. the larger the intercept the greater is the boundary layer effect (Mall et al., 2006). The straight line deviation from the origin may be because of the difference in the rate of mass transfer in the initial and final stages of adsorption. In some cases the plot q_t versus square root time can show multilinearity which indicates that several steps occur in the process (Dawood and Sen, 2012; Dotto and Pinto, 2011; Mall et al., 2006). Each section of the curves represents the different stages in the adsorption process: the first part is due to surface adsorption and external diffusion (boundary layer diffusion). The second part is the gradual adsorption step where the intra-particle diffusion is rate

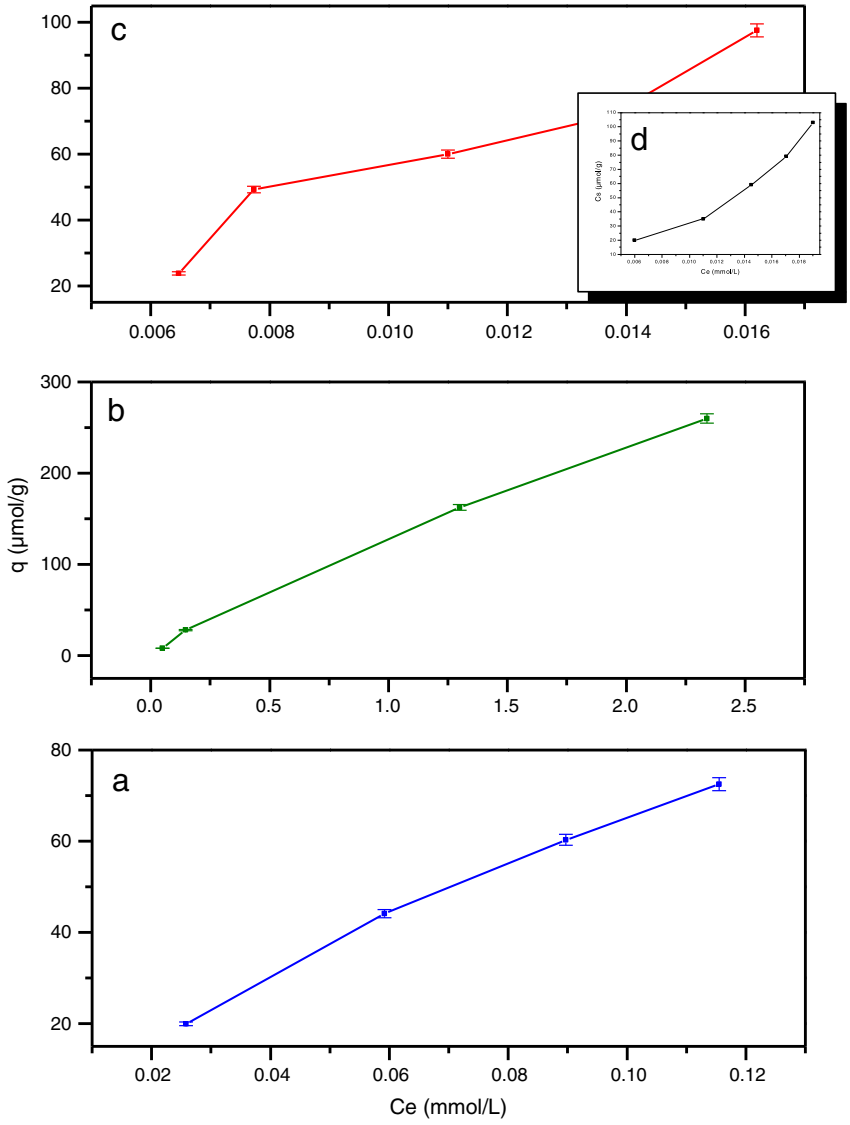

Fig. 5. Intra-particle diffusion model of pesticides adsorption on LDH-Cap.

controlled. The plateau (third part) is the final equilibrium step where the intra-particle diffusion starts to slow down due to the low solute concentration in the solution. In addition, if the regression passes through the origin, the intra-particle diffusion is the only rate-limiting step. The correlation coefficients for the intra-particle diffusion model included in Table 2 show that the adsorption plot is not linear over the whole time range for the three studied pesticides. However, the plot of Eq. (6) for metamitron adsorption, included in Fig. 5, shows three sections. In this case, the bulky molecule of metamitron has an important effect into the control of the rate at the initial time and the limiting step is the boundary layer diffusion or film diffusion. However, the 2,4-DB and linuron plots (Fig. 5) show two different stages: external mass transfer followed by intra-particle diffusion. The pesticide molecules seem to be transported to the external surface of the LDH-Cap through film diffusion and the k_{p1} (the rate constant corresponding to first section included in Fig. 5 as the slope of the line) was higher for linuron than for 2,4-DB where the value of C was lower and then the plateau was reached. This could be due to the different structures of the pesticides and their affinity for the adsorbent which are important to determine the mechanism of the adsorption. Moreover, from Fig. 5 it can be deduced that none of the plots show linear straight line sections that pass through the origin. This indicates that the intra-particle diffusion is involved in the adsorption process but it is not the only rate-limiting step. It can be concluded that the adsorptions of these pesticides on the LDH-Cap were multi-step processes, involving adsorption on the external surface, intra-particle diffusion and chemical interaction (adsorption of the pesticide at the active sites via hydrophobic and/or hydrophilic interaction).

3.2.3. Adsorption equilibrium isotherms

The adsorption isotherms of the three pesticides are given in Fig. 6. According to the classification of Giles et al., 1960, the shape of all adsorption isotherms was C-type. This type of isotherm indicates that there is a minimum or no competition of adsorbate molecules with other anions from the water solution for the adsorbent sites, i.e. there is a constant partition of adsorbate between the adsorbent and the solution.

The maximum amount of pesticide removed from the solution per gram of adsorbent was in the case of metamitron ($q = 260$ μmol/g vs. $q = 72$ μmol/g for linuron and $q = 102$ μmol/g for 2,4-DB), probably due to the higher initial concentrations used in the case of metamitron which was enabled by its higher solubility (Table 2).

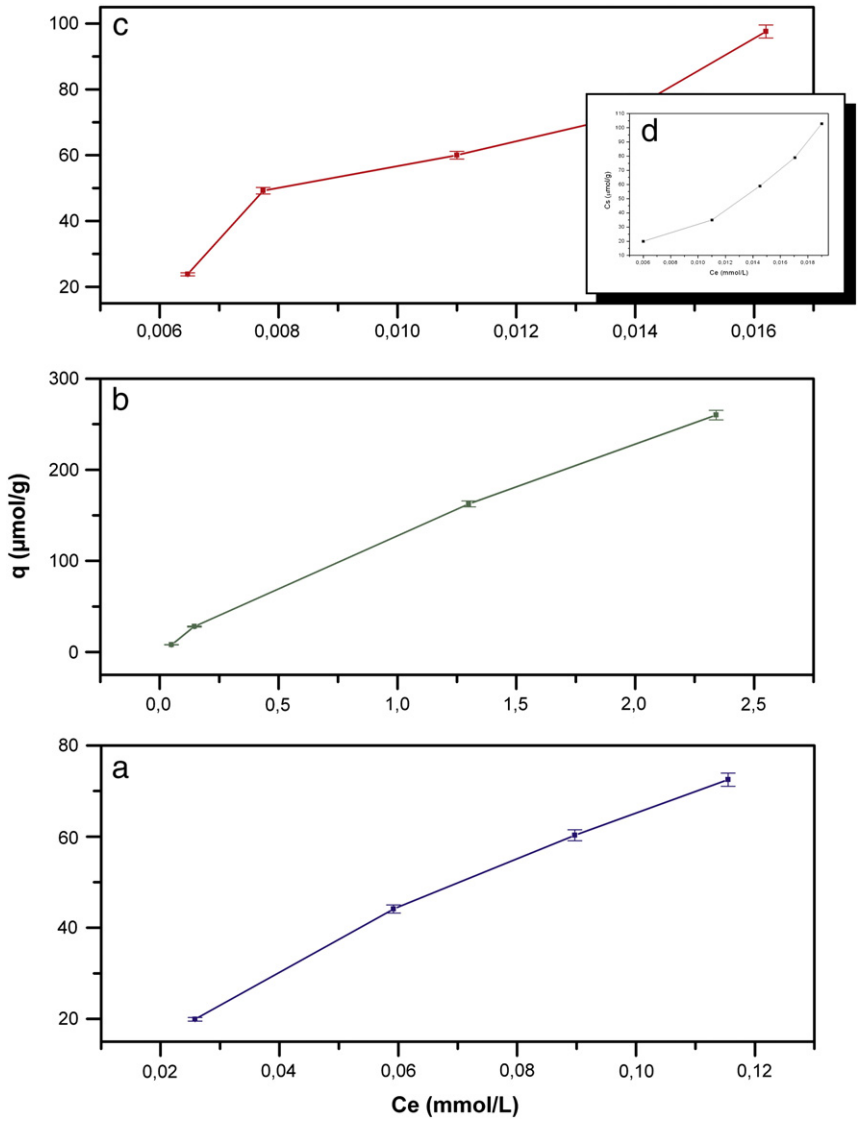

Fig. 6. Adsorption isotherms of a) linuron, b) metamitron, c) 2,4-DB on LDH-Cap and d) 2,4-DB on LDH-Cl.

Notwithstanding, even in this case the isotherm "plateau" was not reached which indicates that under these conditions the maximum adsorption capacity of LDH-Cap was not saturated. However, the amounts of metamitron adsorbed here were higher than those reported for this pesticide on LDH intercalated with dodecyl sulfate, LDH–DDS, (100–170 μmol/g) for the same initial concentrations and under similar experimental conditions (Bruna et al., 2006). In the last case, the adsorption isotherm shape was different from that in the present study and indicated two different types of interactions between the adsorbent and the adsorbate (Giles et al., 1960). The authors suggested that the $-NH_2$ groups of metamitron could be involved in the hydrogen bonding with SO_4^{2-} groups of dodecyl sulfate (DDS), besides the hydrophobic adsorption of the pesticide on the alkyl chains of DDS. On the other hand, the amount of linuron adsorbed here, was similar to that reported for its adsorption on LDH intercalated by sebacate (LDH-SEB) q = 110 μmol/g, but it was lower than that of linuron adsorbed by LDH–DDS (q = 170 μmol/g) under similar experimental conditions (Chaara et al., 2012). Therefore, a different interlayer composition (functional groups and aliphatic tales) and/or the height of the interlayer gallery seems to have some influence in the interaction of metamitron and the hydrophobic part of interlayer anion.

In order to compare the adsorption behavior of the three pesticides studied here, the adsorption experiments were also performed on the inorganic layered double hydroxide, LDH-Cl, under the same experimental conditions. The adsorption of linuron and metamitron on LDH-Cl was negligible (under 5% of the initial concentration) while the adsorption of the 2,4-DB was close to that measured for LDH-Cap (q = 102 μmol/g). The anionic character of this pesticide probably provides more affinity between adsorbent and the adsorbate. Similar adsorption results were reported for the adsorption of herbicide 2,4-dichlorophenoxyacetate (2,4-D) (with similar structure to 2,4-DB) on LDH-Cl (Pavlovic et al., 2005). This suggests that the 2,4-DB pesticide could be adsorbed on organic and inorganic LDH: on the first one by hydrophobic interactions through aromatic ring and on the second by ion–ion interactions between its carboxylic group and the positively charged layers.

The adsorption isotherm data were fitted to the Langmuir and Freundlich equations, but were mostly in agreement with the Freundlich equation where the regression coefficient (R^2) was in the range of 0.880–0.994 while that of Langmuir was ~0.4 (not shown). For the Langmuir model there is an important assumption that the adsorbate is adsorbed in monolayer, all surface sites are energetically equivalent and that the surface is homogeneous. The Freundlich isotherm can also be used to model the adsorption processes on heterogeneous surfaces. In this model, due to its exponential character it is not possible to represent the maximum adsorption on surfaces. The agreement of the adsorption data with the Freundlich equation suggests the existence of heterogeneity of sites and different adsorption energies on the surface and this could be in accordance with the type of adsorbent here used which consists of different components (inorganic and organic) (Bruna et al., 2006; Dawood and Sen, 2012; Lazaridis and Asouhidou, 2003; Travis and Etnier, 1981). The Freundlich parameters are included in Table 3.

3.2.4. Desorption processes

Fig. 7 indicates that only a partial desorption of the studied pesticides occurs with three different solvents. Linuron desorption was quite low with the three solvents used, slightly higher with acetone

Table 3
Freundlich model parameters for pesticide adsorption on HT-Cap.

Sample	$K_f(\mu mol^{1-Nf}\ g\ L^{Nf})$	N_f	R^2
Linuron	1.22 ± 0.08	0.87 ± 0.04	0.994
2,4-DB	2.6 ± 0.9	1.29 ± 0,30	0.880
Metamitron	0.29 ± 0.03	0.88 ± 0.06	0.992

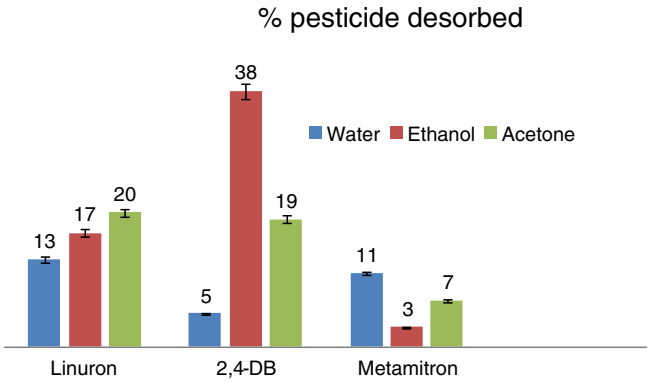

Fig. 7. Desorption percentage of the pesticides with different solvents.

in agreement with its low polarity. The lowest percentages of metamitron desorbed are in agreement with its high affinity for LDH-Cap together with the higher amounts of this pesticide adsorbed in LDH-Cap–pesticide complex compared to the two other pesticides (see adsorption values of the last isotherm points, Fig. 6). As it will be seen below the metamitron is well intercalated in the interlayer LDH-Cap space which makes it less accessible to the solvent under experimental conditions studied here. Higher percentages of 2,4-DB eluted by ethanol are probably related to the higher solvate–solvent affinity due to their similar polarities. The structure of 2,4-DB with two different entities could enable the adsorption of this pesticide on LDH-Cap by involving two different types of host–guest interactions: electrostatic interactions between the carboxylate groups of pesticide with the positive charge of the external particles surface and the hydrophobic ones between the aromatic ring of 2,4-DB and alkylic chains of caprylate, as will be confirmed below in the PXRD study.

3.3. Characterization of the adsorption products

When the PXRD pattern of LDH-Cap was compared to that of the adsorption products LDH-Cap–pesticide (Fig. 8), the appearance of a new peak d_{003} ~ 30 Å was observed in 2,4-DB and metamitron. Taking into account the layer thickness and the pesticides and caprylate lengths (Fig. 1), it could be concluded that these two pesticides are intercalated into the interlayer LDH space after adsorption. A decrease of the intensities of (00 l) reflections in the patterns of the adsorption products LDH-Cap–pesticide has been observed. The incorporation of the pesticide molecules into the interlayer space could account for the decrease of the crystallinity in the adsorption products, due to the interlayer disorder caused by the presence of a new species. A shift to lower angles of the first basal reflection was also observed, giving a spacing that is greater than the original values (from 19.2 to 21.0 Å in Fig. 8). These effects are typical for layered structures which contain stacking fault interstratification effects or other imperfections (Drits and Bookin, 2001). Some of these structural imperfections could be caused here by the adsorption process and the handling during the experiments (interaction with the pesticide, stirring of the suspension, LDH weathering…). In the LDH-Cap–2,4-DB pattern, the presence of two phases could be observed despite their low crystallinity. Thus, there is a phase, with a basal spacing of d_{003} ~ 30 Å and its corresponding higher order reflections, in addition to a phase with a basal reflection of d_{003} ~ 21 Å, which suggests the co-existence of the LDH-Cap–2,4 DB complex phase and the adsorbent LDH-Cap phase. The difference between this pattern (Fig. 8c) and LDH-Cap–metamitron (Fig. 8d), is that there is only one adsorbent–pesticide complex phase observed in the latter (d_{003} ~ 30 Å), which is probably due to the higher amount of metamitron adsorbed (q = 260 μmol/g) compared to that of 2,4-DB (q = 102 μmol/g). An

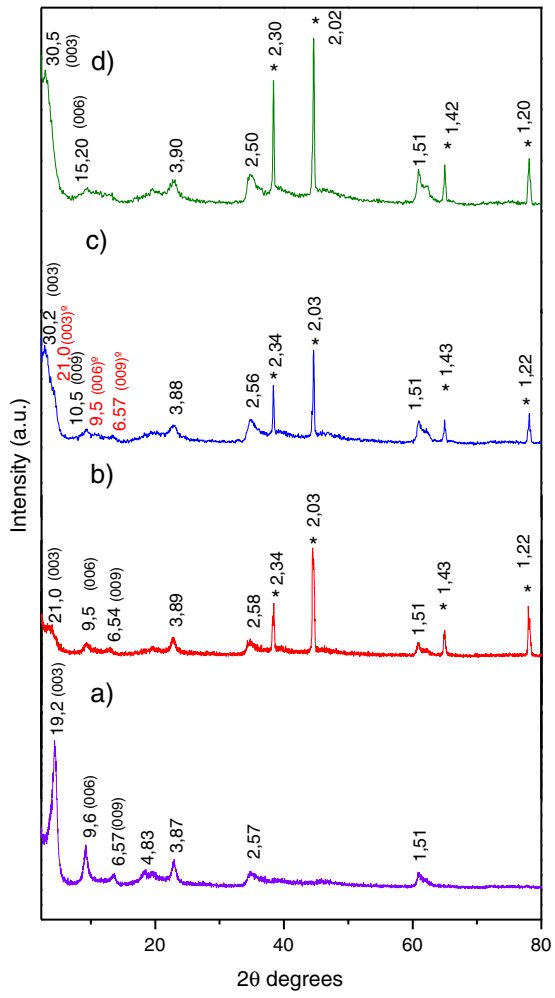

Fig. 8. PXRD patterns of the adsorbent and the adsorbent-pesticide complexes corresponding to the last isotherm point (°LDH-Cap phase, *Al sample holder): a) LDH-Cap, b) LDH-Cap–linuron, c) LDH-Cap-2,4-DB and d) LDH-Cap-metamitron.

important increase of the interlayer space found in the aforementioned metamitron adsorption, however, was not observed in its adsorption on LDH–DDS (Bruna el al., 2006), which is in accordance with higher amounts removed by LDH-Cap. The basal spacing of LDH-Cap–linuron PXRD (Fig. 8b) does not change significantly compared to the pure adsorbent pattern which suggests that this pesticide is probably adsorbed on the external surface of LDH particles. This was also observed in the adsorption of linuron on LDH intercalated with dodecyl sulfate and sebacate (Chaara et al., 2012).

4. Conclusions

The fast adsorption of pesticides studied here and the shapes of their adsorption isotherms on LDH-Cap suggest a great adsorbent/adsorbate affinity.

Comparative study of the adsorption of these pesticides on inorganic LDH-Cl suggests that the organophilic LDH modification improves the uptake of linuron and metamitron, whereas the adsorption of 2,4-DB was almost the same, probably due to the presence of carboxylate group together with the organic entity. Metamitron and linuron uptake by LDH-Cap was also compared to their uptake reported in our previous papers for LDHs with similar organic interlayer anions dodecyl sulfate (DDS) and sebacate (SEB) under similar experimental conditions.

There was no clear relationship observed between pesticide amounts adsorbed and the nature of organic interlayer anions. However, isotherm shapes and d_{003} reflections suggest that a different combination of hydrophobic–electrostatic interactions probably determines the amounts of these pesticides on different organically-tuned LDHs. PXRD results suggest that adsorbed 2,4-DB and metamitron were intercalated in the LDH interlayers while linuron was probably adsorbed on the external particle surface of LDH. The desorption experiments were performed with different solvents but pesticides were desorbed only partially.

Consequently, LDH-Cap could be a suitable water decontaminant with these pesticides, judging by the high percentage of the initial pesticide concentrations removed by it. Notwithstanding, more exhaustive investigations should be carried out in order to study adsorbent behavior in natural conditions, recycling optimization, etc.

Acknowledgments

This work was partially funded by the MCI (CTM 2011-25325) and the Junta de Andalucía through Research Group FQM-214. Fredy González acknowledges a grant from the Fundación Carolina to research at the University of Córdoba (Spain).

References

Bellamy, L.J., 1978. The Infrared Spectra of Complex Molecules. Chapman and Hall, London.
Bolto, B., Dixon, D., Eldridge, R., King, S., Linge, K., 2002. Removal of natural organic matter by ion exchange. Water Research 36, 5057–5065.
Bratermann, P.S., Xu, Z.P., Yarberry, F., 2004. Layered double hydroxides (LDHs). In: Auerbach, S.M., Carrado, K.A., Dutta, P.K. (Eds.), Handbook of Layered Materials. Marcel Decker, Inc., New York, pp. 373–474.
Bruna, F., Pavlovic, I., Barriga, C., Cornejo, J., Ulibarri, M.A., 2006. Adsorption of pesticides carbetamide and metamitron on organohydrotalcite. Applied Clay Science 33, 116–124.
Bruna, F., Pavlovic, I., Celis, R., Barriga, C., Cornejo, J., Ulibarri, M.A., 2008. Organohydrotalcites as novel supports for the slow release of the herbicide terbuthylazine. Applied Clay Science 42, 194–200.
Cavani, F., Trifiro, F., Vaccari, A., 1991. Hydrotalcite-type anionic clay: preparation, properties and application. Catalysis Today 11, 173–301.
Chaara, D., Bruna, F., Draoui, K., Ulibarri, M.A., Barriga, C., Pavlovic, I., 2012. Study of key parameters affecting sorption of the herbicide linuron by organohydrotalcites. Applied Clay Science 58, 34–38.
Cornejo, J., Celis, R., Pavlovic, I., Ulibarri, M.A., 2008. Interactions of pesticides with clays and layered double hydroxides: a review. Clay Minerals 43, 155–176.
Crepaldi, E.L., Pavan, P.C., Valim, J.B., 2000. Anion exchange in layered double hydroxides by surfactant salt formation. Journal of Materials Chemistry 10, 1337–1343.
Cruz-Guzmán, M., Celis, R., Hermosín, M.C., Koskinen, W., Cornejo, J., 2005. Adsorption of pesticides from water by functionalized organobentonites. Journal of Agricultural and Food Chemistry 53, 7502–7511.
Dawood, S., Sen, I.K., 2012. Removal of anionic dye Congo from aqueous solution by raw pine and acid-treated pine cone powder as adsorbents: equilibrium, thermodynamic, kinetic, mechanism and process design. Water Research 461, 1933–1946.
Dotto, G.L., Pinto, L.A.A., 2011. Adsorption of food dyes acid blue 9 and food yellow 3 onto chitosan: stirring rate effect in kinetics and mechanism. Journal of Hazardous Materials 87, 164–170.
Drits, V.A., Bookin, A.S., 2001. Layered double hydroxides: present and future. (Chapter 2) In: Rives, V. (Ed.), Nova Science Publishers, N.Y.
Esplugas, S., Gimenez, J., Contreras, S., Pascual, E., Rodriguez, M., 2002. Comparison of different advanced oxidation processes for phenol degradation. Water Research 36, 1034–1042.
Gámiz, B., Celis, R., Cox, L., Hermosín, M.C., Cornejo, J., 2012. Effect of olive-mill waste addition to soil on sorption, persistence and mobility of herbicides used in Mediterranean olive groves. Science of the Total Environment 429, 292–299.
Gerstl, Z., Nasser, A., Mingelgrin, U., 1998. Controlled release of pesticides into soils from clay–polymer formulations. Journal of Agricultural and Food Chemistry 46, 3797–3809.
Giles, C.H., MacEwan, T.H., Nakhwa, S.N., 1960. Studies in adsorption. Part XI. A system of classification of solution adsorption isotherms and its use in diagnosis of adsorption mechanisms and in measurement specific surface of solids. Journal of the Chemical Society 3973–3993.
Hermosín, M.C., Pavlovic, I., Ulibarri, M.A., Cornejo, J., 1996. Hydrotalcite as sorbent for trinitrophenol: sorption capacity and mechanism. Water Research 30, 171–177.
Ho, Y.S., 2006. Review of second-order models for adsorption system. Journal of Hazardous Materials 136, 681–689.
Houri, B., Legrouri, A., Barroug, A., Forano, C., Besse, J.P., 1998. Use of the ion-exchange properties of layered double hydroxides for water purification. Collection of Czechoslovak Chemical Communications 63, 732–740.
Iyi, N., Sasaki, T., 2008. Deintercalation of carbonate ions and anion exchange of an Al-rich MgAl–LDH (layered double hydroxide). Applied Clay Science 42, 246–251.
Kasprzyk-Hordern, B., 2004. Chemistry of alumina reactions in aqueous solution and its application in water treatment. Advances in Colloid and Interface Science 110, 19–48.

Klumpp, E., Contreras-Ortega, C., Klahre, P., Tino, F.J., Yapar, S., Portillo, C., Stegen, S., Queirolo, F., Schwuger, M.J., 2004. Sorption of 2,4-dichlorophenol on modified hydrotalcites. Colloid Surface 230, 111–116.

LaPara, T.M., Konopka, A., Nakatsu, C.H., Alleman, J.E., 2000. Thermophilic aerobic waste water treatment in continuous-flow bioreactors. Journal of Environmental Engineering 126, 739–744.

Lazaridis, N.K., Asouhidou, D.D., 2003. Kinetics of sorptive removal of chromium (VI) from aqueous solutions by calcined Mg–Al–CO_3 hydrotalcite. Water Research 37, 2875–2882.

Mall, J.I., Srivastava, V.C., Agarwall, R., 2006. Removal of Orange-G and methyl violet dyes study by adsorption onto bagasse fly ash-kinetic study and equilibrium isotherm analyses. Dyes and Pigments 69, 210–223.

Misaelides, P., 2011. Application of natural zeolites in environmental remediation. (A short review) Microporous and Mesoporous Materials 144, 15–18.

Newman, S.P., Jones, W., 1998. Synthesis, characterization and applications of layered double hydroxides containing organic guests. New Journal of Chemistry 22, 105–115.

Pavlovic, I., Barriga, C., Hermosín, M.C., Cornejo, J., Ulibarri, M.A., 2005. Adsorption of acidic pesticides 2,4-D, clopyralid and picloram on calcined hydrotalcite. Applied Clay Science 30, 125–133.

Pavlovic, I., Pérez, M.R., Barriga, C., Ulibarri, M.A., 2009. Adsorption of Cu^{2+}, Cd^{2+} and Pb^{2+} ions by layered double hydroxides intercalated with the chelating agents diethylenetriaminepentaacetate and meso-2,3-dimercaptosuccinate. Applied Clay Science 43, 125–129.

Pérez, M.R., Pavlovic, I., Barriga, C., Cornejo, J., Hermosín, M.C., Ulibarri, M.A., 2006. Uptake of Cu^{2+}, Cd^{2+} and Pb^{2+} on Zn–Al layered double hydroxide intercalated with EDTA. Applied Clay Science 32, 245–251.

Reichle, W.T., 1986. Synthesis of anionic clay minerals (mixed metal hydroxides, hydrotalcite). Solid State Ionics 22, 135–141.

Rives, V., 2001. Layered Double Hydroxides: Present and Future. Nova Science Publishers, Inc., New York.

Tan, B.H., Teng, T.T., Omar, A.K.M., 2000. Removal of dyes and industrial dye wastes by magnesium chloride. Water Research 34, 597–601.

Travis, C.C., Etnier, E., 1981. A survey of sorption relationships for reactive solutes in soil. Journal of Environmental Quality 10, 8–17.

Wang, B., Zhang, H., Evans, D., Duan, X., 2005. Surface modification of layered double hydroxides and incorporation of hydrophobic organic compounds. Materials Chemistry and Physics 92, 190–196.

Weber Jr., W.J., Morris, J.C., 1963. Kinetics of adsorption on carbon from solution. Journal of the Sanitary Engineering Division American Society of Civil Engineers 89, 31–60.

Zouboulis, A.I., Lazaridis, N.K., Grohmann, A., 2002. Toxic metals removal from waste waters by up flow filtration with floating filter medium. I. The case of zinc. Separation Science and Technology 37, 403–416.

Chemical Engineering Journal 254 (2014) 605–611

Contents lists available at ScienceDirect

Chemical Engineering Journal

journal homepage: www.elsevier.com/locate/cej

Removal of Cu^{2+}, Pb^{2+} and Cd^{2+} by layered double hydroxide–humate hybrid. Sorbate and sorbent comparative studies

M.A. González [a], I. Pavlovic [a,*], R. Rojas-Delgado [b], C. Barriga [a]

[a] Dpto. de Química Inorgánica e Ingeniería Química, Instituto Universitario de Química Fina y Nanoquímica (IUQFN), Universidad de Córdoba, Campus de Excelencia Internacional Agroalimentario, 14071 Córdoba, Spain
[b] INFQC, Departamento de Fisicoquímica, Facultad de Ciencias Químicas, Universidad Nacional de Córdoba, Ciudad Universitaria, 5000 Córdoba, Argentina

HIGHLIGHTS

- Layered double hydroxide–humate hybrid was synthetized by ionic exchange method.
- Inorganic matrix was stabilized by humate incorporation.
- High capacity for the Cu^{2+}, Pb^{2+} and Cd^{2+} removal by different mechanisms.
- The simultaneous heavy metal sorption increased the total metal amount sorbed.

GRAPHICAL ABSTRACT

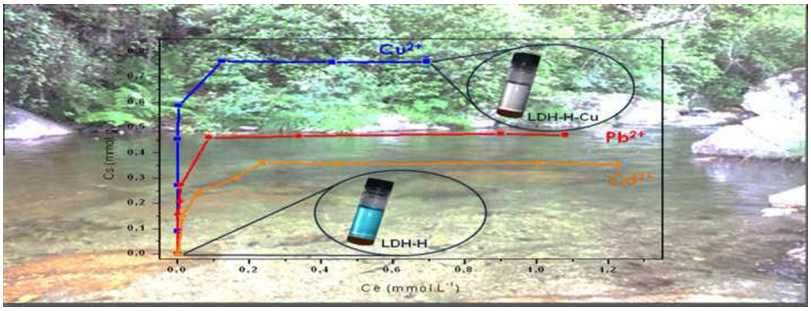

ARTICLE INFO

Article history:
Received 26 March 2014
Received in revised form 28 May 2014
Accepted 29 May 2014
Available online 11 June 2014

Keywords:
Layered double hydroxides
Humic acid
Heavy metals
Sorption

ABSTRACT

The synthesis of a layered double hydroxide-humate (LDH–H) hybrid was purposed for the removal of Cu^{2+}, Pb^{2+} and Cd^{2+} from aqueous solutions. This sorbent has been synthesized by incorporating humate anion into magnesium aluminum layered double hydroxide with chloride as an interlayer anion (LDH–Cl) via ion exchange. The effects of various physic-chemical factors such as pH influence, contact time, initial metal concentration and the simultaneous sorption of the three heavy metal ions onto LDH–H were investigated. The sorption capacities of humic acid (HA), LDH–Cl and LDH–H were compared under the same experimental conditions. The hybrid LDH–H presented better properties, such as greater stability and less pH increase throughout the sorption process. A high affinity and large removal capacity of Cu^{2+}, Pb^{2+} and Cd^{2+} were obtained by complexation and hydroxide precipitation mechanism, being this major for the case of Cu^{2+}, according to its low hydroxide solubility product value.The sorption isotherms were well described by the Langmuir equation. The metal removal efficiency was lower when the three cations were competing for the available adsorbent sites, compared to monocomponent solutions.

1. Introduction

Heavy metals are important pollutants that reach the soils and waters due to natural processes and human activities such as mining, metal plating, batteries and fertilizing industry among many others. They are not biodegradable and their toxicity lies in their bioacumulativity. For humans, extended exposure to heavy metals can result in damage to mental and central nervous function, blood composition, lungs, liver and other vital organs. World Health Organization drinking water guideline values for Cu, Cd and Pb are 2, 0.003 and 0.01 mg/l respectively [1]. Therefore, there is a great interest in the development of processes for heavy metals removal from wastewater ground water and sediments. Methods

* Corresponding author. Address: Facultad de Ciencias, Dpto. Química Inorgánica e Ingeniería Química, Universidad de Córdoba, Campus de Rabanales, Ed. Marie Curie, 14071 Córdoba, Spain. Tel.: +34 957 218648; fax: +34 957 218621.
E-mail address: iq2pauli@uco.es (I. Pavlovic).

http://dx.doi.org/10.1016/j.cej.2014.05.132
1385-8947/

applied in heavy metal removal from aquifers are chemical precipitation as sulfides or hydroxides, filtration, coagulation, inverse osmosis, electrolysis, etc. [2–5]. However, some of them are expensive or unsuitable and there is an increasing interest in the research of low-cost and non-toxic alternatives adsorbents such as zeolites [6], clays and clay minerals [7,8], as well as agricultural and municipal wastes [9].

Thus, heavy metals are immobilized by humic substances (HS), which are the product of decomposed organic matter in soils and waters. Their sorbent properties arise from the presence of humic acid (HA) which is the most abundant fraction of HS. HA are large colloidal molecules with variable composition, but they have a high content of oxygen-containing (carboxylic, phenolic) functional groups [10]. These functional groups exist in anionic form in a large pH range and in bond metal ions through electrostatic interactions and coordinate bonding [11–13]. HA could provoke problems in water treatments for many reasons such as the alteration of color, taste, odor, forming of carcinogenic by-products during the chlorination etc. Consequently, different materials such as activated carbon, alumina, zeolites, clays and clay minerals were proposed for the uptake of HA from waters [14–17]. Moreover, humic acids affect the removal capacity of pollutants such as heavy metal ions by other sorbents, such as carbon nanotubes and zero valent iron nanoparticles [18].

A class of minerals, which are also reported to be good sorbents of both heavy metals and HA, are the layered double hydroxides (LDHs) [16,19]. The structure of LDHs, also known as hydrotalcite-like compounds, are derived from that of brucite ($Mg(OH)_2$) by isomorphic substitution of Mg^{2+} by Al^{3+} ions. The charge excess generated is balanced by intercalation of anions between the layers [20]. The general LDH formula can be represented as $[M^{II}_{1-x}M^{III}_x(OH)_2]X^{n-}_{x/n}\cdot mH_2O$ where M^{II}, M^{III}, and X represent a divalent and trivalent cation and the interlayer anion, respectively. All of them may vary over a wide range and X is quite easy to exchange with other anions [21,22]. These materials are receiving increasing attention due to interesting specific properties such as anion exchange capacity, acid–base buffering capacity, reconstruction from their calcination products, and high customization possibilities. Therefore, LDHs have been studied for their potential applications in diverse areas [23–25], their low toxicity making them suitable for environmental applications [26–30]. Thus, LDHs were used to remove heavy metal by precipitation of the corresponding hydroxides due to their pH buffering capacity and when LDHs are functionalized with chelating ligands such as ethylenediaminetetraacetic acid, diethylenetriaminepentaacetate or meso-(2,3)-dimercaptosuccinate etc., the solids thus obtained showed sorption capacity for heavy metal cations such as Cu^{2+}, Cd^{2+}, Pb^{2+} [31–33]. The objective of this work was to obtain a layered double hydroxide–humate hybrid (LDH–H) and explore its capacity to remove Cu^{2+}, Cd^{2+}, Pb^{2+} from water. Firstly, the sorption capacity of this hybrid was compared to those of chloride intercalated LDH and humic acid. Afterwards, the effect of pH, the contact time and initial metal concentration on LDH–H sorption capacity was assessed and the competition between the three heavy metal ions was evaluated.

2. Experimental

All reagents were reagent grade and purchased from Aldrich. Water was distilled and previously boiled and purged with N_2 to prevent CO_2 presence.

2.1. Synthesis and characterization

The synthesis of the layered double hydroxide–humate hybrid (LDH–H) was carried out in two steps: the preparation of a chloride intercalated precursor (LDH–Cl), obtained by the coprecipitation method [21], which was afterwards dispersed in a sodium humate solution.

LDH–Cl was prepared by drop-wise addition of a 200 mL aqueous solution of 0.75 M of $MgCl_2\cdot 6H_2O$ and 0.25 M of $AlCl_3\cdot 6H_2O$ to a 0.25 M of NaCl solution under vigorous agitation and constant pH = 8, set by addition of 1 M NaOH solution. The synthesis was performed in N_2 atmosphere in order to avoid atmospheric CO_2 dissolution and consequently carbonate incorporation to the solid. The suspension obtained was hydrothermally treated at 80 °C for 24 h, separated by centrifugation and washed. A portion of the precipitate was dried at 60 °C to obtain LDH–Cl, while the remaining slurry was suspended in a 0.13 M sodium humate solution under vigorous stirring and a constant pH = 8 for 24 h. The resulting dispersion (LDH–H) was separated by centrifugation, washed and dried as previously described.

Mg and Al elemental chemical analyses were performed by Inductively Coupled Plasma Mass Spectrometry (ICP-MS) in a Perkin Elmer ELAN DRC-e instrument. The samples were dissolved in concentrated HNO_3 and diluted to meet the calibration range. Powder X-ray diffraction (PXRD) patterns were recorded using a Siemens D-5000 diffractometer with Cu K_α radiation (λ = 1.54050). Fourier-transform infrared (FT-IR) spectra were registered using the KBr disk method on a Perkin Elmer Spectrum One spectrophotometer. TG and DTA curves were recorded on a Setaram Setsys Evolution 16/18 apparatus in an oxidizing atmosphere and at the heating rate of 5 °C/min. Finally, SEM images were recorded in a JEOL JSM 6300 instrument on samples covered with an Au layer.

2.2. Sorption experiments

The optimal sorption conditions (initial pH, contact time) were determined in the sorption experiments performed. 0.05 g of the adsorbent (LDH–Cl or LDH–H) was dispersed in 30 mL, 1 mM aqueous solutions of Cu^{2+}, Pb^{2+} and Cd^{2+} nitrate salts. Sorption isotherms were performed in 30 mL dispersions containing 0.05 g sorbent with increasing initial concentration (C_0) of the corresponding heavy metal ion (C_0 = 0–2 mM). Finally, the competence between the three heavy metals for LDH–H sorbent was studied by dispersing 0.05 g of sorbent in 30 mL solutions containing all three heavy metal ions (C_0 = 1 mM and initial pH 5, each). The initial pH 5 was selected to be sure that the all of the metal ions were dissolved in all cases.

The experiments were performed by duplicate in all cases. The dispersions were shaken at 52 rpm at room temperature, centrifuged and finally filtered on Nylon filters (pore size 0.22 μm). The heavy metal concentration of the resulting supernatants was determined by atomic absorption spectrometry (AAS) in a Perkin Elmer AAnalyst400 instrument, the samples being dissolved in concentrated HNO_3 and diluted to meet the calibration range. These concentrations were used to determine the amount of each metal adsorbed by the sorbents (C_S, mmol g^{-1}):

$$C_S = (C_o - C_e)V/W \quad (1)$$

where C_o and C_e are the initial and equilibrium solution concentrations (mmol L^{-1}), W is the weight of solid (g) and V is the solution volume (L).

The adsorption isotherm data were fitted to the Langmuir model (Eq. (2))

$$C_e/C_S = (1/C_m)C_e + 1/(C_m K_L) \quad (2)$$

where C_m is the maximum sorption capacity at the monolayer coverage (mmol g^{-1}) and K_L (L $mmol^{-1}$) is a constant related to the adsorption energy.

3. Results and discussion

3.1. Characterization of the LDH–Cl and LDH–H

The XRD patterns of LDH–Cl and LDH–H (Fig. 1) portrayed characteristic peaks of hydrotalcite-like compounds [34], sharp, high intensity (00l) peaks at 2θ values below 30°, and broad, low intensity (*hkl*) peaks above this value. The basal spacing obtained for LDH–Cl (7.7 Å) was typical of chloride-intercalated hydrotalcites [34]. LDH–H basal spacing was slightly higher (7.9 Å) and similar to other HA containing LDHs previously reported. Thus, Seida and Nakano [35] suggest that LDH weathering provokes a coagulation of a part of humic acid which is adsorbed on LDH surface, while a small part is bonded by ionic exchange with LDHs interlayer carbonates. Also, Vreysen and Maes [16] propose a ligand exchange between HA and Al-OH groups of the brucite layers as a main mechanism of humic acid bonding to LDH. We consider that the incorporation of HA anions were produced mainly at the surface of the LDH particles, and that a partial intercalation of the humate near the LDH particle edges was concurrent. Humate anions were disposed in a parallel position to the layers, which could explain the slight basal spacing increase.

The FT-IR spectra of LDH–Cl (Fig. 2a) presented bands corresponding to the hydroxylated layers (below 900 cm^{-1}), hydroxyl stretching (above 3000 cm^{-1}), and bending mode of the interlayer water (1630 cm^{-1}) while the bands at 1358 and 1408 cm^{-1} were assigned to the presence of a small fraction of carbonate anions. On the other hand, LDH–H (Fig. 2b) presented characteristic bands of the humate anion (Fig. 2c): 1603 and 1387 cm^{-1} were attributed to antisymmetric and symmetric carboxylate vibration while those at 1105 and 1041 cm^{-1} were assigned to bending =CH vibration of HA [36].

The SEM images of LDH–Cl (Supplementary data, Fig. S1) showed that the sample consisted of well-shaped, regular particles (Fig. S1a and S1b) formed by aggregation of small plate-like units. LDH–H particles (Fig. S1c) presented a broader size range and more irregular edges (Fig. S1d). The increased particle size was assigned to a larger agglomeration of the LDHs platelets related to a higher hydrophobicity and lower particle charge expected for LDH–H particle surface due to the intercalation of an organic anion [37] thus increasing the particle–particle interactions. On the other hand, the irregular shape of LDH–H particles is similar to that obtained for other LDHs that incorporate organic anions at their surface [38].

DTA curves of LDH–Cl and LDH–H and HA are included in Fig. 3. Three endothermic effects at 83, 371 and 421 °C were observed during the thermal treatment of LDH–Cl (Fig. 3a). These thermal

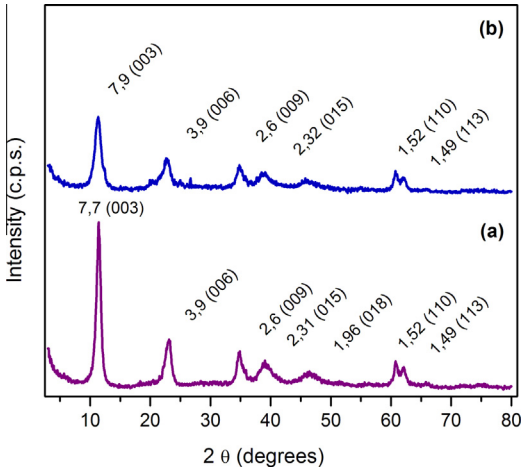

Fig. 1. XRD patterns of (a) LDH–Cl and (b) LDH–H.

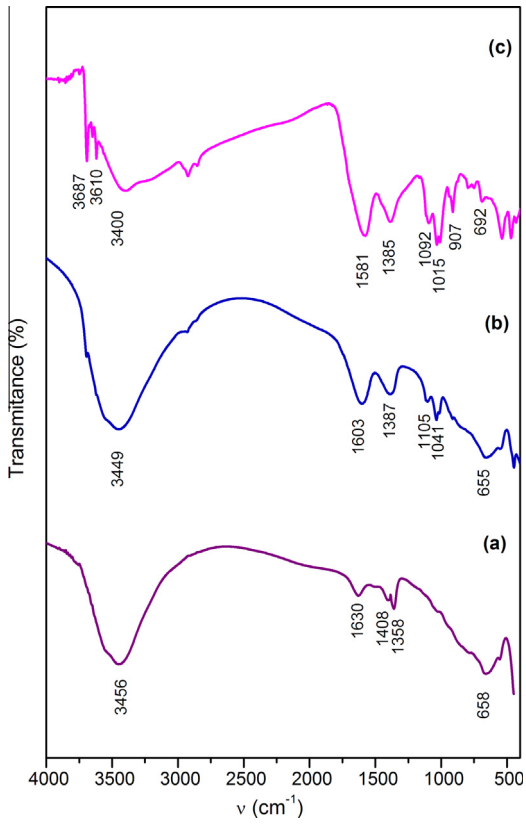

Fig. 2. FT-IR spectra of (a) LDH–Cl, (b) LDH–H and (c) sodium humate (NaH).

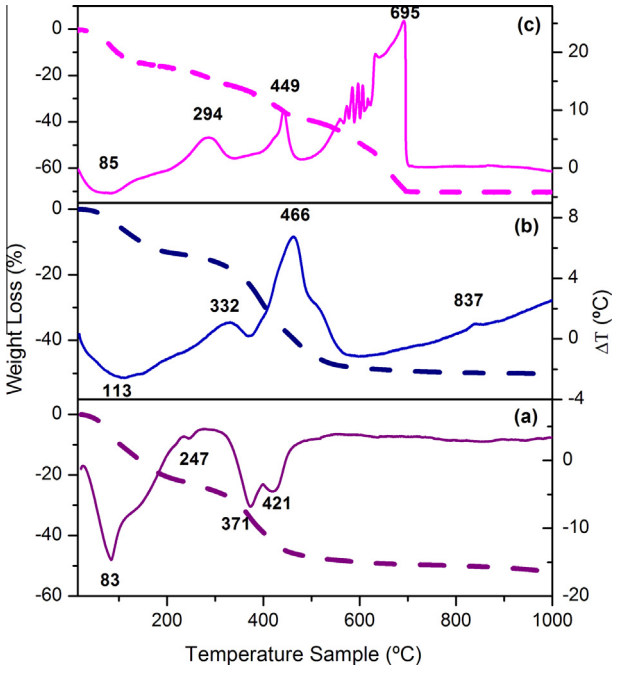

Fig. 3. TG and DTA curves of (a) LDH–Cl, (b) LDH–H and (c) NaH.

effects and their corresponding weight losses were assigned to (1) interlayer water loss, (2) dehydroxylation of the layers and (3) interlayer chloride loss [34]. The DTA curve of the LDH–H hybrid (Fig. 3b) showed the endothermic peak corresponding to the interlayer water, while the endothermic peaks corresponding to the last two effects were overlapped by an exothermic process

Table 1
Chemical analysis results of LDH–Cl and LDH–H.

	% wt		Atomic ratio	Proposed formula
	Mg	Al	Mg/Al	
LDH–Cl	20	8	2.8	$[Mg_{0.74}Al_{0.26}(OH)_2](Cl)_{0.26}{\cdot}0.83H_2O$
LDH–H	15	7	2.4	$[Mg_{0.71}Al_{0.29}(OH)_2](X)_{0.29/n}{\cdot}mH_2O$

X = Cl and/or H (n = 1 and/or 2; m = 0.58–0.71).

of HA oxidation (Fig. 3c). The metal analysis of the LDH–Cl and LDH–H and their proposed formulae are representedin the Table 1.

The results indicated that the molar ratio Mg:Al of the sample LDH–Cl was very close to that in the starting solution, while a decrease had been observed on the sample LDH–H because of a Mg partial dissolution during the HA exchange. According to the Mg/Al ratio and considering that the charge of the layer is only balanced by humate or chloride anion, a formula with a range of substitution was proposed for the LDH–H sample. The number of water molecules has been calculated from the first weight loss in the TG curve and the range has been obtained in accordance to the degree of the anionic substitution. The total weight loss for the proposed formula is consistent with the experimental value obtained by the TG curve, which is ~50% considering a total substitution of chloride by humate. This result confirmed that the HA incorporation was probably produced at the surface of LDH particles along with an important intercalation at the edges of the particles.

3.2. Sorbents comparison

The sorption capacity of LDH–Cl, LDH–H (0.05 g/30 mL, C_i = 1 mM, pH initial = 5, 48 h,) and HA (0.014 g/30 mL, amount equivalent to the total amount of humate adsorbed on 0.05 g of the LDH) was compared and the results are shown in Table 2. Copper was completely removed by LDH–Cl and LDH–H, both sorbents being more effective than HA. In the case of Pb^{2+}, LDH–Cl and LDH–H were capable of producing an almost complete removal, while HA presented lower sorption values. Finally, HA produced the highest Cd^{2+} removal, followed by LDH–H and LDH–Cl, respectively. On the other hand, equilibrium (final) pH values (pH_f) were highly dependent on the sorbent. The buffering capacity of LDH–Cl [39] produced the highest pH values, while the least important pH variation with respect to pH_i was produced for HA. The amounts of Mg and Al released from the solids after metal sorption experiments were also determined. Al^{3+} concentration was negligible in all cases, which was consistent with the low solubility of $Al(OH)_3$ ($K_{SP}(Al(OH)_3) = 5 \times 10^{-33}$). On the other hand, the Mg was detected in all supernatants and it increased upon heavy metal sorption. These results were related to the different sorption mechanisms of the sorbents: in the case of HA heavy metals were bounded by complex formation. Consequently, the heavy metals affinity for HA being determined by the stability of these complexes and the sorption process produced only minor pH variations. In the case of LDH–Cl, its buffering capacity leaded to an important pH increase and heavy metal precipitation as hydroxides was the main sorption mechanism [40]. These hydroxides precipitate either as part of a LDH structure, in a mechanism known as "diadochy" [41] or in a separate phase [42,43]. LDH–Cl affinity for heavy metal was then determined by the solubility products of the their hydroxides ($K_{SP}(Cu(OH)_2) = 1 \times 10^{-20}$, $K_{SP}(Cd(OH)_2) = 3.2 \times 10^{-14}$ and $K_{SP}(Pb(OH)_2) = 2.5 \times 10^{-16}$). Finally, both mechanisms were concurrent in the LDH–H hybrid, humate anions stabilizing and adding complexation capacity to the inorganic matrix. All pH_f values for the heavy metal sorption on LDH–H were lower compared to those of LDH–Cl (Table 2) due to the stabilizing effect of humate anions [44]. Although the pH_f was sufficient to produce an almost complete precipitation of $Cu(OH)_2$, they were not enough for Pb^{2+} and Cd^{2+} due to the higher solubility of the corresponding hydroxides. Nevertheless, LDH–H showed higher Cd^{2+} sorption than LDH–Cl, which confirmed the contribution of the HA complexation mechanism [45].

Table 2
pH final and percenteges of Mg in the supernatants and heavy metals sorbed on different sorbents.

Sample	Metal	pH_{final}	% Mg	% Sorbed
	Cu^{2+}	5.4	–	78
AH	Pb^{2+}	5.0	–	79
	Cd^{2+}	6.8	–	64
	–	9.3	5.9	–
LDH–Cl	Cu^{2+}	9.0	10.0	100
	Pb^{2+}	9.1	9.4	87
	Cd^{2+}	8.2	6.7	37
	–	8.9	5.7	–
LDH–H	Cu^{2+}	8.3	8.9	100
	Pb^{2+}	7.6	7.8	95
	Cd^{2+}	7.8	7.4	56

According to the results obtained, LDH–H presents interesting properties due to (1) the stabilization of LDH matrix, diminishing the layers weathering and the final pH of the supernatants, which in turn, also decrease the environmental impact of the treated effluents and (2) the addition of a complexation mechanism, extending LDH functionalities. Also, due to the recurring presence of HA in the effluents, their interactions with LDHs and the effect on their sorptive behavior are of primary importance. As a consequence, the sorption behavior of the hybrid will be studied in the next section.

3.3. Heavy metal cations sorption by LDH–H

Table 3 shows the effect of pH on the heavy metal sorption capacity of LDH–H. Both Cs and pH_f slightly decreased with decreasing pH_i, as the buffering capacity of LDH–H is exhausted by both heavy metal sorption and proton consumption. It could be noted here that, as Cs decreases from Cu^{2+} to Cd^{2+}, the influence of pH_i in pH_f also decreased, which confirmed that the buffering capacity of LDHs was not consumed, i.e. lower pHs (higher acid concentrations) are necessary to displace the final pH from 7 to 8 range.

The kinetic study results (Fig. 4) showed that sorption was produced into two steps. The first step was fast and produced half of the final sorption within the first 2 h, and the second gradually approached to equilibrium, reaching it within 48 h in the cases of Pb and Cd, and 24 h for the case of Cu. 100%, 95% and 56% of the initial metal concentration were removed for Cu, Pb and Cd, respectively, and the time to reach equilibrium increased in the same sequence as well. A similar kinetic behavior was previously observed for Cu^{2+} on LDH modified by edta [46]: the first, fast step being assigned to the hydroxide precipitation mechanism and the

Table 3
pH influence on the heavy metals sorption on LDH–H.

Sample	pH initial	pH final	Cs (mmol g^{-1})
Cu^{2+}	3	6.1	0.51
	5	8.3	0.57
Pb^{2+}	3	7.4	0.34
	5	7.6	0.40
	7	8.0	0.36
Cd^{2+}	3	7.7	0.23
	5	7.8	0.26
	7	8.0	0.27

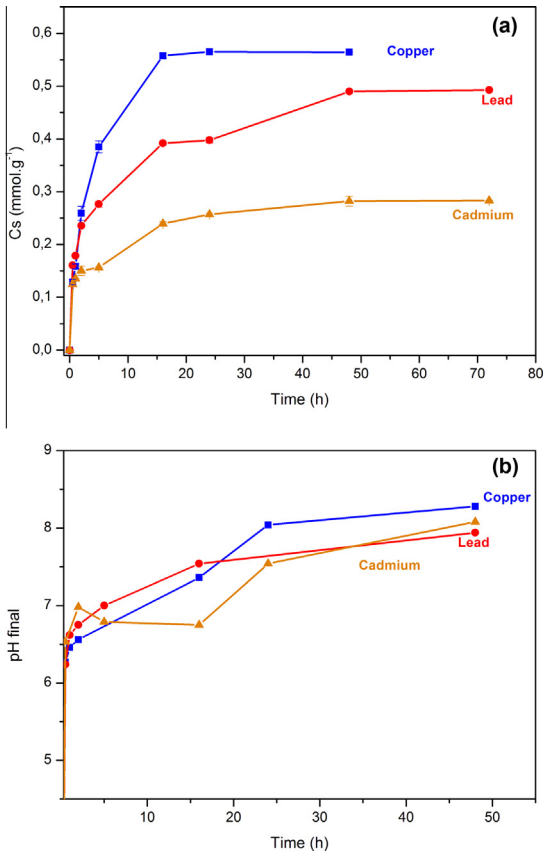

Fig. 4. The evolution of: (a) heavy metals uptake by LDH–H and (b) pH evolution (C_i = 1 mM, pH initial 5).

second step to a cation exchange mechanism at edta complexes located at the interlayer. The only difference here was substitution of edta by HA. The presence of the second mechanism was

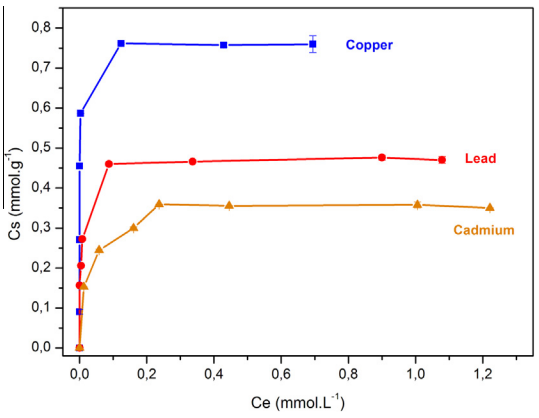

Fig. 5. Sorption isotherms of heavy metals on LDH–H at pH = 5.

Table 4
Langmuir model parameters for heavy metals sorption on LDH–H.

Sample	C_m (mmol g^{-1})	K_L	R^2
Cu^{2+}	0.75	69	0.993
Pb^{2+}	0.48	187	0.999
Cd^{2+}	0.35	114	0.998

confirmed by Fig. 4b, which indicated that the main pH variation, associated with the hydroxide precipitation mechanism, was produced within the first minutes of the experiment in all cases.

The time of 48 h was considered enough to reach equilibrium for the sorption isotherm (Fig. 5). A steep Cs increase was registered in all cases, indicating the high effectiveness of LDH–H as sorbent, the metal ions being completely adsorbed at lower initial concentrations. As determined by the Langmuir model fitting (Table 4), the maximum sorption increased in the sequence Cd (C_m = 0.35 mmol g^{-1}) Pb (C_m = 0.48 mmol g^{-1}) and Cu (C_m = 0.75 mmol g^{-1}). These values were comparable to those obtained for similar

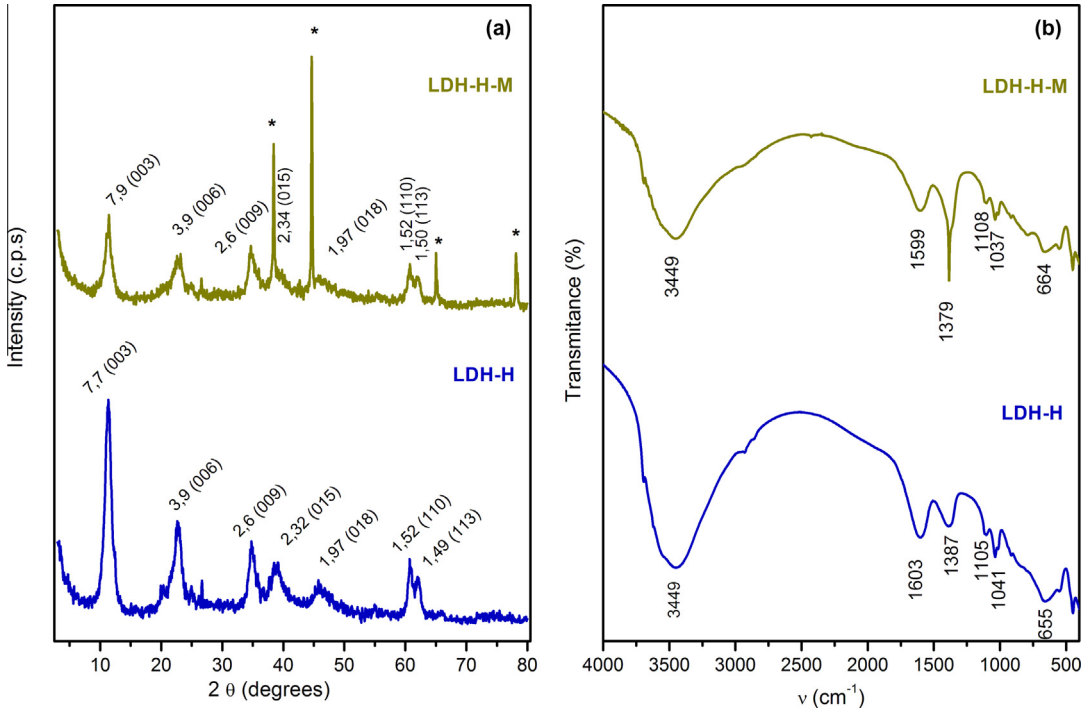

Fig. 6. XRD patterns (a) and FT-IR spectra (b) of the sorption products (M = Cu, Pb and Cd) corresponding to the last isotherm point (*Al sample holder).

Mg–Al–LDHs: between 0.01 and 0.15 mmol g^{-1} for Cd^{2+} sorption by Mg–Al–LDHs containing carbonate and edta, respectively [47], 0.33 and 0.86 mmol g^{-1} for Pb^{2+} sorption by chloride-containing Mg–Al–LDHs [48,49] and between 0.78 and 2.50 mmol g^{-1} for Cu^{2+} sorption by chloride intercalated LDHs either [42,50]. In all cases sorption was assigned to a hydroxide precipitation mechanism, except for the case of Cd^{2+}, which only reaches significant sorption capacity when complexation mechanism is incorporated by intercalating the solid with edta. Similarly, LDH–H showed higher sorption capacity than LDH–Cl or even than the edta intercalated Mg–Al–LDHs.

The sorption products were studied by PXRD and FT-IR (Fig. 6) and there were no important changes observed compared to the pure sorbent pattern (Fig. 1). PDRX of LDH–H–Metal complexes patterns (Fig. 6a) indicated that the crystallinity of the sorption product decreased but the LDH structure was maintained and there was no additional precipitates observed. This is probably due to the low mass of hydroxide formed respect the amount of sorbent in the experiments (less than 10% w/w in all cases, as calculated from C_m values and the formula weight of the corresponding heavy metal hydroxide). The FT-IR spectrum (Fig. 6b) of sorbent after the sorption experiments showed slight displacements of the bands in the 1600–1000 cm^{-1} zone, which is likely to be due to the interaction of the functional groups of the HA with metal ions.

The simultaneous sorption of the three heavy metal ions is represented in Fig. 7. The sorption was slower and the amounts of metal uptaken were lower compared to the monocomponent solutions. The maximum amounts sorbed at the equilibrium time for the multicomponent system were $Cs = 0.46$ mmol g^{-1}, $Cs = 0.21$ mmol g^{-1} $Cs = 0.00$ mmol g^{-1} for Cu, Pb and Cd respectively, vs. $Cs = 0.57$ mmol g^{-1}, $Cs = 0.49$ mmol g^{-1}, $Cs = 0.28$ mmol g^{-1} obtained for the corresponding experiments with a single heavy metal ion. The highest amounts of the metal cations sorbed on LDH–H were reached for copper in both cases, while the sorption of Cd was completely inhibited by the presence of the other two cations probably due to sorption occupation sites by the species with more affinity and/or precipitation of the hydroxides. This behavior was concordant with the sequence of stability of the corresponding metal hydroxides (decreasing K_{PS}) and correlated with the stability constants of M–humate complexes [45], decreasing in the order of Cu > Pb > Cd. Moreover, the sum of Cs for the multicomponent system (0.67 mmol g^{-1}) was larger than the maximum Cs value obtained for the single metal experiments (Cu^{2+} ion, 0.57 mmol g^{-1}), indicating that both precipitation and complexation mechanisms are concurrent and that the different ions were incorporated to different sites. According to this result, Cd^{2+} and Pb^{2+} were competing preferentially for humate complexation sites.

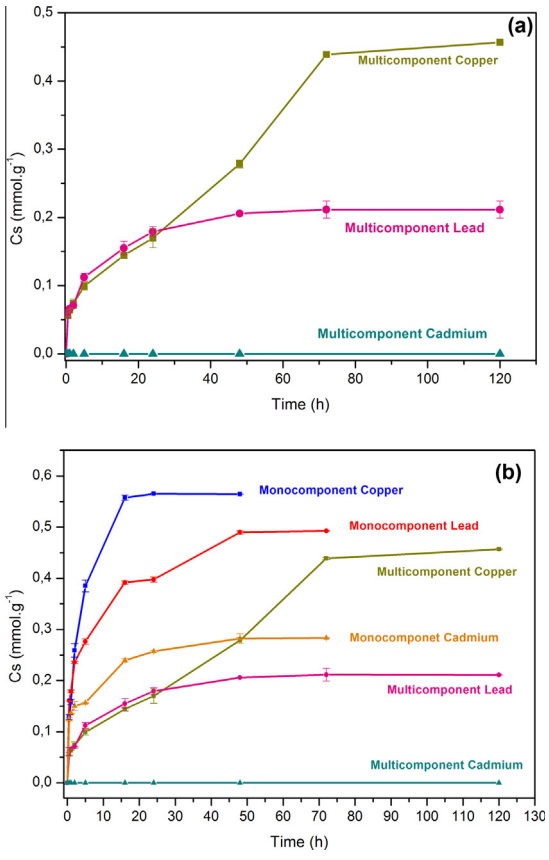

Fig. 7. The evolution of sorption of heavy metals on LDH–H: (a) metal cations coexisting in the solution (multicomponent) and (b) comparing with the monocomponent solution sorption behavior.

4. Conclusions

Layered double hydroxide–humate hybrid (LDH–H) was synthesized by dispersing chloride containing LDH in a humate solution. Humate incorporation was produced at the surface of the particles but also some intercalation at the particles edges was inferred. Humate incorporation produced a stabilization of the inorganic matrix and the resulting hybrid showed sorption capacity of Cu^{2+}, Pb^{2+} and Cd^{2+} due to precipitation and complexation mechanism. As a consequence, LDH–H presented an intermediate behavior compared to LDH–Cl and HA separately. Moreover, LDH–H presents a better stability, resulting in less pH increase during the experiments, which moderates the environmental impact of the sorption process. Also, LDH–H avoids the separation and dewatering problems associated with humic acids. The LDH–H sorption process was fast and was produced in two steps, the first fast step was exclusively associated with hydroxide precipitation, while in the second, slower step, the complexation mechanism was involved. LDH–H presented high affinity for heavy metal ions, leading to low pollutant concentrations at equilibrium while the sorption capacities were similar to other sorbents with similar characteristics. Finally, the presence of more than one heavy metal even increased the overall sorption capacity, indicating that different heavy metals were sorbed by different mechanisms, Pb^{2+} and Cd^{2+} competing for the humate complexation sites.

Acknowledgments

This work was partially funded by the Ministerio de Ciencia e Innovación (CTM 2011-25325) and Junta de Andalucía through Research Group FQM-214. We appreciate the technical assistance received in the SCAI (Universidad de Córdoba) for Electron Microscopy and Elemental Analysis Units (ICP-MS).

Appendix A. Supplementary data

Supplementary data associated with this article can be found, in the online version, at http://dx.doi.org/10.1016/j.cej.2014.05.132.

References

[1] World Health Organization, Guidelines for Drinking-water Quality, Health Criteria and Other Supporting Information, vol. 2, Second ed., WHO, Geneva, 1996.
[2] J.B. Brower, R.L. Ryan, M. Pazirandeh, Comparison of ion-exchange resins and biosorbents for the removal of heavy metals from plating factory wastewater, Sci. Technol. 31 (1997) 2910–2914.
[3] K.G. Karthikeyan, H.A. Elliott, F.S. Cannon, Adsorption and coprecipitation of copper with the hydrous oxides of iron and aluminum, Environ. Sci. Technol. 31 (1997) 2721–2725.

[4] A.T. Heijne, F. Liu, R. Weijden, J. Weijma, C.J.N. Buisman, H.V.M. Hamelers, Copper recovery combined with electricity production in a microbial fuel cell, Environ. Sci. Technol. 44 (2010) 4376–4381.
[5] M.A. Hashim, S. Mukhopadhyay, J.N. Sahu, B.J. Sengupta, J. Environ. Manage. 92 (2011) 2355–2388.
[6] P. Misaelides, Application of natural zeolites in environmental remediation: a short review, Microporous Mesoporous Mater. 144 (2011) 15–18.
[7] M. Cruz-Guzmán, R. Celis, M.C. Hermosín, W. Koskinen, J. Cornejo, Adsorption of pesticides from water by functionalized organobentonites, J. Agric. Food Chem. 53 (2005) 7502–7511.
[8] J. Cornejo, R. Celis, I. Pavlovic, M.A. Ulibarri, Interactions of pesticides with clays and layered double hydroxides: a review, Clay Miner. 43 (2008) 155–176.
[9] A. Bhatnagar, M. Sillanpaa, Utilization of agro-industrial and municipal waste materials as potential adsorbents for water treatment: a review, Chem. Ing. J. 157 (2010) 277–296.
[10] G.W. vanLoon, S.L. Duffy, Environmental Chemistry (a global perspective), Oxford University Press Inc., New York, 2000.
[11] C.A. Coles, R.N. Yong, Humic acid preparation, properties and interactions with metals lead and cadmium, Eng. Geol. 85 (2006) 26–32.
[12] M. Havelcová, J. Mizera, I. Sýkorová, M. Pekar, Sorption of metal ions on lignite and the derived humic substances, J. Hazard. Mater. 161 (2009) 559–564.
[13] Y. Li, Q. Yue, B. Gao, Adsorption kinetics and desorption of Cu(II) and Zn(II) from aqueous solution onto humic acid, J. Hazard. Mater. 178 (2010) 455–461.
[14] B. Bolto, D. Dixon, R. Eldridge, S. King, K. Linge, Removal of natural organic matter by ion exchange, Water Res. 36 (2002) 5057–5065.
[15] A.A.M. Daifullah, B.S. Girgis, H.M.H. Gad, A study of the factors affecting the removal of humic acid by activated carbon prepared from biomass material, Colloids Surf., A 235 (2004) 1–10.
[16] S. Vreysen, A. Maes, Adsorption mechanism of humic and fulvic acid onto Mg/Al layered double hydroxides, Appl. Clay Sci. 38 (2008) 237–249.
[17] Y. Zhan, Z. Zhu, J. Lin, Y. Qiu, J. Zhao, Removal of humic acid from aqueous solution by cetylpyridinium bromide modified zeolite, J. Environ. Sci. 22 (2010) 1327–1334.
[18] W.W. Tang, G.M. Zeng, J.L. Gong, J. Liang, P. Xu, C. Zhang, B.B. Huang, Impact of humic/fulvic acid on the removal of heavy metals from aqueous solutions using nanomaterials: a review, Sci. Total Environ. 468–469 (2014) 1014–1027.
[19] G. Onkal-Engin, R. Wibulswas, D.A. White, Humic acid uptake from aqueous media using hydrotalcites and modified montmorillonite, Environ. Technol. 21 (2000) 167–175.
[20] F. Cavani, F. Trifiro, A. Vaccari, Hydrotalcite-type anionic clays: preparation, properties and applications, Catal. Today 11 (1991) 173–301.
[21] W.T. Reichle, Synthesis of anionic clay-minerals (Mixed metal-hydroxides, hydrotalcite), Solid State Ionics 22 (1986) 135–141.
[22] P.S. Braterman, Z.P. Xu, F. Yarberry, Layered double hydroxides (LDHs), in: S.M. Auerbach, K.A. Carrado, P.K. Dutta (Eds.), Handbook of Layered Materials, Marcel Decker Inc, New York, 2004, pp. 373–474.
[23] J.H. Choy, S.Y. Kwak, J.S. Park, Y.J. Jeong, Cellular uptake behavior of [−32P] labeled ATP–LDH nanohybrids, J. Mater. Chem. 11 (2001) 1671–1674.
[24] D.G. Evans, X. Duan, Preparation of layered double hidroxides and their applications as aditive in polymers, as precursors to magnetic materials and in biology and medicine, Chem. Commun. (2006) 485–496.
[25] J.H. Choy, S.J. Choi, J.M. Oh, T. Park, Clay minerals and layered double hydroxides for novel biological applications, Appl. Clay Sci. 36 (2007) 122–132.
[26] J. Serrano, V. Bertín, S. Bulbulian, Mo-99 sorption by thermally treated hydrotalcites, Langmuir 16 (2000) 3355–3360.
[27] I. Pavlovic, C. Barriga, M.C. Hermosín, J. Cornejo, M.A. Ulibarri, Adsorption of acidic pesticides 2,4-D, clopyralid and picloram on calcined hydrotalcite, Appl. Clay Sci. 30 (2005) 125–133.
[28] F. Bruna, I. Pavlovic, C. Barriga, J. Cornejo, M.A. Ulibarri, Adsorption of pesticides Carbetamide and Metamitron on organohydrotalcite, Appl. Clay Sci. 33 (2006) 116–124.
[29] F. Bruna, I. Pavlovic, R. Celis, C. Barriga, J. Cornejo, M.A. Ulibarri, Organohydrotalcites as novel supports for the slow release of the herbicide terbuthylazine, Appl. Clay Sci. 42 (2008) 194–200.
[30] R. Extremera, I. Pavlovic, M.R. Pérez, C. Barriga, Removal of acid orange 10 by calcined Mg/Al layered double hydroxides from water and recovery of the adsorbed dye, Chem. Eng. J. 213 (2012) 392–400.
[31] M.R. Pérez, I. Pavlovic, C. Barriga, J. Cornejo, M.C. Hermosín, M.A. Ulibarrri, Uptake of Cu^{2+}, Cd^{2+} and Pb^{2+} on Zn–Al layered double hydroxide intercalated with edta, Appl. Clay Sci. 32 (2006) 245–251.
[32] T. Kameda, H. Takeuchi, T. Yoshioka, Uptake of heavy metal ions from aqueous solution using Mg–Al layered double hydroxides intercalated with citrate, malate, and tartrate, Sep. Purif. Technol. 62 (2008) 330–336.
[33] I. Pavlovic, M.R. Pérez, C. Barriga, M.A. Ulibarri, Adsorption of Cu^{2+}, Cd^{2+} and Pb^{2+} ions by layered double hydroxides intercalated with the chelating agents diethylenetriaminepentaacetate and meso-2,3-dimercaptosuccinate, Appl. Clay Sci. 43 (2009) 125–129.
[34] V. Rives, Layered Double Hydroxides: Present and Future, Nova Science Publishers Inc, New York, 2001.
[35] Y. Seida, Y. Nakano, Removal of humic substances by layered double hydroxide containing iron, Water Res. 34 (2000) 1487–1494.
[36] L.J. Bellamy, The Infrared Spectra of Complex Molecules, vol. 1, third ed., Chapman and Hall, London, 1975.
[37] R. Rojas, F. Bruna, C.P. de Pauli, M.A. Ulibarri, C.E. Giacomelli, The effect of interlayer anion on the reactivity of Mg–Al layered double hydroxides: improving and extending the customization capacity of anionic clays, J. Colloid Interface Sci. 359 (2011) 136–141.
[38] Z.P. Xu, P.S. Braterman, Synthesis, structure and morphology of organic layered double hydroxide (LDH) hybrids: comparison between aliphatic anions and their oxygenated analogs, Appl. Clay Sci. 48 (2010) 235–242.
[39] M.L. Parello, R. Rojas, C.E. Giacomelli, Dissolution kinetics and mechanism of Mg–Al layered double hydroxides: a simple approach to describe drug release in acid media, J. Colloid Interface Sci. 351 (2010) 134–139.
[40] X. Liang, Y. Zang, Y. Xu, X. Tan, W. Hou, L. Wang, Y. Sun, Sorption of metal cations on layered double hydroxides: a review, Colloids Surf., A 433 (2013) 122–131.
[41] S. Komarneni, N. Kozai, R. Roy, Novel function for anionic clays: selective transition metal cation uptake by diadocky, J. Mater. Chem. 8 (1998) 1329–1331.
[42] M. Park, C.L. Choi, Y.J. Seo, S.K. Yeo, J. Choi, S. Komarneni, J.H. Lee, Reactions of Cu^{2+} and Pb^{2+} with Mg/Al layered double hydroxide, Appl. Clay Sci. 37 (2007) 143–148.
[43] R. Rojas, Cooper, lead and cadmium removal by CaAl layered double hydroxides, Appl. Clay Sci. 87 (2014) 254–259.
[44] Y. Kameshima, H. Yoshizaki, A. Nakajima, K. Okada, Preparation of sodium oleate/layered double hydroxide composites with acid-resistant properties, J. Colloid Interface Sci. 298 (2006) 624–628.
[45] A.K. Pandey, S.D. Pandey, V. Misra, Stability constants of metal–humic acid complexes and its role in environmental detoxification, Ecotox. Environ. Safe. 47 (2000) 195–200.
[46] R. Rojas, M.R. Pérez, P. Eustaquio, M. Erro, I. Ortiz, M.A. Ulibarri, C.E. Giacomelli, Edta modified LDHs as Cu2+ scavengers: removal kinetics and sorbent stability, J. Colloid Interface Sci. 331 (2009) 425–431.
[47] T. Kameda, S. Saito, Y. Umetsu, Mg–Al layered double hydroxide intercalated with ethylene-diaminetetraacetate anion: synthesis and application to the uptake of heavy metal ions from an aqueous solution, Sep. Purif. Technol. 47 (2005) 20–26.
[48] X. Liang, W. Hou, Y. Xu, G. Sun, L. Wang, Y. Sun, X. Quin, Sorption of lead ion by layered double hydroxide intercalated with diethylenetriaminepentaacetic acid, Colloids Surf., A 366 (2010) 50–57.
[49] D. Zhao, G. Sheng, J. Hu, C. Chen, X. Wang, The adsorption of Pb(II) on Mg_2Al layered double hydroxide, Chem. Eng. J. 171 (2011) 167–174.
[50] Y. Zang, W. Hou, J. Xu, Removal of Cu(II) from $CuSO_4$ aqueous solution by Mg–Al hydrotalcite-like compounds, Chin. J. Chem. 29 (2011) 847–852.

Chemical Engineering Journal 269 (2015) 221–228

Contents lists available at ScienceDirect

Chemical Engineering Journal

journal homepage: www.elsevier.com/locate/cej

Cu(II), Pb(II) and Cd(II) sorption on different layered double hydroxides. A kinetic and thermodynamic study and competing factors

M.A. González, I. Pavlovic, C. Barriga *

Dpto de Química Inorgánica e Ingeniería Química, Instituto Universitario de Química Fina y Nanoquímica (IUQFN), Campus de Excelencia Internacional Agroalimentaio (CeiA3), Universidad de Córdoba, Córdoba, Spain

HIGHLIGHTS

- Higher amounts of metals were sorbed on original LDH-Cl than on humate-modified LDH.
- Kinetics of all sorption systems fitted well to a pseudo second-order model.
- The presence of humate in the solution competes and diminishes metals sorption.
- Copper was sorbed in greater amounts in all cases.
- LDH composition determines order of metal sorption from multicomponent solutions.

GRAPHICAL ABSTRACT

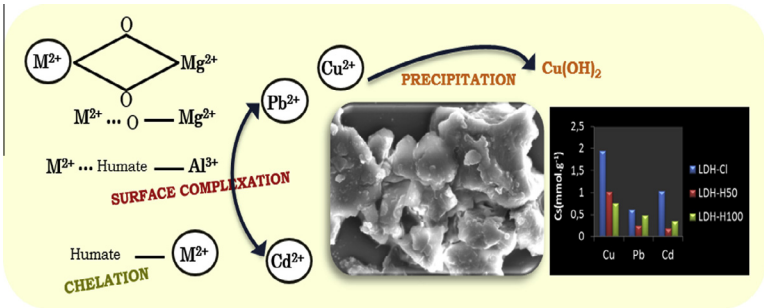

ARTICLE INFO

Article history:
Received 21 November 2014
Received in revised form 22 January 2015
Accepted 24 January 2015
Available online 2 February 2015

Keywords:
Metal sorption
Layered double hydroxide
Kinetic
Humate anion

ABSTRACT

Layered double hydroxide-humate hybrids containing different amounts of humate anions (LDH-H100 and LDH-H50) were synthesized by an ion exchange mechanism from layered double hydroxides intercalated by chloride (LDH-Cl). These LDH-based compounds (LDH-Cl, LDH-H100 and LDH-H50) were proposed as sorbents of Cu^{2+}, $Pb^{2+}$and Cd^{2+} from aqueous solutions. The study of the influence of the initial metal concentration on sorption capacity of LDHs showed that LDH-Cl achieved the best sorption capacity for the potentially toxic metals studied, which is quite unexpected given that humate functional groups have a high affinity for metal cations. The thermodynamic and kinetic studies were carried out and the results confirmed that all sorption processes were spontaneous and thermodynamically favourable, fitting to pseudo second kinetic order. The sorption competition of the metals from binary and ternary metal solutions was also studied in order to obtain a better understanding of metal sorption behaviour on this material.

1. Introduction

The presence of metal cations in water could cause serious environmental and human health problems because of their potentially high toxicity. They reach aquifers as the result of both natural processes and human activities such as agriculture or industrial waste discharge.

As a consequence, this concern generates great interest in the development of methods to remedy the presence of potentially toxic metals in water. Among the different techniques applied with this aim in mind, the most extended one is the precipitation of metals as insoluble metal hydroxides, by increasing the pH [1]. However this could produce large volumes of low density sludge, which make the disposal process difficult. This is one of the reasons why adsorption and ion-exchange methods have been studied

* Corresponding author at: Facultad de Ciencias, Dpto Química Inorgánica e Ingeniería Química, Universidad de Córdoba, Campus de Rabanales, Ed. Marie Curie, 14071 Córdoba, Spain. Tel.: +34 957 218648; fax: +34 957 218621.
E-mail address: cbarriga@uco.es (C. Barriga).

http://dx.doi.org/10.1016/j.cej.2015.01.094
1385-8947/

recently as alternatives for the removal of metallic elements from water.

Layered double hydroxides (LDH) or hydrotalcite-like compounds form part of a family of natural or synthetic materials with the general formula $[M_{1-x}^{II}M_x^{III}(OH)_2]^{x+}A_{x/m}^{m-}\cdot nH_2O$, where M^{II} and M^{III} are a divalent and a trivalent cations, and A is the interlayer anion. In the last few decades, LDHs have received considerable attention for their potential applications in many fields, due to their interesting and unique properties. Low-cost and simple preparation, high sorption efficiency and many other advantages makes these materials suitable for the application in the field of wastewater treatment [2–4].

Although LDH is known to be a good sorbent for anionic pollutants through the ionic exchange of interlayer anions, in recent years these materials were also studied as possible sorbents and scavengers of metal cations from waters [5–9].

On the other hand, humic acids (HA) which are natural polymers formed by the decomposition of biological organisms, could be bonded to metal cations thus affecting their retention and mobility. Their functional groups such as carboxylate, hydroxyl and phenolate could interact with both metals cations and LDHs.

The kinetic and thermodynamic parameters of the metal sorption on different natural substrates as well as their competition with the naturally occurring anions, such as humate, for the sorption sites could be important for understanding the behaviour and fate of these contaminants in the environment.

Therefore, the aim of this work was the study of the kinetic and thermodynamic parameters of the sorption of Cu^{2+}, Cd^{2+} and Pb^{2+} on layered double hydroxides intercalated by (i) chloride (LDH-Cl), (ii) high amounts of the humate anion (LDH-H100) and (iii) low amounts of the humate anion (LDH-H50). Also, the factors affecting the metal sorption such as the competition of the three metals for the sorption sites, as well as their competition with the humate anion from the solution, were studied.

2. Experimental

All the reagents were of analytical grade products and purchased from Aldrich (Spain).

2.1. Synthesis of the sorbents

Three LDHs were synthesized for study as sorbents of potentially toxic metals Cu^{2+}, Cd^{2+} and Pb^{2+}. A layered double hydroxide with chloride as the interlayer inorganic anion (LDH-Cl), was obtained by co-precipitation method and two layered double hydroxide-humate hybrids (LDH-H100 and LDH-H50) were prepared as we have previously described [8] by incorporating of 100% and 50% of humate stoichiometric concentration required to compensate the layer charge (estimated by elemental analysis and TG–DTA study) to the slurry of the sample LDH-Cl.

2.2. Metal sorption experiments

The optimal sorption conditions (initial pH, contact time) were determined in the sorption experiments performed. 0.05 g of the sorbent (LDH-H100, LDH-H50 or LDH-Cl) was dispersed in 30 mL aqueous solutions of Cu^{2+}, Pb^{2+} and Cd^{2+} nitrate salts (initial concentrations $C_0 = 1$ mM). Sorption isotherms were performed in 30 mL dispersions containing 0.05 g sorbent with corresponding metal ion. Initial metal concentrations ranged in all cases between $C_0 = 0$ and 2.5 mM, except in the case of Cu sorption on LDH-Cl, where the initial concentration was increased up to 4.4 mM in order to reach the sorption isotherm plateau. Finally, the competition between two and three metals simultaneously present in the solution (each $C_0 = 1$ mM at pH = 5), was studied by dispersing 0.05 g of sorbent in 30 mL of the metal solutions. Also, the influence of humate presence in the solution ($C_0 = 1$ mM) on sorption for metals on LDH-Cl was studied only for the ternary system (three heavy metals simultaneously present in the solution, each $C_0 = 1$ mM, 0.05 g/30 mL).

The suspensions were shaken and after a suitable time, were centrifuged and the supernatants were filtered and used to determine the amounts of metals by atomic absorption spectrometry (AAS) in a Perkin Elmer AAnalyst 400 instrument. The amounts of metal sorbed per gram of sorbent, C_s (mmol g^{-1}), were calculated as follows:

$$C_s = (C_0 - C_e)V/W \quad (1)$$

where C_0 and C_e are the initial and equilibrium solution concentrations (mmol L^{-1}), W is the weight of solids (g) and V is the metal solution volume (L).

The experimental sorption data were fitted to the Langmuir and Freundlich models, represented in Eqs. (2) and (3), respectively:

$$C_e/C_s = (1/C_m)C_e + 1/(C_m K_L) \quad (2)$$

where C_m is the maximum sorption capacity at the monolayer coverage (mmol g^{-1}) and K_L (L $mmol^{-1}$) is a constant related to the sorption energy:

$$\log C_e = \log K_f + N_f \log C_0 \quad (3)$$

where K_f ($mmol^{1-Nf} L^{Nf} g^{-1}$) and N_f are Freundlich parameters, whose are characteristic of the sorbent–sorbate systems [10].

2.3. Kinetic models

The kinetic models of pseudo-first order and pseudo-second order assume that sorption is a pseudo-chemical reaction, and the sorption rate can be determined for the equations of pseudo-first (Eq. (4)) and pseudo-second order (Eq. (5)) respectively:

$$\log(q_e - q_t) = \log q_e - (k_1/2.303)t \quad (4)$$

$$t/q_t = 1/(k_2 q_e^2) + (1/q_e)t \quad (5)$$

where q_t and q_e are the metal amount sorbed at time t (min) and at equilibrium (mg g^{-1}), respectively, k_1 and k_2 are the rate constants of pseudo-first and pseudo-second-order models, in (min^{-1}) and (g mg^{-1} min^{-1}), respectively.

2.4. Characterization techniques

Mg and Al elemental chemical analyses were performed by Inductively Coupled Plasma Mass Spectrometry (ICP-MS) in a Perkin Elmer ELAN DRC-e instrument. The samples were dissolved in concentrated HNO_3. Powder X-ray diffraction patterns (XRD) were recorded using a Siemens D-5000 instrument with CuK_α radiation. FT-IR spectra were recorded with a Perkin Elmer Spectrum One spectrophotometer using KBr disk method.

3. Results and discussion

3.1. Characterization of the sorbents

XRD patterns corresponding to the three sorbents (Supplementary data, Figure S1) showed that the synthesized samples are hydrotalcite type compounds and the presence of humate anions was confirmed by FT-IR spectrum on the LDH-H100 and LDH-H50 samples (Supplementary data, Figure S2). The elemental analysis indicated that the molar ratio Mg:Al for both hybrids was 2.4, with a content of magnesium and aluminium of 15% and 7%,

respectively. This result shows that the relation of divalent and trivalent cations obtained was close to the LDH-Cl precursor indicating a slight Mg dissolution during the humate incorporation in the synthesis process [8].

3.2. Sorption equilibrium studies

3.2.1. Influence of the initial metal concentration (sorption isotherms)

The Cu^{2+}, Pb^{2+} and Cd^{2+} sorption isotherms on LDH-H100, LDH-H50 and LDH-Cl are included in Fig. 1. The shape of the sorption isotherm was very similar for each metal sorption in the three sorbents and they correspond to type L or H according to the Giles classification [11]. The results showed that the maximum uptake of Cu^{2+} on LDH-H100, LDH-H50 and LDH-Cl was 0.76, 1.02 and 1.95 mmol g^{-1}, respectively. The amounts sorbed of Pb^{2+} were 0.48, 0.25 and 0.61 mmol g^{-1}, and finally for Cd^{2+} were 0.35, 0.18 and 1.03 mmol g^{-1}on LDH-H100, LDH-H50 and LDH-Cl, respectively. In all cases, the removal of the three metals was higher on LDH-Cl. The final pH ~8.2–9 values achieved after sorption processes on LDH-Cl, suggest that the main mechanism of uptake of metals is probably their precipitation as metal hydroxides. These hydroxides can precipitate either as part of the LDH structure by a mechanism known as diadochy or in a separate phase [12]. The higher amounts of metals sorbed on LDH-Cl could be caused by the precipitation of $M(OH)_2$ determined by its solubility product (K_{SP} $(Cu(OH)_2) = 1 \times 10^{-20}$, K_{SP} $(Pb(OH)_2) = 2.5 \times 10^{-16}$, K_{SP} $(Cd(OH)_2) = 3.2 \times 10^{-14}$. The isomorphic substitution in the layer of magnesium for copper due to their similar cation radio ($r^{2+}_{Mg} = 86$ pm and $r^{2+}_{Cu} = 87$ pm [13] could also contribute to the removal of this metal cation. However, the lowest sorption percentage of Pb^{2+} may be due to the large size of its cation ($r^{2+}_{Pb} = 133$ pm), which would cause greater steric hindrance than the other two metal cations which would hinder the cation exchange in the layers. Also, it should be noted here that for LDH-Cl and $C_0 = 0$–2 mM, the metal elimination percentages were

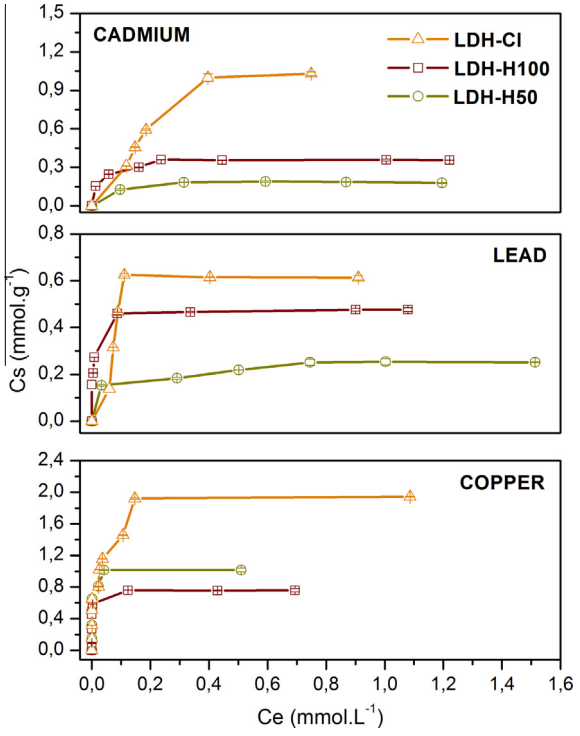

Fig. 1. Sorption isotherms of Cu^{2+}, Pb^{2+} and Cd^{2+} on the sorbents: LDH-H50, LDH-H100 and LDH-Cl.

98%, 80% and 53% for Cu^{2+}, Cd^{2+} and Pb^{2+}, respectively. In the hybrids (LDH-H100 and LDH-H50), the metal sorption behaviour was different, due to an additional bonding mechanism between the metal ions and the humate. The sorption was higher on LDH-H100 than on LDH-H50 for metal cations Pb^{2+} and Cd^{2+}, which is consistent with the additional sorption mechanisms (complexation) of these metals with the functional groups of the hybrid LDHs [14]. Conversely, the Cu^{2+} is sorbed in higher amounts on LDH-H50 than on LDH-H100. One could conclude from this that the precipitation mechanism is the most important for the metal uptake on LDH non-hybrid, since there is a greater proportion of inorganic components on LDH-H50 than on LDH-H100. These results could be comparable and are quite competitive (under similar experimental conditions) with those obtained by other authors; i.e. the maximum amounts of studied metal sorbed on LDHs could be grouped into the following ranges: 0.01–0.5mmol g^{-1} for Cd^{2+}, 0.03–1.78 mmol g^{-1} for Cu^{2+} and 0.03–0.5 mmol g^{-1} for Pb^{2+} [5,6,12,15–20].

3.2.2. Sorption equilibrium models

In order to correlate the experimental data adequately, Langmuir and Freundlich isotherm equations were tested (Eqs. (2) and (3)) to find the best fit using a linear regression coefficient. The results have been included in Table 1 and have shown that the best fit of Cu^{2+}, Pb^{2+} and Cd^{2+} sorption founded on LDH-H100 was the Langmuir model with a $R^2 = 0.998$–0.999, on LDH-Cl with $R^2 = 0.980$–0.999 and on LDH-H50 with $R^2 = 0.997$–0.999. This fact confirms that the sorption processes occur in a monolayer and that the distribution of active sites on the sorbents is homogeneous.

3.2.3. Thermodynamics of sorption

The effect of the temperature on the sorption of metal on LDH-H and LDH-Cl was studied in the temperature range 288–308 K (Fig. 2). The thermodynamic parameters, such as enthalpy (ΔH°), entropy (ΔS°) and Gibb's free energy (ΔG°) were estimated using the relation:

$$\Delta G^\circ = -RT \ln K_L \quad (6)$$

where K_L is the equilibrium constant obtained from Langmuir equation (Table 1)

The standard enthalpy (ΔH°) and entropy (ΔS°) were determined from Van't Hoff equation:

$$lnK_L = \Delta S^\circ/R - \Delta H^\circ/RT \quad (7)$$

the values of ΔH° and ΔS° were obtained from the slope and intersection of the plot of $\ln K_L$ versus $1/T$, and the results are shown in Table 2. The ΔG° values for the temperatures at a range of 288–308 K were obtained between −4.06 and −16.25 kJ/mol. Negative values of free energy changes indicated that the sorption of metal on the LDHs is a spontaneous and a thermodynamically favourable process. These values were in the middle of physisorption (−20–0 kJ/mol) and chemisorption (−80–400 kJ/mol) [21] and it may be concluded that the process was a physical–chemical effect. Positive values of ΔS° indicate the increasing randomness in the sorption process. The positive value of ΔH° indicated that the sorption processes were endothermic in all cases.

3.3. Sorption kinetics

The kinetic of the sorption describes the rate of the removal metal ions on the layered double hydroxides and it is an important aspect of the pollutant removal process control. The kinetic of metal ions uptake is required for selecting optimum operating conditions for the full-scale bath process and gives notable information for designing and modelling the process.

Table 1
Langmuir model parameters for heavy metals sorption on the LDH-H100, LDH-H50 and LDH-Cl sorbents.

Sample	Pollutant	T (K)	C_m (mmol g^{-1})	K_L	R^2
LDH-H100	Cu^{2+}	288	2.109	227	0.998
		298	1.326	260	0.999
		308	1.168	570	0.999
	Pb^{2+}	288	0.286	63	0.999
		298	0.48	187	0.999
		308	0.619	249	0.999
	Cd^{2+}	288	0.177	70	0.999
		298	0.180	123	0.999
		308	0.177	122	0.999
LDH-Cl	Cu^{2+}	288	0.80	41	0.995
		298	0.61	64	0.999
		308	0.57	125	0.980
	Pb^{2+}	288	0.531	9	0.999
		298	0.633	41	0.999
		308	1.209	43	0.999
	Cd^{2+}	288	0.466	5.9	0.996
		298	1.264	6	0.980
		308	2.680	11	0.991
LDH-H50	Cu^{2+}	298	1.02	250	0.999
	Pb^{2+}	298	0.265	14	0.997
	Cd^{2+}	298	0.188	48	0.998

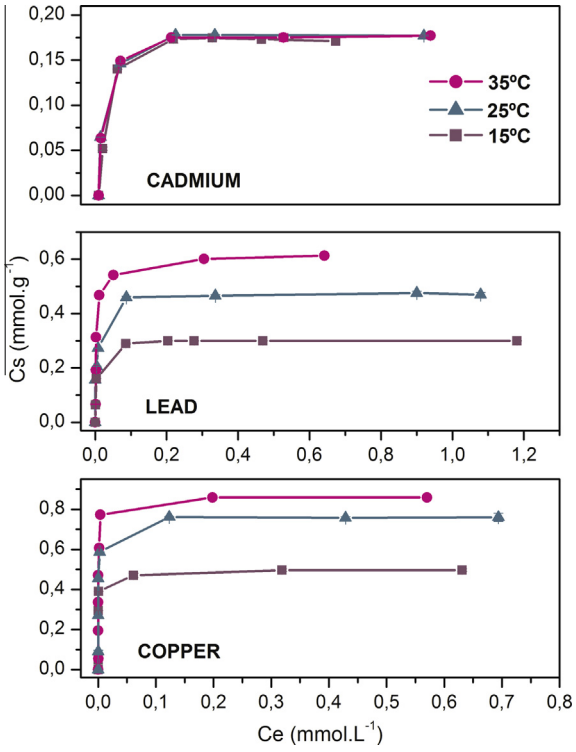

Fig. 2. Sorption isotherms of Cu^{2+}, Pb^{2+} and Cd^{2+} on LDH-H 100 at several temperatures.

3.3.1. The effect of contact time

The studies of the influence of time on the sorption have been included in Fig. 3, showing that the amount of metal sorbed increased with time. In the case of sorption of Cu^{2+} on LDH-Cl, the plateau was reached at 2 h; however, it took 24 h for the LDH-H100 and LDH-H50 sorbents. The removal rates of Pb^{2+} and Cd^{2+} were slower than that corresponding to Cu^{2+}. The equilibrium was reached at 24 h (for LDH-Cl and LDH-H50) and 48 h (for LDH-100) for Pb^{2+} while the equilibrium for sorption of Cd^{2+}occurred at 48 h for the three sorbents. The precipitation process could be less

Table 2
Thermodynamic data for the sorption of Cu^{2+}, Pb^{2+} and Cd^{2+} on the LDH-H100 and LDH-Cl sorbents.

Sample	Pollutant	T (K)	ΔG (kJ mol^{-1})	ΔH (kJ mol^{-1})	ΔS (kJ mol^{-1})
LDH-H100	Cu^{2+}	288	−12.99	33.70	0.161
		298	−13.78		
		308	−16.25		
	Pb^{2+}	288	−9.92	50.97	0.212
		298	−12.96		
		308	−14.13		
	Cd^{2+}	288	−10.17	20.7	0.108
		298	−11.92		
		308	−12.30		
LDH-Cl	Cu^{2+}	288	−8.89	69.7	0.274
		298	−10.30		
		308	−14.38		
	Pb^{2+}	288	−6.34	95.90	0.360
		298	−9.89		
		308	−13.44		
	Cd^{2+}	288	−4.06	18.40	0.078
		298	−4.84		
		308	−5.62		

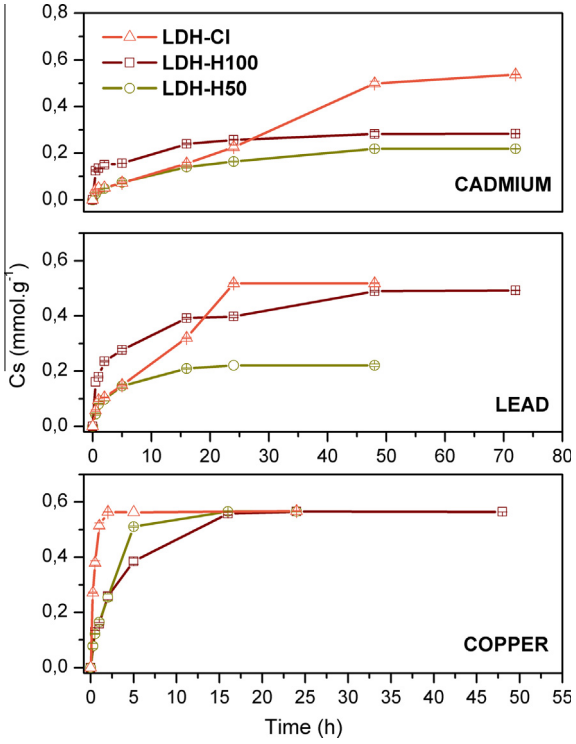

Fig. 3. The evolution of sorption of Cu^{2+}, Pb^{2+} and Cd^{2+} on different sorbents: LDH-H50, LDH-H100 and LDH-Cl at pH = 5.

significant in these last cases due to the fact that $Pb(OH)_2$ and $Cd(OH)_2$ have higher Ks than $Cu(OH)_2$ and a higher concentration of metal in these cases produced a greater interaction between carboxylate groups from the humate anions and the metals ions.

3.3.2. Kinetic models

The kinetic was analysed using different kinetic models such as pseudo-primer-order and pseudo-second-order (Eqs. (4) and (5)).

The parameters of the kinetic models and the linear regression coefficients (R^2) were obtained and shown in Table 3. The kinetic data were fitted better to Eq. (5) for the three sorbents and the three metals based on the correlation coefficient R^2. The q_e values calculated from the pseudo-second-order rate model are very

Table 3
Coefficients of pseudo-first-order, pseudo-second-order and intra-particle diffusion model for sorption of Cu^{2+}, Pb^{2+} and Cd^{2+} on LDH-H100, LDH-H50 and LDH-Cl.

Metal/adsorbent	$q_{e\ Exp}$ (mg/g)	Pseudo-first-order model			Pseudo-second order model			Intra-particle diffusion model		
		$k_1 \times 10^3$ (min^{-1})	q_e (mg/g)	R^2	$k_2 \times 10^3$ (g/mg.min)	q_e (mg/g)	R^2	k_{ip} (mg/g $min^{0.5}$)	C	R^2
Cu/LDH-H 100	36	1.3	17	0.811	0.20	38.5	0.998	0.62	9	0.827
Cu/LDH-H50	36	4.6	50	0.896	0.19	40.0	0.995	0.93	25	0.803
Cu/LDH-Cl	36	4.0	8	0.840	0.05	36.3	0.999	0.38	24	0.385
Pb/LDH-H 100	102	1.8	83	0.909	0.05	105.0	0.995	1.20	34	0.936
Pb/LDH-H50	46	2.1	25	0.840	0.16	47.6	0.999	0.78	12	0.849
Pb/LDH-Cl	108	2.5	114	0.795	0.01	124.0	0.935	2.11	−2	0.845
Cd/LDH-H 100	32	1.6	21	0.993	0.22	32.3	0.998	0.33	13	0.916
Cd/LDH-H50	24	2.3	39	0.864	0.08	27.0	0.985	0.38	2	0.996
Cd/LDH-Cl	61	1.4	89	0.914	0.006	83.3	0.673	1.00	−5.64	0.938

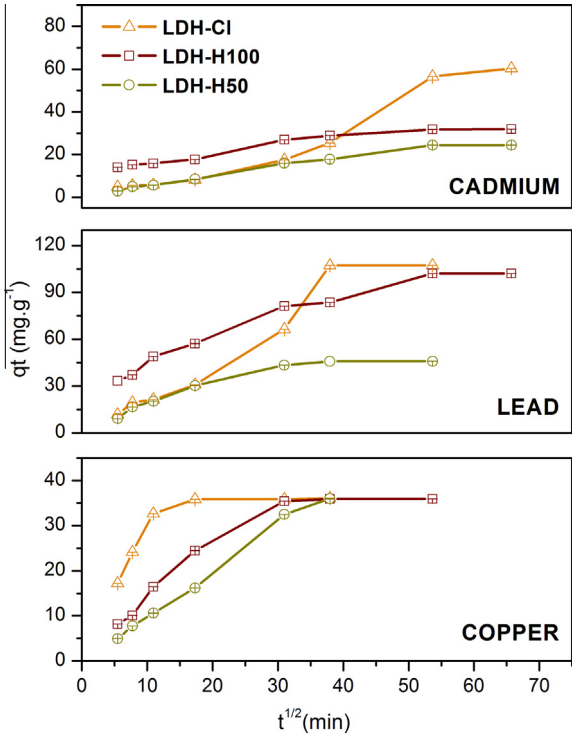

Fig. 4. Intraparticule diffusion plot for the sorption of Cu^{2+}, Pb^{2+} and Cd^{2+} on LDH-H50, LDH-H100 and LDH-Cl.

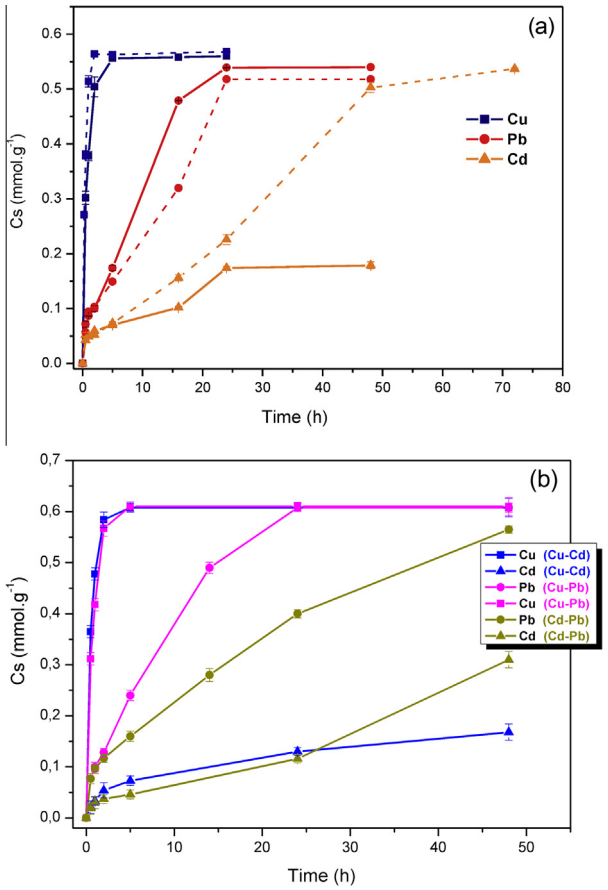

Fig. 5. The evolution of removal of Cu^{2+}, Pb^{2+} and Cd^{2+} on LDH-Cl at pH = 5 and $Ci_{(Cu,Pb,Cd)}$ = 1 mM. (a) From ternary solution (solid line) and single solution (dash line). (b) From binary system.

consistent with the experimental q_e values. This indicates that the experimental kinetic data for sorption by this type of LDH sorbents work well with this model for the entire time range. These results suggested that the pseudo-second order sorption mechanism was predominant, and that the overall rate of the metal uptake appeared to be controlled by a chemisorption process as was indicated by Ho [22]. The pseudo-second-order rate expression has been widely applied in the description of the sorption of the pollutants from aqueous solutions (pesticides, dyes, metal ions, and organic substances) on different sorbents [23–26]. The advantage of using this model is that there is no need to know the equilibrium capacity (q_e) from the experiments as it can be calculated from the model [22]. The rate k_2 for metals sorption process on LDH-Cl and LDH-H50 presented the following sequence: $Cu^{2+} > Pb^{2+} > Cd^{2+}$ and for LDH-H100; $Cd^{2+} \sim Cu^{2+} > Pb^{2+}$. Given the variety of possibilities of different types and/or degrees of specific interaction between the solute and the sorbent (precipitation of hydroxide, diadochy and/or complexation) [7], it is difficult to identify which has a greater influence on the sequence of the apparent rate constant for the different sorbents used.

3.3.3. Intraparticle diffusion model

The overall rate of the sorption process is explored by plotting of q_t versus $t^{1/2}$. According to Weber and Morris [27], for most sorption processes the uptake varies almost proportionally with $t^{1/2}$ rather than with the contact time and can be represented as follows:

$$q_t = ki_p t^{1/2} + C \tag{8}$$

where ki_p (mg/g $min^{0.5}$) is the rate constant of intra-particle diffusion.

According to Eq. (8), the plot of q_t versus $t^{1/2}$ should be a straight line with a slope k_p, which is the intra-particle diffusion rate constant (mg/g $min^{0.5}$), and with an intercept C, when the sorption mechanism follows the intra-particle diffusion process. The value

of *C* gives an idea about the thickness of the boundary layer i.e. the larger the intersection, the greater the boundary layer effect [28].

If the plot shows multilinearity, this would indicate further complexity of the sorption process; each section representing a distinct mechanism. The first section is the external surface sorption or instantaneous sorption step. The second section is the gradual sorption step where the intra-particle diffusion can be rate controlling. The third section is the final equilibrium step where the intra-particle diffusion starts to slow down due to the extremely low solute concentration in the solution [29].

In our case, Fig. 4 shows the Weber and Morris plots for Cu^{2+}, Pb^{2+} and Cd^{2+}, respectively, on the three sorbents used. It was observed that the plots were not linear in any case and they did not pass through the origin, which indicated that intraparticle diffusion is involved in the sorption process, but it is not the only rate limiting mechanism as some other mechanisms also appeared to play an important role. Surface sorption and intraparticle diffusion probably took place simultaneously, both processes controlling the kinetics of sorbate–sorbent interaction. Moreover, the diffusion rate constants in every stage (k_{pi} where $i = 1, 2, \ldots$) follow the order of $k_{p1} > k_{p2} > k_{p3}$. Therefore the changes of k_{p1}, k_{i2}, and k_{i3} could be attributed to the sorption stages of the exterior surface, interior surface and equilibrium, respectively. This can be illustrated as follows: the first section with a steep slope represents the instantaneous diffusion stage, in which large numbers of metal ions from the bulk phase were sorbed rapidly by the surface of the LDH. After almost all the exterior active sites were occupied, the entry of the sorbate into the pores of the sorbents was enhanced [30] and was then sorbed by the interior surface of the pores, which arose in the second stage. In the third section, the intra-particle diffusion rate constants were close to zero, indicating that the equilibrium state had finally been reached. Furthermore, the diffusion rate constant k_{p1} for the sorption of Cu^{2+} on LDH-Cl is much higher than that of LDH-H100, which might be attributed to more active sites on the surface of LDH-Cl or that the high final pH on the process can induce rapid precipitation of Cu^{2+} [8]. The value of the diffusion rate constant k_{p1} for sorption of Pb^{2+} on LDH-H100 is higher than that on LDH-Cl due to the presence of more active sites on the surface of LDH-H100, thus attracting metal ions and enhancing the diffusion rate.

3.4. Competition experiments

3.4.1. Competition of metal sorption in a multicomponent solution in LDH-Cl

The competitive effects that the metals exert on each other in multicomponent (binary and ternary) solutions and the removal efficiencies of LDH-Cl for each metal in a monocomponent (single metal) and in multicomponent solutions, were studied and included in Figs. 5 and 6.

Comparing the binary and the ternary systems, it could be observed that the Pb^{2+} and Cd^{2+} present in the solution do not affect the high percentage of Cu^{2+} sorption in any case. The referred reaction between Cu^{2+} and LDH hydroxyl groups (greater stability constant) cause a fast surface sorption. The precipitation of Cu^{2+} on LDH-Cl takes place (Fig. 5) which makes it difficult for other metals to reach the sorption sites and/or causes its posterior precipitation in different sheets.

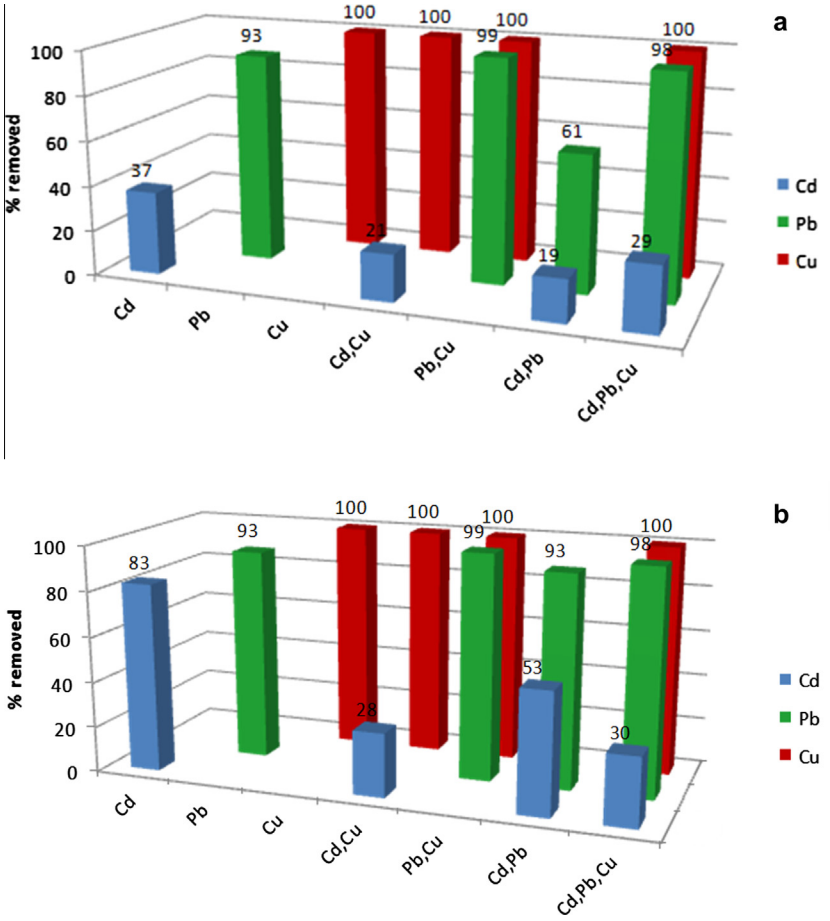

Fig. 6. The evolution of sorption of Cu^{2+}, Pb^{2+} and Cd^{2+} on LDH-Cl from ternary and binary systems (a) at 24 h, and (b) at 48 h.

The results for the multicomponent systems show that the presence of Cd^{2+} has a negligible influence on the sorption of Cu^{2+}- and Pb^{2+} on the LDH-Cl, whereas the sorption of Cd^{2+} is significantly reduced but only if the contact time is 48 h. The results for the binary solution show that the sorption of Cu^{2+} achieved 100% in both the Cu–Cd and Cu–Pb systems. However, the percentage of the removal of Pb^{2+} decreases in the presence of Cd^{2+} in respect to the Cu–Pb system and this value for Cd^{2+} is lower in the presence of Pb^{2+} (Cd–Pb system) than in Cu^{2+} (Cu–Cd system), showing competition between Pb^{2+} and Cd^{2+} during a 24 h period. The decrease in percentage of the removal of the metals on LDH-Cl from the multicomponent solutions in respect to the single solution (non competitive system), may be ascribed to less availability of binding sites. In the multicomponent solutions where metals compete for the same sorption sites of the sorbent metals with a greater affinity, for example; Cu^{2+} could displace others such as Pb^{2+} and/or Cd^{2+} with a weaker affinity [31].

Hence, the order of removal efficiencies of LDH-Cl for the three metal ions was $Cu^{2+} > Pb^{2+} > Cd^{2+}$, implying a stronger affinity of the sorbent for Cu^{2+} than for Pb^{2+} and Cd^{2+}, which agrees with the precipitation of metals as hydroxides and confirms it as the predominant mechanism on LDH-Cl precipitation [8].

3.4.2. Influence of the presence of humate anion on the solution

In order to study the influence of the presence of humate anion on the solution over the metal sorption, some experiments were performed. A simultaneous sorption of these three metals on LDH-Cl in the presence of a humate solution (Fig. 7) was carried out. The maximum amount sorbed of Cu^{2+} at the equilibrium time (in the presence and absence of humate) was the same (C_s = 0.56 mmol g^{-1}). For Pb^{2+} sorption the maximum C_s was 0.54 mmol g^{-1} (in the absence of humate) and 0.49 mmol g^{-1} (in the presence of humate). It could be due to a small part of the metal being complexed with the humate anions present in the solution and remaining there. The Cd^{2+} sorption follows a similar tendency, the C_s values were 0.18 mmol g^{-1} (in the absence of humate) vs 0.12 mmol g^{-1} (in the presence of humate). This could be due to the formation of $Cd(OH)_2$ starting at a higher pH value, the complexation possibly being more favoured (in the presence of NaH) than in the Pb system. This behaviour could indicate that the affinity sequence of metal cations by the humate anion varies, in accordance with the following order: $Cd^{2+} > Pb^{2+} > Cu^{2+}$ (Supplementary data, S3).

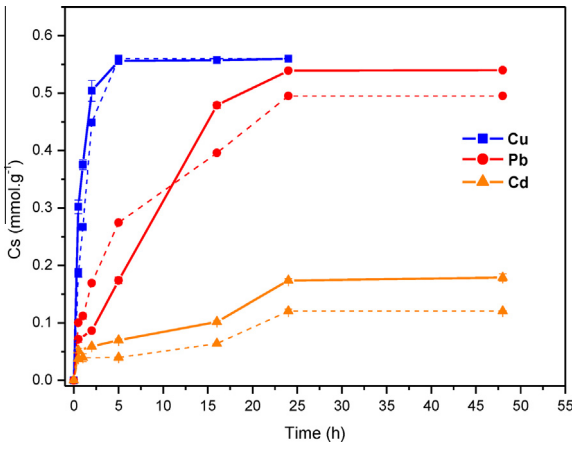

Fig. 7. The evolution of sorption of Cu^{2+}, Pb^{2+} and Cd^{2+} on LDH-Cl from ternary system (solid line) and from ternary solution of metals in presence of humic acid solution (Ci = 1 mM at pH = 5) (dash line).

4. Conclusions

LDHs could uptake metal cations by two mechanisms: (i) chemical precipitation by LDH weathering reactions which lead to a pH increase and precipitation of metal hydroxides and (ii) chelation, if LDH is previously functionalized with a chelating agent. Thus we synthesised LDH intercalated by chloride (LDH-Cl) and two LDH-humate hybrids with different humate loadings (LDH-H50 and LDH-H100) for their study as sorbents of potentially toxic metals from a water solution. LDH-humate is a novel material which we had believed could be very efficient, possibly even more so than LDH-Cl in the metal captions, due to the humate functional groups which could bond metal cations.

However, even though all the sorbents presented high efficiency for the studied metals, maximum sorption was achieved for LDH-Cl, and decreased in the following order: Cu^{2+}, Cd^{2+} and Pb^{2+}. Higher metal amounts sorbed on LDH-Cl suggest that the LDH buffer properties play an important role here, where a slight dissolution of LDH took place, thus inducing precipitation of the metals as hydroxides. In the cases of LDH-H, the LDH moiety is covered by humate, as indicated by characterization analysis, which makes it more stable against dissolution. In this case, humate functional groups are also responsible for the metal uptake.

The thermodynamic parameters indicate that the sorption process is endothermic, feasible and thermodynamically favoured. The pseudo second-order model was found to be more adequate to describe the kinetic of the sorption system in each case. The competitive metal sorption (both in the presence and the absence of humate anions) from binary and ternary solutions for LDH-Cl showed the following sorption order: $Cu^{2+} > Pb^{2+} > Cd^{2+}$. This competing behaviour was related to different factors such as the solubility product constants, complex formation stabilities and/or contact time.

The results suggest that the LDHs studied here are efficient sorbents of potentially toxic metals. Nevertheless, a more detailed research, such as sorbent recyclability and the influence of other ions currently present in water, is needed to optimize this application. Notwithstanding, the novel LDH-humate materials provide an effective solid matrix for immobilizing metals without substantially altering environmental pH values, and could be suitable, as well as LDH-Cl, in the decontamination of water of toxic metallic elements.

Acknowledgements

The financial support from the Spanish Junta de Andalucía (research group FQM214) and MCYT (Project CTM2011-25325) is gratefully acknowledged. We appreciate the technical assistance received in the SCAI (Universidad de Córdoba) for Elemental Analysis Units (ICP-MS).

Appendix A. Supplementary data

Supplementary data associated with this article can be found, in the online version, at http://dx.doi.org/10.1016/j.cej.2015.01.094.

References

[1] M.A. Hashim, S. Mukhopadhyay, J.N. Sahu, B. Sengupta, Remediation technologies for heavy metal contaminated groundwater: a review, J. Environ. Manage. 92 (2011) 2355–2388.
[2] C. Forano, T. Hibino, F. Leroux, C. Taviot-Guého, Layered double hydroxides, in: F. Bergaya, B.K.G. Theng, G. Lagaly (Eds.), Handbook of Clay Science, Elsevier Ltd., 2006, pp. 1021–1095.
[3] U. Costantino, M. Nocchetti, M. Sisani, R. Vivani, Recent progress in the synthesis and application of organically modified hydrotalcites, Z. Kristallogr. 224 (2009) 273–281.
[4] J.H. Choy, S.J. Choi, J.M. Oh, T. Park, Clay minerals and layered double hydroxides for novel biological applications, Appl. Clay Sci. 36 (2007) 122–132.

[5] M.R. Pérez, I. Pavlovic, C. Barriga, J. Cornejo, M.C. Hermosín, M.A. Ulibarrri, Uptake of Cu^{2+}, Cd^{2+} and Pb^{2+} on Zn–Al layered double hydroxide intercalated with EDTA, Appl. Clay Sci. 32 (2006) 245–251.
[6] I. Pavlovic, M.R. Pérez, C. Barriga, M.A. Ulibarri, Adsorption of Cu^{2+}, Cd^{2+} and Pb^{2+} ions by layered double hydroxides intercalated with the chelating agents diethylenetriaminepentaacetate and meso-2,3-dimercaptosuccinate, Appl. Clay Sci. 43 (2009) 125–129.
[7] X. Liang, Y. Zang, Y. Xu, X. Tan, W. Hou, L. Wang, Y. Sun, Sorption of metal cations on layered double hydroxides: a review, Colloids Surf., A. 433 (2013) 122–131.
[8] M.A. González, I. Pavlovic, R. Rojas-Delgado, C. Barriga, Removal of Cu^{2+}, Pb^{2+} and Cd^{2+} by layered double hydroxide-humate hybrid. Sorbate and sorbent comparative studies, Chem. Eng. J. 254 (2014) 605–611.
[9] R. Rojas, Copper, lead and cadmium removal by Ca Al layered double hydroxides, Appl. Clay Sci. 87 (2014) 254–259.
[10] C.C. Travis, E.L. Etnier, A survey of sorption relationships for reactive solutes in soil, J. Environ. Qual. 10 (1981) 8–17.
[11] C.H. Giles, T.H. MacEwan, S.N. Nakhwa, D. Smith, Studies in adsorption. Part XI. A system of classification of solution adsorption isotherms and its use in diagnosis of adsorption mechanisms and in measurement of specific surface areas of solids, J. Chem. Soc. (1960) 3973–3993
[12] S. Komarneni, N. Kozai, R. Roy, Novel function for anionic clays: selective transition metal cation uptake by diadochy, J. Mater. Chem. 8 (1998) 1329–1331.
[13] J.E. Huheey, E.A. Keiter, R.L. Keiter, Inorganic Chemistry: Principles of Structure and Reactivity, fourth ed., Harper Collins College Publishers, New York, 1993.
[14] S. Vreysen, A. Maes, Adsorption mechanism of humic and fulvic acid onto Mg/Al layered double hydroxides, Appl. Clay Sci. 38 (2008) 237–249.
[15] T.S. Anirudhan, P.S. Suchithra, Synthesis and characterization of tannin immobilized hydrotalcite as a potential adsorbent of heavy metal ions in effluent treatments, Appl. Clay Sci. 42 (2008) 214–223.
[16] R. Rojas, M.R. Perez, E.M. Erro, P.I. Ortiz, M.A. Ulibarri, C.E. Giacomelli, EDTA modified LDHs as Cu^{2+} scavengers: removal kinetics and sorbent stability, J. Colloid Interface Sci. 331 (2009) 425–431.
[17] T. Kameda, S. Saito, Y. Umetsu, Mg–Al layered double hydroxide intercalated with ethylene-diaminetetraacetate anion: synthesis and application to the uptake of heavy metal ions from an aqueous solution, Sep. Purif. Technol. 47 (2005) 20–26.
[18] H. Nakayama, S. Hirami, M. Tsuhako, Selective adsorption of mercury ion by mercaptocarboxylic acid intercalated Mg–Al layered double hydroxide, J. Colloid Interface Sci. 315 (2007) 177–183.
[19] X. Liang, W. Hou, Y. Xu, G. Sun, L. Wang, Y. Sun, X. Qin, Sorption of lead ion by layered double hydroxide intercalated with diethylenetriaminepentaacetic acid, Colloids Surf., A 366 (2010) 50–57.
[20] D. Zhao, G. Sheng, J. Hu, C. Chen, X. Wang, The adsorption of Pb(II) on Mg_2Al layered double hydroxide, Chem. Eng. J. 171 (2011) 167–174.
[21] F. Renault, N. Morin-Crini, F. Gimbert, P. Badot, G. Crini, Cationized starch-based material as a new ion-exchanger adsorbent for the removal of C. I. Acid Blue 25 from aqueous solutions, Bioresour. Technol. 99 (2008) 7573–7586.
[22] Y.S. Ho, Review of second-order models for adsorption system, J. Hazard. Mater. B136 (2006) 681–689.
[23] A. Bhatnagar, M. Sillanpää, Utilization of agro-industrial and municipal waste materials as potential adsorbents for water treatment: a review, Chem. Eng. J. 157 (2010) 277–296.
[24] L.D.L. Miranda, C.R. Bellato, M.P.F. Fontes, M.F. de Almeida, J.L. Milagres, L.A. Minim, Preparation and evaluation of hydrotalcite–iron oxide magnetic organocomposite intercalated with surfactants for cationic methylene blue dye removal, Chem. Eng. J. 254 (2014) 88–97.
[25] J. Febrianto, A.N. Kosasih, J. Sunarso, Y.H. Ju, N. Indraswati, S. Ismadji, Equilibrium and kinetic studies in adsorption of heavy metals using biosorbent: a summary of recent studies, J. Hazard. Mater. 162 (2009) 616–645.
[26] T.S. Anirudhan, P.S. Suchithra, Heavy metals uptake from aqueous solutions and industrial wastewaters by humic acid-immobilized polymer/bentonite composite: kinetics and equilibrium modeling, Chem. Eng. J. 156 (2010) 146–156.
[27] W.J. Weber, J.C. Morris, Kinetics of adsorption on carbon solution, J. Sanit. Eng. Div. ASCE 89 (1963) 31–59.
[28] J.I. Mall, V.C. Srivastava, N.K. Agarwall, Removal of Orange-G and Methyl Violet dyes study by adsorption onto bagasse fly ash-kinetic study and equilibrium isotherm analyses, Dyes Pigments 69 (2006) 210–223.
[29] G.L. Dotto, L.A.A. Pinto, Adsorption of food dyes acid blue 9 and food yellow 3 onto chitosan: stirring rate effect in kinetics and mechanism, J. Hazard. Mater. 87 (2011) 164–170.
[30] Y. Ren, H.A. Abbood, F. He, H. Peng, K. Huang, Magnetic EDTA-modified chitosan/SiO_2/Fe_3O_4 adsorbent: preparation, characterization, and application in heavy metal adsorption, Chem. Eng. J. 226 (2013) 300–311.
[31] F. Qin, B. Wen, X.Q. Shan, Y.N. Xie, T. Liu, S.Z. Zhang, S.U. Khan, Mechanisms of competitive adsorption of Pb, Cu, and Cd on peat, Environ. Pollut. 144 (2006) 669–680.

PCCP

PAPER

Cite this: *Phys. Chem. Chem. Phys.*, 2016, **18**, 1838

Capturing Cd(II) and Pb(II) from contaminated water sources by electro-deposition on hydrotalcite-like compounds†

M. A. González,[a] R. Trócoli,*[b] I. Pavlovic,[a] C. Barriga[a] and F. La Mantia*[bc]

Received 2nd September 2015,
Accepted 17th November 2015

DOI: 10.1039/c5cp05235a

www.rsc.org/pccp

Two different hydrotalcite-like compounds were prepared and used as substrates for the electrochemical removal of extremely toxic pollutant cations, such as Cd(II) and Pb(II), from aqueous solutions, and their subsequent recovery for further potential applications. By deposition on the hydrotalcite electrode, it was possible to remove 75% of Cd(II) contained in a starting 5.2 mM solution of $CdCl_2$, which was subsequently recovered and concentrated up to 14.3 mM in a single step. A removal of almost 100% was obtained in the case of Pb(II). Its recovery was largely hindered by the formation of several inert phases, among which is some stable formation of hydroxycarbonate. Our results suggest that the removal of these contaminants by hydrotalcite-like compounds occurs by the combination of two parallel processes: electro-deposition and adsorption. It was possible to achieve a removal capacity for Cd(II) and Pb(II) equal to 763 mg $g_{a.m.}^{-1}$ and 1039 mg $g_{a.m.}^{-1}$, respectively. These removal capacities, accompanied by an excellent posterior eluent-free recovery of Cd(II), suggest that this new method could be an environmentally friendly alternative to the conventional adsorption wastewater treatment.

Introduction

Heavy metals are extremely toxic pollutants, which are directly or indirectly discharged into natural water from different sources, such as metal plating, mining operations, pesticides, textile and dyeing, paper industries, and battery manufacturing, as well as natural rock mineralization processes. Many of them are soluble in water and therefore become more available for living organisms. Their toxicity lies in their bio-accumulation characteristics, *i.e.* they are not biodegradable and thus accumulate in living systems. Lead and cadmium are recognized to be the most hazardous pollutants to various ecosystems and human health[1] since they bind to soft tissues and bones,[2] thus inducing complex changes in plants at genetic, biochemical and physiological levels and leading to phytotoxicity.[3] World Health Organization drinking water guideline values for Cd and Pb are 0.003 and 0.01 mg l^{-1} respectively. Therefore, several remediation technologies such as adsorption by complex formation,[4] co-precipitation,[5] flotation,[6] ion exchange,[7] coagulation,[8] inverse osmosis, nanofiltration,[9] electrolysis,[10] biosorption,[11] *etc.* have been applied to remove the pollutants from contaminated water. Notwithstanding that in many places two or more techniques can work synergistically for better results, new processes can improve the efficiency and functionality of waste water treatment. Among the different techniques applied with this aim in mind, the most extensively used is the precipitation of metals as insoluble metal hydroxides, obtained by increasing the pH of the solution. However, this process consumes a large amount of chemicals and produces large volumes of low density sludge, which is difficult to dispose. One of the most promising emerging technologies in this field is the biological or biochemical techniques but there are several challenges related to the extreme complexity of soil chemistry.[12] Even active carbons, which have been widely used as an adsorbent, present several disadvantages, among which are its high cost and difficulty to be separated from the aquatic system after utilization.[13]

Electro-deposition is an attractive technology due to its high efficiency. The electrochemical treatment techniques offer good removal yields, rapidity, lower volume of sludge, eco-friendly processing, and the possibility of obtaining excellent removal capacities even at high concentration of pollutants.[14] The substrate used to deposit heavy metals from wastewaters plays an important role during the electrochemical process, affecting the formation of dendrites, the occurrence of side reactions (H_2 evolution), and the stability of the process. So, it is necessary to find a low-cost and non-toxic material as a substrate with the purpose to get good electrochemical performance. To this aim,

[a] *Dpto de Química Inorgánica e Ingeniería Química, Campus de Excelencia Internacional Agroalimentaio (CeiA3), Universidad de Córdoba, Córdoba, Spain*
[b] *Semiconductor and Energy Conversion, Zentrum für Elektrochemie – CES, Ruhr-Universität Bochum, Germany. E-mail: rafael.trocolijimenez@rub.de*
[c] *Energiespeicher- und Energiewandlersysteme, Universität Bremen, Germany*

† Electronic supplementary information (ESI) available. See DOI: 10.1039/c5cp05235a

some of the most promising materials are the hydrotalcite-like compounds (layered double hydroxides, LDHs). These materials have attracted attention because of their interesting applications in many fields, and their singular structural characteristics and properties.[15–19] The LDHs exist as minerals, as well as synthetic phases, and their structure could be derived from those of brucite by Al-for-Mg substitution, which results in an excess of positive layer charge that is balanced by interlayer carbonate anions. LDHs have the general chemical formula $[M^{II}_{1-x}M^{III}_{x}(OH)_2]X^{n-}_{x/n}\cdot mH_2O$, where M(II), M(III) and X^{n-} are divalent (Mg^{2+}, Zn^{2+}, Ni^{2+}, *etc.*), trivalent (Al^{3+}, Fe^{3+}, Cr^{3+}, *etc.*) cations, and the interlayer anion, respectively.[20,21] Thus, it is possible to obtain a huge variety of LDH compounds by modifying the nature of these three components.

Recently, these materials have found increasing interest also in electrochemistry because of their layered structure[22] and many attractive properties, such as magnetic, redox, and catalytic functions.[23] The LDHs have been used as an anode material in Zn–Ni secondary batteries, showing lower corrosion, better reversibility and superior electrochemical stability in galvanostatic charge/discharge processes.[24]

For these multiple reasons, this work deals with the incorporation of LDH materials as a substrate component of the electrodes used in the electrochemical deposition of heavy metals. The control of secondary reactions, the metal concentration in the electrolyte, the amount of LDHs, current rate, *etc.* are crucial parameters during the removal process, which should be optimized. Therefore, the first aim of this work was to find out an effective removal method based on the electrochemical deposition of Pb(II) and Cd(II) and using LDH compounds as a substrate. Based on the previously developed mixed entropy, desalination and lithium recovery technologies,[25–28] the second objective of this study was to investigate the possibility of recovering and concentrating the removed metals in a recovery water stream, which could be used for other industrial purposes, such as the production of Pb and Ni–Cd batteries, metallic coatings, dyes, stabilizers for plastics, alloys, fertilizers, *etc.* To this aim, two different hydrotalcite-like materials where prepared: one consisting of Zn/Al layers with carbonate as the balancing anion (ZnAl-CO_3), and another with an organic anion humate (H) between the Mg/Al layers (MgAl-H).

Materials and methods

All the reagents were of analytical grade products and purchased from Sigma-Aldrich. To synthesize Mg–Al-H, distilled water previously boiled and purged with N_2 to prevent CO_2 presence was used.

Preparation of ZnAl-CO_3 and MgAl-H

The hydrotalcite $[Zn_4Al(OH)_{10}]_2(CO_3)\cdot mH_2O$, named ZnAl-$CO_3$, was synthesized using the previously reported coprecipitation method at room temperature.[29] A mixed aqueous solution of 0.40 M $Zn(NO_3)_2\cdot 6H_2O$ and 0.10 M $Al(NO_3)_3\cdot 3H_2O$ was dropped from a funnel into 50 mL of water solution of 1.5 M NaOH and 0.2 M Na_2CO_3, under vigorous agitation and maintaining the basic pH. The suspension obtained was hydrothermally treated at 85 °C for 24 h, separated by centrifugation, washed with distilled water, and dried overnight at 60 °C. The hydrotalcite $[Mg_3Al(OH)_8]_2(H)\cdot mH_2O$, named MgAl-H, was prepared in two steps: a chloride intercalated precursor (Mg_3Al-Cl) was synthesized using the coprecipitation method, which was afterwards dispersed (second step) in a sodium humate solution obtaining the final product by anion exchange. Mg_3Al-Cl was prepared by the dropwise addition of a 200 mL aqueous solution of 0.75 M of $MgCl_2\cdot 6H_2O$ and 0.25 M of $AlCl_3\cdot 6H_2O$ to a 0.25 M of NaCl solution under vigorous agitation and constant pH = 8, set by the addition of 1 M NaOH solution. The synthesis was performed in a N_2 atmosphere in order to avoid atmospheric CO_2 dissolution and consequently carbonate incorporation into the solid. The suspension obtained was hydrothermally treated at 80 °C for 24 h, separated by centrifugation, and washed. A portion of the precipitate was dried at 60 °C to obtain Mg_3Al-Cl, while the remaining slurry was suspended in a 0.13 M sodium humate solution under vigorous stirring and a constant pH = 8 for 24 h.

Characterization of Zn/Mg-Al hydrotalcites

X-ray diffraction patterns (XRD) of powder samples were recorded using a Siemens D-500 diffractometer under CuKα radiation (λ = 1.54050 Å). The Fourier-transform infrared (FT-IR) spectra were registered on a Perkin Elmer Spectrum One Spectrometer using the KBr disc method. Elemental chemical analyses for Zn, Mg and Al were carried out by inductively coupled plasma mass spectrometry (ICP-MS) using a Perkin Elmer ELAN DRC-e instrument. The samples were dissolved in concentrated HNO_3. Thermogravimetric (TG) and differential thermal analysis (DTA) curves were recorded on a Setaram Setsys Evolution 16/18 apparatus in an oxidizing atmosphere under the heating rate of 5 °C min^{-1}. Scanning electron microscopy (SEM) images were recorded using a Quanta 3D FEG instrument equipped with an energy dispersive X-ray analyser (EDAX). Cadmium concentrations were determined by atomic absorption spectroscopy (AAS) on an Analytik Jena AAS 6 Vario instrument and lead concentrations were analyzed by inductively coupled plasma mass spectrometry (ICP-MS) by Wessling GmbH according to the ISO 11885A standard.

Preparation of electrodes based on Zn/Mg-Al hydrotalcites

To prepare the electrodes, a slurry consisting of an active material (LDH or Ag), C65 carbon black (Timcal Super P C60), polyvinylidene fluoride (Solef S5130, Solvay) binder solution in *N*-methyl pyrrolidone (25 mg mL^{-1}), and graphite (Timcal SFG6) in a 75 : 10 : 15 and 80 : 9 : 9 : 2 by weight proportion for LDH and Ag respectively were mixed thoroughly for 30 min at 4000 rpm using an ultra-turrax disperser (Ika). The electrodes, with an approximate area of 2.9 cm^2, were prepared by hand-painting on a carbon cloth (Fuel Cell Earth) current collector with a mass loading of 7 mg of LDH per cm^2 for the removal process from a 5.2 mM solution of $CdCl_2$, and 7 and 14 mg of LDH per cm^2 when 2.5 mM and 5 mM solutions of $PbCl_2$

were respectively used. Prior to use, the electrodes were dried at 60 °C.

Electrochemical measurements

Electrochemical deposition of metals was performed on a flooded three-electrode cell containing 40 mL of the respective solution (5.2 mM $CdCl_2$, 2.5 mM $PbCl_2$ or 5 mM $PbCl_2$), the LDH-based electrode as the working electrode, Ag as the counter electrode, and Ag/AgCl (3 M KCl) as the reference electrode. Prior to the electro-deposition process, argon was bubbled for 10 minutes in solution, and a slow flow was kept during the measurements to avoid the presence of oxygen. After the deposition process, the volume of the cell was reduced to 10 mL and the same configuration described above was used for the recovery process. For the calculation of the current density, the amount of cations in the starting solution was used. Current rates of C/5.2 and C/20.8 were applied for the reduction/oxidation of cadmium and C/20 in the case of lead, where a rate of C/*n* represents a complete reduction (deposition step) or oxidation (recovery step) of all the amount of cations in *n* hours. Electrochemical measurements were performed using a Biologic VSP-300 instrument.

Results and discussion

Structural characterization of the hydrotalcites

The ZnAl-CO_3, MgAl-Cl and MgAl-H samples were characterized using the XRD powder method. Their XRD patterns, included in Fig. 1, correspond to hydrotalcite-like compounds with a rhombohedral symmetry and a basal spacing of 7.6 Å for ZnAl-CO_3, 7.7 Å for MgAl-Cl and 7.9 Å for MgAl-H samples. The XRD reflections of ZnAl-CO_3 were sharper and more symmetric than MgAl-H, showing a good crystallized system. The modification of the hydrotalcite with organic anions (humate) caused a broadening of the diffraction lines and a decrease of the intensities in the hydrotalcite-system. The basal spacing, d_{003} obtained for ZnAl-CO_3 (7.6 Å) corresponds to carbonate containing hydrotalcite,[30] for MgAl-H the basal spacing was 7.9 Å, close to MgAl-Cl used as a precursor.[31] The slight modification of the interlayer spacing during the exchange was consistent with others LDHs containing humic acid.[32–34] The FT-IR spectra of the ZnAl-CO_3, and MgAl-H samples are given in Fig. 2. The broad absorption peak in both spectra between 3600 and 3300 cm^{-1} is due to the ν(OH) mode of the hydroxy groups, both from the brucite-like layers and from interlayer water molecules. Interlayer water also gives rise to the broad, medium-intensity, absorption between 1600 and 1500 cm^{-1}, $\delta(H_2O)$. Hydrogen bonding of water with interlayer carbonate anions also shows a shoulder at 3038 cm^{-1} in the spectrum of the ZnAl-CO_3 sample. The very intense absorption band at 1362 cm^{-1} in the spectrum of Fig. 2a corresponds to the ν_3 mode of the carbonate species. Absorption below 800 cm^{-1} is due to lattice vibrations, involving metal–oxygen stretching modes and, in the case of the ZnAl-CO_3 sample, also modes ν_2 (out-of-plane deformation) and ν_4 (in plane bending) of carbonate at 868 and 670 cm^{-1} respectively.[35] In the case of MgAl-H, the bands at 1114 and 1035 cm^{-1} confirmed the presence of humate anions in the hydrotalcite and the bands at 1603 cm^{-1} and 1387 cm^{-1} were associated with antisymmetric and symmetric vibration of the carboxylate groups.[31,36]

The chemical analysis of the ZnAl-CO_3 and MgAl-H hydrotalcites is shown in Table 1. The molar ratio of Zn:Al was approximately 4, close to the one of the starting solutions used to prepare the sample, which evidenced that co-precipitation was practically complete. The results for MgAl-H indicated that a partial dissolution of Mg^{2+} could have occurred in the sample with respect to the composition of the precursor MgAl-Cl used during the synthesis.[31] The number of water molecules has been calculated from the total weight loss in the TG curves (Appendix 1 ESI,† Fig. S1) attributed to the loss of physically

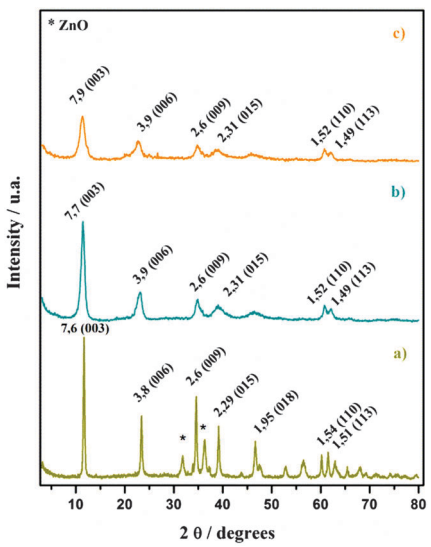

Fig. 1 X-ray patterns of ZnAl-CO_3 (a), MgAl-Cl (precursor of MgAl-H) (b) and MgAl-H (c) hydrotalcites.

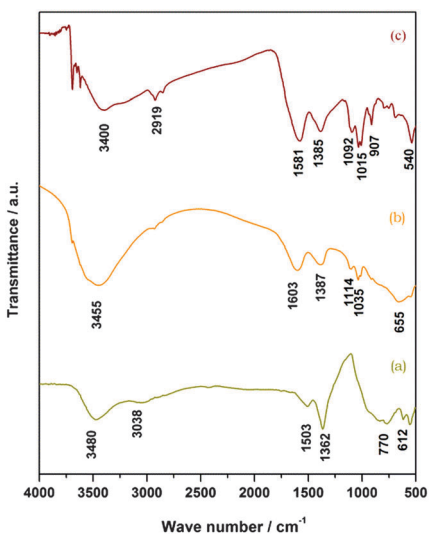

Fig. 2 FT-IR spectra of ZnAl-CO_3 (a) and MgAl-H (b) hydrotalcites. A pattern of humic acid solution salt was added for comparison (c).

Table 1 Chemical analysis results of ZnAl-CO_3, MgAl-Cl and MgAl-H hydrotalcites

	% wt		Atomic ratio	
	M(II)[a]	Al	M(II)/Al	Proposed formula
ZnAl-CO_3	50	5.4	3.8	$[Zn_{0.79}Al_{0.21}(OH)_2](CO_3)_{0.105}\cdot 0.33H_2O$
MgAl-Cl	20	8	2.8	$[Mg_{0.74}Al_{0.26}(OH)_2](Cl)_{0.26}\cdot 0.83H_2O$
MgAl-H	15	7	2.4	$[Mg_{0.71}Al_{0.29}(OH)_2](X)_{0.29/n}\cdot mH_2O$[b]

[a] M = Zn or Mg. [b] X = Cl and/or H (n = 1 and/or 2; m = 0.58–0.71).

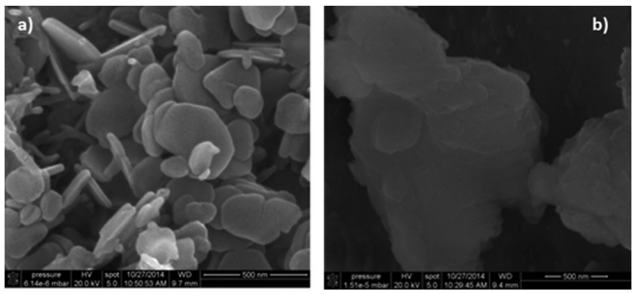

Fig. 3 SEM images of ZnAl-CO_3 (a) and MgAl-H (b) hydrotalcites.

adsorbed and interlayer water, dehydroxylation and decarbonation of the sample ZnAl-CO_3, and for the MgAl-H hydrotalcite was calculated from the first water loss, in the TG curves. In the latter case, two assumptions were used to define the extreme value of the hydration range: all humate molecules are substituting the chlorides in the interlayer; humate is sitting only on the surface.[31,37]

The SEM images of the substrates containing different matrices of LDHs are included in Fig. 3. ZnAl-CO_3 showed thin platelets and a regular shape, which is consistent with a good crystallized structure. The primary particle size was in the range 85–250 nm. The morphology of the MgAl-H sample kept the structural homogeneity after the incorporation of humate anions but a loss of crystallinity and aggregation of the layered particles were observed (SEM image of MgAl-Cl, a precursor of MgAl-H is included in Appendix 2 ESI,† Fig. S2).

Finally, the aggregation of the primary particles can reach a size of more than 300 nm, likely due to the presence of humate anions.

Electrochemical removal of cadmium

Fig. 4 shows the electrochemical deposition of Cd(II) on both ZnAl-CO_3 and MgAl-H, at two different current densities. The process can be described by the following reaction:

$$CdCl_{2(el)} + LDH_{(e)} + 2Ag \leftrightarrow Cd_{(e)} - LDH + 2AgCl \quad (1)$$

where subscripts (el) and (e) indicate the electrolyte and electrode phases respectively. When a negative current was applied, Cd^{2+} was reduced on the LDH to Cd^0 (from left to right in the reaction (1)) and simultaneously 2 Ag were oxidized in the counter electrode. Under the experimental conditions used in this study, the limiting diffusion current is 3.73 mA (more details in Appendix 3 ESI†). The current applied for

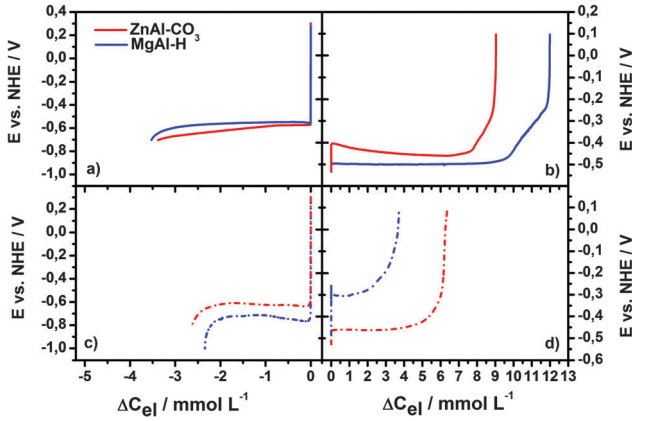

Fig. 4 Electrochemical removal of cadmium at C/20.8 (a) and C/5.2 (c) and their posterior recovery (b and d).

electro-deposition under C/5.2 was close to this value and equal to 2.14 mA, which implies that a high concentration overpotential is required to reduce Cd^{2+} in these measurements. This effect was evidenced in Fig. 4, where the initial overvoltage was 43 mV (E_{eq} = −0.471 V *vs.* NHE) for both double layered hydroxides when a rate of C/20.8 was used, but it increased to 119 mV and 248 mV when the current rate was increased to C/5.2, for ZnAl-CO_3 and MgAl-H, respectively.

Table 2 summarizes the modifications in the concentration of cadmium after the electro-removal process (ΔC_{el}). The value of ΔC_{el} was calculated from the charge flow using the Faraday law. The amounts of cadmium in solution of 3.38 and 3.53 mM decreased when ZnAl-CO_3 and MgAl-H were respectively used at C/20.8. These values indicate the reduction of the pollutant ions of 65.0% and 67.8% respectively. Upon increasing the current rate, the percentage of the cadmium removal decreased to 50.3% (ZnAl-CO_3) and 45% (MgAl-H), respectively. These lower values are in agreement with the fact that the electrodeposition process was controlled by diffusion limitation at this current rate. It is noteworthy to mention that the duration required in the faster experiments was 4 times shorter compared to when a rate of C/20.8 was used. Therefore, it is possible to select the current rate in order to reach the desired objective, *i.e.* shorter times or higher removal fraction. Additionally, the combination of different current densities permits achieving multiple targets, for example, a high initial current to decrease the concentration of the pollutant very fast, followed by a low current to increase the total amount of removed metal ions.

Table 2 Analysis of variation of the concentrations of cadmium (ΔC) in the electrolyte after deposition and recovery processes on ZnAl-CO_3 and MgAl-H at different rates, (Ci_{el} = 5.20 mM)

		Deposition	Recovery	Deposition	Recovery
Sample	Rate	ΔC_{el} (mM)	ΔC_{el} (mM)	ΔC_A (mM)	ΔC_A (mM)
ZnAl-CO_3	C/5.2	−2.62	6.37	−3.18	6.65
ZnAl-CO_3	C/20.8	−3.38	9.04	−3.84	10.55
MgAl-Cl	C/5.2	−2.34	3.72	−2.65	2.75
MgAl-H	C/20.8	−3.53	11.99	−3.91	14.33

Furthermore, if higher percentages of removal are desired, it is enough that a lower current density is applied. It would be possible also to combine this technology with the previously reported adsorption process based on similar LHDs,[31,37] whose effectiveness is limited to the concentration of pollutants lower than 2.5 mM. Therefore, after the electro-deposition step it could be possible to use an adsorption step, to remove all the remaining pollutants from the solution. To measure the real variation of the concentration in the electrolyte, the solutions after and before the electrochemical processes were analysed by AAS. In all the cases, the values of cadmium elimination observed by means of AAS (ΔC_A, Table 2) were higher than the value of ΔC_{el}. It would have been expected that the value of ΔC_{el} would be larger than ΔC_A, due to a non-unitary efficiency in the electrochemical process, maybe caused by hydrogen evolution. The observed differences were associated with the adsorption properties of the double layered hydroxides, able to remove a fraction of cadmium by a simple contact of the electrode with the electrolyte. An estimation of the contribution of the adsorption process to the total removal of metal is described in Appendix 4 ESI.† When this effect is taken into account, an efficiency lower than 1 was obtained for the electrochemical process. The electrochemical removal capacities were equal to 622 mg $g_{a.m.}^{-1}$ ($g_{a.m}$ = gram of active material) and 518 mg $g_{a.m.}^{-1}$ when ZnAl-CO_3 and MgAl-H were respectively used as a substrate with a current rate of C/5.2. These values increased to 749 mg $g_{a.m.}^{-1}$ and 763 mg $g_{a.m.}^{-1}$ when the current rate was equal to C/20.8. These removal capacities are considerably higher than the traditional values obtained by the adsorption process alone, which generally ranges from 10^{-3} mg g^{-1} to 270 mg g^{-1} of the adsorbent.[38] The presence of a pollutant was reduced by 61.2% and 73.8% for ZnAl-CO_3, and 50.9% and 75.2% for MgAl-H, when the current rate was equal to C/5.2 and C/20.8, respectively. To confirm the critical role of the LDHs in the electrochemical deposition of Cd and to evaluate the contribution of the current collector (carbon cloth) and additives used to prepare the electrodes (carbon black, polyvinylidene fluoride, and graphite), a removal process was performed using an electrode composed only by carbon black, graphite, and a binder at a current rate of C/20.8 (Appendix 5 ESI,† Fig. S3a). The electro-deposition of Cd using such a substrate was limited to just 6.5% of the initial amount, confirming that the LDH plays a critical role (Table 2).

After the removal process, the volume of the cell was reduced to 10 mL and the cadmium was recovered by applying a positive current (from right to left in the reaction (1), Fig. 5). A recovery of 60.7% and 39.7% of the cadmium deposited was obtained when ZnAl-CO_3 and MgAl-H were used at C/5.2, respectively. When the current applied was decreased to C/20.8, the values of 84.2% and 66.8% were achieved. These percentages are greater than the recovery obtained (close to 38%) using adsorption methods that have removal capacities similar to the ones of this work.[39] This methodology permitted us to increase the concentration of cadmium up to 14.33 mM, 4.5 times higher than that obtained by other effective absorbents, and without the need to use any eluent.[40] The recovery solution could be used for other applications, such as the reactant in flow cadmium batteries; this technology permits us to convert wastewater into an added-value product. Additionally, the reduction of the volume used for the recovery process and the possibility of reusing the same solution would permit us to increase the concentration of cadmium to the desired values, as we previously demonstrated in an equivalent method for lithium recovery from brines.[27,28]

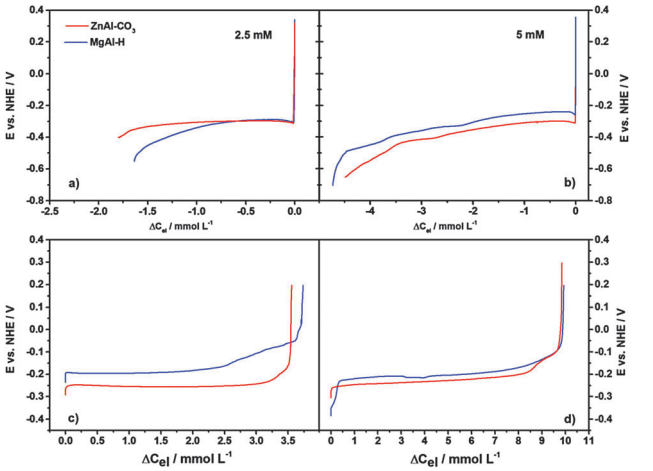

Fig. 5 Electrochemical removal of lead from 2.5 mM (a) and 5 mM $PbCl_2$ (b) and their posterior recovery (c and d).

Electrochemical removal of lead

Fig. 5 shows the electrochemical deposition of Pb(II) on both ZnAl-CO_3 and MgAl-H hydrotalcites, at two different concentrations of the electrolyte. Similar to the one reported previously in the case of cadmium, the process can be described by the following reaction:

$$PbCl_{2(el)} + LDH_{(e)} + 2Ag \leftrightarrow Pb_{(e)} - LDH + 2AgCl \quad (2)$$

where subscripts (el) and (e) indicate the electrolyte and electrode phases respectively. When a negative current was applied Pb^{2+} was reduced on the LDH to Pb^0 (from left to right in the reaction (2)) and simultaneously 2 Ag were oxidized in the opposite electrode. In the case of lead, the applied current was always far from the diffusion limiting current, thus polarization observed at lower concentrations of Pb(II) can be attributed to the deposition mechanism itself, which is kinetically slow. The variations of lead concentration are summarized in Table 3. The Pb(II) concentration was reduced by 1.8 mM and 1.64 mM when ZnAl-CO_3 and MgAl-H were respectively used in a solution containing an initial concentration of 2.5 mM of $PbCl_2$, decreasing the starting amount of Pb(II) by 72% and 65.6%, respectively.

When a solution with initial concentration equal to 5 mM was used, it was possible to decrease the concentration of the pollutant by 4.48 mM (ZnAl-CO_3) and 4.73 mM (MgAl-H), reaching percentages of removal equal to 89.6% and 94.6%. The concentration of Pb(II) in the solution after the removal process was analyzed by ICP-MS. Again, higher values of ΔC_A

Table 3 Analysis of the variation of the concentrations of lead (ΔC) after the deposition and recovery process on ZnAl-CO_3 and MgAl-H at different concentrations of electrolyte (Ci_{el})

		Deposition	Recovery	Deposition	Recovery
Sample	Ci_{el}	ΔC_{el} (mM)	ΔC_{el} (mM)	ΔC_A (mM)	ΔC_A (mM)
ZnAl-CO_3	2.5	−1.80	3.56	−2.09	1.31
ZnAl-CO_3	5	−4.48	9.85	−4.60	0
MgAl-Cl	2.5	−1.64	3.73	−1.95	2.16
MgAl-H	5	−4.73	9.93	−5.07	3.32

were obtained with respect to the values of ΔC_{el} calculated from the Faraday law. These differences were in the same range of the one observed for Cd, and it was verified that they were due to the inevitable adsorption process occurring during the contact of the hydrotalcite with the solution containing the pollutant (more details in Appendix 4 ESI†). Considering the combination of the electrochemical removal process and the adsorption effect, the percentages of Pb eliminated from a 2.5 mM solution the reached values of 83% and 78% for ZnAl-CO_3 and MgAl-H respectively, these values increased up to 92% and 100% when a 5 mM solution was used, achieving a nearly total removal of Pb(II). The highest removal capacity was obtained by the sample MgAl-H from a 5 mM Pb(II) solution, reaching 1039 mg $g_{a.m.}^{-1}$, 2.7 times higher than the best adsorption method.[41] As in the case of the electro-deposition of Cd, the presence of LDH in the electrode was vital to the process. Without LDH in the electrode a removal of Pb(II) equal to just 4.4% was achieved when a 5 mM $PbCl_2$ solution was treated with a current rate of C/20. This clearly shows that LDHs play a critical role in the electro-deposition of these highly toxic metals. After the removal process, the volume of the cell was reduced to 10 mL and lead was recovered by applying a positive current (from right to left in reaction (2), Fig. 5). Although from Fig. 5c and d, it could be supposed that the recovery of the deposited lead was successful, the ICP analysis (Table 3) showed that there was no or little recovered lead, so that the final solution after recovery had a lower concentration than the initial one. With the aim to clarify the mechanism of lead depletion during the recovery process, the electrodes were analyzed by X-ray diffraction (Fig. 6). The XRD patterns showed a complex system containing several phases: lead metal, oxide, hydroxide, hydroxycarbonate, and chloride of lead. Three possible mechanisms of re-adsorption of Pb(II) on LDHs during the recovery process, or their combination, could explain the differences observed between the electrochemical and ICP-MS data, as they are schematically shown in Fig. 7. The first mechanism is given by precipitation as hydroxycarbonate of lead. The presence of carbonate as an interlayer anion in the structure of the hydrotalcite helps in producing this compound. The lower values of recovery obtained using ZnAl-CO_3 (Table 3) and comparing with MgAl-H are in agreement with the higher amount of carbonate inside ZnAl-CO_3, so the possibility of removing this anion to form hydroxycarbonate of lead is plausible. This assumption was confirmed by the blank measurements, which showed higher removal values of this

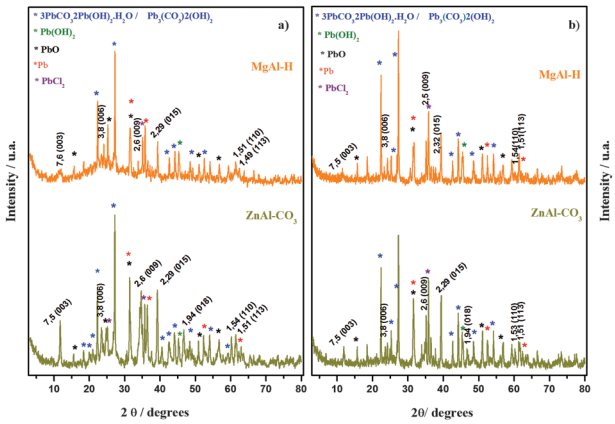

Fig. 6 X-ray diffractograms of the substrates after the recovery process from 2.5 mM (a) and 5 mM (b) lead solutions as electrolytes.

$$Pb_{(e)}{-}LDH \rightarrow Pb^{2+}_{(el)} + LDH_{(e)} \xrightarrow{mechanism\ 1} Pb_x(CO_3)_y(OH)_z \downarrow$$
$$\xrightarrow{mechanism\ 2} Pb(OH)_2 \quad \leftarrow 2OH^- + H_2 \leftarrow 2H_2O$$
$$\xrightarrow{mechanism\ 3} PbCl_2 \leftarrow 2Cl^-_{(el)}$$

Fig. 7 Possible mechanisms of lead depletion during the recovery process.

HT (more details in Table S2, ESI†). Pavlovic *et al.* also found $PbCO_3$ precipitated in ZnAl-LDH intercalated with DMSA ligands and Park *et al.* in Mg/Al-LDH.[21,42] The humate anion contained in MgAl-H could contribute to the sorption process *via* complexation/chelation between the metallic cation and the functional groups of humate. This mechanism was confirmed by XRD, several peaks associated with this phase are shown in Fig. 6. The uptake of lead by precipitation as hydroxide on the LDH is the second mechanism proposed. The local increase of pH caused by possible H_2 evolution during the deposition process could induce its precipitation. Finally, the third mechanism involves the formation of $PbCl_2$. During the recovery process the concentration of Pb(II) in the surrounding of the electrode increases and simultaneously Cl^- anions are attracted from the bulk owing to the positive current applied, generating locally an oversaturated solution and the precipitation of $PbCl_2$. However, there was neither a clear evidence of the presence of hydroxide nor chloride of lead, which could occur in a negligible amount or could be rebalanced very rapidly, once the current is interrupted. The identification of both phases could also be complicated by the fact that the main peaks of the XRD pattern are overlapping with the diffraction lines of different species of hydroxycarbonate, whose phase is the majority. In any case the XRD patterns indicate the high complexity of these systems that hinder the recovery of lead and its concentration to values higher than 3.3 mM.

Due to the nature of the reactions involved in the removal process investigated in this study (reactions (1) and (2)), the integrity of the LDHs is not compromised by oxidation/reduction of their components or structural stress. Therefore

we expect a long cycle life and good stability of the LDHs, similar to that reported by Huang *et al.*[24] The authors demonstrated that LDH-based electrodes had a cycle life superior to 500 cycles. The silver electrode showed a good stability, and was cycled at least 30 times in 5.2 mM $CdCl_2$ and 5 mM $PbCl_2$ at least 30 times (Appendix 6 ESI,† Fig. S4), reaching a capacity close to 60 mA h g^{-1}.

Conclusions

The electrochemical method for the removal of Cd(II) and Pb(II) developed in this article is based on the use of ZnAl-CO_3 and MgAl-H hydrotalcites as substrates. The structural characterization of these compounds confirms the hydrotalcite-like structure with a good crystallization of the samples. The utilization of these materials permits the elimination of pollutants by two simultaneous processes; electrochemical reduction of M^{2+} to M^0, and adsorption. This combined methodology shows the removal values of 763 mg $g_{a.m.}^{-1}$, and 1039 mg $g_{a.m.}^{-1}$ of Cd(II) and Pb(II), respectively, removing 75% and 100% of the heavy metals from the water stream. These values are considerably higher than the traditional values obtained by using other materials as adsorbents. We have shown that the presence of the LDH is vital to the electro-deposition process, and only negligible removal is reached in electrodes that do not contain the hydrotalcite-like compounds. Additionally, it was possible to recover 27% of the removed lead in a separate solution; in the case of cadmium it was possible to reach a recovery value of 84.2%, thus obtaining a solution with a concentration of 14.3 mM, 4.5 times higher than the best cadmium recovery method using adsorbents and without the need to use any eluent. This recovery solution could be used for other applications, such as a reactant in flow cadmium batteries, without further treatment. The lower amount of lead recovered was attributed to the formation of different species of this metal resorbed on the LDH. This was also confirmed by XRD. Future work should focus on replacing silver as the counter electrode with more suitable materials, in terms of cost and effectiveness.

Acknowledgements

The financial support from the Spanish Junta de Andalucía (research group FQM214) and MCYT (Project CTM2011-25325), the Federal Ministry of Education, Research (BMBF) in the framework of the project "Energiespeicher" (FKZ 03K3005), and the Cluster of Excellence RESOLV (EXC 1069) funded by the Deutsche Forschungsgemeinschaft (DFG) are gratefully acknowledged.

References

1 S. Mol, *Biol. Trace Elem. Res.*, 2011, **143**, 974.
2 G. Yuan, S. Dai, Z. Yin, H. Lu, R. Jia, J. Xu, X. Song, L. Li, Y. Shu and X. Zhao, *Food Chem. Toxicol.*, 2014, **65**, 260.
3 G. Drazic and N. Mihailovic, *Plant Sci.*, 2005, **168**, 511.
4 M. R. Pérez, I. Pavlovic, C. Barriga, J. Cornejo, M. C. Hermosin and M. A. Ulibarri, *Appl. Clay Sci.*, 2006, **32**, 245.
5 K. G. Karthikeyan, H. A. Elliot and F. S. Cannon, *Environ. Sci. Technol.*, 1997, **31**, 2721.
6 J. Rubio, M. L. Souza and R. W. Smith, *Miner. Eng.*, 2002, **15**, 139.
7 S. Y. Kanga, J. U. Leeb, S. H. Moona and K. W. Kima, *Chemosphere*, 2004, **56**, 141.
8 Q. Chang and G. Wang, *Chem. Eng. Sci.*, 2007, **62**, 4636.
9 H. A. Qdais and H. Moussa, *Desalination*, 2004, **164**, 105.
10 A. T. Heijne, F. Liu, R. Weijden, J. Weijma, C. J. N. Buisman and H. V. M. Hamelers, *Environ. Sci. Technol.*, 2010, **44**, 4376.
11 N. Ahalya, T. V. Ramachandra and R. D. Kanamadi, *Res. J. Chem. Environ.*, 2003, **7**, 71.
12 M. A. Hashim, S. Mukhopadhyay, J. N. Sahu and B. Sengupta, *J. Environ. Manage.*, 2011, **92**, 2355.
13 Q. Jiuhui, *J. Environ. Sci.*, 2008, **20**, 1.
14 F. Fu and Q. Wang, *J. Environ. Manage.*, 2011, **92**, 407.
15 A. E. Palomares, J.-M. López-Nieto, F. J. Lazaro, A. Lopez and A. Corma, *Appl. Catal., B*, 1999, **20**, 257.
16 D. G. Evans and X. Duan, *Chem. Commun.*, 2006, 485.
17 J.-H. Choy, S.-J. Choi, J.-M. Oh and T. Park, *Appl. Clay Sci.*, 2007, **36**, 122.
18 F. Bruna, I. Pavlovic, R. Celis, C. Barriga, J. Cornejo and M. A. Ulibarri, *Appl. Clay Sci.*, 2008, **42**, 194.
19 R. Extremera, I. Pavlovic, M. R. Pérez and C. Barriga, *Chem. Eng. J.*, 2012, **213**, 392.
20 P. S. Braterman, in *Handbook of Layered Materials*, ed. S. M. Auerbach, *et al.*, Marcel Dekker, Inc., New York, Basel, 2004, pp. 373–474.
21 I. Pavlovic, M. R. Pérez, C. Barriga and M. A. Ulibarri, *Appl. Clay Sci.*, 2009, **43**, 125.
22 P. Vialat, F. Leroux, C. Taviot-Gueho, G. Villemure and C. Mousty, *Electrochim. Acta*, 2013, **107**, 599.
23 C. Obayashi, M. Ishizaka, T. Konishi, H. Yamada and K. Katakura, *Electrochemistry*, 2012, **80**, 879.
24 T. Wang, Z. Yang, B. Yang, R. Wang and J. Huang, *J. Power Sources*, 2014, **257**, 174.
25 F. La Mantia, M. Pasta, H. D. Deshazer, B. E. Logan and Y. Cui, *Nano Lett.*, 2011, **11**, 1810.
26 M. Pasta, C. D. Wessells, Y. Cui and F. La Mantia, *Nano Lett.*, 2012, **12**, 839.
27 M. Pasta, A. Battistel and F. La Mantia, *Energy Environ. Sci.*, 2012, **5**, 9487.
28 R. Trócoli, A. Battistel and F. La Mantia, *Chem. – Eur. J.*, 2014, **20**, 9888.
29 W. T. Riechle, *Solid State Ionics*, 1986, **22**, 135.
30 I. Crespo, C. Barriga, V. Rives and M. A. Ulibarri, *Solid State Ionics*, 1997, **101–103**, 729.
31 M. A. González, I. Pavlovic, R. Rojas-Delgado and C. Barriga, *Chem. Eng. J.*, 2014, **254**, 605.
32 Y. Seida and Y. Nakano, *Water Res.*, 2000, **34**, 1487.
33 S. J. Santosa, E. S. Kunarti and Kamato, *Appl. Surf. Sci.*, 2008, **254**, 7612.
34 S. Vreysen and A. Maes, *Appl. Clay Sci.*, 2008, **38**, 237.

35 V. Rives, *Layered Double Hydroxides: Present and Future*, Nova Science Publishers, Inc., New York, 2001.
36 L. J. Bellamy, *The Infrared Spectra of Complex Molecules*, Chapman and Hall, London, 1975.
37 M. A. González, I. Pavlovic and C. Barriga, *Chem. Eng. J.*, 2015, **269**, 221.
38 D. Purkayastha, U. Mishra and S. A. Biswas, *Journal of Water Process Engineering journal*, 2014, **2**, 105.
39 V. Singh, A. K. Sharma and S. Maurya, *Ind. Eng. Chem. Res.*, 2009, **4**, 4688.
40 K. C. Justi, V. T. Fávere, M. C. M. Laranjeira, A. Neves and R. A. Peralta, *J. Colloid Interface Sci.*, 2005, **291**, 369.
41 K. Kesenci, R. Say and A. Denizli, *Eur. Polym. J.*, 2002, **38**, 1443.
42 M. Park, C. L. Choi, Y. J. Seo, S. K. Yeo, J. Choi, S. Komarneni and J. H. Lee, *Appl. Clay Sci.*, 2007, **37**, 143.